University of Alberta
Department of Civil &
Environmental Engineering

Beam-to-Column Shear Connections with Slotted Holes

by

Jack C.Y. Man

Gilbert Y. Grondin

and

Robert G. Driver

January, 2006

Beam-to-Column Shear Connections with Slotted Holes

by

Jack C.Y. Man

Gilbert Y. Grondin

and

Robert G. Driver

Structural Engineering Report 260

Department of Civil & Environmental Engineering
University of Alberta
Edmonton, Alberta

February, 2006

ABSTRACT

Slotted holes in web framing angles of beam to column connections provide greater fabrication tolerance and can facilitate both fabrication and erection of steel structures. The current North American steel design standards require plate washers to completely cover the slots in connections with long slotted holes in the outer plies of the joint. Although plate washers are required in connections that require pretensioned bolts, their need in bearing-type connections is questionable.

Tests on beam-to-column shear connections with slotted holes were conducted to investigate the influence of a wide range of parameters on their strength and behaviour. The angle leg connected to the supporting column was also investigated.

The test program indicated that plate washers are required with long slotted holes to develop the expected shear capacity. The North American standards were not able to predict the capacity of web framing angles failing in the leg connected to the column and failing within the edge distance. New prediction models are proposed for these failure modes.

ACKNOWLEDGEMENTS

TABLE OF CONTENTS

LIST OF TABLES

LIST OF FIGURES

viii

LIST OF SYMBOLS

A_{gv}	=	Gross shear area (mm^2)
A_{nt}	=	Net tensile area (mm^2)
A_{nv}	=	Net shear area (mm^2)
B_u	=	Bearing capacity of a bolt in a connection (N)
d	=	Bolt diameter (mm), or
D_c	=	Cope depth on coped beam (mm)
d_h	=	Bolt hole diameter of angle leg (mm)
D_h	=	Bolt hole diameter on beam web (mm)
d_{slot}	=	Diameter of the slot (mm)
e_g	=	Edge distance of angle leg (mm)
E_g	=	Edge distance of beam web (mm)
e_s	=	End distance of angle leg (mm)
E_s	=	End distance on beam end, from centre of bolt hole to the outside face of flange, or to the coped end (mm)
F_y	=	Material yield strength (MPa)
F_u	=	Material ultimate strength (MPa)
L	=	Horizontal distance from the vertical load to the centre of top bolt hole (mm)
L_c	=	Cope length on coped beam (mm)
l_c	=	Clear distance in the direction of applied force (mm)
l_e	=	End distance in the direction of applied force, from centre of bolt hole to the end of material (mm)
l_{slot}	=	Slot length (mm)
M_p	=	Plastic moment at the plastic hinge (N.mm)
θ	=	Vertical angle of top bolt force R_1
p	=	Vertical spacing between bolt holes or slotted holes of angle leg (mm)
P	=	Predicted connection capacity using modified ICR method (N)
P_c	=	Collapse load of end distance at the end of angle (N)
P_r	=	Tension and shear block capacity (N)

R	=	Force in the bolts connecting the angle to the column (N)
r	=	Distance from the Instantaneous Centre of Rotation to each bolt (mm)
r_o	=	Horizontal distance from the Instantaneous Centre of Rotation to the top bolt (mm)
R_t	=	Tension stress correction factor
R_v	=	Shear stress correction factor
S	=	Vertical spacing between bolt holes on beam web (mm)
S_r	=	Shear contribution of the inclined tension and shear block failure capacity (N)
t	=	Thickness of connected material (mm)
T_r	=	Tension contribution of the inclined tension and shear block failure capacity (N)
V_u	=	Nominal connection shear capacity (N)
w	=	Beam web thickness (mm)
$\mu\varepsilon/min$	=	Mircostrain per minute or 10^{-6}mm/mm/min
σ_b	=	Applied bearing stress of bolt acting on the bolt hole by the fastener (MPa)

1 Introduction

1.1 Statement of Problem

Single or double angle bolted connections are often used in beam-to-column connections as simple framing connections. When these connections have to accommodate large rotations or when beams have to be erected at a slope, slotted holes, either in the beam web or in the framing angles, are an economical means of achieving the larger required tolerances (Shneur, 2003). Since the first application of high-strength bolts in 1947, bolt holes 1/16 in. or 2 mm larger than the nominal bolt diameter have been used for assembly (Kulak *et al.*, 1987). Slotted holes are bolt holes with 2 mm clearance in the transverse axis and oversized in the longitudinal axis. The slot length depends on the amount of adjustment required during construction or to accommodate beam end rotation. In this respect, slots are classified as either short slots or long slots. Short slots have a length up to about 1.4 times the bolt diameter whereas long slots have slot lengths up to 2.5 times the bolt diameter.

The current North American steel design standards require that for connections with long slotted holes in the outer plies of the joint, a plate washer (or a continuous bar 8 mm or greater in thickness with standard holes) must be installed that completely covers the slots. However, high strength bolts in connections with short slotted holes require only the use of conventional hardened washers. Because of the significant amount of material loss around a bolt in a long slotted hole, proper bolt preload is not achievable unless plate washers are used. However, their need in bearing-type connections, where bolt pretension is not required, has not been well demonstrated. It is believed that pull-out of the bolt head or nut through the slot could occur in a connection without plate washers when the holes deform sufficiently. However, no testing has shown that pull-out of the bolts does, in fact, occur in these connections.

Extensive research has been conducted on single or double angle connections. However, the majority of this past research emphasized the moment vs. rotation behaviour and the rotational restraint provided by the connections, rather than the shear capacity of the connections. Consequently the connections were not loaded to their

ultimate load carrying capacity. Moreover, the number of parameters investigated was very limited. Therefore, a research program is initiated to acquire a better understanding of bolted single and double angle connections with slotted holes with the slots in the outer plies.

1.2   Objectives and Scope

The main objective of this research program was to investigate the strength and behaviour of slotted-hole connections and the influence of various parameters on the connection capacity. The research program consisted of a series of tests on full-scale connections and assessment of predicted capacities using the current North American steel design standards. Recommendations for improvement of the current prediction models will be made when required.

The experimental program consisted of 40 tests. The parameters investigated include: angle loaded end distance, plate washers, slot length, bolt pretension, torsion brace, bolt pitch, flange cope, beam end rotation, web thickness and bolt diameter. In addition, the effect of parameters related to failure in the leg connected to the supporting column was also investigated. These parameters include: top end distance, top edge distance, angle thickness and number of bolts on the angle leg connected to the supporting column. The effect of the above parameters is assessed from a comparison of the capacity and the load vs. deformation response of the test specimens.

In order to assess the adequacy and level of conservatism offered by the current North American steel design standards on connections with slotted holes, the capacity of all the specimens based on the relevant design equations is compared with the test results. All the possible failure modes and the corresponding capacities are investigated. Additionally, new prediction models for single angle shear connections with slotted holes and eccentrically loaded single angle connections are proposed. These new predictions models are also compared with the test results.

1.3   Organization of the Report

This report is divided into six chapters. A review of the relevant literature on the strength and behaviour of shear connections and slotted hole connections is presented in Chapter 2. A description of a test program on full-scale test connections is presented in Chapter 3. The results of the test program are presented in Chapter 4 and in Appendices A and B. Chapter 5 present an assessment of the current Canadian and American steel design standards through a comparison of the design equations with the observed test results. The same chapter presents proposed models for the prediction of failure modes observed in the tests but poorly predicted by the current design equations. A summary, conclusions and recommendations for future work are presented in Chapter 6.

2 Literature Review

2.1 Introduction

Angle connections are a common type of simple framing connection. Slotted holes are often used in the angles, primarily to accommodate construction tolerances in the field, but they also permit erection of beams on a slope while keeping the holes in the beam perpendicular to the axis of the beam. The current North American steel design standards require that plate washers be used for connections with long slotted holes, i.e., those having slot lengths from about 1.4 to 2.5 times the bolt diameter. Plate washers are not required, however, in connections with short slotted holes, i.e., those with slot lengths up to about 1.4 times the bolt diameter. In the case of bearing-type connections, plate washers are required for long slots because it is feared that bolts might pull-out in a connection without plate washers. However, until recently no testing has been completed to show that pull-out of the bolt does in fact occur in these connections. In order to investigate the behaviour of slotted hole connections without plate washers, five pilot tests on single angle connections with slotted holes and without plate washers were conducted by Franchuk *et al.* (2002). Slot lengths varying from 1.65 to 2.4 times the bolt diameter were investigated. Other parameters included in the tests were bolt diameter, location of the bolt within the slot, and number and spacing of the bolts in the connection.

Although very limited research on slotted hole connections without plate washers has been conducted, extensive research has been conducted on single angle, single shear plate, and double angle connections over the past few decades. A review of the research conducted on single angle, single plate, and double angle connections is presented. A review of tests conducted on slotted hole connections is presented as well.

2.2 Experimental and theoretical studies on slotted hole, single plate shear, single angle and double angle connections

Steel angles are often used as connecting elements to transfer shear between the beams and columns in steel structures. Beam-to-column shear connections can use either one or two angles and can either be bolted or welded. Single angle and double angle

connections are often designed as flexible connections as they are assumed in design to act as pin connections that possess no rotational restraint. Over the past few decades, extensive research has been conducted on single and double angle beam-to-column connections. However, most of the research has focused on the moment vs. rotation behaviour and the rotational restraint developed in these connections, rather than the shear capacity. This section summarizes on single and double angle shear connections and connections with shear plates. Both connections with circular holes and slotted holes are reviewed.

2.2.1   Double Angle Connections

Rathbun (1936) was one of the first researchers who conducted tests on beam-to-column steel connections. The main objectives of his research were to investigate the rotational restraint on various types of riveted beam-to-column connections, and to apply the test results on the existing analysis methods, including slope deflection and moment distribution. He obtained 18 moment vs. rotation curves from 18 test specimens. Seven of these tests were conducted on double angle riveted connections. Elastic properties for each type of connection with different geometry were derived from the experimental moment vs. rotation curves. The elastic and rotational properties of the test connections were incorporated into analysis methods.

Munse *et al*. (1961) conducted four tests on both riveted and bolted beam-to-column connections. The work focused on the moment vs. rotation characteristics, moment resisting capacity, position of center rotation, slip and shear deformation of connections, and deformation of fasteners. The angles from three of the specimens were connected to the supporting column flange with ASTM A325 bolts and to the beam web by rivets of ASTM A141 materials. The angles of the remaining specimen were connected to the beam and column flanges with rivets. It was observed that failure of double angle web connections was mainly due to flexure of the angles rather than failure of bolts or rivets. The tests showed that the behaviour of double angle web connections was independent of the moment-to-shear ratio. Moreover, it was found that standard or flexible connections, which are assumed to behave as hinged connections, provide some rotational restraint.

In order to verify the significant increase in allowable bolt bearing stress in CSA standard S16.1–74 and in the Specification for Structural Joints Using ASTM A325 or A490 Bolts (RCRBSJ, 1976), Birkemoe and Gilmor (1978) conducted two tests on double angle shear connections: one test on a coped beam and one test on an uncoped beam. The test specimens consisted of a W410x67 beam and L102x89x9.5 angles. The beams were made of G40.21 300W steel. Two failure modes were observed: bearing failure and edge distance rupture was observed in the uncoped beam and tension and shear block failure was observed in the coped beam. These tests revealed that tension and shear block failure, which involves a combination of tension fracture and shear failure, could be more critical than bolt bearing failure in coped beams. The capacity of the coped beam was reduced by 24% compared to its full-flange counterpart. A strength prediction model was proposed that combined the tensile resistance along the net tension area at the bottom bolt hole and the shear resistance of the web along the net shear area. The proposed model showed reasonable agreement with the test results.

Yura *et al.* (1982) completed nine tests on beam web shear connections. The objective of the test program was to verify the provisions of the 1978 AISC Specification for edge distance, end distance and bearing stresses on bolted beam web connections. In this series of tests, the connections were subjected to shear only. The test program was conducted on W460x89 beams of grade ASTM A36 steel. Coped and uncoped beams, single and double line of bolts, and circular and slotted holes (the slots were located in the beam web) were incorporated in the test matrix. Number of bolts, bolt pitch, end and edge distance were investigated. The specimens were fabricated with three or five ASTM A325 3/4 in. bolts. They found that an increase in end distance from 25 mm to 50 mm resulted in an increase in capacity of 16%. Connections with two lines of holes had less strength that expected.

Ricles and Yura (1983) extended the work of Yura *et al.* (1982) by completing eight additional tests on double angle connections. The additional test specimens were two-line connections and all specimens, except for one, were fabricated with a coped beam. The same size and grade of steel beams as used by Yura *et al.* (1982) were used for the additional tests, except that four specimens were from a different heat of steel. Although an increase in beam web edge distance from 25 mm to 50 mm resulted in an

6

increase in capacity of 18%, a similar increase in end distance resulted in an increase in capacity of only 9%.

2.2.2   Single Angle and Single Plate Shear Connection

Lipson (1968) presented the results of an early study on single angle and single plate framing connections. He investigated three types of connections: single angle bolted to both the beam web and the supporting member, single vertical plate welded to the supporting member and bolted to the beam, and single angle welded to the supporting member and bolted to the beam. All bolts were ASTM A325 3/4 in. diameter bolts and all welds were made using E60 and E70 SMAW electrodes. The parameters investigated were: number of bolts, angle thickness, gauge distance, angle leg size and loading condition. The connections were tested under combinations of vertical shear and moment. The author's interest was on the behaviour of connections under working loads, maximum rotation capacity, and a consistent factor of safety and to determine whether the connections can be treated as flexible connections. His work demonstrated the feasibility of the three types of connections.

Lipson (1977) later examined the behaviour of welded and bolted single angle connections. Five series of tests, consisting of 43 tests in total, were conducted. The angles were bolted to the beam with 2 to 12 bolts and welded to the column. All the connections were loaded and rotated to 0.024 rad to simulate actual service conditions, in which the beam ends rotate under the action of the applied loads. The test specimens were subjected to monotonic loading up to 2.5 times the working load of the bolts permitted by the AISC and CSA steel design standards in 1969 for designing steel structures. The moment vs. rotation characteristics were obtained for each test. The results showed that the factors of safety for the bolts and welds were greater than 2.5 and the rotation of 0.024 rad could be achieved in all connection sizes. For the connections under cyclic load, the hysteretic loop were stable for at least three cycles at 2.5 times the allowable working load permitted by AISC and CSA steel design standards in 1969.

Richard *et al.* (1980) investigated the moment vs. rotation characteristics of single plate shear connections. The research program consisted of 126 single bolt, single shear

7

load vs. deformation tests with different bolt diameter, plate thickness, end distance and steel grade. A finite element analysis, which used the results of single bolt shear tests, was conducted and used to develop theoretical moment vs. rotation curves for single plate shear connections. The finite element analysis was validated from results of five full-scale tests on single plate shear connections. Although the finite element analysis results showed good agreement with the test results, the connections were not loaded to their maximum capacity and consequently, the ultimate limit state was not identified. A design procedure was proposed to account for the moment resistance of single plate shear connections.

Hormby *et al*. (1984) later extended the work by Richard *et al*. (1980) to include connections with slotted holes on shear tab connections. Of eight tests conducted on shear tab connections, six were on test specimens with slotted holes. The primary objective of the test program was to investigate the effect of slotted holes and off-axis bolt groups (centre of gravity of bolt groups does not coincide with the central axis of the beam) on the beam eccentricity, defined as the distance from the location of zero moment along the beam to the connection. The beam was loaded at midspan and beam eccentricity was measured using strain gauges mounted on the beam flanges at different loading stages. Tests conducted on connections with circular holes and slotted holes with pretensioned bolts showed similar behaviour. It should be noted, however, that the tests were conducted at load levels that did not cause slip in the bolted joints.

Astaneh *et al*. (1989) reported the results of five tests on shear tab connections conducted to full capacity of the connection. All the test specimens were prepared with circular holes and the connections were loaded in shear and controlled rotation. All the connections failed by rupture of bolts in shear.

Three cyclic tests on single plate shear connections were conducted by Crocker and Chambers (2004). The tests were conducted to determine the maximum deformation demand on bolts in single plate shear connections under cyclic rotation. The test specimens, which consisted of a single plate shear connection at the end of a 4 m long cantilever beam, were subjected to bending moment and minimal shear. Connections with three, four and six bolts were tested. The maximum imposed rotation on the

connection was 0.06 rad. Of the three tests, only the six-bolt connection failed by bolt rupture. The connections with three and four bolts did not fail after reaching the specified connection rotation. The authors suggested using a value of 8.6 mm as the limiting value of deformation for ASTM A325 bolts in single plate shear connections.

2.2.3 Connections with Slotted Holes

2.2.3.1 Lap Joints with Slotted Holes

Allan and Fisher (1968) conducted 21 tests on standard, oversized and slotted hole double lap joints. The test program was designed to investigate the effect of oversized and slotted holes on the slip resistance and ultimate strength of bolted joints. The specimens were made of four plies of 1 in. steel plates of grade ASTM A36 steel, connected by two lines of 1 in. ASTM A325 bolts with a pitch of 133 mm (5 ¼ in.). Slot lengths equal to 2.5 times the bolt diameter were used that were either oriented parallel or transverse to the applied load. The plates with slotted holes were placed in the two inner plies, covered with the outer plates. The bolts were installed using the turn-of-nut method. All of the test joints were tested in tension. Of 21 specimens, 15 were designed as slip-critical joints, including the joints with slots parallel to the applied load. The slip behaviour of the test specimens was observed and the tests were stopped when the joints went into bearing. The remaining six specimens were designed to carry load in bearing and were tested to their ultimate capacity. Bolt pretension was measured in six specimens and the pretension was monitored over time. Oversized or slotted holes did not affect the pretension over time following installation. All test specimens with slotted holes placed perpendicular to the line of action of the load did not show a reduction in tensile strength of the plate or the shear strength of the bolts.

Wald *et al*. (2002) reported the results of 73 tests on double lap joints to determine the bearing resistance, stiffness and ductility of cover plates with transverse slotted holes of different lengths: standard size holes (bolt diameter+2 mm), short slots (diameter+6 mm), long slots (up to 2.5 times the bolt diameter), and extra long slots (up to 3.5 times the bolt diameter). Based on the observed test results the researchers proposed a strength reduction factor β for slotted holes. Different reduction factors were

recommended for different slot lengths: 0.9 for short slotted holes, 0.7 for long slots, and 0.6 for extra long slots. This reduction factor was obtained as the ratio of the measured capacity for the slotted hole joint to the capacity of the joint with circular holes.

2.2.3.2 Single and Double Angle Connections with Slotted Holes

As mentioned previously, Yura *et al*. (1982) conducted eight tests on double angle connections, including three connections with slotted holes in the beam web. The authors found that the slotted hole connections showed about 20% less capacity compared to connections with standard circular holes.

Bergson and Galambos (1998) conducted an experimental investigation of the strength and behaviour of single angle bolted shear connections with short slots. Six full-scale connections were tested and the observed failure mode consisted of overall connection twisting, which was influenced by the bracing condition, tension and shear block failure in the beam web, and fracture of the angle. The limit states checked for strength prediction consisted of bolt failure, bearing failure of the supported beam web, yielding of the angle, fracture of the angle and formation of a plastic hinge in the beam. The capacities computed from these limit states were compared to the ultimate capacity of the test specimens. It was noted that all of the test connections reached a higher capacity than expected based on the calculations. In addition, they were not able to predict the failure mode accurately. All the test specimens were expected to fail in bearing of the web when none of them did. The effect of slotted holes on single angle connections could not be clearly identified. Both the failure mode and the test capacity could not be predicted accurately using the current design specifications.

As described previously, Franchuk *et al.* (2002) conducted five tests on single angle beam-to-column connections with slotted holes in the angles. Three-bolt and four-bolt slotted hole connections were tested without plate washers on the outer plies. The four-bolt connections failed by shear rupture of the net area in the leg of the angle connected to the beam, while the three-bolt connections failed by tearing of bottom end distance of angle and top edge distance of beam web, followed by severe tilting of the middle bolt. Tilting of the middle bolt was not expected. Bolt pull-out was not observed in any of the tests.

2.2.3.3 Single Plate Shear Connections with Slotted Holes

Hormby *et al*. (1984) also investigated the effect of slotted holes on the moment resistance of single plate shear connections. For the case where the bolts were pretensioned, the moment resistance of the connections with slotted holes was the same as the resistance of joints with circular holes.

2.3 Summary and Conclusions

A review of the literature has shown that the research on single and double angle connections mainly focused on the moment vs. rotation behaviour of connections. Many test programs did not investigate the behaviour up to the ultimate capacity of the joint. No research programs reported in the literature on single and double angle connections provide comprehensive tests to assess the behaviour of joints with slotted holes in the outer plies. CSA–S16–01 and AISC 2005 require that long slots be covered with plate washers that cover the slots entirely. Although only few tests on connections with slotted hole connections without plate washers have been conducted, there is no evidence that the bolts might have the tendency to pull-out of the joint. However, the number of tests on this type of joint is insufficient to draw definite conclusions. Moreover, the effect of plate washers on the behaviour of the connections with long slots in the outer plies is not well identified. More research is therefore required to study the strength and behaviour of connections with slotted hole in the outer plies.

3 Experimental Program

3.1 Introduction

A review of the literature has indicated that test data on slotted hole shear connections are scarce and the behaviour of such connections is not well understood. Therefore, the main objectives of this research program are to investigate the strength and behaviour of slotted hole shear connections, to increase the pool of available experimental data, and to assess the ability of current prediction models to predict the failure mode and strength of these connections. A description of the test program, the test-setup, instrumentation, specimen installation, testing procedure and ancillary tests is presented in the following.

3.2 Test Specimens Designation

The specimens used in this test program consisted of 3.6 m long wide flange beams with connections fabricated at both ends. Single and double angle shear connections were investigated. The test specimens were designated by an alphanumeric identifier. The first two characters consist of either 1L or 2L to indicate whether the connection is a single angle or a double angle connection. This is followed by a number that designates the test number within each of the two groups of tests. The letter 'a' following the specimen designation indicates the single angle specimen had pretensioned bolts connecting the angle to the column. The double angle specimens with letter 'a' after the designations consisted of angle section L152x102x9.5 with the larger size leg connected to the supporting column, while the remaining double angle specimens consisted of angle section L102x102x9.5. The capital 'E' in the designation of test specimen 1L2aE indicates that the test specimen was fabricated with a larger end distance of 47 mm at the bottom end of the angle compared to the other test specimens, which were fabricated with the minimum end distance. Three additional tests were carried out to investigate the effect of end distance and edge distance on the capacity of the angle leg connected to the column. These test specimens were identified as 1L12, 1L13 and 1L14.

The as-built dimensions of all the connections are presented in Table 3-1. Variables specified in this table are defined in Figure 3-1. The nominal dimensions for all connections are illustrated in Figures 3-2 and 3-3 and 'w', listed in column (24) of Table 3-1, is the beam web thickness. All bolt holes in the beam web were drilled to a diameter 2 mm (1/16 in.) larger than the bolt diameter. The long slots on the angle were sub-punched and reamed to the desired dimension. The short slots and circular holes on the angles were punched to the required diameter. The test matrix summarizing the parameters investigated in this test program is shown in Table 3-2. The test matrix for specimens 1L12, 1L13 and 1L14, used to investigate the angle leg connected to the column is shown in Table 3-3.

3.3 Full-scale Test Setup

A test apparatus similar to the one used in an earlier test program (Franchuk *et al*., 2002) was used to test full-scale shear connections under controlled end rotation. A diagram of the test setup is illustrated in Figure 3-4, and a photograph of the overall test setup is shown in Figure 3-5. The setup was designed to test a beam-to-column connection under shear, with controlled rotation. The beam was connected to a reaction column with either a single or double angle shear connection. Each angle was bolted to the reaction column with two 1 in. ASTM A325 bolts, in either a snug-tight or pretensioned condition. The single angle specimens identified with the letter 'a' in their designation were installed with pretensioned bolts to the column. The other single angle connections were installed with bolts to the column in a snug-tight condition. The purpose of pretensioning the bolts on the column side in some single angle specimens was to reduce the twist of the connection about the axis of the beam in the connections. All the double angle connections were installed with bolts connecting to the reaction column in a snug-tight condition. The beam was connected to the angle with three ASTM A325 bolts.

For the tests with an imposed beam end rotation as a variable, the rotation was controlled by adjusting the support hydraulic actuator at the end opposite to the test connection. A knife-edge was placed between the beam and the hydraulic actuator to simulate a simple support and a load cell was used to measure the reaction force.

13

Figure 3-6 shows a photograph of the support at the beam end opposite to the test connection.

A vertical load was applied to the beam at approximately 400 mm from the connection with a 890 kN hydraulic actuator. A spherical bearing assembly was used to allow rotation in the plane of the beam web and allow free rotation about the axis of the beam. A roller bearing was also used to prevent unwanted displacement restraint along the axis of the beam. A diagram showing the section of test frame at the load point is illustrated in Figure 3-7. A photograph illustrating the various elements of the loading frame is shown in Figure 3-8.

Lateral supports were provided at two locations along the beam length. The load point was laterally braced near the top flange with two pairs of rollers mounted on the reaction frame columns and sliding on two pairs of HSS 51x25x3.2 clamped to the beam near the load point, as shown in Figure 3-9. This simulates a beam element in a floor system where the top flange is often laterally braced by the floor slab. At the reaction end (end opposite to the test connection) of the beam, the top flange and bottom flanges were supported by rollers riding on adjacent support columns as illustrated in Figure 3-10. A rubber mallet was used to tap on the lateral supports to release any friction forces developed between the test specimen and the lateral supports during the tests. Photographs of the lateral bracing system at the loading frame and the reaction frame are shown in Figures 3-11 and 3-12, respectively. In order to prevent web buckling at the load point, bearing stiffeners, consisting of a pair of HSS 76x51x4.8 clamped to the web of the beam as shown in Figure 3-11. A close-up of the bracing system and roller assembly at the reaction frame is depicted in Figure 3-13.

3.4   Instrumentation

Vertical and lateral displacements, end rotation, applied load and reaction force were measured electronically during the test. Figure 3-14 presents a summary of the instrumentation used in the tests. Cable transducers were used to measure the vertical displacement at the bottom flange under the load point and to measure the vertical displacement at the reaction actuator. The vertical displacements of the beam at the load

point were also measured at regular load intervals using a dial gauge to check the measurements obtained using electronic transducers. A 890 kN load cell was used to measure the force applied with the load actuator. A second load cell was placed on top of the reaction actuator to measure directly one of the two reaction forces. The connection reaction force was obtained by subtracting the measured end reaction from the applied load. Friction at the lateral supports was assumed negligible. At the connection, vertical and lateral displacements of the angle and the beam were measured. The vertical displacement of the angle was measured using two LVDTs installed just above and below the connection (deflections Δ_5 and Δ_6 in Figure 3-15). Two cable transducers (Δ_7 and Δ_8 in Figure 3-15) were used to measure the top and bottom flange vertical displacement of the beam. To assess the angle of twist of the angle and the beam, the lateral displacements of the angle and the beam were measured independently using four LVDTs ($\Delta_1, \Delta_2, \Delta_3$ and Δ_4 in Figure 3-15). The angle of twist of the connection was computed from the difference between the top and bottom lateral displacements and the distance between the measurement points. A rotation transducer was also installed near the connection on the beam web to provide an additional measurement of the beam end rotation.

The measured displacements were recorded at regular intervals during the test using an electronic data acquisition system.

3.5   Specimen Installation

The beam was first positioned on the knife-edge and load cell assembly at the end of the beam opposite to the test connection. The beam was centered on the load cell to ensure accurate measurement of the reaction load.

Test angles were loosely attached to the column using two ASTM A325 1 in. high strength bolts in each angle. For the thin single angle specimens fabricated with L102x102x6.4 (1LA, 1LB, 1LAa and 1LBa), an additional half-inch thick doubler plate was placed on the angle leg connected to the column to minimize the shear angle distortion during loading.

The position of the beam along its axis was adjusted so that the holes of the beam were centered with the slots in the shear angle. The bolts in the angle to the beam joint were installed and tightened to a snug-tight or pretensioned condition, depending on the required test condition. In the case of single angle connections, the bolts in the connection were installed with the head on the angle side and the nut on the beam side, with a single standard hardened washer placed between the beam and the nut. All the plate washers used in the current test program were 9.5 mm thick, which satisfies the requirement of 8 mm minimum thickness for plate washers in CAN/CSA–S16–01 and AISC 2005. A spherical bearing and roller assembly was then placed on the beam under the load actuator. The beam was then braced laterally close to the load point with two HSS 51x25x3.2 clamped on either side of the beam and rollers installed on the reaction frame column as depicted in Figure 3-11. The roller and HSS assembly provided lateral restraint to the top flange without restraining the vertical displacement of the beam.

3.6 Test Procedure

Prior to each test, the surface of the test specimens was whitewashed in the connection area in order to visually detect the onset of yielding. The test connections were loaded quasi-statically under stroke control. Static load readings were recorded at every 100 kN in the ascending part of the loading curve and at approximately every 3 mm displacement of the connection in the remaining part of the loading curve. For the test conducted under large end rotation, a rotation of 3.5°, measured using the rotation transducer, was imposed at the connection end of the test specimen by adjusting the end reaction actuator. The beam end rotation angle was maintained at 3.5° during the tests by regularly adjusting the end support reaction actuator.

3.7 Ancillary Tests

In order to obtain the material properties of the beams and angles in the connection, tension coupon tests were conducted on both the beam web and angle sections. The coupons were fabricated in accordance to ASTM A370 (ASTM, 1997). Sheet-type coupons were cut from both angle and beam sections. Typical coupon dimensions are shown in Figure 3-16. The cross-sectional dimensions of each coupon

16

were measured at various locations along the final gauge length. The average area, which was taken as the representative coupon cross-sectional area, was computed from the measured dimensions. The strain was recorded using a 50 mm gauge length extensometer. A pair of strain gauges was mounted on one coupon from each group of thickness to verify the extensometer readings.

The stress was computed from the recorded machine load and the as-measured initial cross-sectional area. During each coupon test, two values of static yield stresses were obtained along the yield plateau. The testing machine was stopped for about five minutes along the yield plateau and the load was recorded after each pause. The mean static yield was taken as the average of the two values recorded along the yield plateau. The upper yield strength was taken as the highest point on the stress versus strain curve, just before the yield plateau. The lower yield strength was taken as the lowest point on the stress vs. strain curve within the yield plateau. In contrast to the static yield strength, the lower yield is obtained under dynamic loading condition. Static stress values were also obtained at ultimate. The rupture stress and rupture strain were obtained from the stress versus strain curve at the time of fracture. The strain-hardening strain was taken as the strain where the stress started to increase after the yield plateau. Strain at ultimate stress was obtained where the maximum load was reached. After each tension coupon test, the two fractured ends of the coupon were fitted together and the gauge length was measured. The reduced of area at the fractured location was also measured to obtain the true stress at rupture. The reduction area was computed from the as-measured original area and the reduced area. The strain rates used in the elastic, yield plateau and strain-hardening ranges were approximately $1500\,\mu\varepsilon/\min$, $8000\,\mu\varepsilon/\min$ and $60000\,\mu\varepsilon/\min$, respectively.

3.7.1 Beam

Three sheet-type coupons were obtained from each web plates from the midspan after the experimental program. The coupons were oriented perpendicular to the axis of the beam so that the material properties in the direction of loading at the end connection could be assessed. Coupon tests were conducted on eight of the beam sections that failed at the web. The typical location of coupons on the beam web material sample is shown in

Figure 3-17. The plate material sample shown in the figure was cut at the midspan of the beam to assure that no yielding has taken place. The specified grade of steel for the beams was CAN/CSA–G40.21 350W (CSA, 1998).

3.7.2   Angle

Additional lengths of angle of each size were ordered from the same heat as the ones used for the test specimens. Three sheet-type coupons were fabricated and tested from each piece of angle. The orientation of the coupon is the same as the direction of loading. The coupons were oriented along the length of the angle as shown in Figure 3-18. The grade of all the angle sections was CAN/CSA–G40.21 300W (CSA, 1998).

Table 3-1 As-built Connection Dimensions

Test Specimen	Angle (refer to Figures 3-1a and 3-1b)															Beam (refer to Figures 3-1c and 3-1d)							
	e_{s1}	p_1	p_2	e_{s2}	e_g	d_{slot}	l_{slot}	t	e_{s3}	p_3	e_{s4}	e_{g1}	e_{g2}	d_{h1}	d_{h2}	E_s	S_1	S_2	E_g	D_h	D_c	L_c	w
(1)	(2)	(3)	(4)	(5)	(6)	(7)	(8)	(9)	(10)	(11)	(12)	(13)	(14)	(15)	(16)	(17)	(18)	(19)	(20)	(21)	(22)	(23)	(24)
1LA	24.1	102.0	102.1	25.7	24.5	20.6	31.2	6.59	50.1	152.0	51.9	36.4	36.3	26.8	26.9	26.1	101.3	101.6	25.4	20.7	34.9	75.5	7.32
1LB	31.0	102.2	102.0	32.4	33.5	27.7	40.4	6.55	58.0	151.9	58.0	36.7	36.6	26.8	26.8	32.1	100.8	100.9	30.8	26.5	36.1	81.7	6.91
1LAa	26.2	102.0	102.0	24.7	23.8	20.7	31.7	6.42	52.1	152.5	50.8	35.9	36.2	27.0	27.3	24.8	101.4	101.1	25.0	20.4	35.9	74.0	6.92
1LBa	33.5	102.4	101.6	31.6	33.9	28.9	45.0	6.39	58.9	152.3	58.3	36.4	36.4	27.2	27.2	32.4	101.1	101.6	32.0	26.9	36.1	81.9	6.92
1L1	32.0	75.7	76.2	32.5	30.2	25.6	55.0	9.88	31.8	151.7	32.9	37.1	36.9	26.6	26.8	58.4	76.0	75.8	30.4	23.8	–	–	7.21
1L2	31.4	101.4	102.2	33.2	28.8	24.3	55.1	9.63	57.5	152.4	59.7	36.4	36.7	27.1	27.2	62.6	99.9	102.4	29.1	23.7	–	–	6.98
1L3	32.0	101.6	102.0	32.9	30.1	24.7	55.0	9.83	58.1	152.0	59.4	37.5	37.1	26.8	26.9	65.8	100.6	101.7	28.6	23.5	–	–	8.98
1L4	31.0	101.5	101.8	34.2	29.4	25.1	54.8	9.66	57.5	152.3	59.6	36.6	36.9	27.0	26.9	61.1	101.9	101.3	29.0	23.7	–	–	7.05
1L5	30.8	101.5	101.8	34.4	29.6	25.5	54.8	9.59	57.3	152.7	60.0	36.3	36.5	27.1	27.4	62.0	102.4	101.9	29.7	23.9	–	–	7.02
1L6	30.9	101.8	101.7	34.6	29.7	25.7	54.8	9.69	56.6	151.9	59.8	36.5	36.2	26.7	26.7	61.9	100.9	102.1	30.6	24.1	–	–	7.08
1L7	32.0	76.7	77.1	32.3	30.4	25.7	55.0	9.94	32.8	151.8	32.2	36.3	36.5	26.8	26.7	57.5	76.3	77.0	29.3	23.8	–	–	7.09
1L8	31.8	75.0	76.2	32.8	30.4	25.9	55.0	9.90	31.8	151.9	33.2	37.0	36.8	27.0	27.1	29.7	75.6	75.4	30.3	24.1	35.9	78.9	6.91
1L9	31.4	102.1	102.0	33.5	30.3	23.7	28.3	9.63	57.5	151.8	59.2	36.0	36.1	26.7	26.8	61.7	101.6	101.4	29.5	23.9	–	–	7.06
1L10	31.7	76.2	77.1	34.5	29.8	24.6	28.6	9.59	32.9	152.2	32.8	36.5	36.5	26.7	26.8	60.2	74.8	74.7	30.0	23.5	–	–	7.26
1L1a	46.1	75.9	76.2	33.4	32.5	25.9	53.8	9.41	46.7	152.9	33.6	86.4	86.4	27.5	27.6	75.4	75.9	75.6	29.6	23.5	–	–	6.92
1L2a	46.1	101.6	101.4	34.0	27.5	24.9	55.1	9.46	72.7	152.2	59.3	86.0	86.2	27.1	27.2	75.7	100.9	101.3	29.5	23.6	–	–	7.21
1L2aE	48.6	102.3	102.0	46.3	33.5	25.2	53.6	9.51	74.4	152.1	73.3	86.2	86.1	27.3	27.2	75.1	101.9	102.0	29.6	23.6	–	–	7.32
1L3a	46.2	102.1	102.1	33.9	28.3	24.9	53.9	9.44	72.7	152.4	59.6	85.9	86.1	27.2	27.2	43.9	101.9	101.8	30.5	23.9	36.2	83.0	9.78
1L4a	45.9	102.0	102.0	33.7	27.8	25.5	54.6	9.39	72.9	152.7	59.8	86.3	86.3	27.5	27.6	76.3	101.0	100.9	30.2	23.6	–	–	7.22
1L5a	46.2	101.6	102.3	33.9	27.4	24.8	55.3	9.49	72.8	152.2	59.4	86.0	86.1	27.1	27.2	45.8	101.9	102.1	30.0	24.1	28.0	82.2	7.25
1L6a	46.5	101.7	101.7	34.3	27.8	25.0	55.0	9.51	72.9	152.8	59.7	86.0	86.4	27.4	27.7	46.2	101.9	101.5	29.4	23.9	29.3	82.5	7.22
1L7a	44.9	75.4	76.0	33.4	32.4	25.5	53.3	9.37	45.0	152.7	33.5	85.9	86.1	27.4	27.6	75.2	75.4	75.2	29.4	23.5	–	–	6.98
1L8a	46.2	76.5	75.8	33.6	32.7	26.0	53.1	9.45	46.9	152.4	33.3	86.1	86.4	27.4	27.7	45.0	75.1	76.0	29.9	23.5	36.7	79.4	6.89
1L9a	48.0	101.9	102.0	31.5	29.9	23.8	29.2	9.49	74.4	152.3	57.7	86.2	86.1	27.2	27.3	76.5	101.6	101.0	30.8	23.7	–	–	7.31
1L10a	46.6	76.0	76.1	33.5	31.6	23.8	28.5	9.53	32.0	153.0	33.2	79.5	79.7	27.3	27.5	76.1	75.5	75.2	30.9	23.6	–	–	6.92
1L11a	45.9	75.5	75.8	35.6	32.5	26.3	53.3	9.44	46.9	152.4	35.0	86.3	86.3	27.4	27.6	75.8	75.7	75.4	30.4	23.7	–	–	6.99

Note: All dimensions are in millimetres.

19

Table 3-1 As-built Connection Dimensions (cont'd)

Test Specimen	Angle (refer to Figures 3-1a and 3-1b)															Beam (refer to Figures 3-1c and 3-1d)							
	e_{s1}	p_1	p_2	e_{s2}	e_g	d_{slot}	l_{slot}	t	e_{s3}	p_3	e_{s4}	e_{g1}	e_{g2}	d_{h1}	d_{h2}	E_s	S_1	S_2	E_g	D_h	D_c	L_c	w
(1)	(2)	(3)	(4)	(5)	(6)	(7)	(8)	(9)	(10)	(11)	(12)	(13)	(14)	(15)	(16)	(17)	(18)	(19)	(20)	(21)	(22)	(23)	(24)
1L12	51.8	75.7	75.7	52.6	31.7	23.7	—	9.48	32.2	152.6	73.0	33.7	33.6	27.2	27.4	75.7	75.5	75.3	30.2	23.6	—	—	6.93
1L13	52.4	76.1	76.0	52.8	31.9	23.7	—	9.49	31.9	152.4	73.0	50.2	50.0	27.0	27.1	75.6	76.0	75.7	29.7	23.6	—	—	6.85
1L14	52.2	75.8	76.1	52.4	32.7	23.7	—	9.46	32.1	76.2/76.5[1]	73.3	33.0	33.0	27.3	27.3	75.5	75.3	75.4	30.6	23.5	—	—	6.93
2L1	31.9	75.9	75.7	33.2	29.4	24.4	55.3	9.72	32.2	151.9	33.2	36.9	36.8	27.0	27.0	57.4	75.8	74.7	29.7	23.8	—	—	7.04
	32.4	76.3	76.0	32.2	29.4	24.7	55.8	9.87	32.4	152.3	32.2	36.5	36.4	26.8	26.7	—	—	—	—	—	—	—	—
2L2	31.9	101.6	102.1	33.1	30.1	25.3	55.1	9.83	57.5	152.1	58.7	37.1	37.3	26.9	27.0	62.0	100.9	101.1	29.8	23.7	—	—	7.10
	31.8	101.8	102.1	32.6	29.8	25.3	55.0	9.77	59.0	151.9	58.6	36.9	37.0	26.9	27.0	—	—	—	—	—	—	—	—
2L3	30.5	102.5	101.5	33.8	29.3	25.2	55.6	9.70	57.5	152.0	59.2	35.9	35.9	26.9	27.1	65.7	101.6	101.2	30.4	23.6	—	—	9.29
	31.6	102.2	101.7	33.6	30.0	25.2	55.3	9.71	58.3	152.0	59.5	36.8	37.0	26.9	27.0	—	—	—	—	—	—	—	—
2L4	31.6	101.6	101.7	33.3	29.7	25.2	55.1	9.82	57.6	152.0	59.0	37.2	36.8	27.1	27.1	62.0	102.0	101.8	29.7	24.3	—	—	7.03
	31.7	101.9	102.0	32.6	29.5	25.2	55.1	9.71	57.7	151.7	58.5	37.0	36.9	27.1	27.0	—	—	—	—	—	—	—	—
2L5	32.7	101.9	102.1	31.9	29.6	25.3	55.1	9.86	58.7	152.1	57.8	36.7	36.7	26.9	26.9	62.4	100.4	101.4	30.6	24.1	—	—	7.01
	30.5	102.5	101.5	33.8	29.3	25.2	55.6	9.70	57.5	152.0	59.2	35.9	35.9	26.9	27.1	—	—	—	—	—	—	—	—
2L6	32.0	75.5	75.6	33.2	29.6	25.1	55.9	9.77	25.8	146.1	32.8	31.5	36.6	26.3	26.5	61.0	76.0	75.5	30.3	23.6	—	—	6.98
	31.8	75.3	76.5	33.5	29.7	24.8	55.4	9.80	31.9	151.9	33.3	36.8	36.9	26.6	26.8	—	—	—	—	—	—	—	—
2L7	32.4	76.6	75.9	31.7	30.2	25.8	55.0	9.79	32.2	151.6	32.4	36.9	36.9	26.9	27.1	28.6	74.8	74.4	29.4	24.0	35.9	75.7	6.87
	31.9	75.5	75.9	32.3	29.8	24.3	54.9	9.75	32.1	151.9	33.0	37.0	36.6	26.9	26.9	—	—	—	—	—	—	—	—
2L1a	33.6	76.1	75.9	31.6	28.2	25.5	54.3	9.44	33.3	152.7	32.0	80.1	79.5	27.7	27.4	60.7	76.2	75.7	30.5	23.5	—	—	6.87
	31.3	76.1	75.9	33.3	28.1	25.0	54.6	9.41	32.0	153.0	33.2	79.5	79.7	27.3	27.5	—	—	—	—	—	—	—	—
2L5a	33.5	102.2	102.2	31.3	28.2	25.7	54.1	9.39	59.7	152.6	57.8	79.9	79.8	27.6	27.3	60.6	101.5	101.5	30.4	23.6	—	—	6.93
	31.6	101.6	102.5	33.4	27.8	24.4	54.2	9.44	57.9	152.5	59.4	79.6	79.7	27.3	27.5	—	—	—	—	—	—	—	—
2L6a	33.6	76.1	76.5	31.0	28.9	25.9	54.3	9.48	33.4	152.8	31.6	79.8	79.7	27.5	27.4	60.6	75.8	75.9	30.0	23.6	—	—	6.92
	31.5	75.8	76.1	32.8	28.6	25.7	54.2	9.45	32.2	152.6	33.0	79.6	79.9	27.4	27.6	—	—	—	—	—	—	—	—
2L8a	31.5	102.2	102.0	33.7	28.4	25.9	53.8	9.38	57.9	152.7	59.5	79.3	79.8	27.4	27.5	29.8	101.8	101.9	30.2	23.7	30.5	78.1	6.93
	33.8	101.3	102.0	31.2	28.2	25.3	54.2	9.35	59.5	152.7	57.9	79.6	79.7	27.3	27.5	—	—	—	—	—	—	—	—

[1] Specimen 1L14 is fabricated with 3 bolt holes at the angle leg connected to the column. The numbers shown are the spacing between the three bolt holes.
Note: All dimensions are in millimetres.

Table 3-2 Test Matrix Used to Investigate Angle Leg Connected to Beam

Test Specimen	No. of Angles	Slot Length[1]	Plate Washer	Beam Web	Pre-tension	Bolt Pitch[2]	Torsion Brace	Beam Rotation[3]	Flange Cope	Angle	Beam
(1)	(2)	(3)	(4)	(5)	(6)	(7)	(8)	(9)	(10)	(11)	(12)
1LA [4]	1L	Long [6]	Yes	Thin	No	Large	No	No	Yes	A5	B5
1LB [5]	1L	Long [6]	Yes	Thin	No	Large	No	No	Yes	A6	B6
1LAa [4]	1L	Long [6]	Yes	Thin	No	Large	No	No	Yes	A5	B5
1LBa [5]	1L	Long [6]	Yes	Thin	No	Large	No	No	Yes	A6	B6
1L1	1L	Long	No	Thin	No	Std.	No	No	No	A1	B1
1L2	1L	Long	No	Thin	No	Large	No	No	No	A2	B2
1L3	1L	Long	No	Thick	No	Large	No	No	No	A2	B3
1L4	1L	Long	Yes	Thin	No	Large	No	No	No	A2	B2
1L5	1L	Long	Yes	Thin	Yes	Large	No	No	No	A2	B2
1L6	1L	Long	No	Thin	No	Large	Yes	No	No	A2	B2
1L7	1L	Long	No	Thin	No	Std.	No	Yes	No	A1	B1
1L8	1L	Long	No	Thin	No	Std.	No	No	Yes	A1	B4
1L9	1L	Short	No	Thin	No	Large	No	No	No	A3	B2
1L10	1L	Short	No	Thin	No	Std.	No	Yes	No	A4	B1
1L1a	1L	Long	No	Thin	No	Std.	No	No	No	C1	D1
1L2a	1L	Long	No	Thin	No	Large	No	No	No	C2	D2
1L2aE [7]	1L	Long	No	Thin	No	Large	No	No	No	C7	D2
1L3a	1L	Long	No	Thick	No	Large	No	No	Yes	C2	D3
1L4a	1L	Long	Yes	Thin	No	Large	No	No	No	C2	D2
1L5a	1L	Long	Yes	Thin	Yes	Large	No	No	Yes	C2	D2a
1L6a	1L	Long	No	Thin	No	Large	No	No	Yes	C2	D2a
1L7a	1L	Long	No	Thin	No	Std.	No	Yes	No	C1	D1
1L8a	1L	Long	No	Thin	No	Std.	No	No	Yes	C1	D4
1L9a	1L	Short	No	Thin	No	Large	No	No	No	C3	D2
1L10a	1L	Short	No	Thin	No	Std.	No	Yes	No	C4	D1
1L11a	1L	Long	No	Thin	No	Std.	Yes	No	No	C1	D1
2L1	2L	Long	No	Thin	No	Std.	No	No	No	A1	B1
2L2	2L	Long	No	Thin	No	Large	No	No	No	A2	B2
2L3	2L	Long	No	Thick	No	Large	No	No	No	A2	B3
2L4	2L	Long	Yes	Thin	No	Large	No	No	No	A2	B2
2L5	2L	Long	Yes	Thin	Yes	Large	No	No	No	A2	B2
2L6	2L	Long	No	Thin	No	Std.	No	Yes	No	A1	B1
2L7	2L	Long	No	Thin	No	Std.	No	No	Yes	A1	B4
2L1a	2L	Long	No	Thin	No	Std.	No	No	No	C1d	B1
2L5a	2L	Long	Yes	Thin	Yes	Large	No	No	No	C2d	B2
2L6a	2L	Long	No	Thin	No	Std.	No	Yes	No	C1d	B1
2L8a	2L	Long	No	Thin	No	Large	No	No	Yes	C2d	D2da

All bolts are 22.2 mm (7/8 in.) diameter unless noted otherwise.

All plate washers are 9.5 mm thick.

Notes: 1: Long slot length = 55 mm, short slot length = 28 mm

2: Large bolt pitch = 102 mm, standard pitch = 76 mm

3: Beam end rotation = 3.5° for specimens with imposed rotation

4: Bolt diameter = 19.1 mm

5: Bolt diameter = 25.4 mm

6: Slot length = 1.65 times bolt diameter

7: With bottom end distance of 47 mm

**Table 3-3 Test Matrix Used to Investigate the Angle Leg Connected to the Column**

| Test Specimen	Nominal Distances Top End e_{s3} (mm)	Edge e_{g1} (mm)	Angle	Beam	Number of bolts connected to column
(1)	(2)	(3)	(4)	(5)	(6)
1L12	32	32	C8	D1	2
1L13	32	50	C9	D1	2
1L14	32	32	C10	D1	3
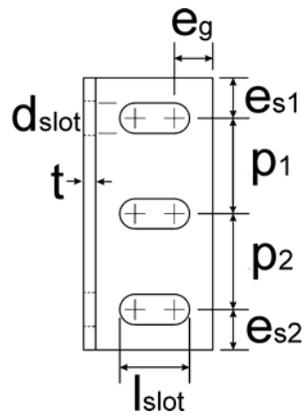
a) Typical Outstanding Leg of Angle
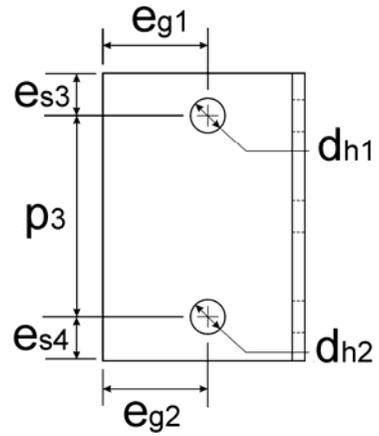
b) Typical Leg of Angle Connected to the Column
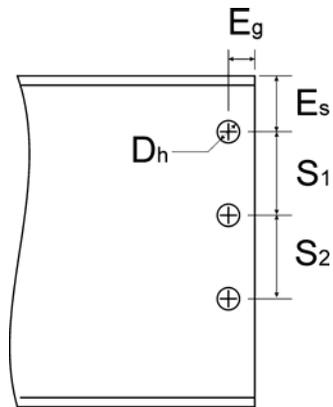
c) Typical Beam with Full Flange
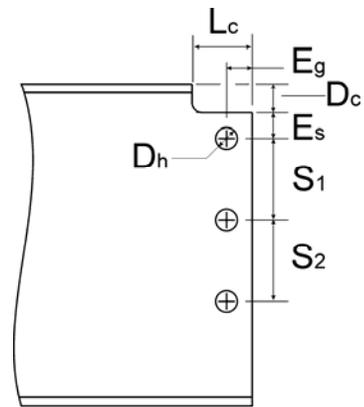
d) Typical Beam with Coped Flange

**Figure 3-1 Test Specimens Dimensions**

a) A1
Test 1L1, 1L7, 1L8,
2L1, 2L6, 2L7

b) A2
Test 1L2, 1L3, 1L4, 1L5, 1L6,
2L2, 2L3, 2L4, 2L5

c) A3
Test 1L9

d) A4
Test 1L10

e) A5
Test 1LA, 1LAa

f) A6
Test 1LB, 1LBa

Notes:
- A1 to A4 are fabricated from L102x102x9.5
- A5 and A6 are fabricated from L102x102x6.4
- C1d and C2d are fabricated from L152x102x9.5

g) C1d
Test 2L1a, 2L6a

h) C2d
Test 2L5a, 2L8a

Figure 3-2 Nominal Angle Dimensions

24

j) C1
Test 1L1a, 1L7a, 1L8a, 1L11a

k) C2
Test 1L2a, 1L3a, 1L4a, 1L5a, 1L6a

l) C3
Test 1L9a

l) C4
Test 1L10a

n) C7
Test 1L2aE

p) C8
Test 1L12

Notes:
- C1 to C4 and C7 are fabricated from L152x102x9.5
- C8 to C10 are fabricated from L102x102x9.5

q) C9
Test 1L13

r) C10
Test 1L14

Figure 3-2 Nominal Angle Dimensions (cont'd)
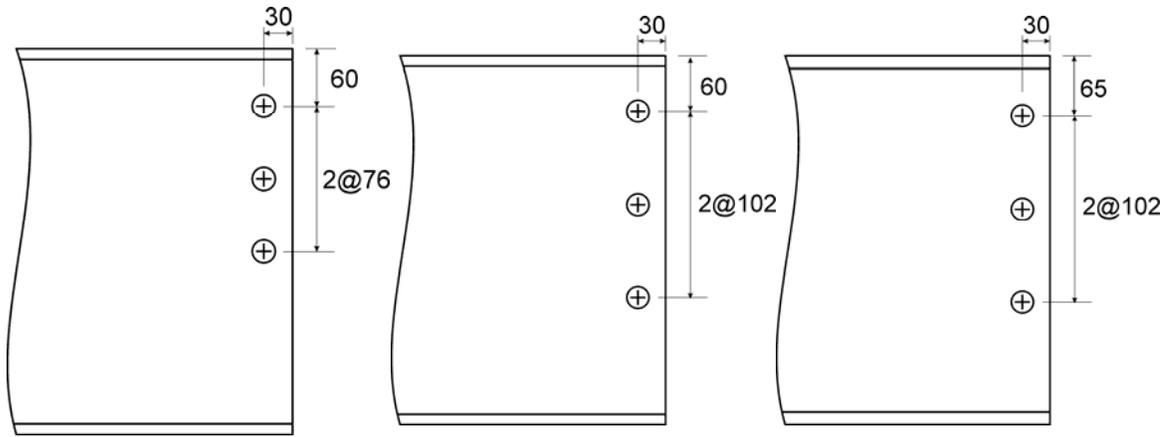
a) B1
Test 1L1, 1L7, 1L10, 2L1, 2L6, 2L7, 2L1a, 2L6a

b) B2
Test 1L2, 1L4, 1L5, 1L6, 1L9, 2L2, 2L4, 2L5, 2L5a

c) B3
Test 1L3, 2L3

d) B4
Test 1L8, 2L7

e) B5
Test 1LA, 1LAa
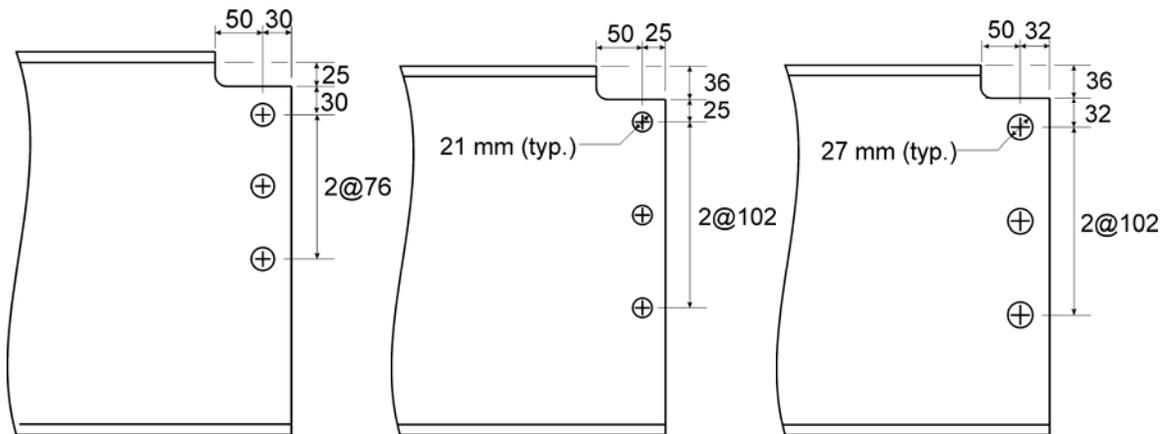
f) B6
Test 1LB, 1LBa

Notes: All dimensions are in millimetres
All hole diameters are 24 mm unless noted otherwise

Figure 3-3 Nominal Dimensions of Beam Connections
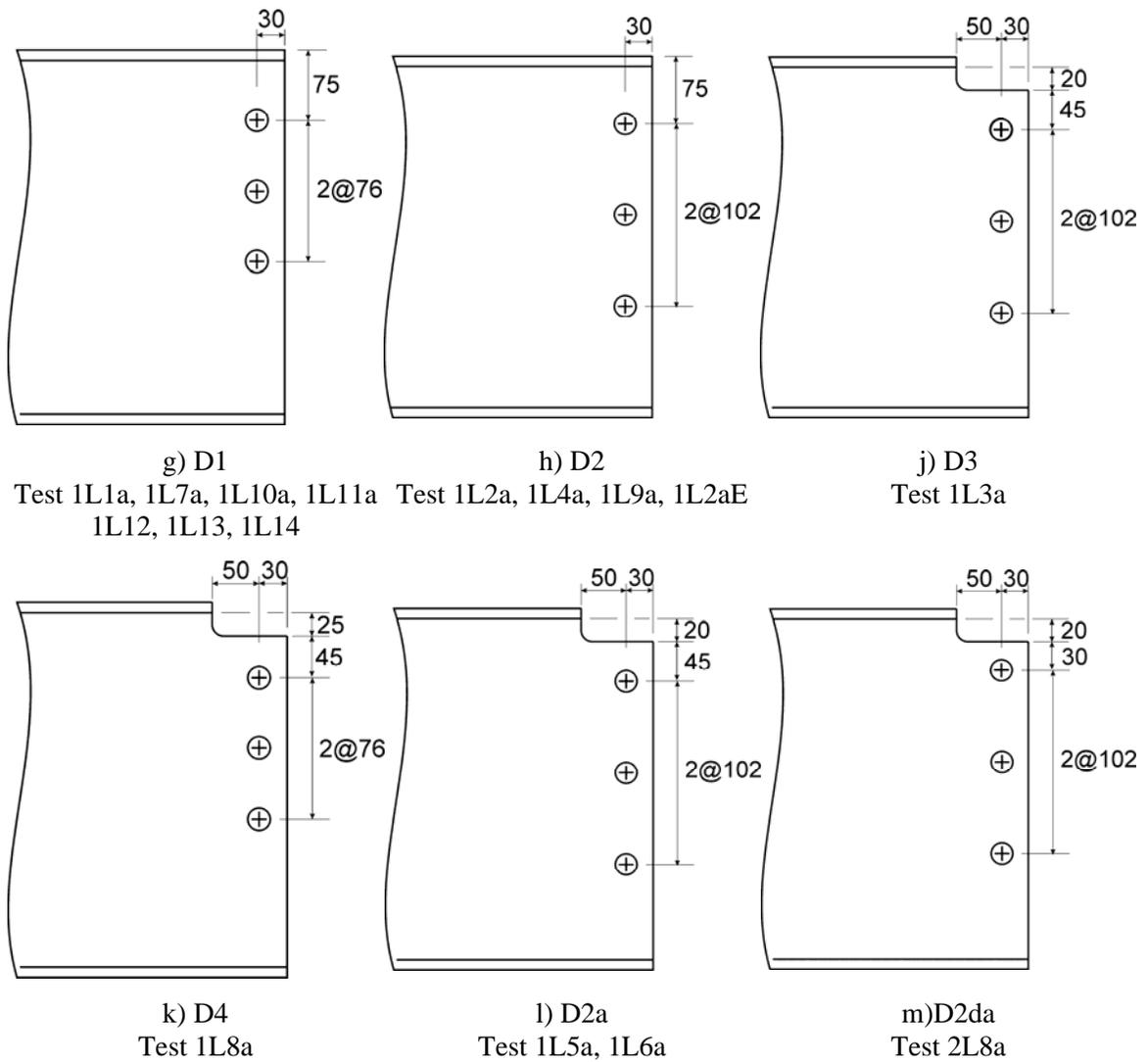
26

g) D1
Test 1L1a, 1L7a, 1L10a, 1L11a
1L12, 1L13, 1L14

h) D2
Test 1L2a, 1L4a, 1L9a, 1L2aE

j) D3
Test 1L3a

k) D4
Test 1L8a

l) D2a
Test 1L5a, 1L6a

m) D2da
Test 2L8a

Notes: All dimensions are in millimetres
        All hole diameters are 24mm unless noted otherwise
        All beams are W410x46 except B3 and D3
        B3 is a W410x74
        D3 is a W410x100

**Figure 3-3 Nominal Dimensions of Beam Connections (cont'd)**

27
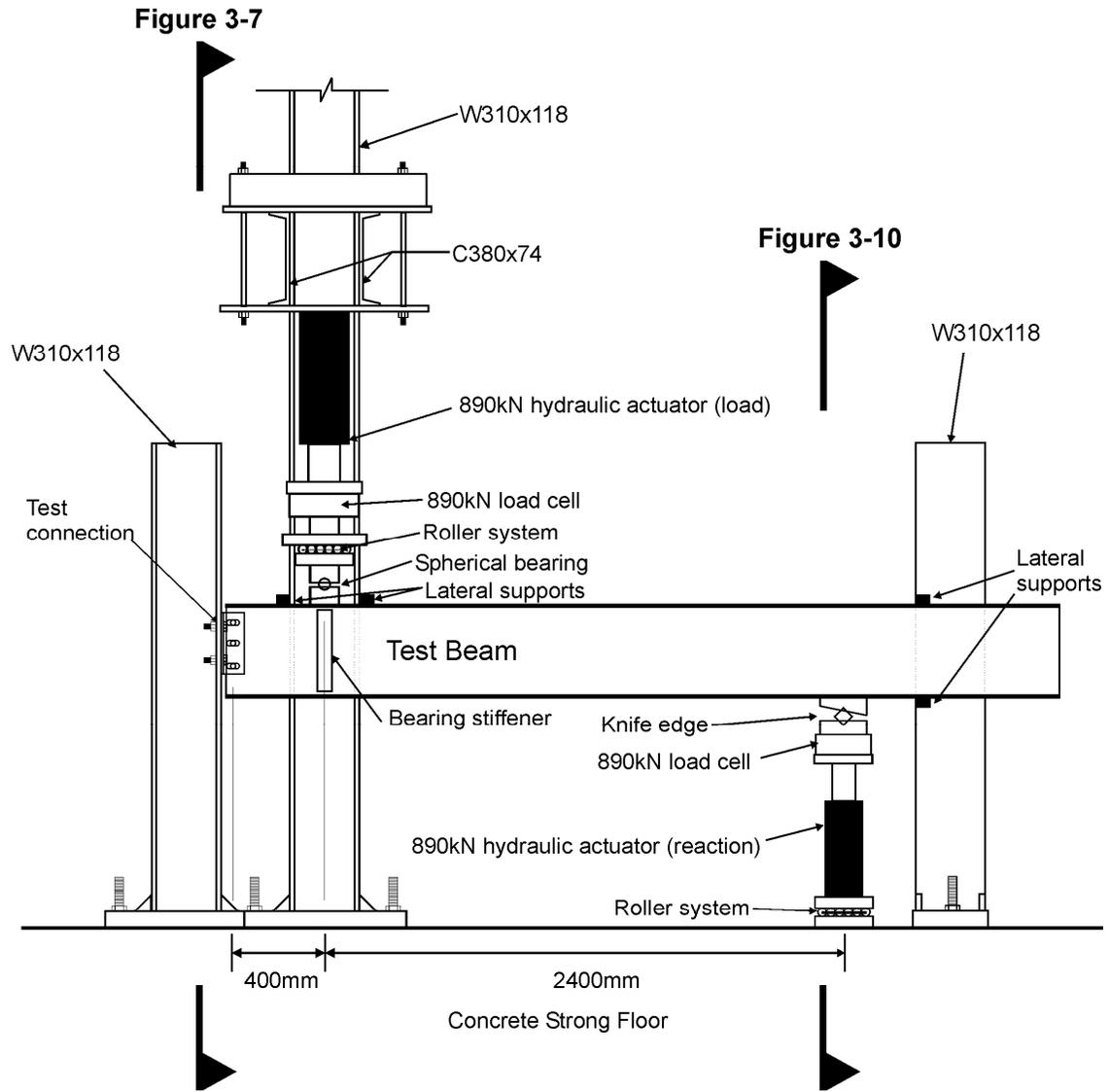
Figure 3-4 Elevation View of Test Setup
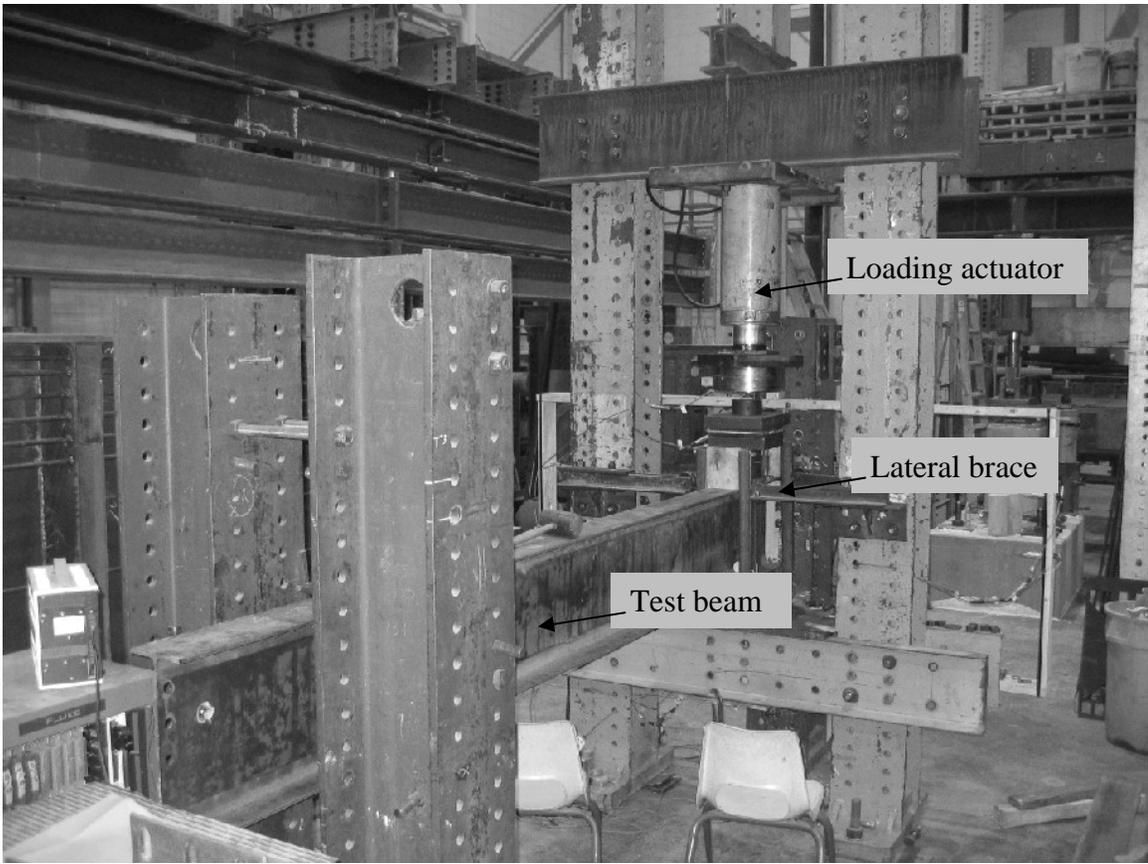
Figure 3-5 Overall Test Setup

Knife edge

890kN load cell

890kN reaction actuator

Cable transducer for support displacement monitoring.
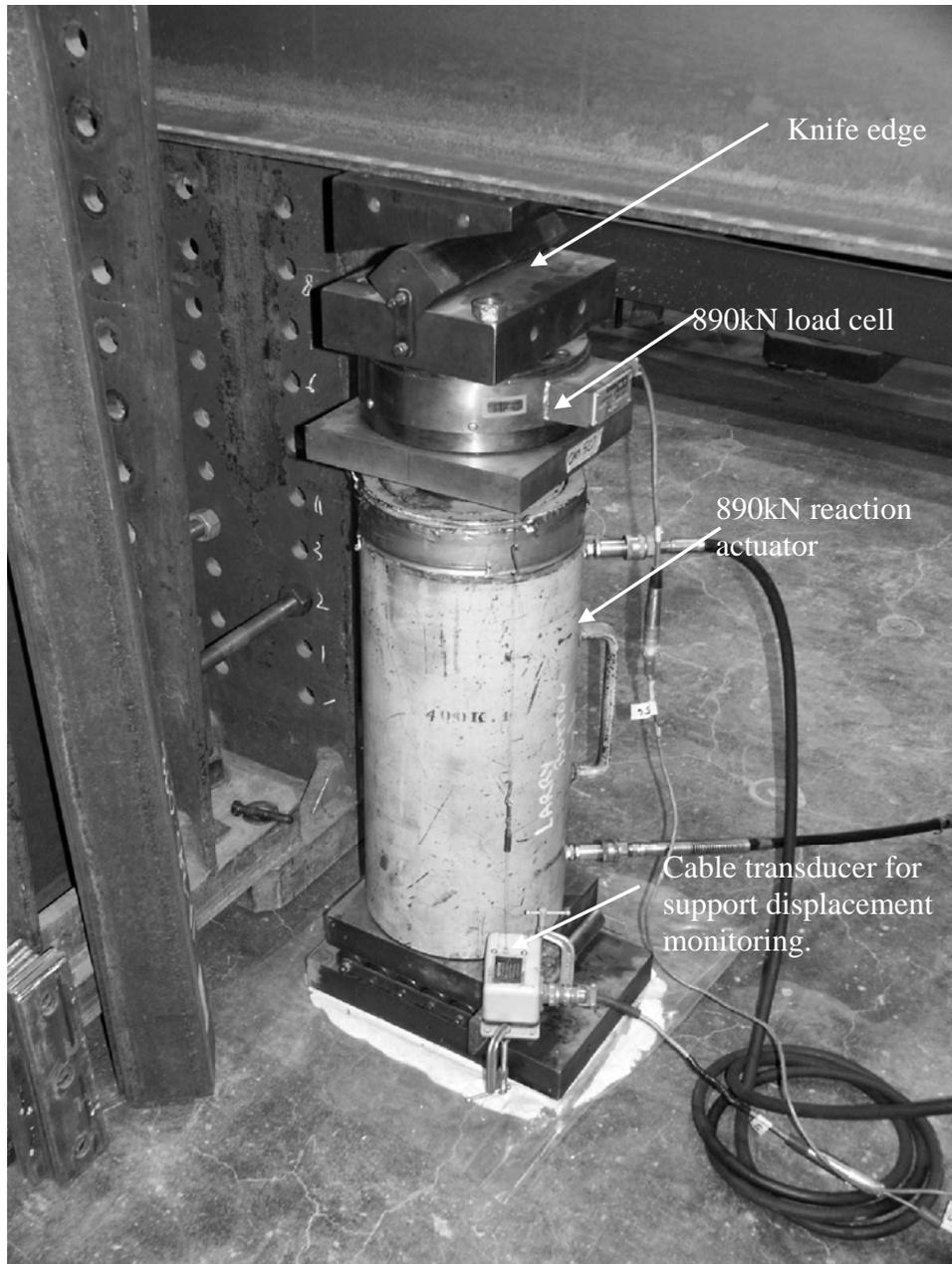
Figure 3-6 Reaction Actuator with Load Cell and Knife Edge
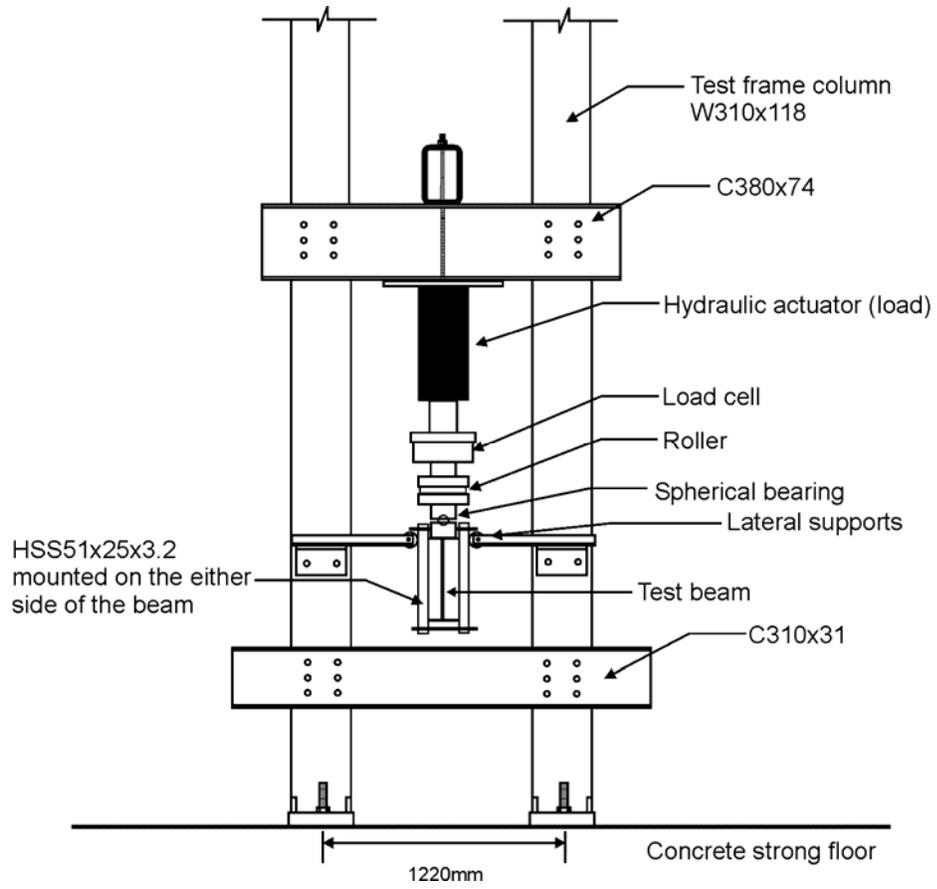
Figure 3-7 Section of Test Setup at Load Point (refer to Figure 3-4)

890 kN load
actuator

890 kN load
cell

Roller
assembly

Spherical
bearing
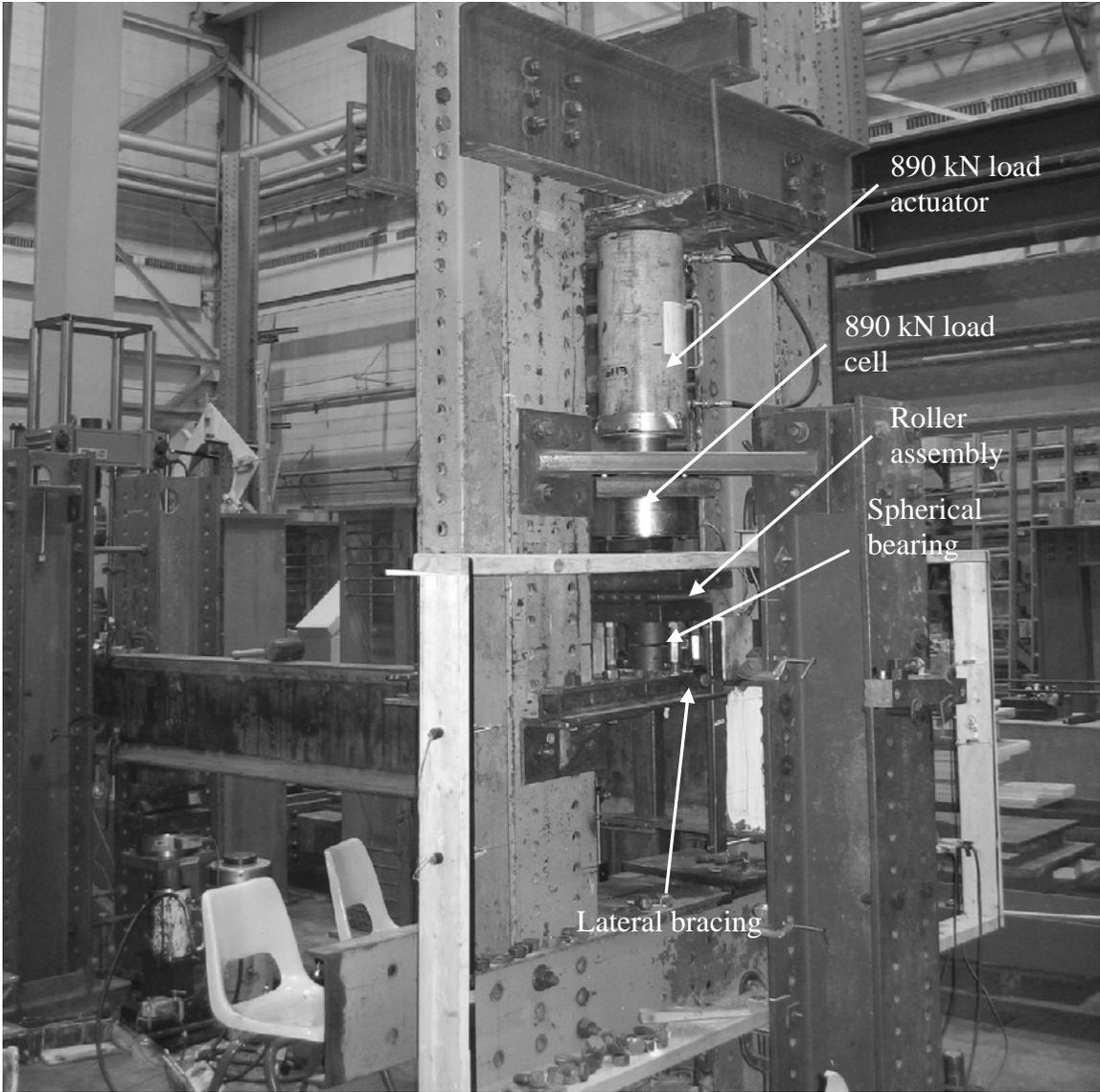
Lateral bracing

Figure 3-8 Loading Frame near the Connection
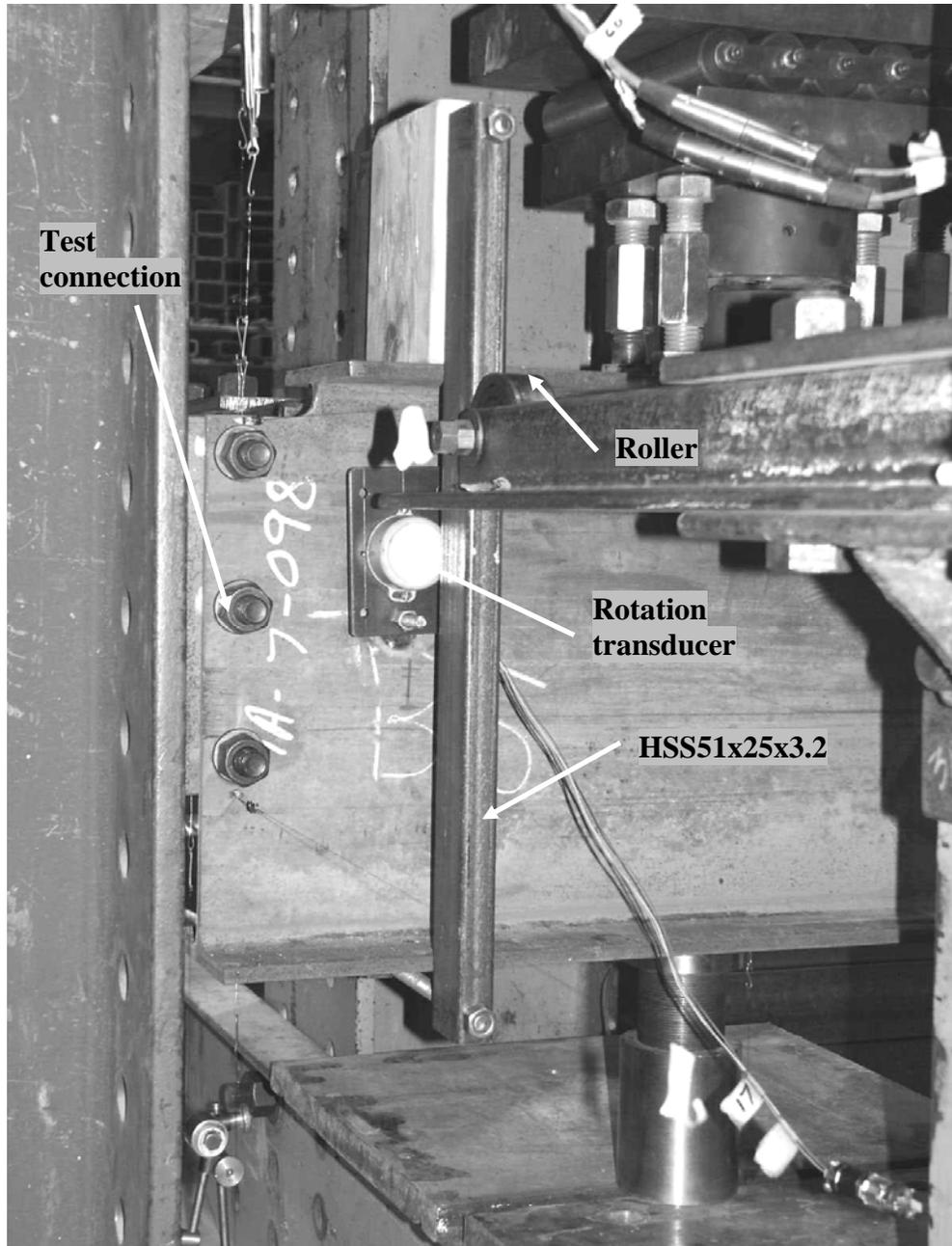
Figure 3-9 Lateral Bracing Near Test Connection

Test frame column
W310x118

Lateral supports

Test beam

Knife edge

890kN load cell

Hydraulic actuator (reaction)

Concrete strong floor
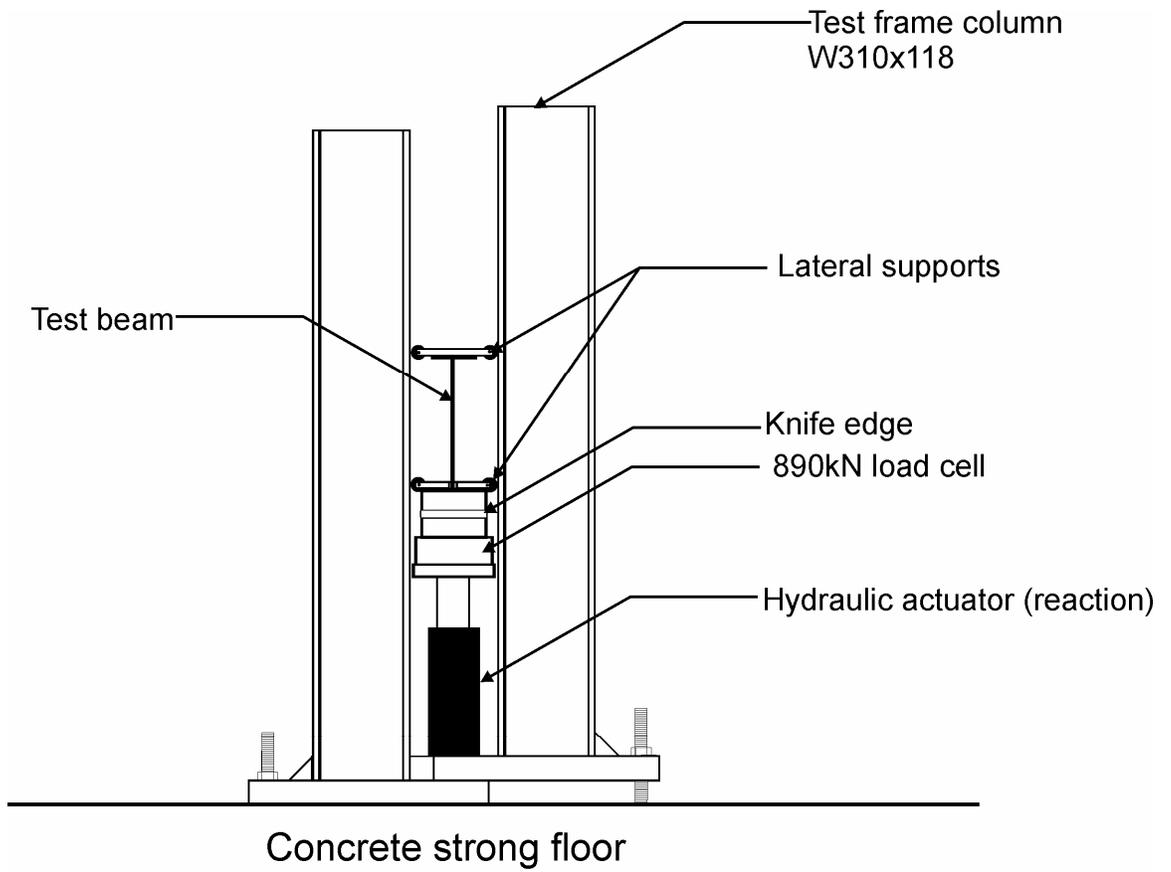
Figure 3-10 Section of Test Setup at Reaction Frame (refer to Figure 3-4)
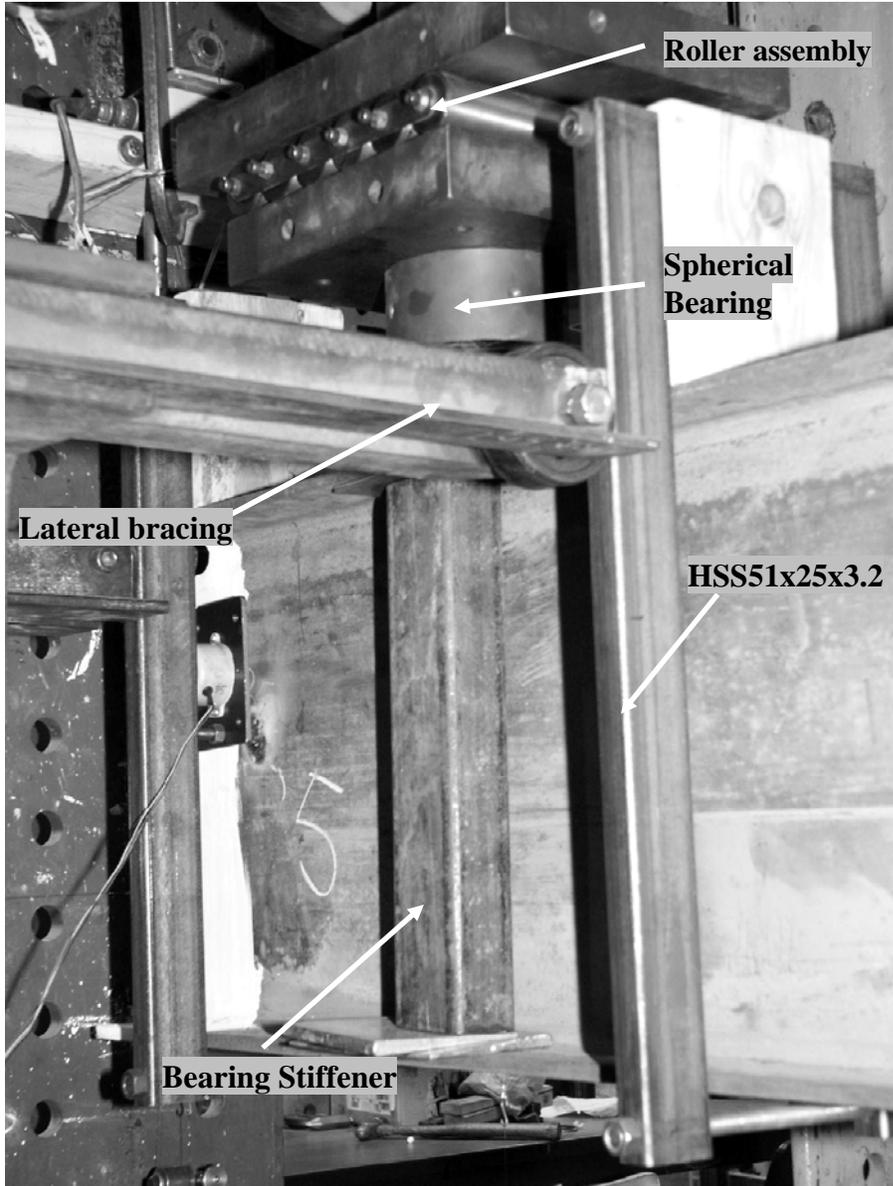
Figure 3-11 Lateral Bracing at Load Point
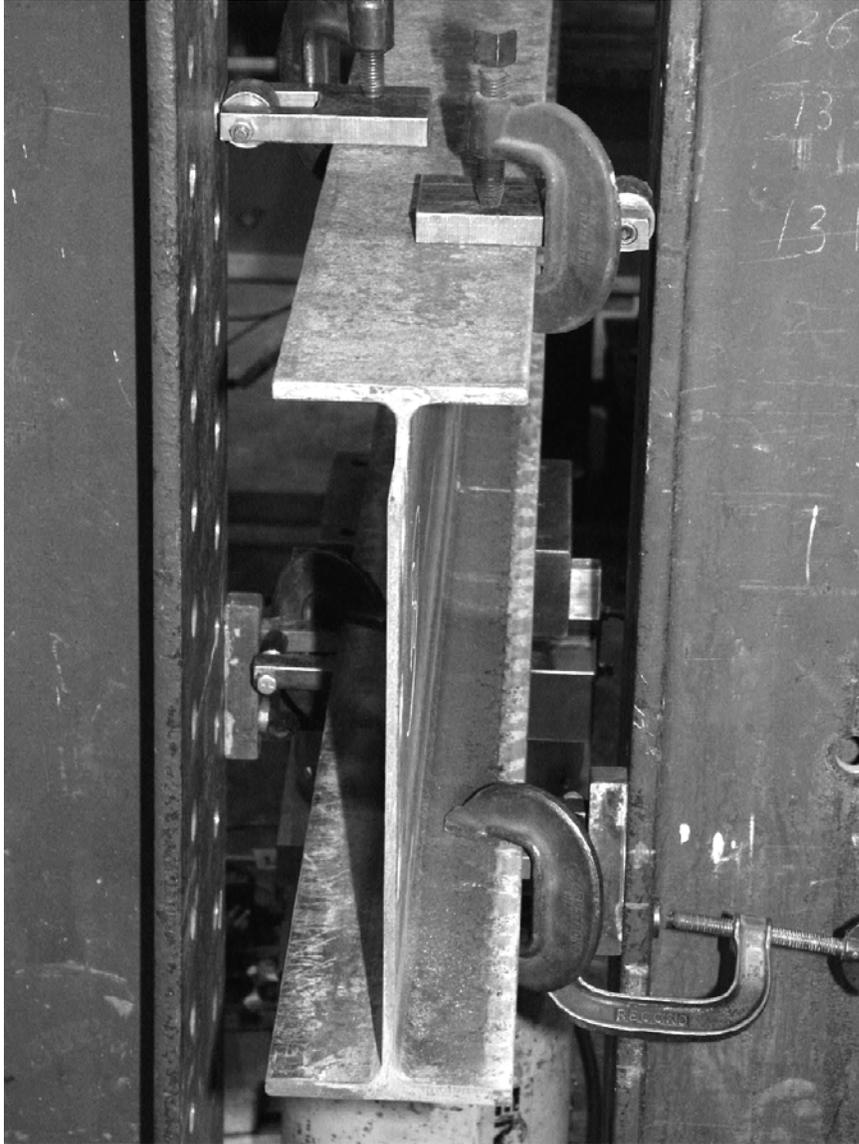
Figure 3-12 Lateral Bracing at Reaction Frame
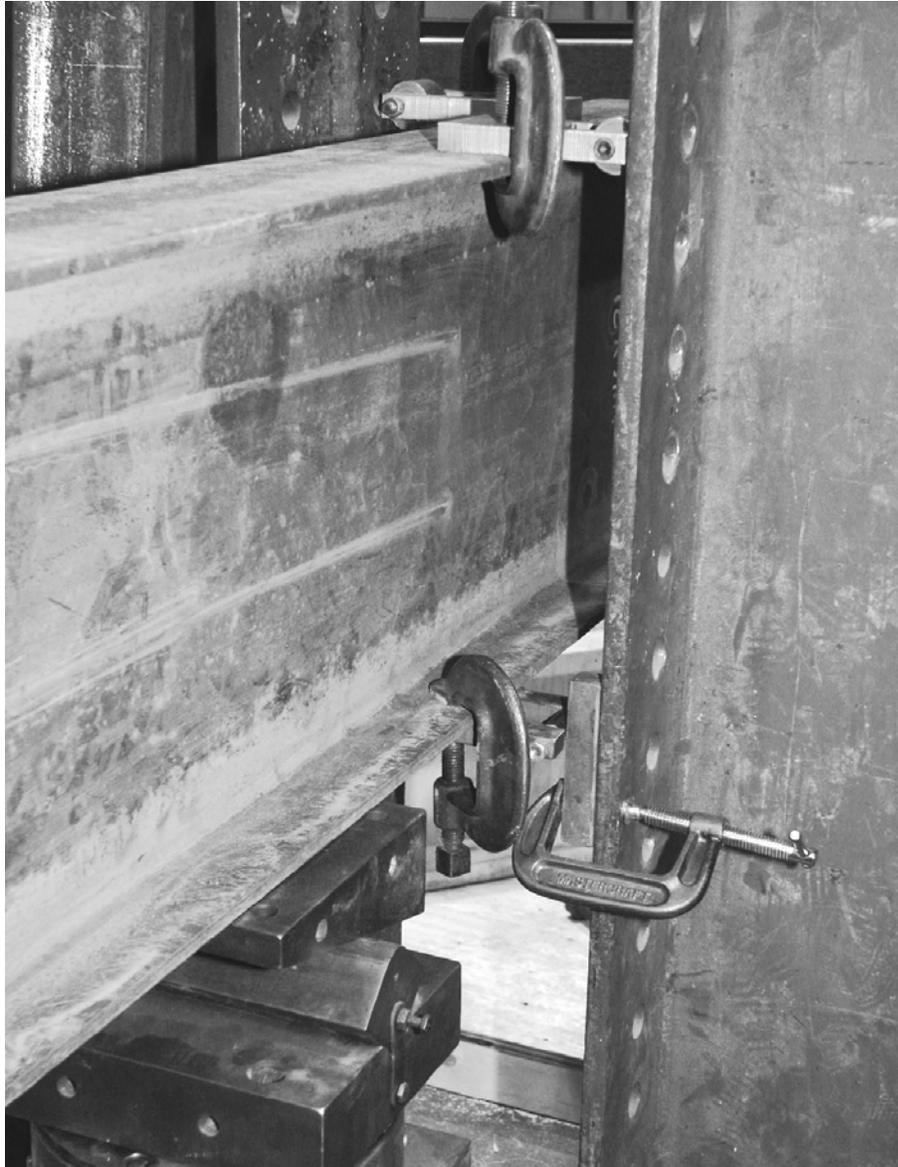
Figure 3-13 Lateral Bracing at Reaction Frame
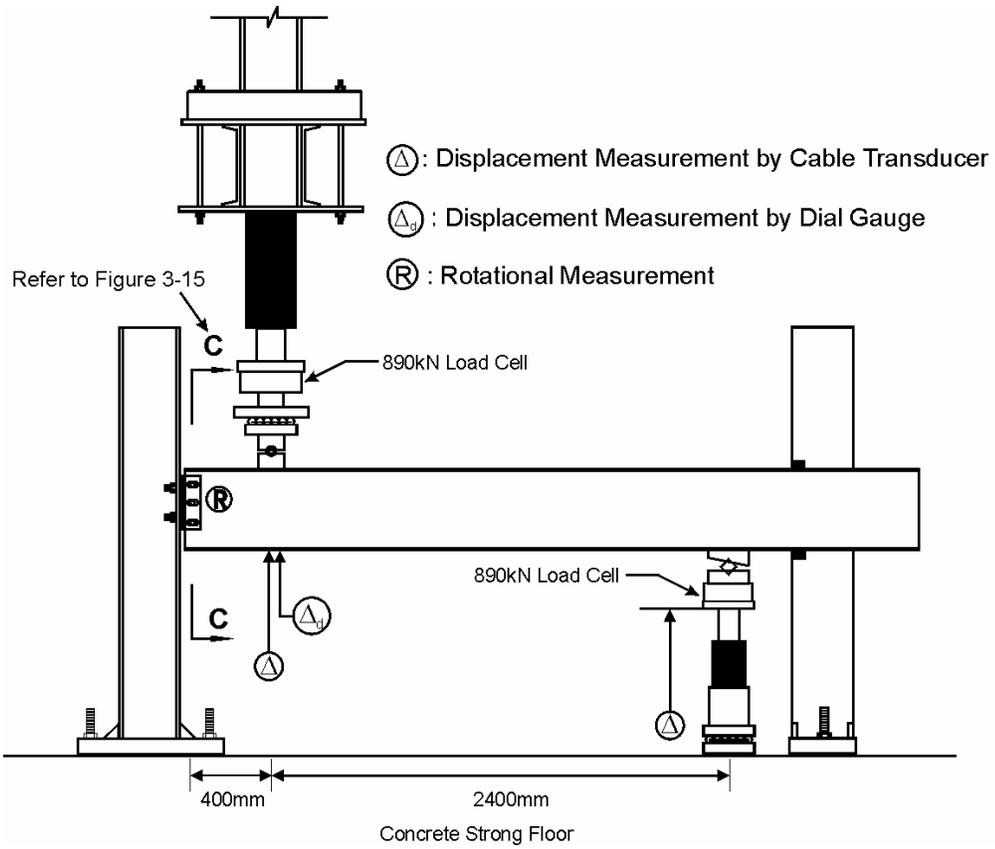
Figure 3-14 Instrumentation
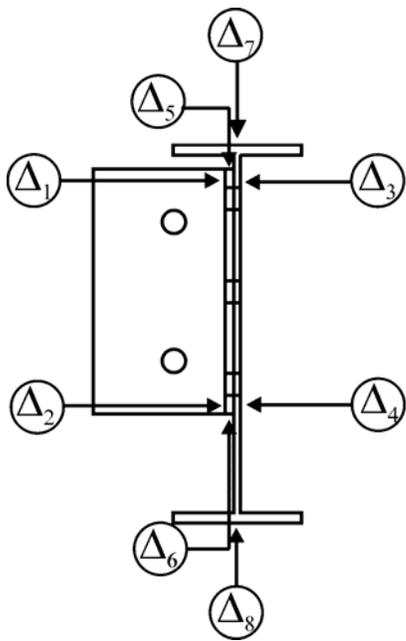
Δ_1, Δ_2: Measurement of lateral displacement of angle

Δ_3, Δ_4: Measurement of lateral displacement of beam

Δ_5: Measurement of displacement of angle at the top

Δ_6: Measurement of displacement of angle at the bottom

Δ_7: Measurement of displacement of top flange of the beam

Δ_8: Measurement of displacement of bottom flange of the beam

Section C-C in Figure 3-14

Figure 3-15 Details of Instrumentation at Connection

38
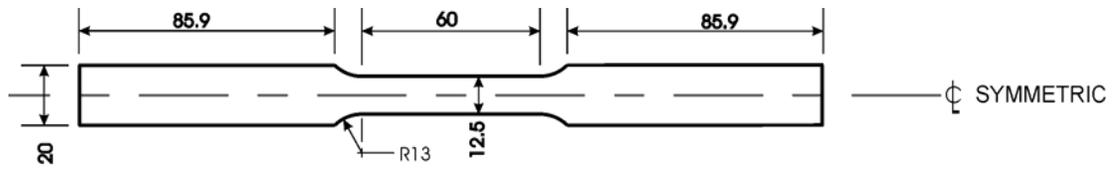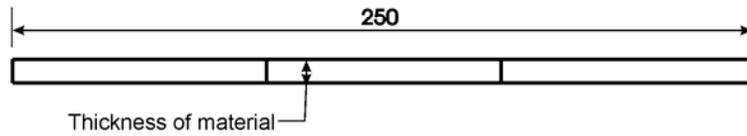
Figure 3-16 Typical Tension Coupon Dimensions
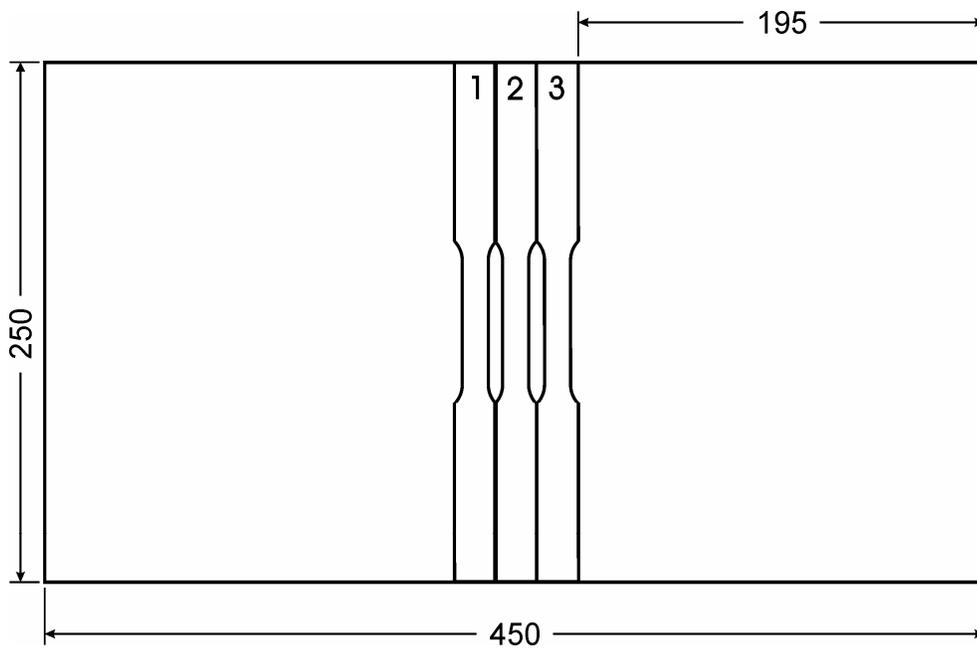
Figure 3-17 Typical Coupon Locations on Beam Web Material Sample
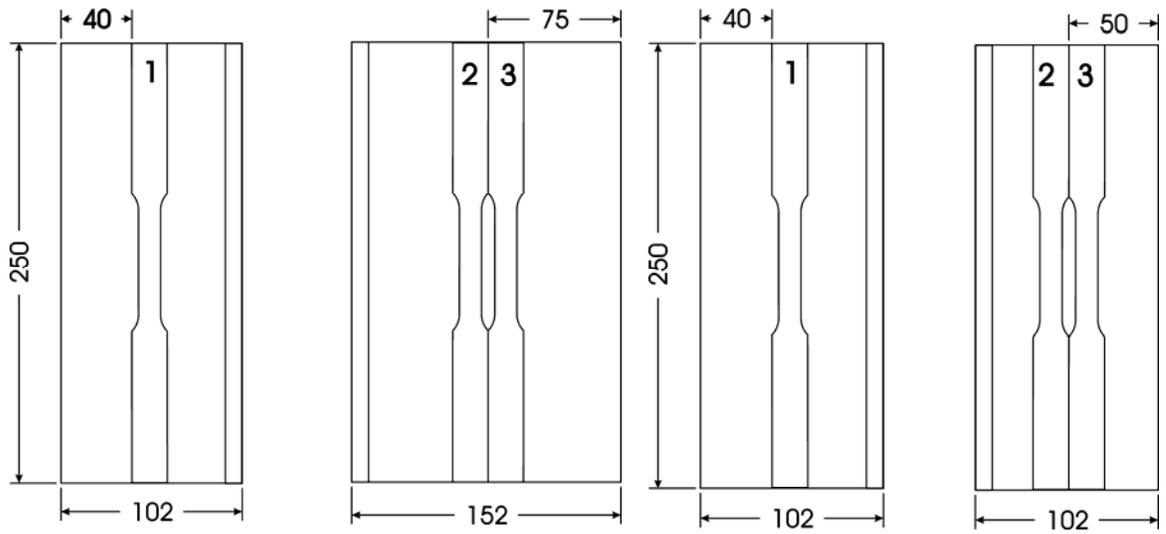
a) Location of Coupons

on Angle L152x102x9.5

b) Location of Coupons

on Angle L102x102x9.5
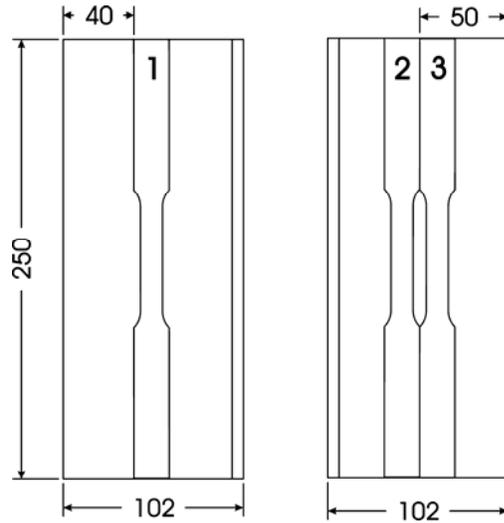
c) Location of Coupons

on Angle L102x102x6.4

Figure 3-18 Location of Coupons on Angle Sections

4 Test Results

This chapter presents the results of the test program described in Chapter 3. The observed failure mode and the general behaviour of the test specimens are described and the effects of the test parameters are assessed by comparisons of the test results. The influence of various parameters on the shear and bearing capacity of the slotted hole connections is investigated through the comparison of test results.

4.1 Description of Failure Modes

The following presents the test results in groups according to the observed failure mode. Photographs of typical test specimens illustrate the various failure modes observed in the test program. The failure modes that were observed include:

- Angle end tearing failure – The leg of the angle connected to the beam failed at the bottom end distance. The failure started with fracture initiated from the bottom bolt hole of the angle leg and propagated to the bottom end of the angle. Eventually the bottom end distance failed and fractured. Bearing of the top two bolts on the slotted holes caused local yield in the bearing area and large plastic deformation of the slots. The end distance failure corresponds to the peak load for specimen 1L2aE, 1L3a, 1L4a, 1L6a, 1L8a and 1L9a. Test specimens 1L1a, 1L2a, 1L5a, 1L7a and 1L11a failed primarily by end tearing, but the load increased after the end tearing failure. These five specimens were able to carry from 5% to 13% more load after the angle bottom end distance failed. Nevertheless, the primary failure mode for these five specimens was still angle end tearing and large deflections (approximately 30 mm in the connection) were required to reach the ultimate load past the end tearing failure. For this reason, the capacity of these specimens was taken as the load at which end distance tearing took place. Photographs of failed specimens 1L1a and 1L2a are shown in Figures 4-1a and 4-1b, respectively. Test specimens 1LAa and 1LBa failed by angle bottom end tearing as well. The failure initiated near 95% to 100% of the peak load when tears propagated from the bottom of bolt hole to the end of the angle. The bottom

end fractured completely eventually. Unlike the other specimens with end tearing failure, the angle failed by shear fracture after the angle bottom end failed. The shear failure path intersects the slotted holes closer to the supporting column, as shown in Figures 4-2a and 4-2b, respectively.

- Beam web edge distance tearing failure – Test specimens 2L1a, 2L2, 2L3, 2L4, 2L5a and 2L6a failed in the beam web by tearing of the edge distance at peak load. This failure mode has similarities to the tension and shear block failure mode described below. However, the top flange was not coped and a tension and shear block failure could not take place. Large deformation of the top flange was observed. Photos of failed specimens 2L1a and 2L2 are shown in Figures 4-3a and 4-3b, respectively.

- Beam web tension and shear block failure – Two of the double angle specimens, namely, 2L7 and 2L8a, failed by beam web tension and shear block tearing. This failure mode initiates by a tension rupture of the edge distance, followed by shear rupture. As illustrated in the photos of failed specimens 2L7 and 2L8a in Figures 4-4a and 4-4b, respectively, shear rupture does not take place at the same time as the tension rupture.

- Failure of angle leg connected to the column – Failure of the angle leg connected to the column characterized the failure mode for the test specimens with standard bolt pitch (76 mm), namely, specimens 1L1, 1L7, 1L10 and 1L10a. In this failure mode, the top end distance of the angle leg connected to the column fractured at the peak load. Photographs of failed specimens 1L1 and 1L7 are shown in Figures 4-5a and 4-5b, respectively. Two double angle specimens, namely, 2L1 and 2L6, also experienced this type of failure mode. The top (loaded) end distance of one of the angle leg connected to the column severed just before the load peaked. For the test specimens with a large pitch (102 mm) (specimens 1LB, 1L2, 1L3, 1L4, 1L5, 1L6 and 1L9), the top corner of angle fractured as the load reached its peak value. Photographs of the failed angle from specimens 1LB and 1L2 are shown in Figures 4-6a and 4-6b, respectively. Test specimen 1LA experienced a large twist (approximately 4°) before the test was terminated. An examination of the tested

specimen showed that a tear had formed around the top bolt hole, indicating that it was close to failing at the angle leg connected to the column. Test specimens 1L12, 1L13 and 1L14 were designed to investigate this failure mode further. These three specimens were fabricated with either minimum end or edge distance at the top bolt hole of the angle leg connected to the column. Moreover, it is suspected that the use of minimum top end and top edge distance at the angle leg connected to the column would result in a capacity similar to that of specimens 1L1 to 1L10. The capacity of these specimens ranged from 288 kN to 430 kN. To ensure failure in the angle leg connected to the column, standard holes were used in the angle leg connected to the beam, and uncoped beams were used. As a result, the predicted shear and bearing capacity of the connection on the beam side was ensured to exceed the capacity of the angle leg connected to the column (maximum capacity observed previously = 430 kN). The angle leg connected to the column for these three specimens failed as expected, as shown in Figure 4-7.

- Web crippling under the load point – Test specimen 2L5 failed by web crippling under the load point, which is believed to have resulted from improper installation of the bearing stiffeners. The beam web buckled under the load point and, unfortunately, the ultimate load of the connection could not be reached. This failure mode is shown in Figure 4-8.

A summary of the test results is presented in Table 4-1, where the peak load is shown in column (2). The numbers presented in brackets for specimens 1L1a, 1L2a, 1L5a, 1L7a and 1L11a are the load when the angle failed by angle end tearing. The angle rotation about the beam axis and the angle of twist of the beam at the peak load are presented in columns (3) and (4), respectively. The vertical displacement at the bottom of the connection measured at the peak load is presented in column (5). Finally, column (6) tabulates the observed failure mode. Photographs of each specimen, showing the failed element of the connection, are presented in Appendix A. Load vs. deformation response and the twist of connection vs. deformation response of all the specimens are presented in Appendix B.

43

4.2 Material Properties

Tension coupon tests were conducted to determine the material properties of the angles and beam material used to fabricate the test specimens. Sheet-type coupons were fabricated and tested according to ASTM standard A370 (ASTM, 1997). The properties recorded from the tension coupon tests are the elastic modulus, the upper yield and lower yield strength when visible, the static yield strength and static ultimate strength, the stress at rupture, the strain at onset of strain hardening, the strain at the ultimate stress, the strain at rupture, and the reduction in area. A summary of material properties is presented in Table 4-2.

4.2.1 Beam Material Properties

A total of 24 coupons fabricated from the beam web were tested. The tension coupons were obtained from the web in order to obtain material properties more relevant to the failure modes observed during the test program, namely, failure in the beam web for some of the test specimens. The mechanical properties for all the beams met the requirements of CAN/CSA–G40.21–98 350W steel (CSA, 1998)[1]. The 1998 edition of G40.21 Structural Quality Steel (CSA, 1998) was the latest edition when the experimental work was conducted. As shown in Table 4-2, the beams were from four heats of steel, and the static yield strength and ultimate strength show slight variation among them. The variation of static yield and static ultimate strength are accounted for in the comparison of test results. Figure 4-9a shows a typical stress vs. strain response for a tension coupon obtained from one of the beams.

4.2.2 Angle Material Properties

A total of 17 coupons were tested from the angle sections. A summary of measured material properties is presented in Table 4-2. All the angle sections meet the mechanical properties requirements of CAN/CSA–G40.21–98 300W steel (CSA, 1998). Except for coupons identified as V and Z, all the coupons were obtained from a virgin section of

---

[1] Note that CAN/CSA–G40.21–98 requires the tension coupons to be sampled from the flanges when the flange width of the W shape is greater than 150 mm. The same strength requirements are used in this project even if the coupons were obtained from the web.

angle. Specimens identified as V and Z, however, were obtained from test specimens after testing. Therefore, it is possible that the measured yield strength is higher than normal due to the strain-hardening effect. All the tension coupons from the V series showed no yield plateau and yield strength, obtained by the 0.2% offset method, significantly higher than the yield strength obtained from virgin material. Although the static yield and static ultimate strengths are slightly lower than 300 MPa and 450 MPa, the dynamic yield and ultimate strength for coupons X are higher than the prescribed minimum of 300 MPa and 450 MPa, respectively, which is considered to be satisfactory. A typical stress vs. strain response for coupons V and Y series are shown in Figures 4-9b and 4-9c, respectively. Coupon V was obtained from the tested angles, whereas coupon Y was obtained from virgin untested angles. As shown in Figure 4-9b, the yield plateau cannot be identified on the stress vs. strain curve for the tested coupon V, whereas it can be identified on the stress vs. strain curve of coupon Y as shown in Figure 4-9c.

4.3   Effect of Test Parameters on Connection Capacity and Behaviour

An analysis of the test results is presented in this section. The test program was designed to investigate the effect of the following parameters: web angle bottom end distance, plate washer, slot length, bolt pretension, torsion brace, bolt pitch, flange cope, beam end rotation, web thickness and bolt diameter.

The test results for specimens that failed in the beam-to-angle connection are discussed first. The parameters are discussed in their order of importance, starting with the parameter that had the most significant effect on the connection strength and behaviour. The load vs. deformation response, the observed behaviour, the failure mode and the capacity of the test specimens are used as a basis of comparison. The measured angle of twist is also used as a basis for comparison in all the single angle test specimens. It should be noted that the load vs. deformation responses are not normalized in the comparisons. However, if the material properties varied greatly between the two specimens being compared, their material strengths are accounted for in the comparison.

For the case where the test specimens showed some increase in load carrying capacity after the angle end tearing, the end tearing load is taken as the capacity of the

test specimen since large deformation (approximately 35 mm measured at the bottom flange) were required for these specimens to reach the higher capacity.

The results of tests on specimens that failed in the angle leg connected to the column are discussed second. The effects of the following parameters are investigated: angle thickness, top edge distance, top end distance, number of bolts and number of angles. The failure mode and capacity of these specimens are used a basis of comparison.

4.3.1   Comparison with Tests from Franchuk *et al.* (2002)

Two single angle test specimens from Franchuk *et al.* (2002), namely, tests IV and V, and two from the current test program, namely, 1LAa and 1LBa, can be compared directly. All four specimens were fabricated with L102x102x6.4 angle sections and W410x46 coped wide flange beam sections. The as-built dimensions and material properties of the test specimens from Franchuk *et al.* are shown in Table 4-3 and Table 4-4, respectively. A summary of the test results for these two tests is presented in Table 4-5.

All four test specimens were fabricated with a nominal bolt pitch of 102 mm, slot lengths of 1.65 times the bolt diameter and coped beam. Specimens IV and 1LAa used 3/4 in. A325 bolts whereas specimens V and 1LBa used 1 in. A325 bolts. All bolts were in the snug tight condition. Specimens IV and V were tested without plate washers whereas specimens 1LAa and 1LBa were tested with a 9.5 mm plate washer. The yield and ultimate strengths for the angle material used in specimens IV and V are 358 MPa and 492 MPa, respectively, compared to 320 MPa and 470 MPa, respectively, for specimens 1LAa and 1LBa, respectively.

Test specimens IV and V are reported to have failed by loaded end distance tearing, followed by tilting of the middle bolt in a three bolt connection. Tearing of the bottom end distance of the angle and top edge of the beam web at the connection occurred at approximately 95% to 100% of the ultimate capacity, leaving only the middle bolt to carry the load. The middle bolt titled about the axis of the beam in the direction of eccentricity. The test-to-predicted ratio for test specimens IV and V were only 0.69 and 0.76, respectively. A detailed description of the test results can be found in Franchuk *et*

al. (2002). Test specimens 1LAa and 1LBa of the current test program were prepared with the same dimensions as specimen IV and V, except that plate washers were used to cover the slots. Specimens 1LAa and 1LBa, failed by angle bottom end tearing near the peak load, followed by the fracture of shear area.

4.3.1.1 Effect of Plate Washer

As shown in Figure 4-10 and Figure 4-11, the test specimens with plate washer, 1LAa and 1LBa, had capacities of 24% and 27% higher than their counterparts without plate washer, IV and V. The increase in capacity was likely due to the change in failure mode from end tearing followed by tilting of the middle bolt to shear fracture of the angle. It is suspected that test specimens IV and V were not capable of developing the full net shear capacity of the angle because of the bolt tilting problem. The test specimens had reached 95% to 100% of the test capacity when the bottom end distance of the angle and the top edge distance of the beam web fractured. Although the material strength in specimens IV and V was slightly higher than in specimens 1LAa and 1LBa, the strength of the connection was significantly lower. It is believed that the plate washer prevented the bolt tilting phenomenon in thin single angle connections, allowing the full shear capacity to develop. The effect of the plate washer is further investigated with thicker angles in the next section. It should be noted that the shear angles used for specimens IV, V, 1LAa and 1LBa were thinner than the minimum recommended angle thickness from the AISC Manual of Steel Construction (AISC, 1999). However, the Canadian design practice (CISC, 2004) does not limit the thickness of web framing angles.

4.3.2 Comparison of Tests in Current Experimental Program

4.3.2.1 Effect of Plate Washer

In this comparison, four test specimens are included: two single angle specimens, namely 1L2a and 1L4a, and two double angle specimens, 2L2 and 2L4. All angles have a nominal thickness of 9.5 mm, compared to 6.4 mm used for the comparison presented in section 4.3.1.1.

Figure 4-12 shows that test specimen 1L2a (without plate washer) had a 19% lower peak load than specimen 1L4a (with plate washer). If we take the angle end tearing as the failure load, as explained above, the reduction of capacity then becomes 29%. The angle of twist of the beam and of the shear angle were very close throughout the test for the specimen with plate washer (1L4a). Figure B-42 and Table 4-1 show a difference of 0.8° of the twist between the beam and the angle at the peak load. On the other hand for the specimen without plate washer (1L2a), the angle of twist of the beam was approximately 2° larger than the angle of twist of the shear angle at ultimate, as shown in Figure B-36 and Table 4-1. The larger angle of twist observed in the beam than in the angle for the test specimen 1L2a is possibly a result of a slight pullout of the top bolt through the slot, although the bolt did not completely pull out of the hole during the test. It is believed that the slight pullout and the separation between the beam and the angle did not contribute to the loss of capacity observed in the test specimens without a plate washer. The bolts were not pulled out enough to lose bearing. Inspection of failed specimens after the test showed that yielding occurred around the bottom bolt hole in the plate washer. It seems that one of the roles of the plate washer in the test specimens was to redistribute the load between the bolts after the angle end tearing.

Test specimens 2L2 (without plate washer) and 2L4 (with plate washer) are compared to assess the effect of plate washer on double angle connections. In both cases, the specimens failed by edge distance rupture of the beam web. From Figure 4-13, it is seen that specimen 2L4 had a 14% higher capacity than that of 2L2. An examination of the failed specimens indicated that the angles underwent very little deformation when plate washers are used, whereas the shear angle in 2L2 failed by angle end tearing after reaching the ultimate capacity. It is suspected that the higher capacity of the specimen with the plate washers, 2L4, is possibly due to the increased rigidity of the angles, indicated by the observations of the failed specimens, and the friction developed between the faying surfaces of the connection.

The plate washers have been found to improve the connection strength, significantly. Calculations presented in Chapter 5 indicate that two specimens without plate washer, namely, 1L2a and 2L2, have test-to-predicted ratios of 0.68 and 0.69,

respectively, as predicted by CSA–S16–01, whereas the specimens with plate washer, 1L4a and 2L4, have test-to-predicted ratios of 0.97 and 0.80, respectively.

4.3.2.2   Effect of Loaded End Distance

Test specimen 1L2aE was fabricated with a larger bottom end distance (47 mm) than test specimen 1L2a (32 mm, which is the minimum for 7/8 in. diameter bolts). The as-built end distance of 1L2aE was 36% larger than that of 1L2a. The difference in geometry between the two specimens resulted in an increase in as-built gross shear area of 6.2% and net shear area of 7.8% on the angle leg connected to the beam. The primary failure mode for both specimens was angle end tearing. As shown in Figure 4-14, test specimen 1L2a was able to carry more load after end tearing of the angle (from 321 kN to 364 kN). The peak load was reached when the edge distance of the web ruptured at a measured connection displacement of about 32 mm. Test specimen 1L2aE, which had a larger end distance than 1L2a, showed a load carrying capacity 53% larger than specimen 1L2a, fabricated with minimum end distance. A comparison of peak loads shows an increase of capacity of 35% as the as-built end distance is increased by 36%.

4.3.2.3   Effect of Slot Length

The effect of slot length can be assessed by comparing test specimens 1L2a (long slot) and 1L9a (short slot). Both test specimens were tested without a plate washer. Figure 4-15 shows that the test specimens had the same initial stiffness. However, the test specimen with short slots reached a capacity 25% higher than the connection with long slots. The load at angle end tearing of the short slot specimen was 41% larger than the load at end tearing of the specimen with long slots. Specimen 1L2a was able to carry more load after the angle failed whereas the capacity of 1L9a dropped from 454 kN to about 400 kN after angle end tearing.

The separation between the angle and beam web at the connection was larger for the specimen with long slots (1L2a), as shown in Figures B-36 and B-52. The larger separation between the beam and angle of specimen 1L2a was likely due to the large deformation of slots in the load direction and greater flexibility of the material between the slots, thus allowing the bolt head to pull through the slot partially. Nevertheless, the

partial pull-out of the bolt head occurred at a large deflection (about 30 mm). It is therefore concluded that slot length does have a significant effect on capacity.

4.3.2.4 Effect of Bolt Pretension

The effect of bolt pretension can be assessed from a comparison of test 1L6a (snug tight bolts) with test 1L5a (pretensioned bolts with a plate washer). In both tests, the angle failed by end tearing, followed by beam web edge distance rupture. Figure 4-16 shows that specimen 1L5a had 24% higher ultimate capacity and 18% higher angle failure capacity than specimen 1L6a. The general behaviour of the two specimens was similar, but the specimen with pretensioned bolts had a slightly higher stiffness and load carrying capacity. The increase in stiffness and capacity was likely due to friction developed between the faying surfaces at the connection.

The effect of bolt pretension on double angle connections with slotted holes can be assessed by comparing specimen 2L4 to 2L5a. Both specimens had plate washers on the outer plies of the connection to cover the slotted holes. Test specimen 2L5a was installed with pretensioned bolts connecting the angle to the beam, whereas specimen 2L4 had only snug-tight bolts. Both test specimens showed a similar beam web failure mode, that is, the beam edge distance next to the bottom bolt ruptured at a load close to the peak load. Figure 4-17 shows that specimen 2L5a had a capacity 13% higher than that of 2L4. It is also noted that the test specimen with snug tight bolts had stiffness 50% lower than that of the specimen with pretensioned bolts. Both the increase in capacity and initial stiffness displayed by the specimen with pretensioned bolts are likely due to the friction contribution. Since there was no visible sign of bolt deformation after the test, it is suspected that the bolts maintained most of their pretension during the tests. The beneficial effect of bolt pretension is not expected to be applicable when the connection fails at a load capacity close to the shear capacity of the bolts since the plastic shear deformations observed in bolts under this condition have the effect of releasing the pretension force.

4.3.2.5 Effect of Torsion Bracing

The effect of torsion bracing can be assessed by comparing specimen 1L1a (top flange braced only) to 1L11a (torsionally braced). Both exhibited similar behaviour and end tearing of the angle, which was the primary failure mode for both specimens. Although the difference in end tearing capacity between the two specimens was only 5%, the two specimens showed different behaviour after the angle end tearing failure. As shown in Figure 4-18, for specimen 1L11a bolt bearing failure was observed around the top two bolts followed by tearing of the beam web edge distance at the middle bolt hole at peak load. On the other hand, the capacity of specimen 1L1a was limited by twisting of the beam, which caused the top bolt head to pull partially through the slot. The test was stopped when the angle of twist of the beam became large (approximately 8°) (See Figure B-34). The ultimate capacity for the torsionally braced specimen (1L11a) was 12% higher than the capacity of specimen 1L1a. Moreover, due to the torsional bracing, the beam angle of twist in specimen 1L11a was smaller than 1° at the peak load, as shown Figure B-56. It is believed that a torsion brace affects the ultimate connection capacity and behaviour of single angle connection at large deflections (about 25 mm), although its benefit on the angle end tearing capacity is small.

4.3.2.6 Effect of Bolt Pitch

Four tests are used to assess the effect of bolt pitch in single angle connections, namely, 1L1a, 1L2a, 1L6a and 1L8a. Two of them (1L1a and 1L8a) were fabricated with a 76 mm bolt pitch and the other two (1L2a and 1L6a) were fabricated with a 102 mm bolt pitch. Figure 4-19 shows a comparison of load versus deformation response of test specimens 1L1a and 1L2a. Both test specimens failed by angle end tearing, followed by beam web edge distance tearing for specimen 1L2a, and a combination of beam twisting and top bolt pullout for specimen 1L1a. From Figure B-34 and B-36, the separation between the angle and the beam at the connection was about 3° for specimen 1L1a and 2° for specimen 1L2a at peak load. The peak capacity of the specimen with a larger bolt pitch (1L2a) was 11% larger than that observed for a smaller pitch (1L1a), which is likely due to different behaviour and failure modes observed after the angle failed by end

tearing. The difference in angle end tearing capacity was only 3% despite a 23% larger gross area and a 32% larger net shear area in the angle leg connected to the beam web.

Test specimens 1L8a and 1L6a had identical configurations to 1L1a and 1L2a, respectively, except that the beams were coped. Both specimens failed by angle end tearing initially, which also corresponds to the peak load for both specimens. Following the angle end tearing failure, the net shear area between the middle and bottom slotted hole fractured at a displacement of about 35 mm for test specimen 1L8a. Tearing of the web edge distance next to the middle bolt was observed in specimen 1L6a at a deflection of about 35 mm. As shown in Figure 4-20, the peak capacity of specimen 1L6a (large pitch) was only 8% higher than that of test specimen 1L8a, despite the increase of 32% of the net area and 23% of the gross area in specimen 1L6a.

The effect of bolt pitch on double angle connections can be assessed by comparing four tests: 2L1a, 2L2, 2L7 and 2L8a. Two of them (2L1a and 2L7) used a nominal bolt pitch of 76 mm and the other two (2L2 and 2L8a) used a large pitch (102 mm). Figure 4-21 shows the load vs. deformation curves for 2L1a and 2L2. Both test specimens failed at the beam web. The difference in their ultimate capacity is about 1% and they demonstrated similar initial stiffness and ductility. The tensile strength of the beam material in specimen 2L1a was 4% higher than that used in specimen 2L2, as shown by the coupon test results. It is believed that the small difference in ultimate strength of the beam web does not affect the comparison significantly. However, the location of the edge distance rupture was different for the two specimens. Although both specimens failed by tearing of the beam web edge distance, specimen 2L1a failed at the bottom bolt hole, whereas specimen 2L2 failed at the middle bolt hole.

Figure 4-22 shows the load vs. deformation response of specimens 2L7 and 2L8a. Both test specimens were identical to 2L1a and 2L2, except that the top flange of the beam was coped. Both specimens failed by beam web tension and shear block failure. Test specimen 2L8a showed an increase in capacity of 20% over 2L7, which is consistent with an increase in net shear area resulting from the larger bolt pitch. However, inspection of the failed specimens showed a slight difference in the block shear failure mode. Specimen 2L7 had tension failure at the edge distance next to the bottom bolt, and

a shear fracture along the vertical shear area above the bottom bolt. For the specimen with larger bolt pitch (2L8a), tension rupture was observed at the edge distance next to middle bolt, and shear fracture was observed along the vertical shear area above the middle bolt. Only some hole deformation was observed at the bottom bolt. Angle end tearing was observed at peak load on both angles for specimen 2L8a as well.

4.3.2.7   Effect of Flange Cope

The same four single angle connections used in the bolt pitch investigation (1L1a, 1L2a, 1L6a and 1L8a) were also used to assess the effect of flange cope. Figure 4-23 shows a comparison of the load vs. deformation responses for test specimens 1L1a and 1L8a. A comparison of specimen 1L1a (uncoped) with 1L8a (coped) indicates a difference of peak capacity of 8%. Although both specimens failed by angle end tearing at approximately the same load (312 kN versus 306 kN), specimen 1L1a showed an increase of capacity of 5% before failure by excessive beam twisting and partial pullout of head of top bolt. Specimen 1L8a failed by angle end tearing followed by fracture of the net shear area between the bottom and middle slotted hole. The two connections showed similar stiffness and behaviour up to the point where the angle failed. Similar observations can be made about specimens 1L2a (uncoped flange) and 1L6a (coped flange). The peak capacity of specimen 1L2a was 10% higher than that of specimen 1L6a, as shown in Figure 4-24. The load at which angle end tearing took place only differed by 3% between the two test specimens. Since failure took place in the angles rather than in the beam web, no significant difference was observed between the coped and uncoped specimens.

To assess the effect of flange cope on double angle connections, the same four specimens (2L1a, 2L2, 2L7 and 2L8a) used in the bolt pitch comparison are used. The load vs. deformation curves for this comparison are shown in Figures 4-25 and 4-26. Test specimens 2L1a and 2L7 were fabricated with standard pitch (76 mm). Test specimen 2L7, with the coped flange, showed a 27% lower capacity than test specimen 2L1a. Specimen 2L7 failed by tension and shear block failure of the beam web, whereas 2L1a failed by edge distance rupture of the beam web, followed by bolt bearing and elongation of bolt holes. The failure mode is similar to a tension and shear block failure, but the

difference in capacity is possibly attributed to the contribution from the top flange. The top flange provided additional strength in terms of bearing resistance to the connection. This change in failure mode is consistent with the observation by Birkemoe and Gilmor (1978). Although both specimens showed beam web edge distance rupture at an early stage, the residual strength of specimen 2L7 was contributed by the vertical shear area of the beam web at the connection. The contribution to the strength of specimen 2L1a came from the vertical shear area as well as from the top flange, which resulted in an increase in capacity.

A similar comparison can be made between test specimens 2L2 and 2L8a. The coped specimen 2L8 showed a 14% lower capacity than its uncoped counterpart 2L2. Although both specimens had beam web edge distance rupture initially, the decrease in capacity of coped specimens was consistent with the change in failure mode from beam web bearing to tension and shear block failure. It is believed that the presence of top flange contributed to the increase in capacities of double angle specimens.

4.3.2.8   Effect of Beam End Rotation

The effect of beam end rotation on single angle connections can be assessed by comparing test specimens 1L1a (measured rotation of −0.41° at peak load) to 1L7a (measured rotation of 3.5° at peak load). Positive beam end rotation indicates rotation created by lowering the reaction actuator at the end of member opposite to the connection. Both test specimens failed by angle end tearing with a small increase in load carrying capacity before the end of testing due to excessive twist. Figure 4-27 shows that both test specimens displayed a similar load vs. deformation response. Table 4-1 indicates that the peak load for specimen 1L1a was 5% larger than the peak load for specimen 1L7a. The angle end tearing load was 8% larger than for specimen 1L7a.

A comparison of test specimen 2L1a (measured rotation of −0.25° at peak load) with 2L6a (measured rotation of 3.5° at peak load) shows less than 3% difference in capacity. The load response is shown in Figure 4-28. The initial stiffness and behaviour were nearly identical up to the peak load. Both test specimens failed by tearing of the beam web edge distance. The beam web edge distance of test specimen 2L6a ruptured at

54

the middle bolt hole, combined with bottom end tearing of both angles near the ultimate load. On the other hand, the beam web edge distance of specimen 2L1a ruptured at the bottom bolt hole. Despite the difference of web edge distance rupture location, the failure modes are similar. It is therefore concluded that beam end rotation has little effect on the connection capacity. This observation is consistent with earlier observations by Franchuk *et al.* (2002).

4.3.2.9 Effect of Web Thickness

The effect of beam web thickness can be assessed by comparing specimen 1L6a (nominal web thickness of 7.0 mm) to 1L3a (nominal web thickness of 10.0 mm). In both cases, the specimens reached their peak capacity when the angle failed by end tearing. Figure 4-29 shows that the connection capacity of specimen 1L3a (nominal web thickness of 10.0 mm) is only 4% larger than that of 1L6a (nominal web thickness of 7.0 mm). As expected, web thickness has negligible effect on angle failure capacity.

The effect of web thickness on double angle connections is assessed by comparing specimens 2L2 (nominal web thickness of 7.0 mm) and 2L3 (nominal web thickness of 9.7 mm). Both specimens used double angles with large bolt pitch and long slots. The load vs. deformation response for both specimens is shown in Figure 4-30. Test specimen 2L3 shows a 19% higher capacity than specimen 2L2, which can be attributed partly to the difference of 31% in actual web thickness. However, the ultimate strength of the web material of specimen 2L3 is 6% greater than that of specimen 2L2. From the difference in material properties and web thickness, the difference in capacity between specimens 2L2 and 2L3 should have been greater than observed. Angle end tearing has been observed in both test specimens near the peak load. The angles were of the same nominal thickness and from the same heat of steel. Therefore, it is suspected that the angle end tearing partly contributed to the failure as well.

4.3.2.10 Effect of Bolt Diameter

The effect of bolt diameter can be assessed by comparing test specimen IV with V from Franchuk *et al.* (2002), and test specimen 1LAa with 1LBa from the current test program. Figure 4-31 shows the comparison of test specimen IV with V, which had

19.1 mm and 25.4 mm bolts, respectively. Test specimen V showed a capacity 12% greater than that of test specimen IV, despite of a 2.5% larger as-built net area of specimen IV. It is believed that the increase in capacity is likely due to the increase in minimum end distance from 25 mm to 32 mm to accommodate the change in bolt diameter. As mentioned previously, test specimens IV and V failed by the rupture of angle bottom end distance rupture and beam web top edge distance, followed by tilting of the middle bolt. The increase in net or gross shear area did not contribute significantly to the increase in capacity.

Similar conclusions can be drawn from a comparison of test specimens 1LAa and 1LBa. In both cases, the connections failed by angle bottom end tearing near the peak load. The angle used in test specimen 1LAa has a 4.7% larger as-built net shear area than 1LBa. However, specimen 1LBa showed a capacity 14% larger than that of 1LAa, as shown in Figure 4-32. The increase in capacity is likely due to the increase in end distance of 1LBa (32 mm) over 1LAa (25 mm). It was observed that the failure initiated by tearing of bottom end distance, and both connections reached about 95% of the peak load when the end distance failed. Rupture of the remaining shear area followed, and the load decreased significantly afterward. The angles from both tests were from the same heat of steel, thus the variations in material properties were negligible.

4.3.3 Discussion of Specimens that Failed in the Leg Connected to the Column

All of the tests in the current test program were designed so that failure would take place on the beam side. However, several specimens showed an unexpected failure of the angle leg connected to the column, giving the opportunity to study an additional failure mode. The specimens that failed with this type of failure mode include 1LA, 1LB, 1L1 to 1L10, 1L10a, 2L1 and 2L6. In addition, three tests, namely 1L12, 1L13 and 1L14, were designed specifically to investigate this failure mode. The parameters investigated were top end distance (e_{s3}), top edge distance (e_{g1}), thickness of angle (t), number of bolts and number of angles (single or double). These parameters were found to have an effect on the capacity of connections with this type of failure mode. A summary of the test parameters is shown in Table 4-7. As shown in the table, the test specimens 1LB, 1L1 to

1L10, 2L1 and 2L6 are divided into four groups. The nominal dimensions of specimens within each group were identical. For comparison, the connection capacity of each group is taken as the average of the capacities of the specimens within the group.

4.3.3.1   Effect of Angle Thickness

The test specimens from group 1 and the test specimens from group 3 are compared to assess the effect of angle thickness. For all the test specimens in this group, the nominal dimensions of the angle leg connected to the column are the same. The top end distance, e_{s3}, is 58 mm and the edge distance, e_{g1}, is 37 mm. Specimen 1LB was fabricated with a 6.4 mm thick L102x102x6.4 angle, whereas the specimens from group 3 were fabricated with L102x102x9.5 angles. The test results presented in Figure 4-33 indicate that an increase of angle thickness of 48% (from 6.4 mm to 9.5 mm) results in an increase in capacity of 30%. It should be noted that the yield and ultimate strengths of the angles used in group 1 were 45% and 12% higher, respectively, than the ones used for the test specimens of group 3, accounting for part of the difference.

4.3.3.2   Effect of Top End Distance

In order to assess the effect of top end distance, e_{s3}, test specimens from group 2 are compared to specimens from group 3. The top end distance of specimens from group 2 was 32 mm, whereas the one from group 3 was 58 mm, while the edge distance, e_{g1}, for both groups was 37 mm. As shown in Figure 4-34, an increase of top end distance of 81%, or by 26 mm, results in an increase of average capacity by 29%. Angles used in both groups of tests were from the same heat of steel, thus the variation in material properties was negligible.

4.3.3.3   Effect of Edge Distance

Specimens 1L12 and 1L13 are compared to assess the effect of edge distance, e_{g1}, on the capacity of the connection. The baseline test in this comparison is specimen 1L12, which was fabricated with the minimum edge distance of 32 mm as required by CSA–S16–01 (CSA, 2001). Specimen 1L13 was fabricated with an edge distance of 50 mm. Both specimens had a top end distance, e_{s3}, of 32 mm. As shown in Figure 4-35, an

increase of edge distance of 56%, or 18 mm, resulted in an increase in capacity of 24%. Again, the angle sections used in both specimens came from same heat of steel.

4.3.3.4 Effect of Number of Bolts Connecting the Angle to the Column

The effect of number of bolts on the connection capacity of a single angle connection that failed in the angle leg connected to the column can be assessed by comparing specimen 1L12 with 1L14. The angle in specimen 1L12 was connected to the column with two ASTM A325 1 in. diameter bolts, whereas the one in specimen 1L14 was connected to the column using three ASTM A325 1 in. diameter bolts. Figure 4-36 shows that an increase of 2 bolts to 3 bolts results in a 21% increase in capacity.

4.3.3.5 Effect of Number of Web Framing Angles

The effect of number of angles (either single or double angles) on connection capacity can be assessed by comparing the specimens from group 2 with the specimens from group 4. Specimens from group 2 were single angle connections whereas specimens from group 4 were double angle connections. The nominal dimensions of angle leg connected to the column are identical for both groups. The failure path crossed the top end of the angles in both groups. However, only one of the two angles failed in the double angle for specimens in group 4. It is likely due to slight initial imperfection in fabrication of the angles so that one of the top end distances of the angle is shorter than the other. Figure 4-37 shows that the double angle specimens (group 4) had a 34% higher capacity than the ones with single angle (group 2).

4.4 Conclusions

The effect of a wide range of parameters on the strength and behaviour of connections with slotted holes was investigated. The main findings from an examination of test results (40 tests from this test program and two from an earlier test program) are:

- Plate washers are beneficial for thin (nominal thickness = 6.4 mm) single angle connections. They increased the capacity as well as the stability of the connection (change in failure mode from tearing of loaded end distance followed by

58

bolt-tilting to shear failure of angle). The observed increase in capacity was from 24% to 27% for the specimens with plate washers as compared to equivalent specimens without. Thicker single web framing angle (nominal thickness = 9.5 mm) specimens fabricated with a plate washer showed a 41% greater capacity than the specimens without a plate washer. Double angle specimens with plate washers (2L4) showed a 14% higher capacity than the specimen without plate washers (2L2). The test-to-predicted ratio of 2L4 is 0.8, compared to 0.69 of test specimen 2L2. The predicted capacities of both specimens are calculated based on web bearing failure. However, it is suspected that the beam web edge distance failed and the web bearing strength was not fully developed. As a result, the test capacities of both specimens did not reach the expected capacities. The double angle specimen with plate washers (2L4) has a higher capacity than the one without plate washers (2L2), possibly due to the increased rigidity of the angle, as well as the friction developed between the faying surfaces at the connection.

- The increase in capacity for single angle web framing connections with a plate washer was possibly due to the difference in the load transfer mechanism at the angle end. For the single angle specimen with a plate washer (1L4a), part of the load was shared by the plate washer during the angle end tearing, allowing for a better transfer of load from the end bolt to the other two bolts. This is indicated by the observed yielding of the plate washer around the bottom bolt hole. Double angle connections also showed an increase in capacity compared to the specimens without plate washers. The possible cause of the increase in this case is the friction contribution between the faying surfaces and increased rigidity of the angles due to the installation of plate washers on the outer plies. Although the bolts are in the snug-tight conditions, some friction might be developed between the faying surfaces at the connection.

- The loaded end distance had a significant effect on the capacity of single web framing angle connections that failed by angle end tearing. An increase in actual bottom end distance of 36% was found to lead to an increase in connection capacity of as much as 53%. As shown in Chapter 5, the test-to-predicted values

using CSA–S16–01 Clause 13.11(a) (tension and shear block failure) for a specimen with a 47 mm nominal bottom end distance (1L2aE) is 0.98, compared to 0.68 for a specimen with 32 mm nominal bottom end distance (1L2a). The failure mode of these two connections combines tearing of the bottom end distance and bearing failure at the bolts on the top two slotted holes. For specimen 1L2a, it is suspected that the bottom end distance failed before the rest of the connection could mobilize its full bearing strength. Therefore, this specimen has a significantly lower test-to-predicted ratio compared to the specimen with a larger loaded end distance. It was also observed that the loaded end distance of connections with long slots did not fail by shear and end splitting, but rather by a combination of bending and bearing failure, as shown in Figures 4-2a and 4-2b. The 2005 AISC specification has provisions for an exterior bolt failing by end spitting, but the equation was based on the shear rupture of the net shear area in front of the bolt hole. In order to address this issue, new prediction models are developed in Chapter 5 to predict the capacity of slotted hole connections with angle end tearing failure.

- Single angles with short slots showed a 41% higher angle failure capacity than connections with long slots that failed by angle end tearing.

- Connections with pretensioned bolts showed a higher capacity (18% higher angle end tearing capacity in single angle connections and 13% in double angle connections) and initial stiffness (about 50%) than connections with snug tight bolts.

- Connections with a larger bolt pitch did not show any significant increase (from 3% to 8%) in capacity, except for double angle specimens that failed by tension and shear block. The single angle connections with different bolt pitch failed by angle end tearing. Therefore, the increase in bolt pitch had little effect on the capacity.

- Torsionally braced beams showed much less twisting (7° less) in the connection and a higher capacity at large deflection (approximately 25 mm). However, the angle failure capacity was only increased by 5%.

- For specimens that failed in the angle leg connected to the column, it was found that increasing the thickness of angles, the loaded end distance, the edge distance and the number of bolts all lead to an increase in capacity. Double angle specimens with this type of failure mode also showed a higher capacity (34%) than its single angle counterpart.

Table 4-1 Summary of Test Results

Test specimen	Peak test capacity	Rotation of angle at peak load[1,2]	Beam end twist at peak load[2]	Displacement of bottom of connection at peak load	Failure Mode
	(kN)	(degrees)	(degrees)	(mm)	
(1)	(2)	(3)	(4)	(5)	(6)
1LA	280	3.52	3.58	19.5	Excessive twist of connection
1LB	288	2.31	2.42	29.6	Angle leg connected to the column failed
1LAa	299	1.64	1.71	28.3	Angle end tearing
1LBa	342	1.43	1.53	26.1	Angle end tearing
1L1	306	0.79	1.35	24.7	Angle leg connected to the column failed
1L2	346	4.67	5.23	24.7	Angle leg connected to the column failed
1L3	430	2.73	2.69	30.0	Angle leg connected to the column failed
1L4	378	4.41	4.49	23.4	Angle leg connected to the column failed
1L5	362	4.24	4.09	16.5	Angle leg connected to the column failed
1L6	368	0.75	1.63	31.1	Angle leg connected to the column failed
1L7	276	0.82	1.49	21.6	Angle leg connected to the column failed
1L8	290	0.31	0.28	21.0	Angle leg connected to the column failed
1L9	360	3.79	3.82	19.6	Angle leg connected to the column failed
1L10	291	0.84	0.72	17.7	Angle leg connected to the column failed
1L1a	329 (312)[3]	2.94	7.60	41.8 (21.2)[3]	Angle end tearing
1L2a	364 (321)[3]	3.15	5.20	31.5 (16.2)[3]	Angle end tearing
1L2aE	490	4.38	4.85	39.9	Angle end tearing
1L3a	345	1.03	1.40	14.4	Angle end tearing
1L4a	452	4.12	4.89	41.7	Angle end tearing
1L5a	412 (391)[3]	1.57	1.98	31.3 (17.1)[3]	Angle end tearing
1L6a	331	0.67	0.98	14.7	Angle end tearing
1L7a	312 (288)[3]	1.84	5.60	31.0 (13.1)[3]	Angle end tearing
1L8a	306	0.56	1.37	18.3	Angle end tearing
1L9a	454	3.50	3.85	29.3	Angle end tearing
1L10a	376	-0.07	2.30	30.5	Angle leg connected to the column failed
1L11a	367 (327)[3]	-1.16	0.68	34.1 (20.3)[3]	Angle end tearing
1L12	299	1.86	1.79	10.9	Angle leg connected to the column failed
1L13	372	1.97	1.62	14.6	Angle leg connected to the column failed
1L14	362	3.29	3.15	17.4	Angle leg connected to the column failed
2L1	400	0.50	0.92	15.8	Angle leg connected to the column failed
2L2	482	-0.33	-0.50	20.2	Beam web edge distance tearing
2L3	574	-0.45	-0.56	14.6	Beam web edge distance tearing
2L4	551	-0.39	-0.39	31.3	Beam web edge distance tearing
2L5	542	1.31	1.31	12.6	Beam web crippling under the load point
2L6	377	1.59	0.25	16.9	Angle leg connected to the column failed
2L7	347	-0.08	-0.11	13.5	Beam web tension and shear block failure
2L1a	476	-0.30	0.30	39.4	Beam web edge distance tearing
2L5a	620	0.16	0.18	17.0	Beam web edge distance tearing
2L6a	463	-0.72	-0.90	24.1	Beam web edge distance tearing
2L8a	415	-0.09	-0.20	15.0	Beam web tension and shear block failure

Notes: [1] Rotation about axis of the beam
[2] Positive angle of twist indicates twist in the direction of eccentricity
[3] At angle end tearing

Table 4-2 Material Properties

(1)	(2) Section Size	(3) Used in Test	(4) Heat	(5) Coupon ID	(6) Coupon Mark	(7) Elastic Modulus MPa	(8) Upper Yield Stress MPa	(9) Lower Yield Stress MPa	(10) Mean Static Yield Stress, F_y [1] MPa	(11) Static Ultimate Stress, F_u MPa	(12) Rupture Stress MPa	(13) Strain-hardening Strain %	(14) Strain at Ultimate Stress %	(15) Rupture Strain %	(16) Reduction of Area %
Beam W410x46	2L2	**1**		**A**	**1**	214000	410	389	379	492	429	2.75	22.9	32.3	56.4
					2	212000	422	389	381	493	423	2.89	18.7	31.3	57.4
					3	214000	415	383	368	500	424	2.55	17.3	30.2	51.6
					Mean	**213300**	**416**	**387**	**376**	**495**	**425**	**2.73**	**19.6**	**31.3**	**55.1**
W410x46	2L4, 2L5	**1**		**B**	**1**	208000	419	391	370	486	418	2.94	20.1	32.5	53.5
					2	212500	415	389	374	487	433	2.72	21.3	31.6	53.5
					3	208000	413	394	374	485	423	2.61	22.1	32.5	54.4
					Mean	**209500**	**416**	**391**	**373**	**486**	**425**	**2.76**	**21.1**	**32.2**	**53.8**
W410x46	2L7	**1**		**C**	**1**	209000	423	398	383	495	472	2.63	19.9	31.4	53.4
					2	211000	420	401	382	496	427	2.82	20.9	31.6	54.9
					3	210500	410	400	389	500	476	2.72	21.5	28.8	49.3
					Mean	**210000**	**418**	**400**	**385**	**497**	**458**	**2.72**	**20.8**	**30.6**	**54.2**
W410x74	2L3	**2**		**D**	**1**	207000	455	436	430	526	482	2.90	17.3	21.1	48.6
					2	209000	462	444	429	527	482	2.92	17.2	19.5	52.3
					3	217000	462	433	430	518	478	2.94	16.2	21.4	51.8
					Mean	**211000**	**460**	**438**	**430**	**524**	**481**	**2.92**	**16.9**	**20.7**	**50.9**
W410x46	1L2a	**3**		**E**	**1**	213500	446	423	411	478	444	3.78	21.6	28.6	41.6
					2	214000	435	418	404	470	394	4.03	18.6	32.1	49.4
					3	213500	443	418	403	473	478	4.42	19.3	26.0	36.1
					Mean	**213500**	**441**	**420**	**406**	**474**	**439**	**4.08**	**19.9**	**28.9**	**42.3**

Note: [1] From two individual readings

63

Table 4-2 Material Properties (cont'd)

Section Size	Used in Test	Heat	Coupon ID	Coupon Mark	Elastic Modulus	Upper Yield Stress	Lower Yield Stress	Mean Static Yield Stress, F_y^1	Static Ultimate Stress, F_u	Rupture Stress	Strain-hardening Strain	Strain at Ultimate Stress	Rupture Strain	Reduction of Area
					MPa	MPa	MPa	MPa	MPa	MPa	%	%	%	%
(1)	(2)	(3)	(4)	(5)	(6)	(7)	(8)	(9)	(10)	(11)	(12)	(13)	(14)	(15)	(16)
W410x100	1L3a	**3**	**F**	**1**	215500	446	419	413	481	409	4.40	18.4	32.6	57.1
				2	216000	452	417	410.5	483	407	3.76	18.4	35.0	57.2
				3	208500	441	416	403	480	415	3.95	19.7	32.1	55.7
				Mean	**213000**	**446**	**417**	**409**	**481**	**410**	**4.04**	**18.8**	**33.3**	**56.7**
Beam W410x46	2L1a, 2L6a	**4**	**G**	**1**	209000	438	413	401	513	461	2.79	17.8	30.5	49.7
				2	209000	450	416	406	509	468	2.82	19.8	29.7	48.0
				3	212500	442	422	409	520	463	2.70	19.0	28.2	50.0
				Mean	**210000**	**443**	**417**	**405**	**514**	**464**	**2.77**	**18.9**	**29.4**	**48.8**
W410x46	2L5a, 2L8a	**4**	**H**	**1**	209500	436	412	397	509	443	2.47	19.4	30.9	52.3
				2	220500	459	427	418	530	453	2.63	16.7	32.4	56.4
				3	210500	437	411	400	510	478	2.72	17.8	27.7	44.4
				Mean	**213500**	**444**	**417**	**405**	**516**	**458**	**2.61**	**18.0**	**30.3**	**54.3**

Note: [1] From two individual readings

Table 4-2 Material Properties (cont'd)

(1)	(2) Section	(3) Used in Test	(4) Coupon ID	(5) Coupon Mark	(6) Elastic Modulus	(7) Upper Yield Stress	(8) Lower Yield Stress	(9) Mean Static Yield Stress, F_y^1	(10) Static Ultimate Stress, F_u	(11) Rupture Stress	(12) Strain-hardening Strain	(13) Strain at Ultimate Stress	(14) Ultimate Strain	(15) Rupture Reduction of Area
					MPa	MPa	MPa	MPa	MPa	MPa	%	%	%	%
Angle	**L102x102x6.4**	1LA, 1LB	**V**	**1**	233000	—	—	548[2]	583	478	—	3.6	4.4	51.0
				2	198000	—	—	462[2]	541	539	—	3.5	3.6	50.0
				3	191500	—	—	424[2]	518	496	—	4.0	4.6	54.0
				4	203500	—	—	401[2]	511	516	—	6.2	6.4	57.0
				5	184000	—	—	421[2]	520	415	—	8.3	18.0	58.0
				Mean	**202000**	**—**	**—**	**451**	**535**	**489**	**—**	**5.1**	**7.4**	**54.0**
	L102x102x9.5	1L1 to 1L10 2L1 to 2L7	**W**	**1**	207000	347	313	311	476	392	1.52	20.1	34.8	57.0
				2	200000	335	318	309	477	391	1.50	18.0	34.1	58.0
				3	209500	348	325	312	474	402	1.85	16.7	34.2	56.0
				Mean	**205500**	**343**	**319**	**311**	**476**	**395**	**1.62**	**18.3**	**34.4**	**57.0**
	L152x102x9.5	1L1a to 1L11a 1L2aE 2L1a, 2L5a 2L6a, 2L8a	**X**	**1**	198500	343	308	293	447	346	2.84	23.6	37.8	65.5
				2	209000	330	311	296	449	345	2.21	21.1	36.1	64.2
				3	210500	328	306	290	441	339	2.08	22.6	38.6	63.3
				Mean	**206000**	**334**	**308**	**293**	**446**	**343**	**2.38**	**22.4**	**37.5**	**64.3**
	L102x102x6.4	1LAa, 1LBa	**Y**	**1**	206500	355	338	324	469	370	2.81	20.8	36.8	60.9
				2	205500	357	331	317	469	371	2.45	21.8	36.1	60.4
				3	204000	372	333	318	471	380	2.25	22.6	32.4	60.3
				Mean	**205000**	**361**	**334**	**320**	**470**	**374**	**2.50**	**21.7**	**35.1**	**60.5**
	L102x102x9.5	1L12 to 1L14	**Z**	**1**	209500	347	340	325	521	421	0.79	16.3	29.1	57.3
				2	202000	—	—	444[2]	551	445	—	7.8	19.5	52.5
				3	212000	341	335	327	521	431	0.95	18.0	28.4	56.8
				Mean	**208000**	**344**	**338**	**365**	**531**	**432**	**0.87**	**14.0**	**25.7**	**55.5**

Notes: [1] From two individual readings
[2] 0.2% offset yield strength

Table 4-3 As-built Dimensions of Test Specimens IV and V from Franchuk *et al.* (2002)

Test Specimen	e_{s1} (mm)	p_1 (mm)	p_2 (mm)	e_{s2} (mm)	e_g (mm)	d_{slot} (mm)	l_{slot} (mm)	t (mm)
(1)	(2)	(3)	(4)	(5)	(6)	(7)	(8)	(9)
IV	24.8	102.3	101.8	22.7	27.4	20.3	31.4	6.477
V	31.7	103.3	102.2	33.0	33.8	26.8	42.1	6.342
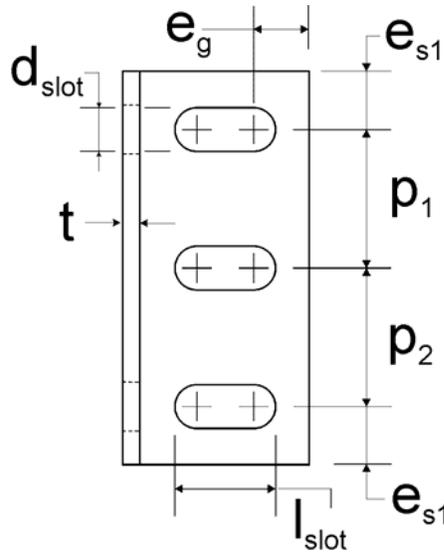
Table 4-4 Material Properties of Angle from Franchuk *et al.* (2002)

Coupon ID	Modulus of Elasticity (MPa)	Mean Static Yield (MPa)	Static Ultimate Strength (MPa)
(1)	(2)	(3)	(4)
1	203300	357	489
2	207400	360	495

Table 4-5 Summary of Franchuk *et al.* (2002) Tests Results IV and V

Test specimen	Peak test capacity (kN)	Displacement of bottom of connection at peak load (mm)	Beam end twist at peak load[1] (degrees)	Rotation of angle at peak load[1] (degrees)
(1)	(2)	(3)	(4)	(5)
IV	240	10.2	-0.54	-0.06
V	269	10.1	0.04	-0.09

[1] Positive angle of twist indicates twist in the direction of eccentricity

Table 4-6 Summary of Test Parameters - Current Test Program

| Parameter | Test Specimen | | Nominal Values of Parameters | | Constants in each comparison | | | |
					Bolt pitch	Slot Length	Beam	Plate Washer
(1)	(2)	(3)	(4)	(5)	(6)	(7)	(8)	(9)
Bottom end distance	1L2a	1L2aE	32	47	Large	Long	Uncoped	No
Plate washer	1L2a	1L4a	No	Yes	Large	Long	Uncoped	
	2L2	2L4	No	Yes	Large	Long	Uncoped	
Slot length (mm)	1L2a	1L9a	55	28	Large		Uncoped	No
Pretension	1L5a	1L6a	Yes	No	Large	Long	Coped	No
	2L4	2L5a	No	Yes	Large	Long	Uncoped	Yes
Torsion brace	1L1a	1L11a	No	Yes	Standard	Long	Uncoped	No
Bolt pitch (mm)	1L1a	1L2a	76	102		Long	Uncoped	No
	1L8a	1L6a	76	102		Long	Coped	No
	2L1a	2L2	76	102		Long	Uncoped	No
	2L7	2L8a	76	102		Long	Coped	No
Coped flange	1L2a	1L6a	Uncoped	Coped	Large	Long		
	1L1a	1L8a	Uncoped	Coped	Standard	Long		No
	2L1a	2L7	Uncoped	Coped	Standard	Long		No
	2L2	2L8a	Uncoped	Coped	Large	Long		No
Beam end rotation (^{o})	1L1a	1L7a	-0.41 [1]	3.5 [1]	Standard	Long	Uncoped	No
	2L1a	2L6a	-0.25 [1]	3.5 [1]	Standard	Long	Uncoped	No
Web thickness (mm)	1L3a	1L6a	10.0	7.0	Large	Long	Coped	No
	2L2	2L3	7.0	9.7	Large	Long	Uncoped	No
Bolt diameter (mm)	IV	V	19.1	25.4	Large	Long [2]	Coped	No
	1LAa	1LBa	19.1	25.4	Large	Long [2]	Coped	Yes

Notes: [1] Measured beam end rotation at peak load
[2] 1.65 times of bolt diameter

- Nominal large bolt pitch = 102 mm
- Nominal standard bolt pitch = 76 mm
- Nominal long slot length = 55 mm
- Nominal short slot length = 28 mm
- Nominal plate washer thickness = 9.5 mm
- All bolts are 22.2 mm (7/8 in.) diameter ASTM A325 bolts unless noted otherwise

Table 4-7 Summary of Test Parameters for Specimens that Failed at Angle Leg Connected to the Column

Parameter	Test Specimen		Nominal Values of Parameters	
(1)	(2)	(3)	(4)	(5)
Thickness (mm)	Group 1 [1]	Group 3 [3]	6.4	9.5
Top end distance, e_{s3} (mm)	Group 2 [2]	Group 3 [3]	32	58
Edge distance, e_{g1} (mm)	1L12	1L13	32	50
No. of bolts	1L12	1L14	2	3
No. of angles	Group 2 [2]	Group 4 [4]	Single	Double

Notes: [1] Group 1 includes test specimens: 1LB (capacity = 288 kN)
  [2] Group 2 includes test specimens: 1L1, 1L7, 1L8 and 1L10 (average capacity = 291 kN)
  [3] Group 3 includes test specimens: 1L2 to 1L6 and 1L9 (average capacity = 374 kN)
  [4] Group 4 includes test specimens: 2L1 and 2L6 (average capacity = 389 kN)
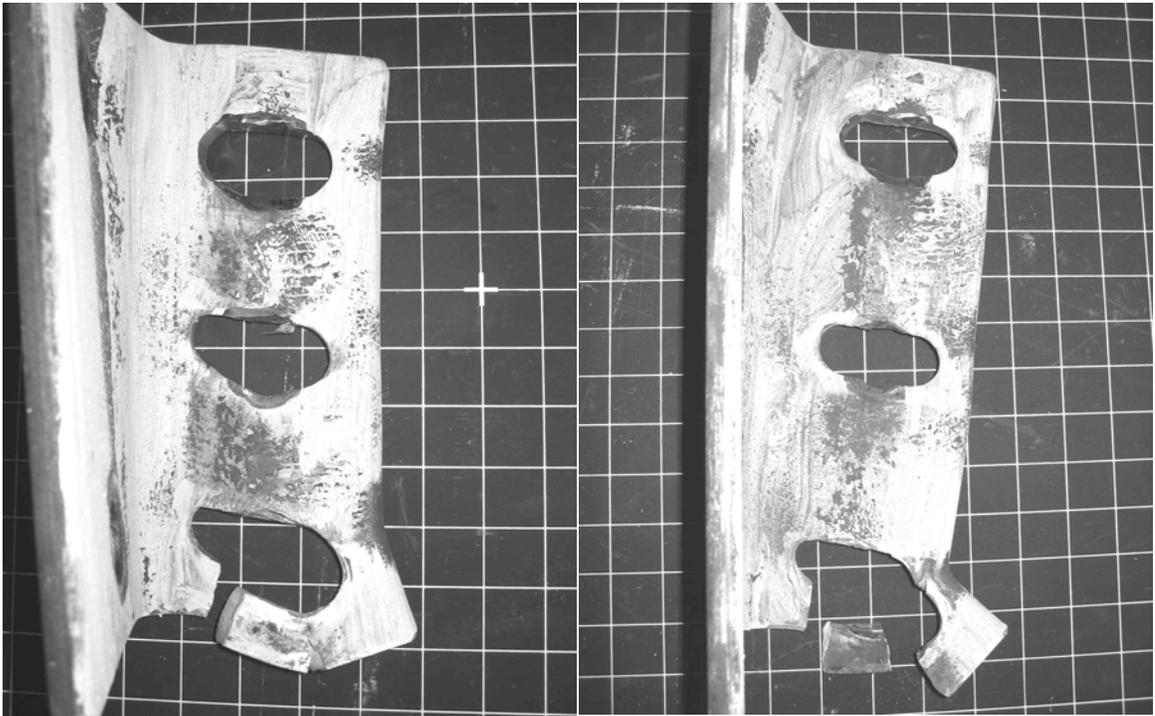
a) Test Specimen 1L1a   b) Test Specimen 1L2a

Figure 4-1 Angle End Tearing Failure
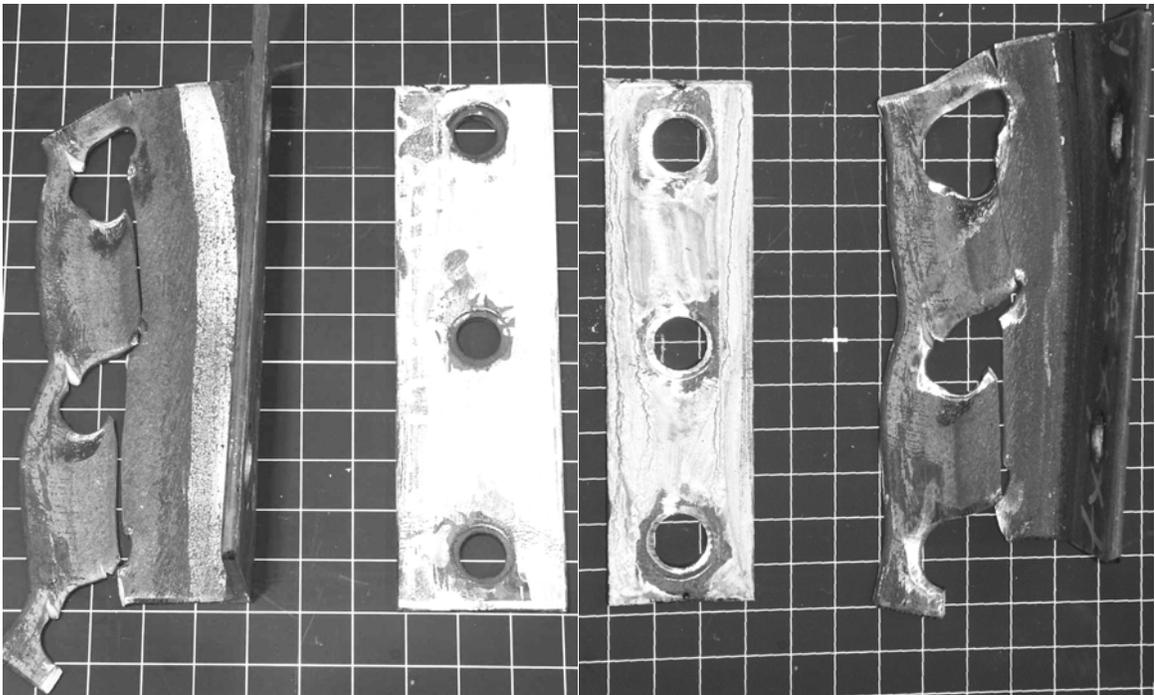
a) Test Specimen 1LAa   b) Test Specimen 1LBa

Figure 4-2 Angle End Tearing Failure (Followed by Rupture of Shear Area)

a) Test Specimen 2L1a b) Test Specimen 2L2

Figure 4-3 Beam Web Edge Distance Tearing Failure
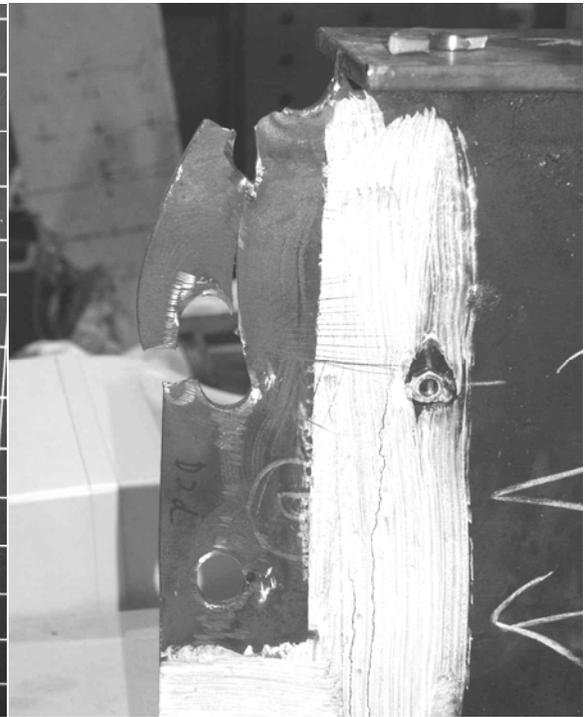
a) Test Specimen 2L7 b) Test Specimen 2L8a

Figure 4-4 Tension and Shear Block Failure of Coped Beam Web
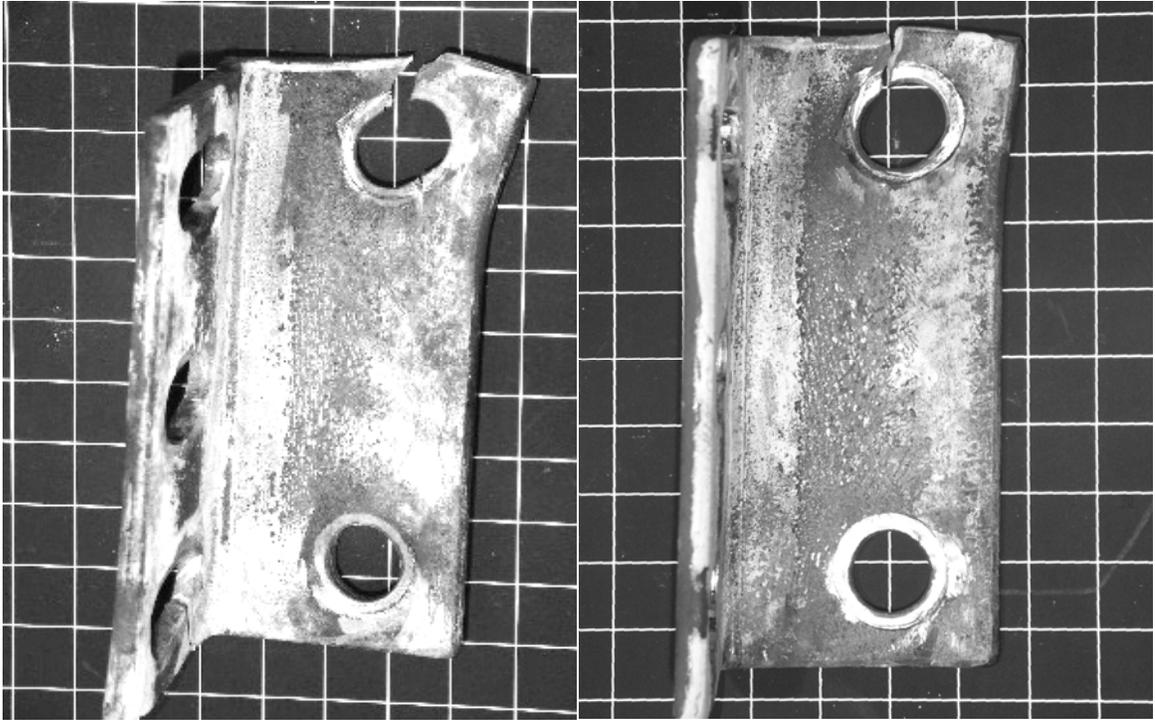
a) Test Specimen 1L1	b) Test Specimen 1L7

Figure 4-5 Failure of Angle Leg Connected to the Column (Top End Distance Tearing)
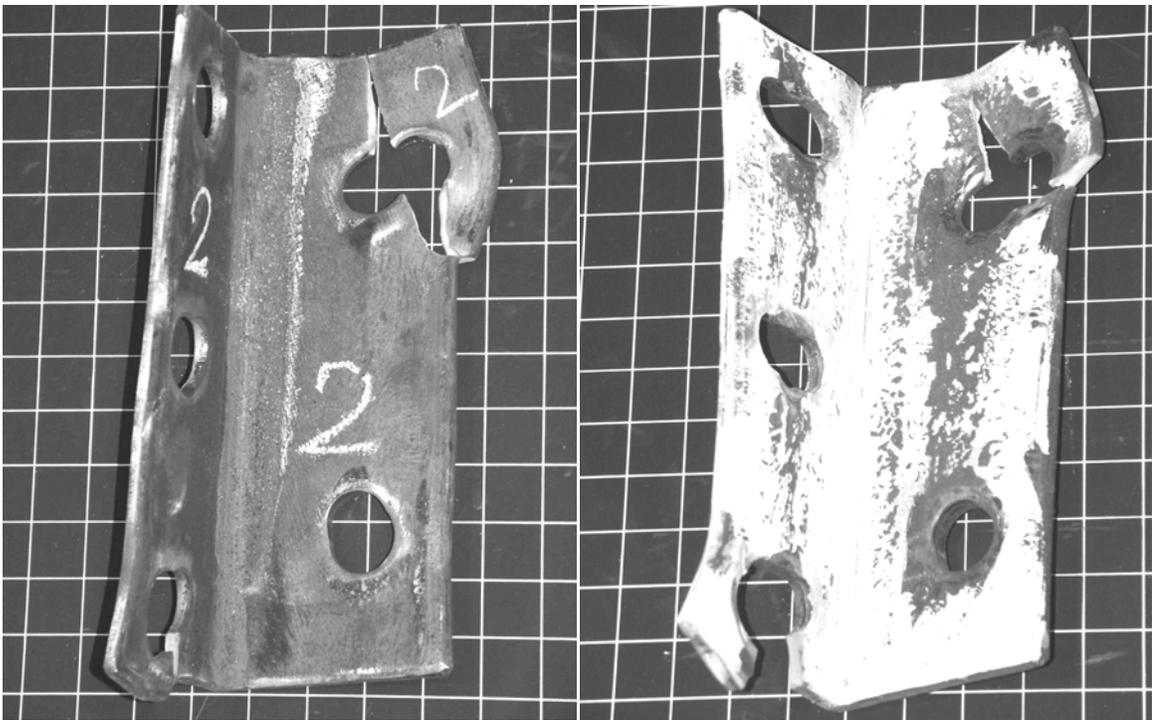
a) Test Specimen 1LB	b) Test Specimen 1L2

Figure 4-6 Failure of Angle Leg Connected to the Column (Top Corner Tearing)
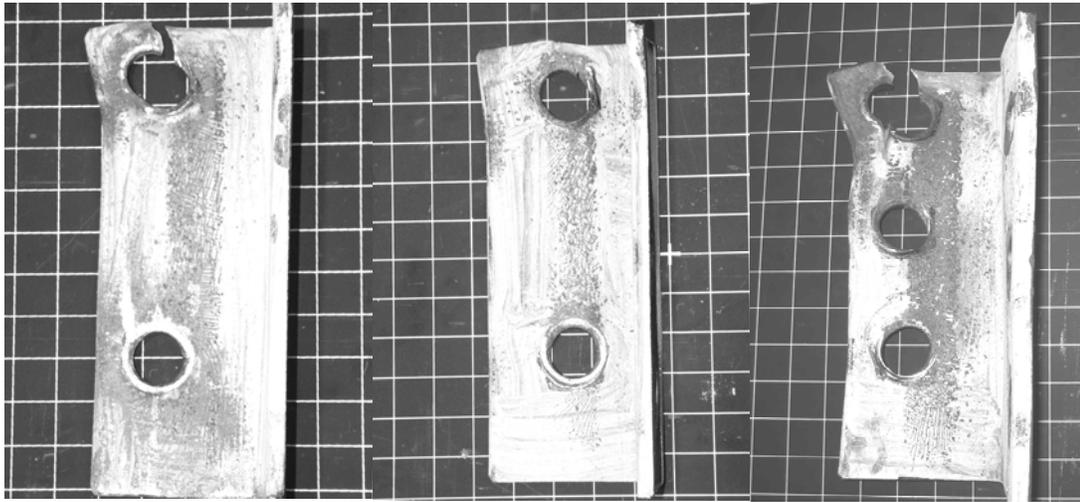
a) Test Specimen 1L12   b) Test Specimen 1L13   c) Test Specimen 1L14

Figure 4-7 Failure of Angle Leg Connected to the Column (Top End Distance Tearing)

Test Specimen 2L5

Figure 4-8 Failure by Web Crippling
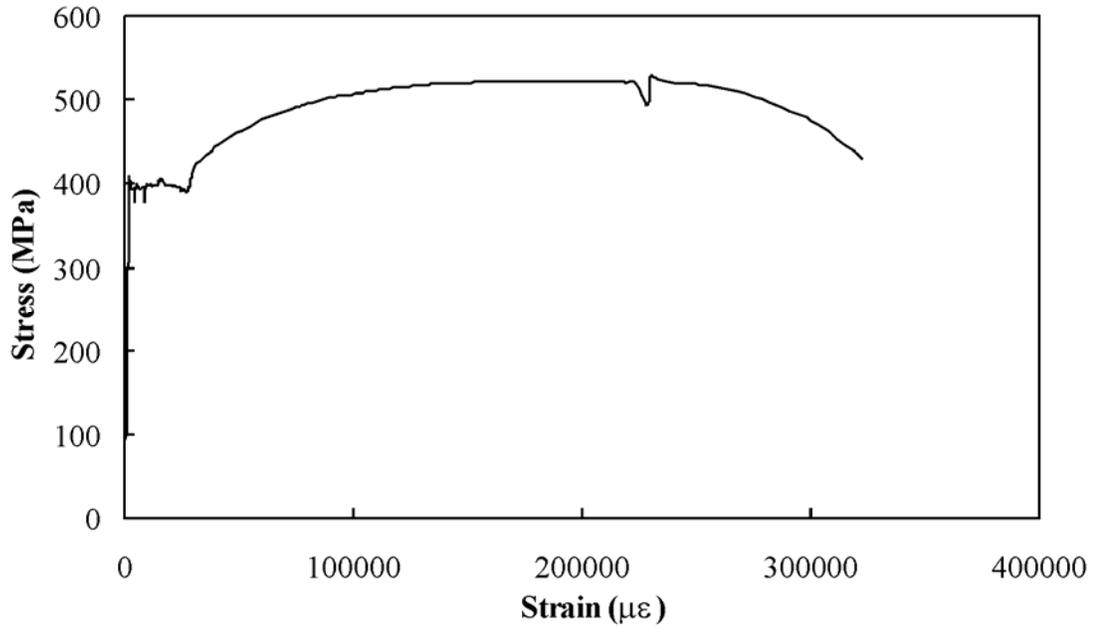
a) Beam Material (Coupon A1)
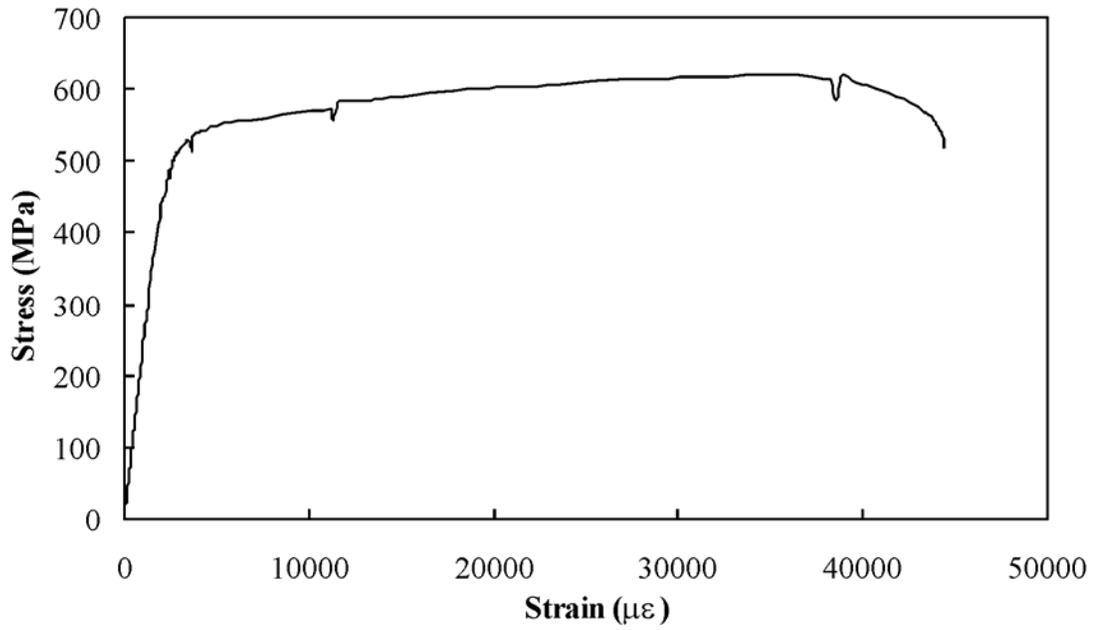
b) Tested Angles (Coupon V1)

Figure 4-9 Typical Tension Stress vs. Strain Response
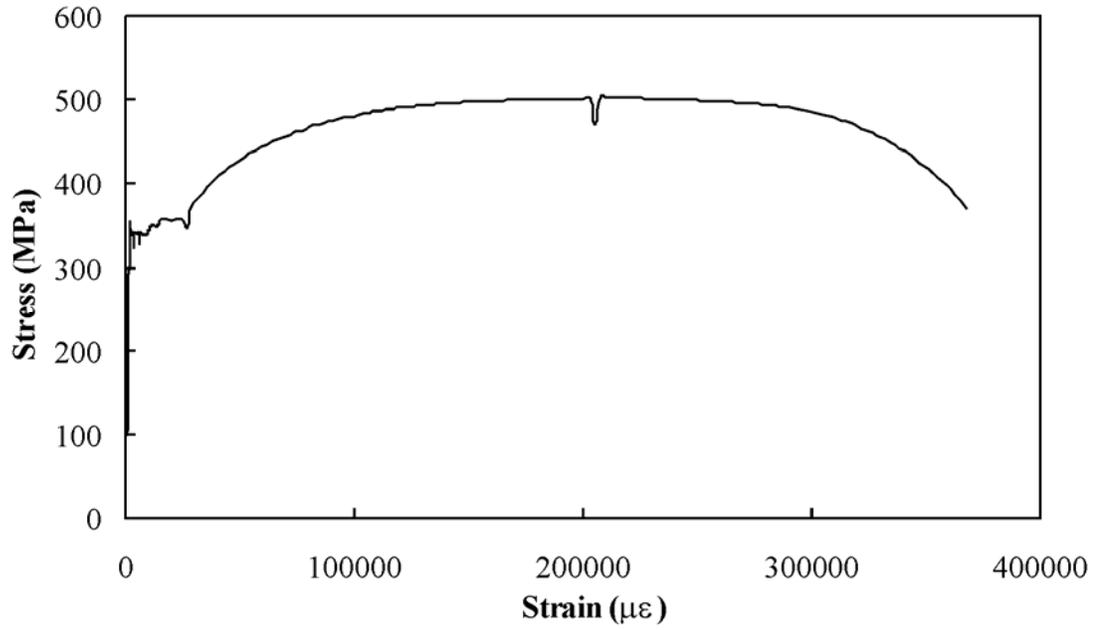
c) Virgin Angles (Coupon Y1)

Figure 4-9 Typical Tension Stress vs. Strain Response (cont'd)
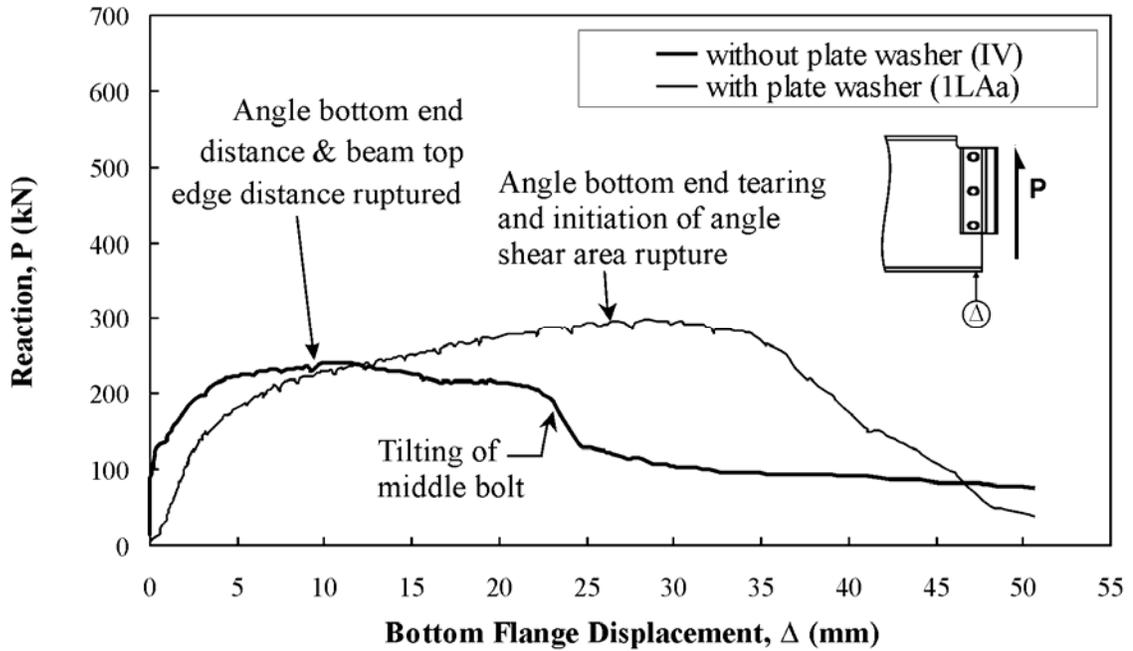
Figure 4-10 Connection Reaction vs. Bottom Flange Displacement – Effect of Plate Washer
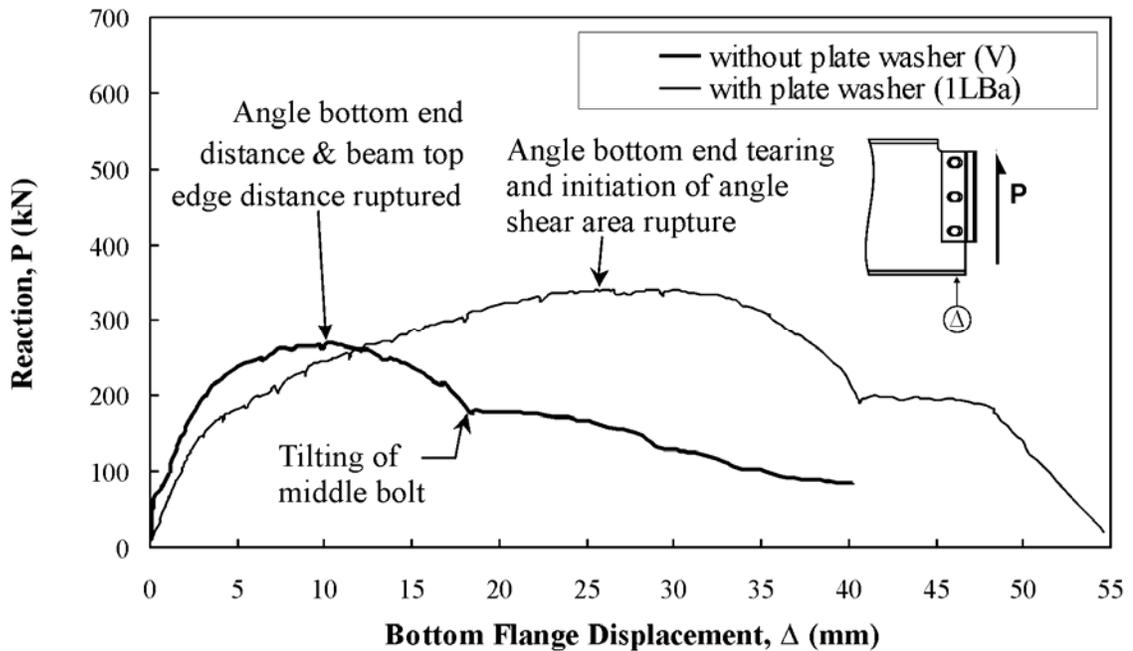
Figure 4-11 Connection Reaction vs. Bottom Flange Displacement – Effect of Plate Washer
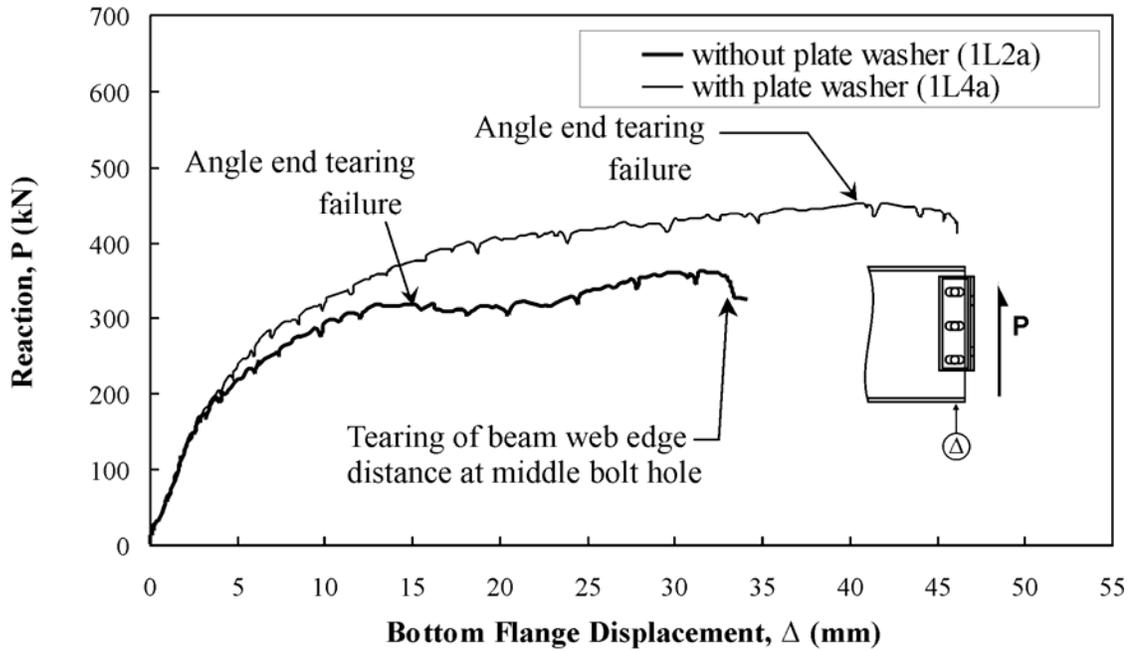
Figure 4-12 Connection Reaction vs. Bottom Flange Displacement – Effect of Plate Washer
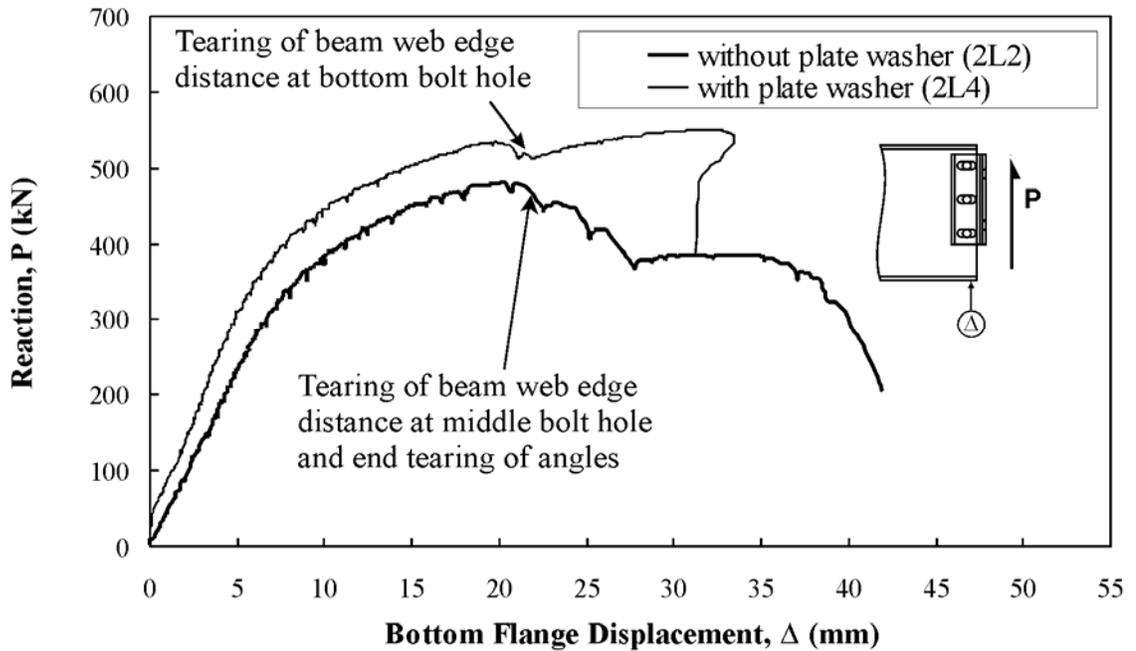
Figure 4-13 Connection Reaction vs. Bottom Flange Displacement – Effect of Plate Washer
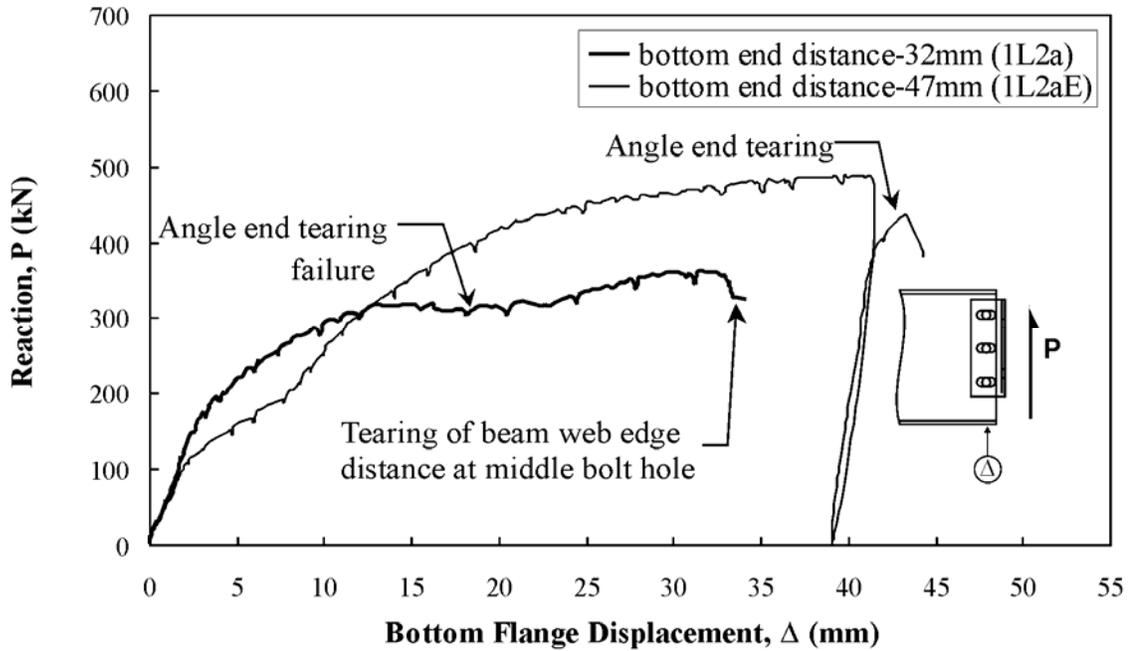
Figure 4-14 Connection Reaction vs. Bottom Flange Displacement – Effect of Bottom End Distance
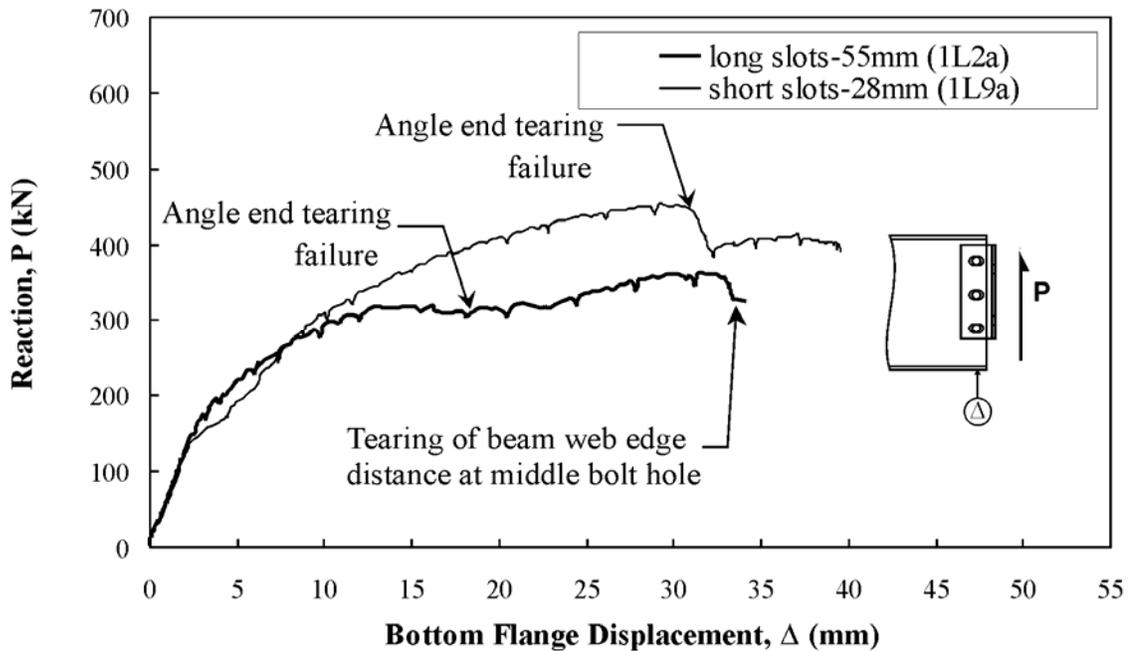
Figure 4-15 Connection Reaction vs. Bottom Flange Displacement – Effect of Slot Length
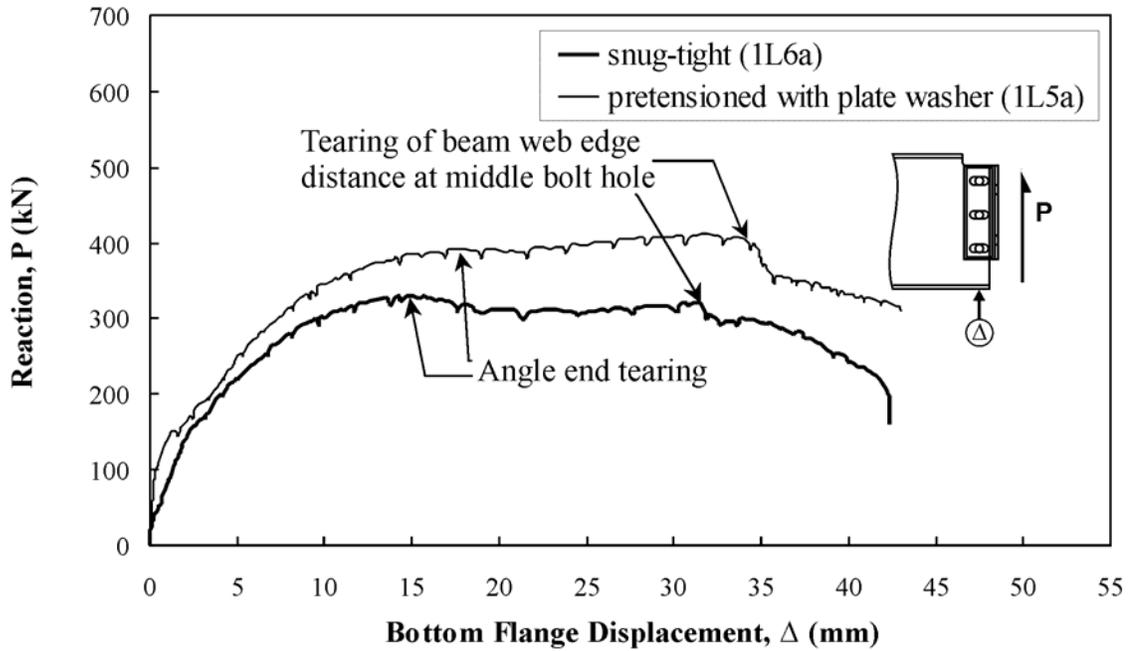
Figure 4-16 Connection Reaction vs. Bottom Flange Displacement – Effect of Bolt Pretension
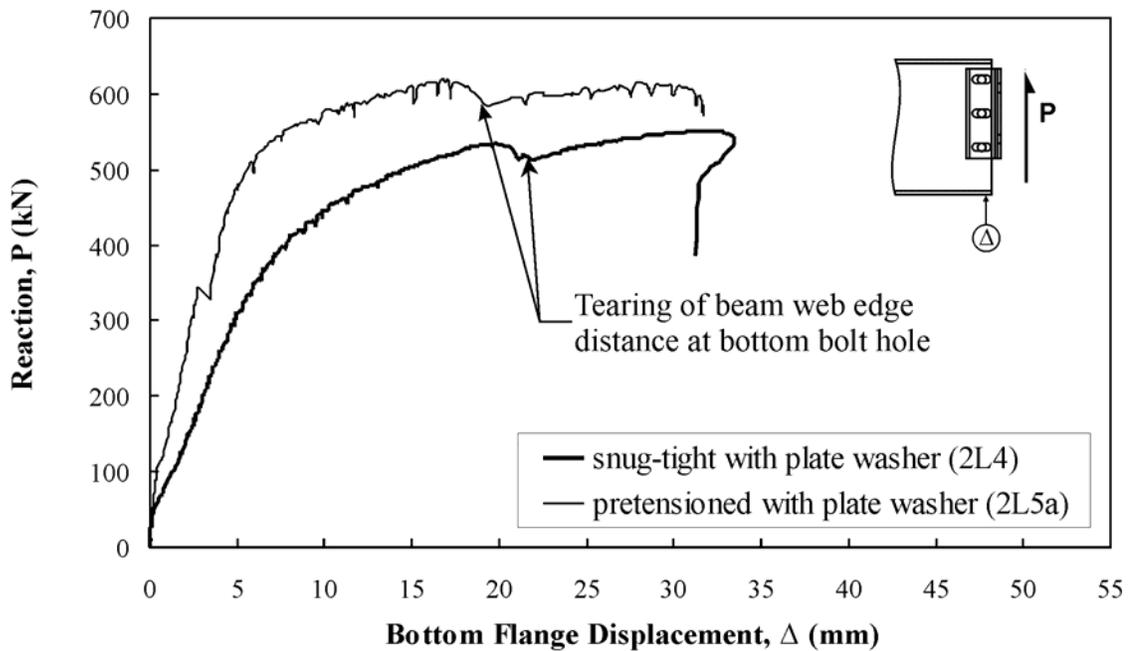
Figure 4-17 Connection Reaction vs. Bottom Flange Displacement – Effect of Bolt Pretension

78
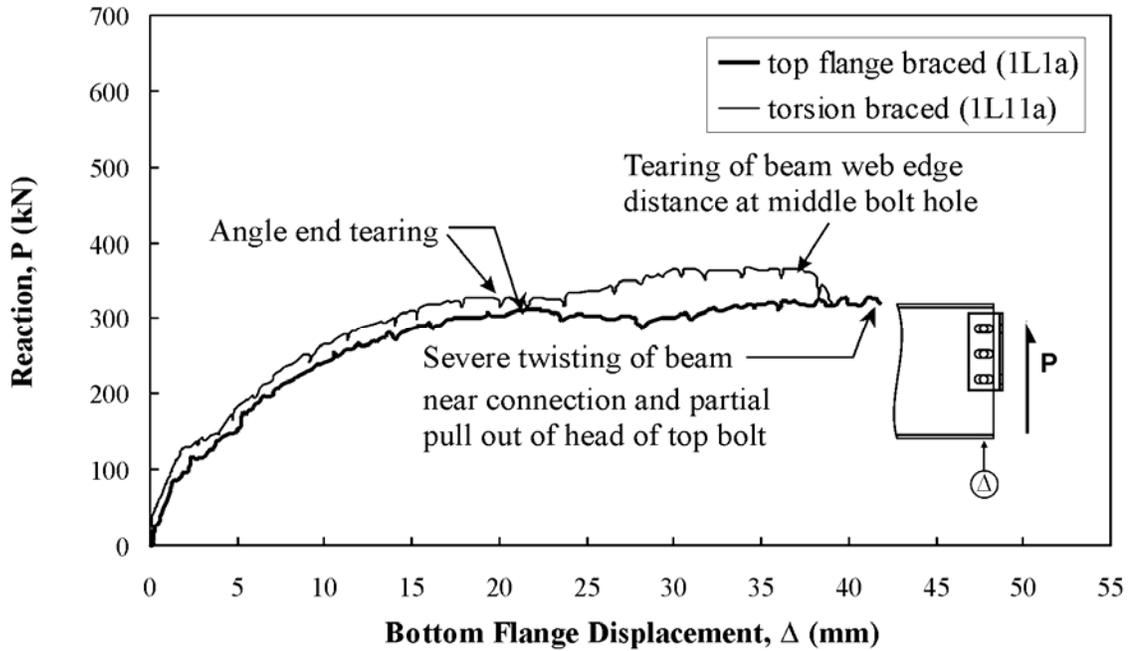
Figure 4-18 Connection Reaction vs. Bottom Flange Displacement – Effect of Torsion Bracing
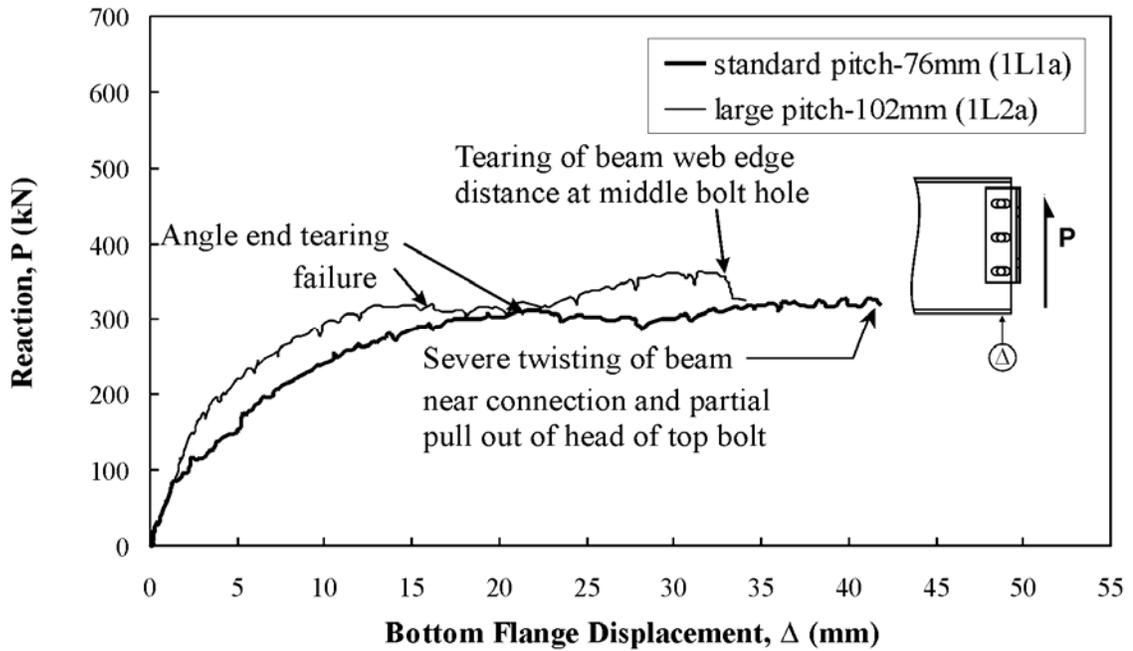
Figure 4-19 Connection Reaction vs. Bottom Flange Displacement – Effect of Bolt Pitch

79
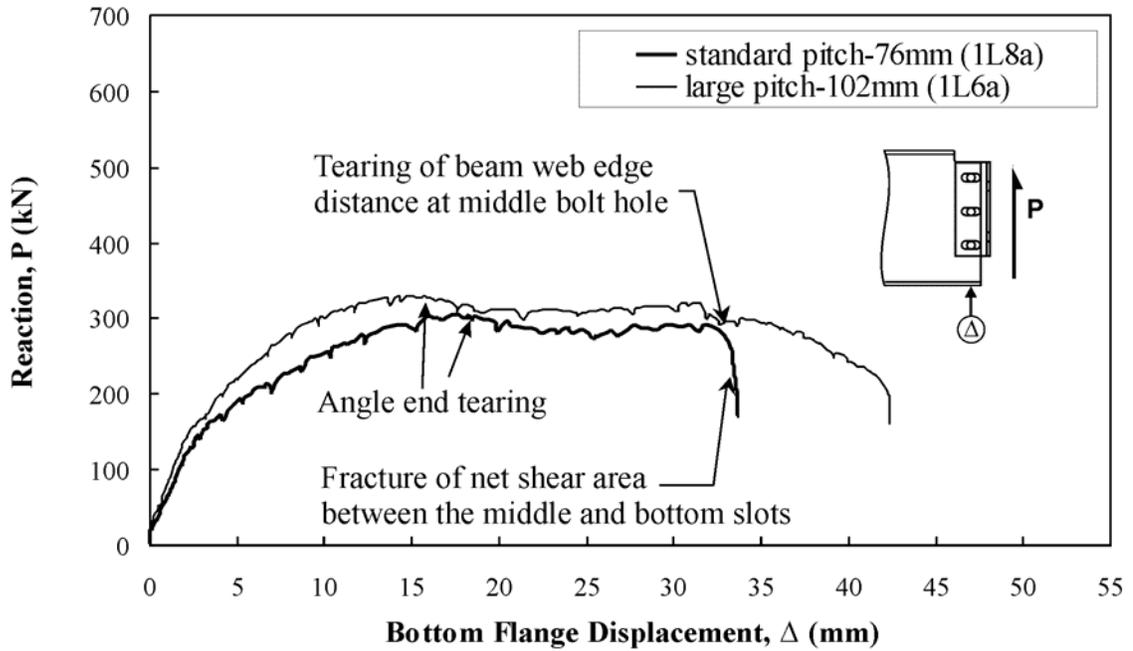
Figure 4-20 Connection Reaction vs. Bottom Flange Displacement – Effect of Bolt Pitch
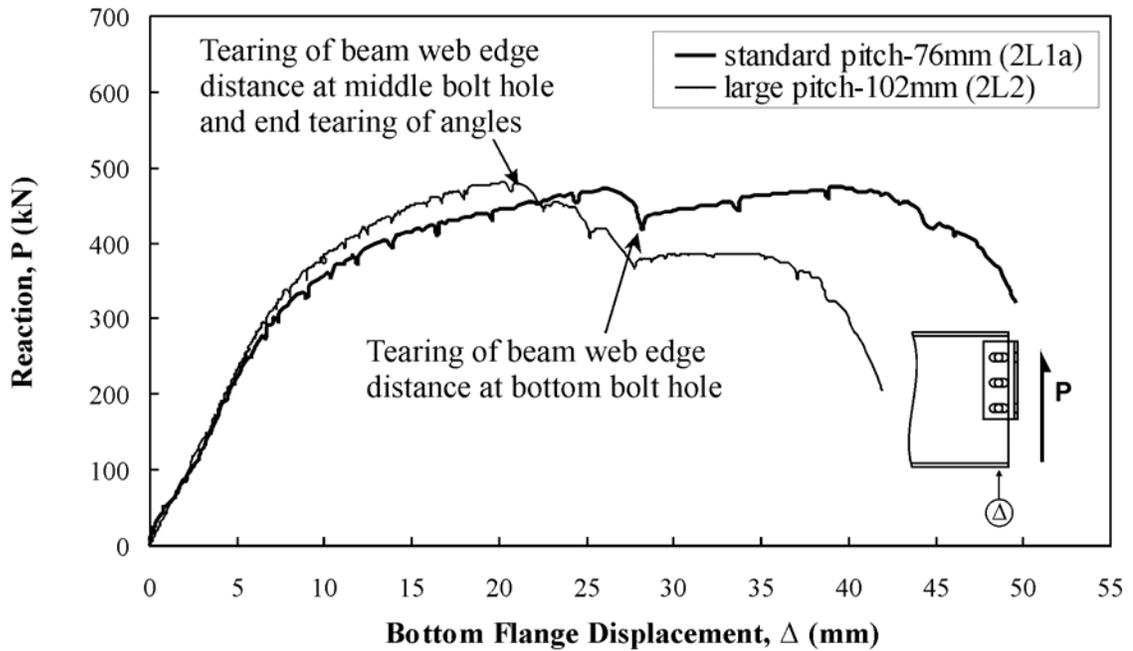
Figure 4-21 Connection Reaction vs. Bottom Flange Displacement – Effect of Bolt Pitch
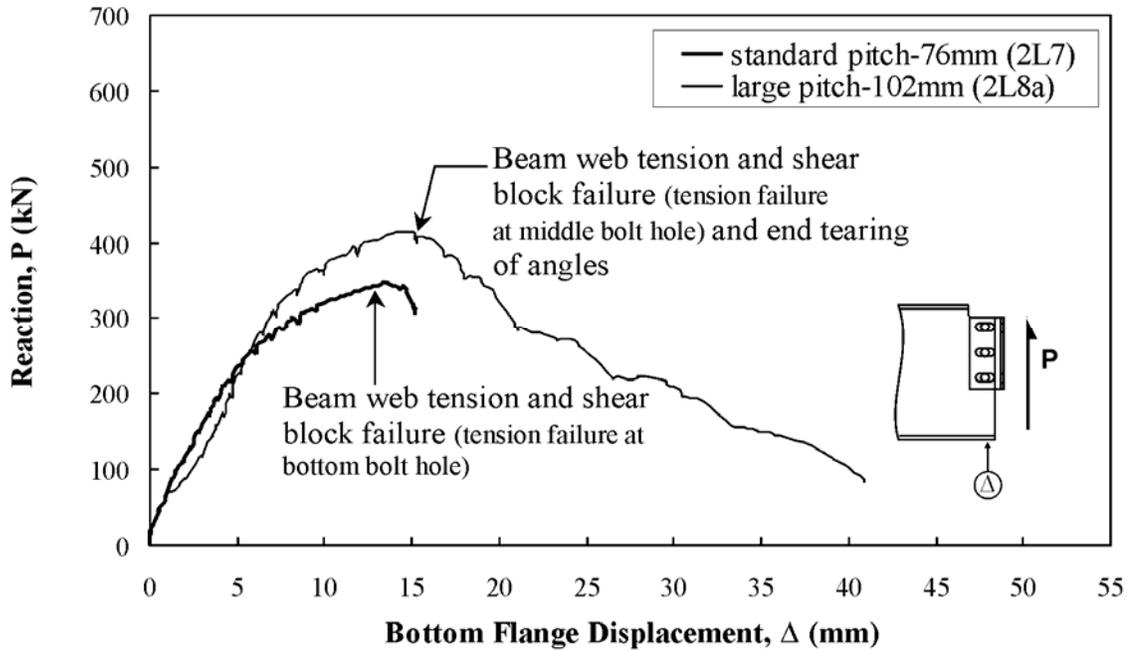
Figure 4-22 Connection Reaction vs. Bottom Flange Displacement – Effect of Bolt Pitch
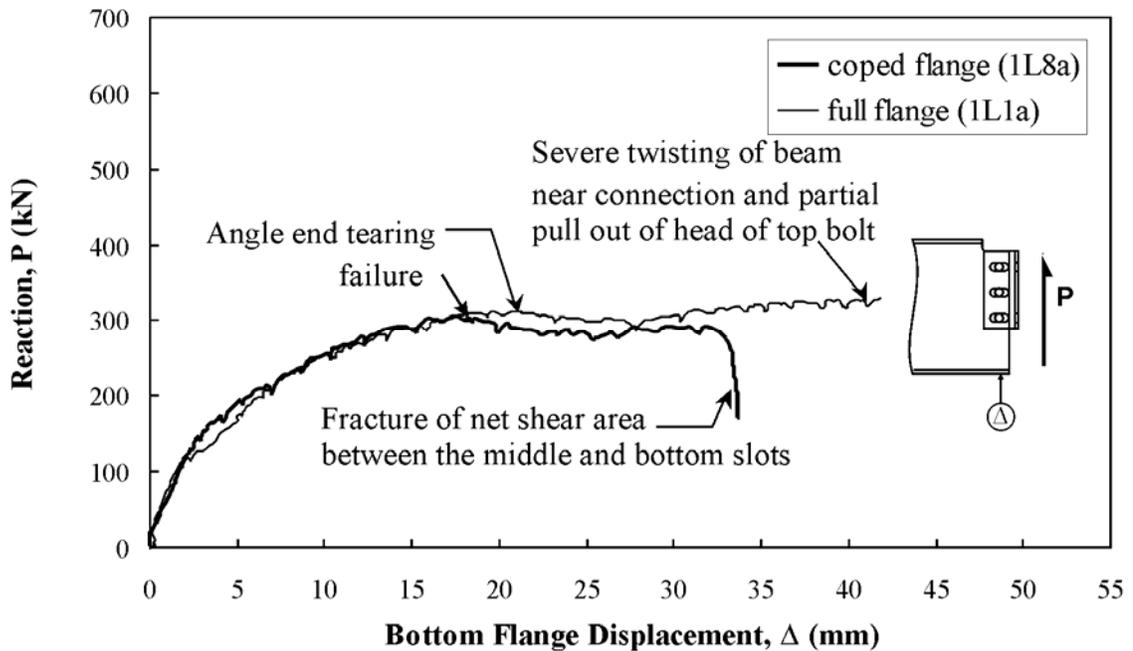
Figure 4-23 Connection Reaction vs. Bottom Flange Displacement – Effect of Flange Cope
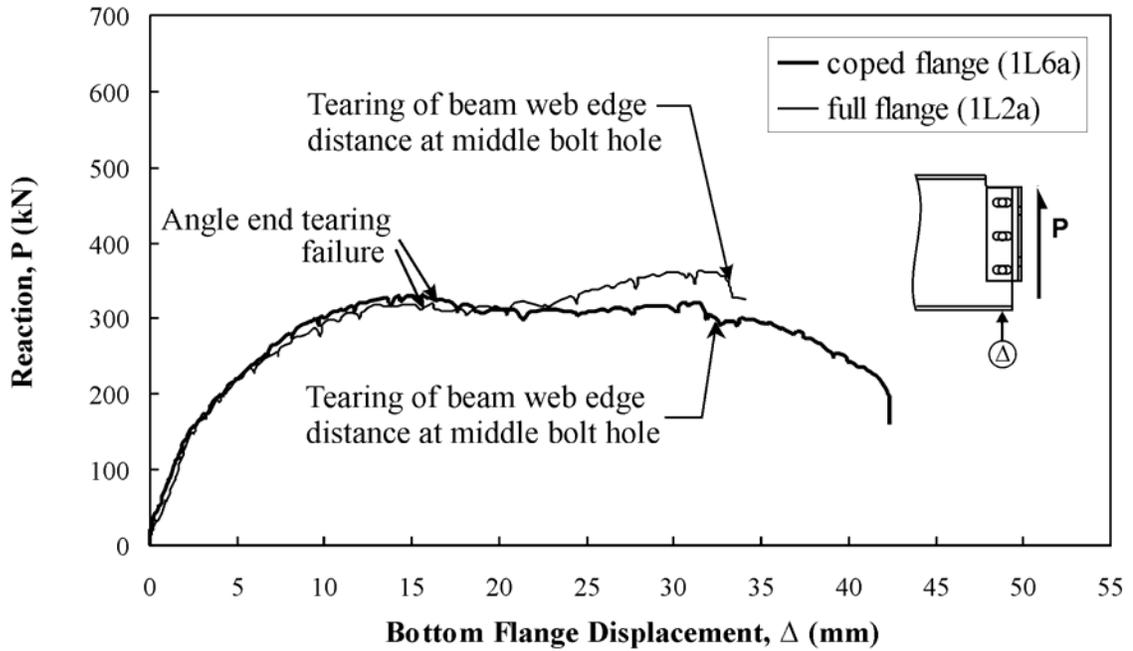
Figure 4-24 Connection Reaction vs. Bottom Flange Displacement – Effect of Flange Cope
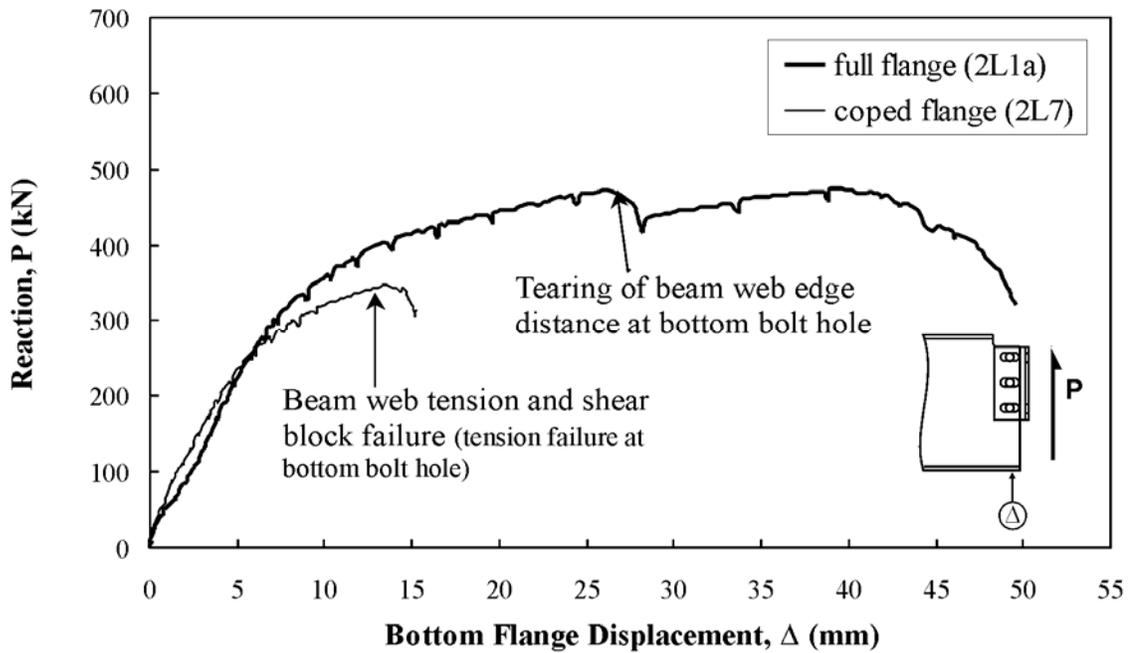
Figure 4-25 Connection Reaction vs. Bottom Flange Displacement – Effect of Flange Cope

82
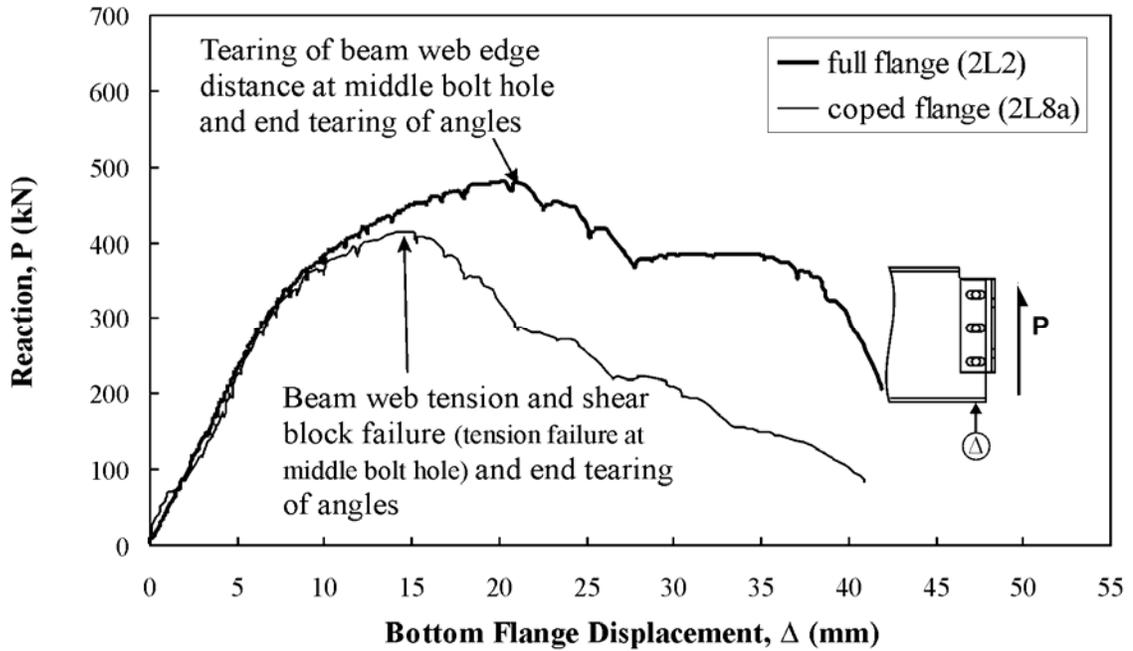
Figure 4-26 Connection Reaction vs. Bottom Flange Displacement – Effect of Flange Cope
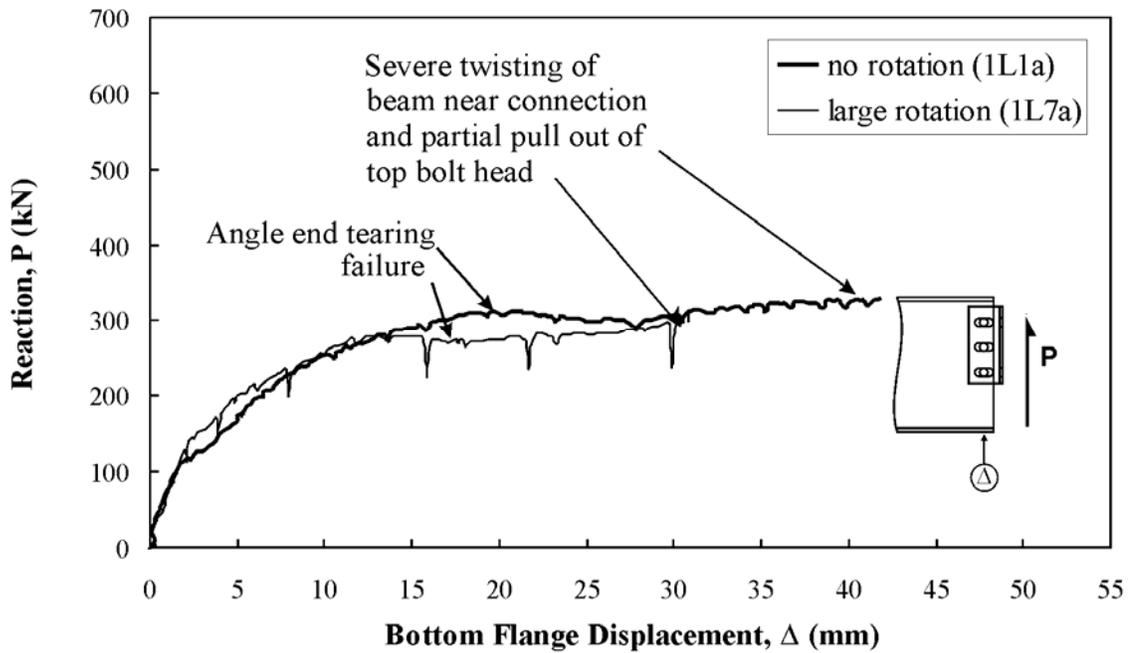
Figure 4-27 Connection Reaction vs. Bottom Flange Displacement – Effect of End Rotation
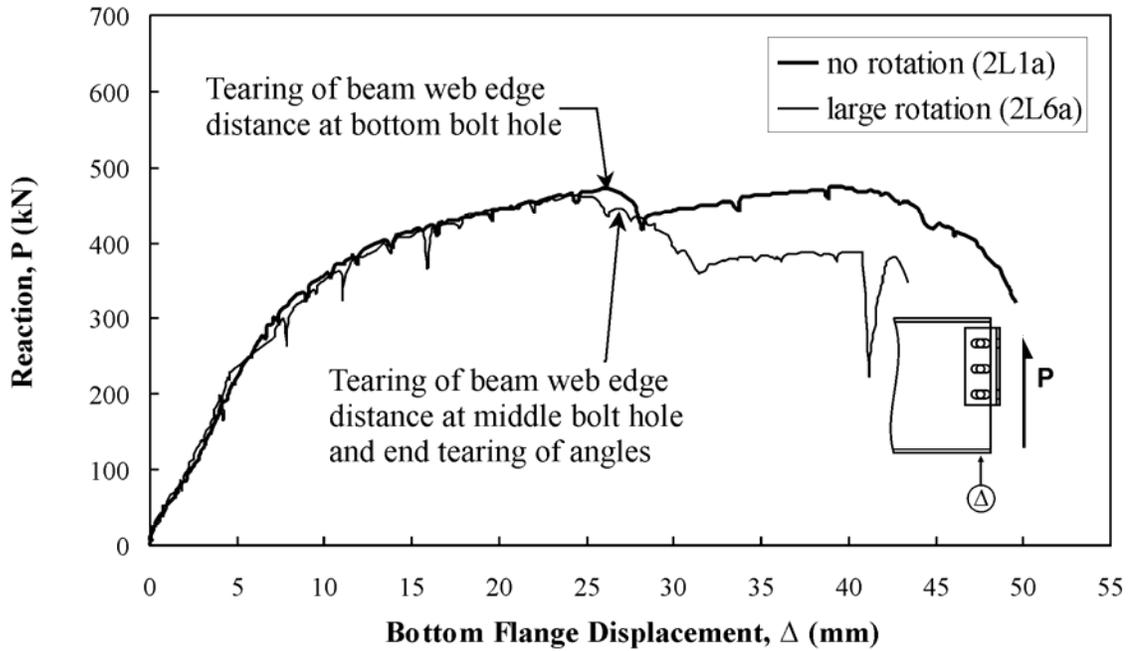
Figure 4-28 Connection Reaction vs. Bottom Flange Displacement – Effect of End Rotation
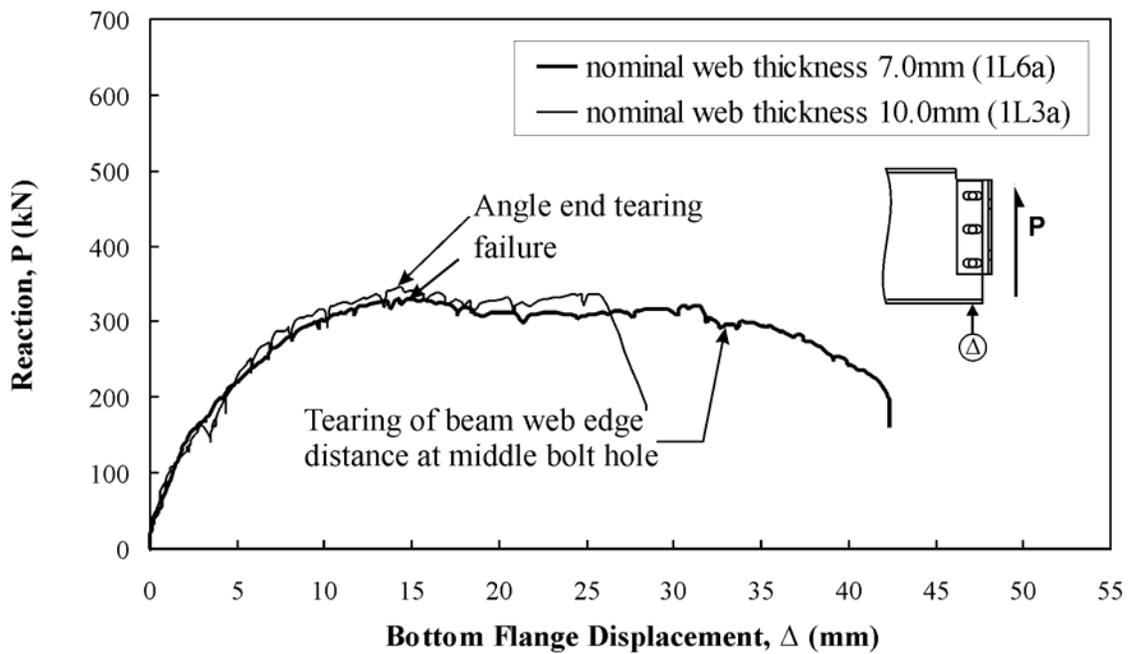
Figure 4-29 Connection Reaction vs. Bottom Flange Displacement – Effect of Web Thickness
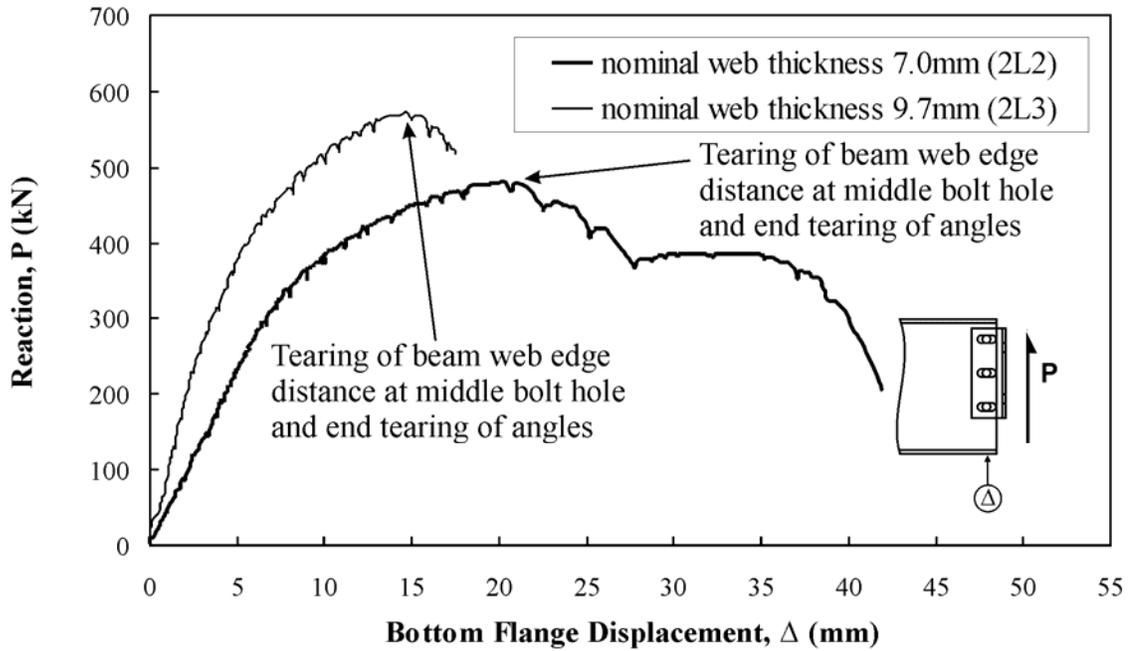
Figure 4-30 Connection Reaction vs. Bottom Flange Displacement – Effect of Web Thickness
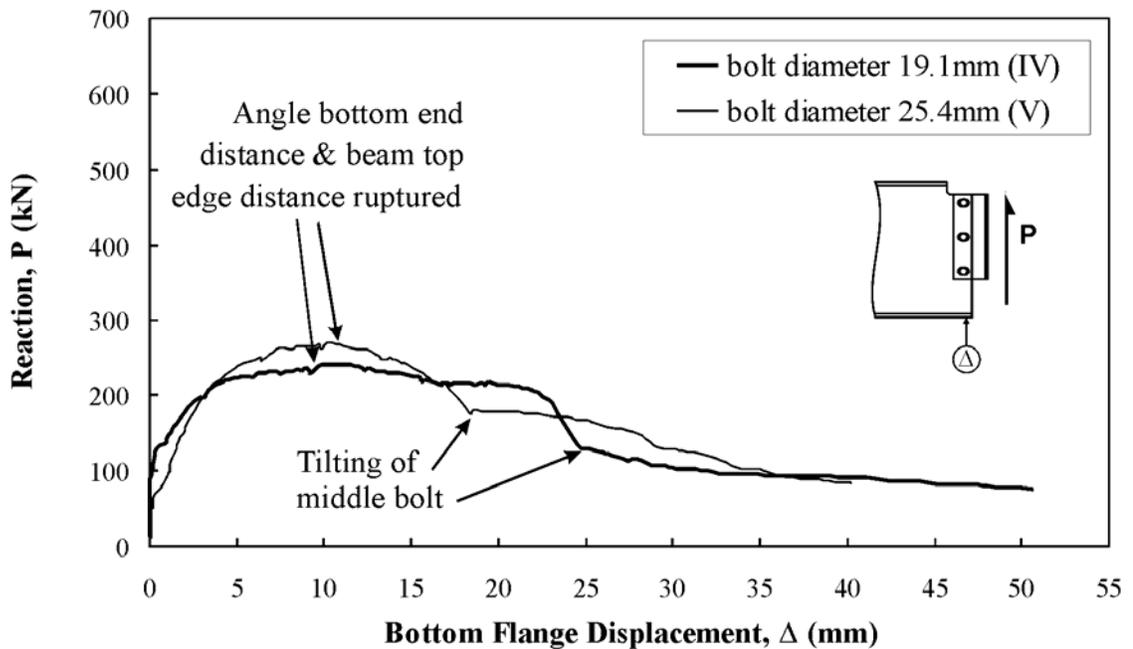
Figure 4-31 Connection Reaction vs. Bottom Flange Displacement – Effect of Bolt Diameter
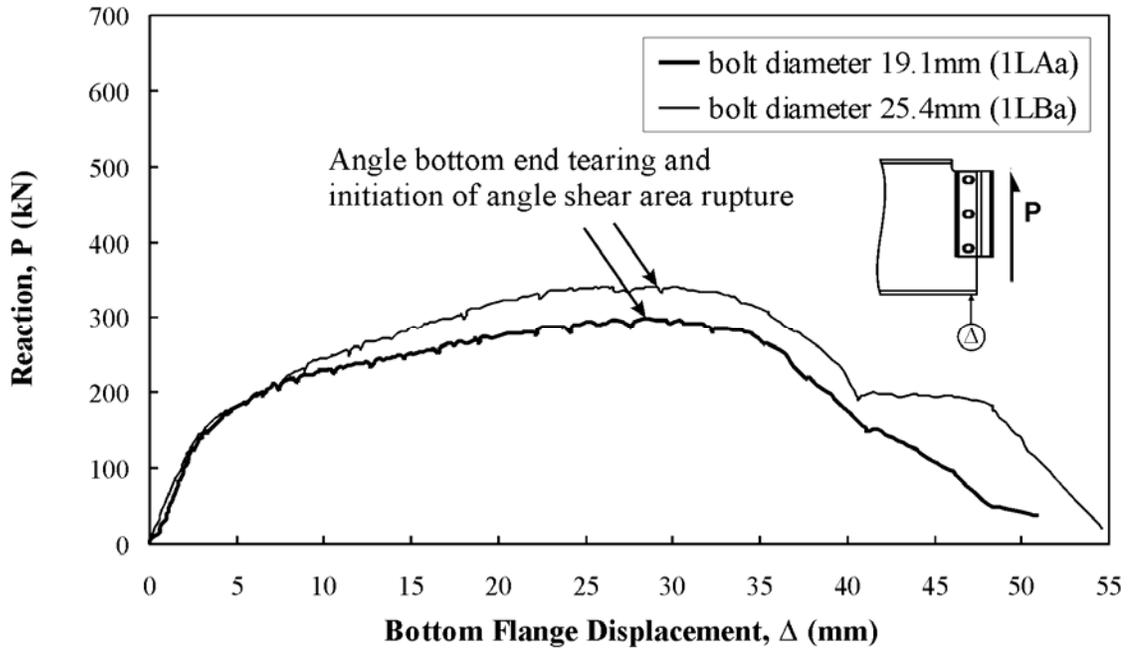
Figure 4-32 Connection Reaction vs. Bottom Flange Displacement – Effect of Bolt Diameter
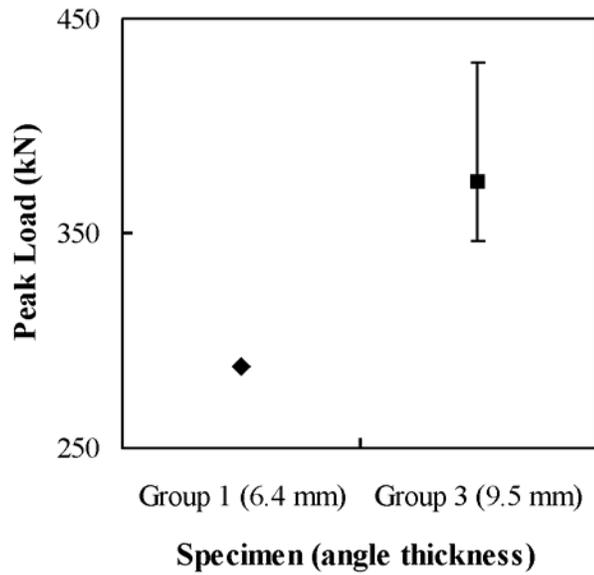
Figure 4-33 Effect of Angle Thickness on Capacity of Connection

that Failed in the Leg Connected to the Column
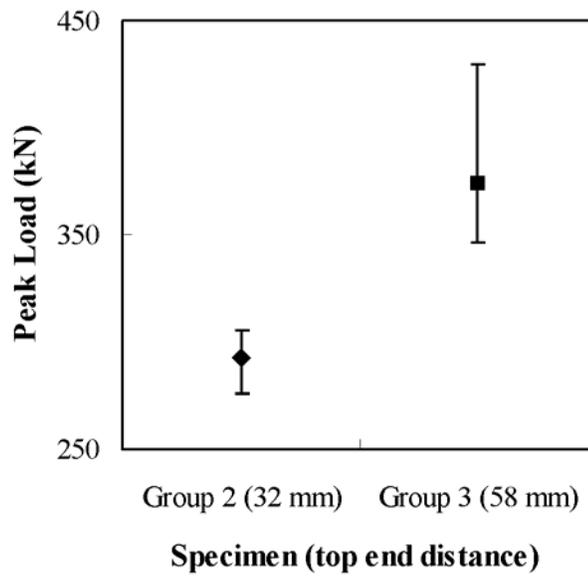
Figure 4-34 Effect of Top End Distance on Capacity of Connection that Failed in the Leg Connected to the Column
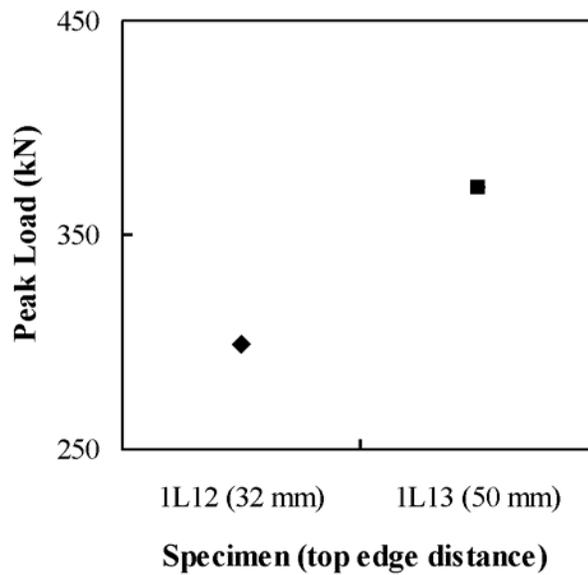
Figure 4-35 Effect of Edge Distance on Capacity of Connection that Failed in the Leg Connected to the Column
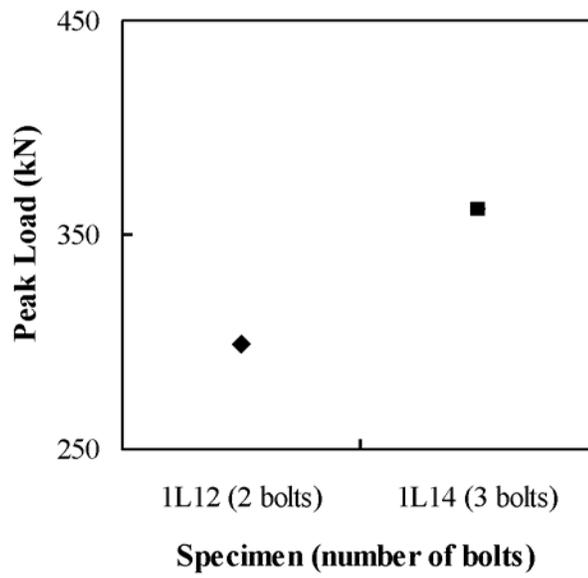
Figure 4-36 Effect of Number of Bolts on Capacity of Connections
that Failed in the Leg Connected to the Column
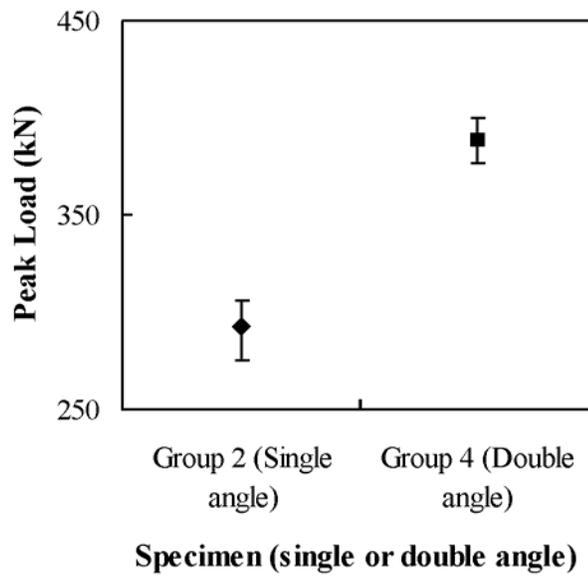
Figure 4-37 Effect of Number of Angles on Capacity of Connections
that Failed in the Leg Connected to the Column

5 Prediction of Test Results

This section presents the predicted capacities for the test specimens in the experimental program. A wide range of failure modes were observed: shear failure of angle leg connected to the beam, beam web tension and shear block failure, edge distance tearing of the beam web, angle loaded end tearing, failure of angle leg connected to the column, and crippling of the beam web under the load point. A total of 40 tests were conducted in this research program. In predicting the capacities of the specimens, test specimen 2L5 is not included due to the fact that it did not fail at the connection. The beam web crippled under the load point before the connection failed.

Assessments of current North American steel design standards, namely, CAN/CSA–S16–01 (CSA, 2001) and AISC 2005 (AISC, 2005) are presented. Both their ability to predict the observed failure modes and the load carrying capacities are assessed.

The capacities predicted from various design equations are based on as-built dimensions and measured material properties for the test specimens included in this test program. The as-built dimensions and measured material properties can be found in Table 3-1 and Table 4-2, respectively. The holes in the beam web were drilled and the long slotted holes in the angles were sub-punched and reamed to the required size. However, the short slots and circular holes on the angles were punched. In order to be consistent with current design practice, a 2 mm allowance is made for punched holes in the net area calculations. In all cases, the resistance factor is taken as 1.0.

5.1 Prediction Models

5.1.1 Angle End Tearing Failure

Of all the 29 single angle specimens in the current test program, 13 specimens failed by angle end tearing. As discussed in sections 4.1 and 4.3, five of these specimens were able to carry more load after the angle end tearing failure. In predicting the capacity of the connections, the angle end tearing load will be considered as the connection capacity since very large deformations (about 35 mm of bottom flange deflection) were required for these specimens to reach the higher capacity observed in the tests.

A description of this failure mode and photographs of failed specimens are presented in Chapter 4. Failure of the angle took the form of bending and tearing of the angle end distance. No sign of beam web failure was observed in any of these test specimens when the angle failed by end tearing, except for some localized yielding near the bearing area.

Three possible related failure modes predicted by the current North American steel design standards are investigated, namely, shear rupture of the angle through the slotted holes, yielding of gross area, and bolt bearing on the beam web and angle leg. According to CSA–S16–01 and AISC 2005, the shear capacity of web framing angles is equal to the lesser of:

$$V_u = 0.6 \, A_{gv} \, F_y \qquad\qquad [5\text{-}1]$$

$$V_u = 0.6 \, A_{nv} \, F_u \qquad\qquad [5\text{-}2]$$

where,

V_u is the nominal connection shear capacity,

A_{gv} is the gross shear area, taken as the product of total length of the angle and the angle thickness,

A_{nv} is the net shear area, taken as the product of the vertical net length across the centres of the bolt holes and the angle thickness,

F_y is the material yield strength, and

F_u is the material tensile strength.

The shear capacity is governed by either yielding of the gross shear area (Equation [5-1]) or rupture through the net shear section (Equation [5-2]).

The bearing capacity of bolted connections predicted by CSA–S16–01 can be expressed as:

$$B_u = 3.0 \, t \, n \, d \, F_u \qquad\qquad [5\text{-}3]$$

where,

B_u is the nominal bearing capacity,

t is the thickness of connected material,

n is the number of bolts in bearing, and

d is the bolt diameter.

Although it is possible that one bolt in a bolt group may have a smaller capacity (e.g., the bolt closest to a free end), the current version of CSA–S16 does not specifically address this issue. According to CSA–S16–01, all bolts in a bolt group have the same bolt bearing capacity. Furthermore, the bearing capacity is the same for all types of holes, including standard holes, oversized holes, short slots and long slots.

The bearing provisions of AISC 2005 vary with the type of bolt hole. The nominal bearing capacity of a bolt in a standard hole or short slot, where deformation of the bolt holes at service load is not a design consideration is given as:

$$B_u = 1.5\, l_c\, t\, F_u \leq 3.0\, d\, t\, F_u \qquad\qquad [5\text{-}4]$$

where,

l_c is the clear distance, in the direction of applied force, between the bolt holes or to the edge of the material.

The left part of Equation [5-4] consists of the shear tearing resistance of the clear distance between the bolt holes or between the outer bolt and the unloaded end of the connected plate. The upper limit expressed in Equation [5-4] is identical to the bearing capacity used in CSA–S16–01. From Equation [5-4], it can be seen that the full bearing capacity of a bolt is not developed until the clear distance is at least 2.0 times the bolt diameter, d.

The bearing capacity for a plate with a long slotted hole perpendicular to the direction of the force is given as:

$$B_u = 1.0 \, l_c \, t \, F_u \leq 2.0 \, d \, t \, F_u \hspace{3cm} \text{[5-5]}$$

All the angles used in the experimental program were fabricated with the minimum bottom end distance, e_{s2}, specified in CSA–S16–01 and AISC 2005 for ASTM A325 bolts, except for specimen 1L2aE. The minimum end distance requirement in CSA–S16–01 and AISC 2005 for is approximately 1.75 times the bolt diameter for sheared edges, and 1.25 times the bolt diameter for rolled, sawn, or gas-cut edges. Moreover, for beam-framing angles with sheared edges installed with 7/8 in. (22.2 mm) and 1 in. (25.4 mm) bolts, an end distance of 32 mm is allowed by both standards. This is the case for the specimens in the current test program that failed by angle end tearing.

Kulak *et al*. (1987) proposed a minimum end distance for bolts as a function of the applied bearing stress, σ_b, as follows:

$$\frac{l_e}{d} \geq 0.5 + 0.715 \, \frac{\sigma_b}{F_u} \hspace{3cm} \text{[5-6]}$$

where l_e is the end distance from the centre of the fastener to the unloaded end and σ_b is the bearing stress exerted on the plate material by the fastener. According to Equation [5-6], the end distance requirements of 1.75 times the bolt diameter for sheared edges and 1.25 times the bolt diameter for rolled, sawn or gas-cut edges, as described in CSA–S16–01, correspond to a ratio of bearing stress to material tensile strength of 1.75 and 1.0, respectively.

Kulak *et al*. (1987) also report various requirements that must be satisfied for the end distance of bolted connections in limit states design. One of the requirements relates to the minimum end distance of 1.5 times the bolt diameter for any type of edge connections. This represents the average of 1.75 times the bolt diameter for sheared edges and 1.25 times the bolt diameter for rolled, sawn, or gas-cut edges as specified in the current North American design standards. Another requirement consists of satisfying Equation [5-6] at the end zone of a connection. Lastly, a limit of 3.0 times of the material ultimate tensile strength, F_u, is placed on the bearing strength of the plate material in contact with the bolt.

Although the end and edge distance requirements in CSA–S16–01 and AISC 2005 also apply to connections with slotted holes, the failure mechanism at the end of connections with slotted holes is different from the failure mechanism for standard holes. As shown in the photographs of failed specimen in Figures 4-1a and 4-1b, the end distance did not fail by shear and tension splitting: they failed by bending and bearing failure of the end distance. In contrast, tests on connections with standard holes have shown that failure occurs by splitting out of the fastener through the end of the plate due to insufficient end distance (Kulak *et al.*, 1987). Tests by Wald *et al.* (2002) also showed that the end distance failure results in a lower strength for slotted holes than for standard holes.

5.1.1.1 Proposed Prediction Method for Angle End Tearing Failure

It was observed that the bottom end distance below a slotted hole did not fail by shear and splitting, as is usually observed with circular holes. Instead, the bottom end distance failed in a combined bending and bearing mode with eventual tearout below the bolt. Moreover, as discussed later, the current design standards do not provide a good prediction of the failure mode and the capacity for the test specimens that failed by angle end tearing. To address these issues, a new prediction model is proposed to predict the bearing capacity for a bolt in a slotted hole connection.

The method proposed here combines the bearing capacity of bolts on the connected material, shear resistance of the clear distance or the collapse capacity of the clear distance below the bolt. The capacity of each bolt in a connection is taken as the least of the above capacities. A prediction model for the end distance of a connection with slotted holes was derived based on the plastic collapse mechanism illustrated in Figure 5-1. Figure 5-1a shows the definition of slot length, l_{slot}, the diameter of the ends of the slot, d_{slot}, and the clear end distance, l_c. From the collapse mechanism shown in Figure 5-1b, the collapse load P_c can be readily obtained from:

$$ P_c = \frac{8\, M_p}{(l_{slot} - d_{slot})} \qquad\qquad [5\text{-}7] $$

where,

P_c is the collapse load of end distance at the end of angle,

l_{slot} is the slot length, and

d_{slot} is the diameter of the slot.

M_p is the plastic moment capacity of the clear end distance, given as:

$$M_p = \frac{l_c^2 t}{4} F_y \qquad [5\text{-}8]$$

Substitution of Equation [5-8] into Equation [5-7] leads to the following expression for the bolt force required to cause plastic collapse of the clear end distance, l_c:

$$P_c = \frac{2 \, l_c^2 \, t \, F_y}{(l_{slot} - d_{slot})} \qquad [5\text{-}9]$$

Equation [5-9] provides an upper limit to the bearing capacity of the bolt closest to the end of the member. The capacity of an end bolt can be limited either by the plastic collapse or shear failure of the clear distance below the bolt. The shear strength is taken as 60% of the tensile strength of the material. The capacity of the clear distance below the bolt is therefore taken as the lesser of:

$$B_u = P_c \qquad [5\text{-}10]$$

$$B_u = 1.2 \, l_c \, t \, F_u \qquad [5\text{-}11]$$

The upper limit of the bearing capacity of the bolts in slotted holes is taken as:

$$B_u = 1.5 \, d \, t \, F_u \qquad [5\text{-}12]$$

This limit is similar to the existing AISC 2005 provisions, except that a coefficient of 1.5 is used instead of 2.0 for connections with long slots. The coefficient of

1.5 is chosen so that the mean test-to-predicted ratio is close to 1.0 and the coefficient of variation (COV) is minimized for the tests conducted in this research program. It is suspected that the end distance of the single angle specimens failed before the rest of the connection mobilized the full bearing strength. The capacity of the connection can be taken as the sum of the capacity of individual bolts in the connection. The general expression for the bearing capacity of a single bolt can therefore be expressed as:

$$B_u = \frac{2\, l_c^2\, t\, F_y}{(l_{slot} - d_{slot})} \le 1.2\, l_c\, t\, F_u \le 1.5\, d\, t\, F_u \qquad [5\text{-}13]$$

5.1.2   Beam Web Edge Distance Tearing

Six of the test specimens with double angles and uncoped beam, namely, 2L1a, 2L2, 2L3, 2L4 and 2L6a, failed by tearing of the edge distance at or near the peak load. Although this mode of failure is different from bolt bearing failure, bolt bearing is still a possible failure mode for this type of connection. CSA–S16–01 and AISC 2005 use Equation [5-3] and Equation [5-4], respectively, as the bearing capacity of bolts in standard circular holes. As seen in Section 5.1.1, the AISC 2005 provisions for slotted holes are a function of deformation requirements.

5.1.2.1   Failure Mechanism

Bearing failure in a bolted connection can be characterized by the splitting of the bolted plate in the end zone due to insufficient end distance, or piling up of material in front of the fastener hole with excessive deformation, or often a combination of the above two failure modes (Kulak *et al.*, 1987). It is assumed that the bearing stress exerted by the bolt on a circular bolt hole or short slots reaches three times of the material tensile strength for the second type of failure to occur. The bearing strength is limited to 2 times material tensile strength for connection with long slots to account for the larger deformation of connection with long slots than the one with short slots and circular holes. These are reflected in Equation [5-3] for standard holes and short slots, and the second part of Equation [5-5] for long slots. However, specimens in the current test program failed by tearing of the beam web edge distance, rather than failing in bearing. The

minimum edge distance used for the fabrication of the steel beams is not sufficient to develop the full bearing capacity of the bolt. It is suspected that the beam web edge distance ruptured and the full bearing strength of beam web was not reached.

5.1.3 Tension and Shear Block Failure of Beam Web

Two double angle specimens with a coped beam (2L7 and 2L8a) failed by tension and shear block failure of beam web. Three prediction models are being compared, namely CSA–S16–01, AISC 2005 and a model proposed by Franchuk *et al.* (2002), which was developed from the analysis of test results from coped beams.

5.1.3.1 Prediction Models

According to CSA–S16–01 the tension and shear block failure of coped beams is taken as the lesser of the following two equations:

$$P_r = 0.5A_{nt}F_u + 0.6A_{gv}F_y \qquad\qquad [5\text{-}14]$$

$$P_r = 0.5A_{nt}F_u + 0.6A_{nv}F_u \qquad\qquad [5\text{-}15]$$

where:

A_{nt} is the net tensile area, A_{gv} is the gross shear area, and A_{nv} is the net shear area.

The constant 0.5 preceding the first term of both equations reflects the non-uniform stress observed on the tension face of the failure plane.

The tension and shear block model in AISC 2005 is taken as the least of the following two equations:

$$P_r = U_{bs}A_{nt}F_u + 0.6A_{gv}F_y \qquad\qquad [5\text{-}16]$$

$$P_r = U_{bs}A_{nt}F_u + 0.6A_{nv}F_u \qquad\qquad [5\text{-}17]$$

where:

U_{bs} is the tension stress correction factor, taken as 1.0 for coped beams with only one line of bolts.

The equations combine rupture of the net tension area and yielding of the gross shear area, with a limitation on the latter to the rupture capacity on the net shear area.

Franchuk *et al*. (2002) proposed an equation for the calculation of the tension and shear block capacity based on a series of tests on coped beams. It combines effective stresses on the net tension area and the gross shear area. It takes the following form:

$$P_r = R_t A_{nt} F_u + R_v A_{gv} \left(\frac{F_y + F_u}{2\sqrt{3}} \right)$$
[5-18]

where:

R_t is a stress correction factor for the tension face, taken as 0.9 for connections with one-line of bolts, and

R_v is a stress correction factor for the shear face, taken as 1.0 for coped beams and 0.9 for shear angles.

The effective shear stress acting on the gross area is taken as the average of the shear yield strength and the shear rupture strength acting on the gross shear area.

5.1.4 Failure of Angle Leg Connected to the Column

5.1.4.1 Description of Failure Mode

Several test specimens (1LA, 1LB, 1L1 to 1L10, 2L1, 2L6 and 1L10a) failed at the angle leg connected to the column. This failure mode was associated with the eccentric loading in the single angle connections, combined with the minimum end or edge distances selected for the top bolt hole in the angle leg. Because of the load eccentricity on the single angle connection, a moment is created in the plane of the supporting column flange as the angle is loaded. It was observed that the top end and edge distance at the top hole of the angle leg connected to the column can affect the connection capacity.

Three test specimens, namely 1L12, 1L13 and 1L14, were designed to investigate the effect of end and edge distances and the number of bolts on the strength of the single angle connection. The top end distance, e_{s3}, and edge distance, e_{g1}, are defined in Figure 3-1.

5.1.4.2 Current Design Practice

Provisions for the type of failure observed in specimen 1LA, 1LB, 1L1 to 1L10, 2L1, 2L6 and 1L10a are provided in the current CISC Handbook of Steel Construction (CISC, 2004) and the AISC Manual of Steel Construction (AISC, 1999) under design of eccentrically loaded bolt groups. The procedure for designing eccentrically loaded bolt groups is based on the instantaneous centre of rotation (ICR) method proposed by Crawford and Kulak (1971). Based on the method proposed by Crawford and Kulak, design tables were derived and presented in the CISC Handbook of Steel Construction and AISC Manual of Steel Construction. The design tables were obtained based on bolt data obtained from 3/4 in. diameter ASTM A325 bolts with ultimate tensile strength of 329 kN and ultimate deformation of 8.64 mm. The strength of a bolt group is reached when the bolt farthest from the ICR reaches its ultimate deformation. However, for the specimens in the test program that failed at the leg connected to the column, the connected material failed by rupture and tearing before the bolt reached its ultimate deformation. Therefore, there is a need for a new design model that addresses this issue. The new design model assumes that the ultimate limit state of the connection is reached when the connected material around the fastener farthest from the ICR fails by a combination of shear and tension rupture.

5.1.4.3 Proposed Modified Instantaneous Centre of Rotation Method

Since current provisions for failure of eccentrically loaded bolt groups are based on bolt failure in shear rather than plate tearing failure, a new model is proposed to predict the capacity of the test specimens that failed in the angle leg connected to the column. The ICR method will be utilized to compute the connection resistance, but it will be modified so that the ultimate limit state is failure of the connected material rather than shearing of the bolts.

When calculating the force in each bolt, the procedure is similar to that of ICR method. At the ultimate limit state, the ICR is located outside of the bolt group. The force in each bolt is assumed to act along a line perpendicular to the radial line joining the bolt to the instantaneous centre. A diagram illustrating the load eccentricity, the location of the ICR and the bolt forces is shown in Figure 5-2. The following assumptions are made in the formulation of the ICR method for eccentrically loaded single shear angles:

1) The vertical load acts through the centre of the beam web.

2) The vertical load is shared equally by all bolts.

3) The capacity of the connection is reached when the top corner of the angle leg connected to the column reaches the tension and shear block limit state.

The data for calculation of ICR for the specimens is shown in Table 5-1. The calculation of the location of the ICR, r_o, defined in Figure 5-2, is illustrated in Table 5-2. The procedure consists of the following steps:

1) From the assumed location of the ICR, r_o, the direction of each bolt force, θ, defined in Figure 5-2, is determined. The direction of the bolt forces are perpendicular to the radial distance between the ICR and the centre of the bolts, namely, r_1, r_2 and r_3 as shown in column (6), (7) and (8) of Table 5-2, respectively.

2) The tension and shear areas of the tension and shear block failure plane are determined and the capacity at the critical bolt, R_1, is determined, as shown in Table 5-3 for various predicted failure models. R_1 is taken as the sum of T_r and S_r calculated using the various predicted failure models described in section 5.1.4.4. T_r and S_r are the tension and shear contribution, respectively, to the calculated tension and shear block failure capacity. Note that the tension area is perpendicular to the bolt force and intersects the edge of the angles whereas the shear area is parallel to the direction of the bolt force and intercepts either the edge or the loaded end of the angle.

3) For a symmetrical joint, the force in the bottom bolt, R_2, will be equal to R_1 and oriented as shown in Figure 5-2. The force in the middle bolt is now defined from the first assumption above.

4) The ratio of P/R_1 is determined from equilibrium of vertical forces, as shown in column (9) of Table 5-2.

5) The ratio of P/R_1 is also determined from equilibrium of moments about the ICR, as shown in column (10) of Table 5-2.

6) If the ratio P/R_1 determined in step 4 is in good agreement with the ratio P/R_1 determined in step 5, the location of ICR, r_o, is correct. Otherwise, the location of the ICR is adjusted and the procedure is repeated.

The value of R_1 is computed in section 5.1.4.4 using various predicted failure models. Different magnitude of effective stress is assigned to the net area and the gross area on the tension and shear block failure planes. Once the force in each bolt is known, the connection capacity, P, can be computed.

The orientation of the shear and tension planes depends on the orientation of the bolt force, θ. The shear plane will be parallel to the force in the top bolt and the tension plane will be perpendicular to the shear plane. Whether the line of action of the bolt force crosses the edge or the top end of the angle depends on the angle θ, illustrated in Figure 5-3, the top end distance of the angle, e_{s3}, and the edge distance of the angle, e_{g1}. It should be noted that for some specimens the calculated line of action of the bolt force intersects the vertical edge of the angle, instead of the top end of angle, as shown in Figure 5-3a. The shear face intercepts the bolt hole and the side edge of the angle, and the tension face intercepts the bolt hole and the top end of the angle for an inclined tension and shear block failure to occur. This is the case for specimens 1LA, 1LB, 1L2 to 1L6, 1L9 and 1L14. The corresponding failure model is illustrated in Figures 5-4e, 5-4g, 5-4i and 5-4k. For the remaining specimens, the line of action of the bolt force intersects the top end of the angle as shown in Figure 5-3b. Thus, the tension face intercepts the bolt hole and the edge of the angle. The corresponding failure model is illustrated in Figures 5-4d, 5-4f, 5-4h, and 5-4j. In all cases, the corner of the angle is included within the block. The ratio of the capacity of the connection to the force in the critical bolt (top bolt) is tabulated in columns (9) and (10) of Table 5-2. The force magnitude in the top bolt depends on the failure capacity of the connected material, i.e., the tension and shear block

tear out capacity of the angle around the top bolt, which can be determined using the procedure in the following section.

5.1.4.4 Calculation of Limiting Bolt Force for the ICR Method

The calculation of the limiting bolt force, R_1, and the predicted capacity of the connection, P, is illustrated in Table 5-3. T_r and S_r are the tension and shear block contributions to the tension and shear block resistance. The sum of T_r and S_r represents the limiting bolt force, R_1. P is computed by multiplying the ratio of P/R_1 in columns (9) and (10) of Table 5-2 by the sum of T_r and S_r. Various failure models are illustrated and discussed in the following.

5.1.4.4.1 *CSA–S16–01 Tension and Shear Block Model*

The observed failure planes for test specimens with a large top end distance, e_{s3}, of 58 mm, (specimens 1L2 to 1L6 and 1L9) suggests a tension and shear block failure analogous to the failure mode observed in connections with coped beams. Therefore, the tension and shear block equation from CSA–S16–01 (CSA, 2001) is used to predict the limiting force on the top bolt required to carry out the calculation outlined in section 5.1.4.3. The tension and shear block resistance given in CSA–S16–01 was presented in Equations [5-14] and [5-15]. The direction of the bolt force and the ratio of the applied joint load to the bolt force are obtained using the modified ICR method as described in the section 5.1.4.3.

Equation [5-14] consists of net tension area fracture plus gross shear yielding, whereas Equation [5-15] consists of net tension area fracture plus net shear area fracture. The failure model predicted by Equation [5-14] is depicted as models D and E in Figure 5-4, whereas the failure model predicted by Equation [5-15] is depicted as models F and G in Figure 5-4. The various failure models presented in the following differ in magnitude of the shear and normal stress assigned to the shear face and the tension face. The observed failure paths in the test specimens and some possible failure paths that were not observed in the specimens tested in this program are also illustrated in Figure 5-4 and Table 5-3.

5.1.4.4.2 *Modified Franchuk et al. (2002) Model*

Equation [5-18], from Franchuk *et al.* (2002), represents a failure mode similar to that of Equation [5-14]. For a coped beam with a single line of bolt, the stress correction factors, R_t and R_v, are taken as 0.9 and 1.0, respectively, leading to the following expression for the tension and shear block capacity:

$$P_r = 0.9\,A_{nt}\,F_u + 1.0\,A_{gv}\left(\frac{F_y + F_u}{2\sqrt{3}}\right) \tag{5-19}$$

The capacity based on the failure models depicted as failure models H and I in Figure 5-4 can be predicted by Equation [5-19].

A modified version of Equation [5-18], with R_t and R_v taken as 0.4 and 1.0, respectively, is also proposed. The stress factors were selected so that the calculated mean test-to-predicted ratio is as close as possible to 1.0, while minimizing the coefficient of variation. The equation takes the following form:

$$P_r = 0.4\,A_{nt}\,F_u + 1.0\,A_{gv}\left(\frac{F_y + F_u}{2\sqrt{3}}\right) \tag{5-20}$$

The failure model predicted by this method is depicted as models J and K in Figure 5-4.

5.2 Comparison of Test Results with Various Prediction Models

In this section, the test results presented in Chapter 4 are compared to the various prediction models presented above. The mean test-to-predicted ratio calculated using CSA–S16–01, AISC 2005 and the proposed prediction models will be assessed in order to determine their adequacy as prediction models. The COV of the test-to-predicted values are also presented. A mean test-to-predicted ratio close to unity with a low COV indicates the design model or equation is a good predictor of the test results.

In the following, the predicted capacities of the test specimens are grouped according to the observed failure mode. The predicted capacities based on possible

failure modes and models from CSA–S16–01 and other models presented above are tabulated for each group of specimens. Finally, a comparison of all the test results with all the various failure modes considered in this chapter is made to assess whether the actual failure mode can be predicted.

5.2.1 Angle End Tearing

The capacity of specimens that failed by angle end tearing was predicted using CSA–S16–01 and AISC 2005 for various failure modes, including rupture of the web framing angle on the net shear area, yielding of the gross shear area, bolt bearing, and tension and shear block failure in the beam. The results of these calculations are presented in Table 5-4. The capacity predicted using Equation [5-18] for angle shear capacity, and Equation [5-13] for the angle end tearing capacity are also shown in the table.

The procedures used in CSA–S16–01 would consider either bolt bearing failure, assuming all bolts in the connection have the same capacity, or shear failure of the angle. This approach can result in a significant overestimate of the capacity as shown in Table 5-4. On the other hand, AISC 2005 provisions account for different capacity of an exterior bolt and interior bolts within a bolt group. However, it overestimates the capacity for all the specimens that failed by angle end tearing. The mean test-to-predicted ratios calculated using the CSA–S16–01 and AISC 2005 standard are both 0.88. The COV of the test-to-predicted values calculated using CSA–S16–01 and AISC 2005 are 0.13 and 0.15, respectively. Equation [5-18] gives a mean test-to-predicted ratio of 0.78, with a COV of 0.14 for predicting angle shear failure capacity. It should be noted that Equation [5-18] is not intended to predict the angle end tearing failure mode, but it will be used to predict the capacity of specimens with tension and shear block failure as shown in section 5.2.3.

The proposed plastic collapse model (Equation [5-13]) is based on the sum of the plastic collapse capacity of the clear bottom end distance, with the upper limit equal to the shear failure along the clear length of the connection, and the bearing capacity of the bolts on the slotted holes. Equation [5-13] gives a test-to-predicted ratio of 1.01 and a

COV of 0.18. As shown in Table 5-4, the low values of test-to-predicted ratio predicted by Equation [5-13] are 0.80, 0.83, 0.85 and 0.86 for test specimens 1L7a, 1L8a, 1L11a and 1L1a, respectively. All of these four specimens had long slotted holes with standard bolt pitch (76 mm) and without plate washer in the outer plies of the joint. It has been shown that the observed capacities of single angle test specimens with standard pitch failed by angle end tearing had slightly lower capacities than their large pitch (102 mm) counterparts. The highest test-to-predicted ratio is 1.33 for specimen 1LAa, which is a thin single angle specimen (6.4 mm) with plate washer on the outer ply. The next largest test-to-predicted ratio is 1.25, obtained for a connection with plate washer on the outer ply but with thicker angles (9.5 mm). The large scatter (COV = 0.18) observed in the test-to-predicted values is likely caused by the effect of many parameters on the connection capacities. For instance, the specimen with plate washer on the outer ply and an uncoped beam (1L4a) had a capacity 41% higher than the one without plate washer (1L2a). The effect of plate washer is not accounted for in calculation of angle end tearing capacities. It is also assumed that all the bolts in the connection reach their capacity simultaneously. However, the bottom end of single angles with minimum end distance is more flexible and possibly has lower strength than the rest of the connection. In fact, the bolts in the connection may not reach their individual capacity simultaneously. Therefore, assuming the bolts reach their capacity at the same time is possibly an unconservative assumption.

Although the COV of 0.18 predicted by Equation [5-13] is higher than the ones predicted by CSA–S16-01 (0.13), AISC 2005 (0.15) and Equation [5-18] (0.14), Equation [5-13] has several advantages compared to the other prediction models. First, the mean test-to-predicted ratio of 1.01 is very close to unity and it is higher than the one predicted by other prediction models. Second, it addresses the end distance failure below the bottom slotted hole correctly, which is something not achieved by other models. The observed failure mode is a combination of bending and bearing failure of end distance. Moreover, Equation [5-13] is able to predict the correct failure mode of the angle end tearing, i.e. collapse of the end distance and bearing of bolt on the slot in the loading direction.

5.2.2 Beam Web Edge Distance Tearing

Six of the specimens failed in the beam web by edge distance tearing, namely, specimens 2L1a, 2L2, 2L3, 2L4, 2L5a and 2L6a. The possible failure mode of bolt bearing on the beam web and the corresponding capacity are investigated. As shown in Table 5-5, both North American design standards underestimate the observed capacity of the test specimen that failed by tearing of the edge distance. The bolt bearing capacity governs for all cases, except for specimen 2L6a for which rupture on the angle net area governs. The mean test-to-predicted ratio of 0.71 and COV of 0.14 predicted by both standards indicate a poor correlation between the observed capacity and the predicted capacity. Since these specimens were fabricated with uncoped beams, it is assumed that they would fail by bolt bearing on the web. However, the low average test-to-predicted ratio and high COV indicate that the bolt bearing model does not describe well the observed edge distance tearing failure mode for cases where the minimum permissible edge distance is used.

5.2.3 Tension and Shear Block Failure of Beam Web

Table 5-5 also presented the predicted capacity of tension and shear block failure by the North American standards and Equation [5-18]. The tension and shear block capacities predicted by CSA–S16–01 are conservative, with a mean test-to-predicted ratio of 1.15 and COV of 0.16. The mean test-to-predicted ratio obtained using the AISC 2005 model is 1.06 and COV of 0.14. Although the two specimens showed a slight difference in tension and shear block failure (different location of tensile failure), the mean test-to-predicted ratios obtained from both standards are both higher than unity.

The test-to-predicted ratio obtained using Equation [5-18] has a mean value of 0.90 and a COV of 0.08. The details about this proposed equation can be found in Franchuk *et al.* (2002). Among all the prediction models, CSA–S16–01 is the most conservative, followed by AISC 2005 and Equation [5-18]. However, Equation [5-18] provides the lowest COV of predicted values, followed by AISC 2005 and CSA–S16–01. It appears that the minimum edge distance used on the beam web prevented the higher shear capacity in Equation [5-18] to be mobilized fully.

5.2.4   Failure of Angle Leg Connected to the Column

The capacities predicted by CSA–S16–01, AISC 2005, Equation [5-18] for angle shear capacity and Equation [5-13] for the specimens that failed in the leg connected to the column are shown in Table 5-6. CSA–S16–01 and AISC 2005 do not have provisions for this type of failure. The failure mode for single angle shear connections considered by these two standards are rupture of the net shear area, yielding of the gross shear area, bolt bearing on the angle, and tension and shear block failure. The mean test-to-predicted ratios obtained using the equations in CSA–S16–01 and AISC 2005 were 0.75 and 0.78, respectively. The two current steel design standards overestimate the capacity of the specimens by a considerably large margin.

The predicted capacities by the four new proposed models are presented in Table 5-3. Equation [5-14] gives a mean test-to-predicted ratio of 1.02 and a COV of 0.16. Equation [5-15] gives a mean test-to-predicted ratio of 1.00 and COV of 0.17. The large COV indicates a wide scatter of test-to-predicted values. It should be noted that the test-to-predicted ratios for specimens 1L10a, 2L1 and 2L6 are substantially lower than the average of the remaining test specimens. This is due to the fact that only specimen 1L10a with this failure mode has a larger angle leg size (152 mm) connected to the column so that the contribution of the tension area was larger than for the specimens with a smaller leg size (102 mm), thus resulting in a larger predicted capacity. On the other hand, specimens 2L1 and 2L6 are double angle connections. The predicted capacities of these two specimens by the above four models are shown for completeness. The same procedure is used to compute the predicted capacity of these two connections. The predicted capacity of the double-angle specimens is taken as the sum of the capacity of each angle in the connection. As a result, the predicted capacities of these two specimens are approximately twice as much as their single angle counterpart, namely 1L1 and 1L7. It should also be noted that the test-to-predicted ratio for specimen 1L14 is larger than the rest of the other specimens. This is possibly attributed to the assumption that all bolts carry the same amount of vertical load. For a connection with three bolts, this simplifying assumption might not represent the actual behaviour of the connection. The location of the ICR depends partly on the distribution of the vertical load among the bolts. Therefore,

the distribution of vertical load affects the connection capacity based on the proposed prediction models. Nevertheless, the predicted capacity is on the conservative side. As shown in Table 5-3, the mean test-to-predicted ratio calculated by Equation [5-19], which uses a value of R_t intended for coped beams with one line of bolt, is 0.67 and COV is 0.17. The predicted capacities are all on the unconservative side. Therefore, Equation [5-19] is modified to improve the prediction.

Equation [5-20] is essentially identical to Equation [5-19], except that the tension stress correction factor, R_t, is taken as 0.4, instead of 0.9. This reduction results in a higher mean value of test-to-predicted ratio (1.05) and a lower COV (0.15), indicating a better prediction than Equation [5-19]. A graphical comparison of test-to-predicted ratios of the four new prediction models is shown in Figure 5-5. Of the four of the prediction models, Equation [5-20] gives a mean test-to-predicted ratio very close to unity and a smallest value of COV, which indicates a better predictor of the test results.

5.3   Summary of All Prediction Models

Table 5-7 presents a summary of the predicted capacities for all the test specimens by CSA–S16–01 as well as proposed equations. The possible failure modes being investigated are bolt bearing, angle shear failure, beam web tension and shear block failure, angle bottom end tearing and failure of angle leg connected to the column. In this summary, all the predicted capacities are predicted using proposed new equations. The tension and shear block and angle shear capacities are calculated using Equation [5-18], which was proposed by Franchuk *et al.* (2002) based on an analysis of test results on coped beams. The angle end tearing capacities are calculated using Equation [5-13]. The capacities at which that angle failed at the leg connected to the column are predicted using Equation [5-20]. Since there are no newly developed prediction models for the bolt bearing failure, the bolt bearing capacities are calculated using the design equation from CSA–S16–01.

As shown in Table 5-7, the bolt bearing capacity of angle and beam web is presented in column (2) and column (3), respectively. The angle shear capacity and beam web tension and shear block capacities predicted using Equation [5-18] are presented in

columns (4) and (5), respectively. The capacity of the web framing angle predicted by Equation [5-13] for angle end tearing capacity is presented in column (6). The tension and shear block capacity of the web framing angle corner tear out as predicted by Equation [5-20] is shown in column (7). The governing capacity predicted by all the prediction models and the corresponding failure mode is shown in columns (8) and (9), respectively. The observed capacity and the observed failure mode are presented in columns (10) and (11), respectively.

The equations from the current design standards and the proposed new models are able to predict the correct failure mode for 32 of the 41 test specimens. Of the nine specimens for which the failure mode was not predicted correctly, six of them are double angle connections with an uncoped beam. The observed failure mode for these six specimens was beam web edge distance tearing. As discussed previously, the current design standards do not have provisions for edge distance tearing of beam webs. The predicted failure modes in these cases are bolt bearing failure against the beam web, angle end tearing and failure of angle leg connected to the column. As shown in Table 5-5, CSA–S16–01 over-predicts the capacity of these specimens by as much as 41% based on the bearing strength of bolt on the beam web. This large discrepancy between the test capacity and the predicted bearing capacity indicates that the current minimum edge distance used in design standards is not sufficient to develop full beam web bearing strength. The predicted failure mode for test specimen V by Franchuk *et al.* (2002) is failure of angle leg connected to the column, but the observed failure mode is angle end tearing. Another two of the nine specimens, namely, 1LA and 1L10a, failed in the leg connected to the column, but the predicted failure mode for both specimens is angle end tearing as predicted by Equation [5-13]. Nevertheless, the predicted capacity is within 5% of the observed capacities for these two specimens.

A combination of new prediction models and the design equation from current design standard provides the tool to predict the capacity and the failure mode for most of the specimen (32 out of 41) being investigated. However, the bearing resistance for bolts in the beam web can be limited by edge distance tearing. There is a need for a new prediction model for this type of failure. An increase in the minimum permissible edge distance is required if the bearing capacity of the bolts in contact with the beam web to be

reached. Similarly, an increase in minimum edge distance is required if the full tension and shear block capacity predicted by Equation [5-18] for coped beam is to be mobilized.

Table 5-1 Data for Instantaneous Center of Rotation Calculation

Test specimen	Angle (east/west)	t	d_{h1}	d_{h2}	e_{g1}	e_{g2}	e_{s3}	p_3	w	Angle material properties F_y	F_u	Observed capacity
		(mm)	(mm)	(mm)	(mm)	(mm)	(mm)	(mm)	(mm)	(MPa)	(MPa)	(kN)
(1)	(2)	(3)	(4)	(5)	(6)	(7)	(8)	(9)	(10)	(11)	(12)	(13)
1LA	—	6.59	27.00	27.30	36.51	36.57	50.17	152.5	7.32	431	535	280
1LB	—	6.56	27.20	27.20	36.87	36.77	58.22	152.3	6.91	431	535	288
1L1	—	9.88	26.60	26.80	37.09	36.93	31.87	151.7	7.21	311	475	306
1L2	—	9.63	27.10	27.20	36.40	36.68	57.49	152.4	6.98	311	475	346
1L3	—	9.83	26.80	26.90	37.46	37.51	58.06	152.0	8.98	311	475	430
1L4	—	9.66	27.00	26.90	36.63	36.58	57.47	152.3	7.05	311	475	378
1L5	—	9.59	27.10	27.40	36.34	36.49	57.34	152.7	7.02	311	475	362
1L6	—	9.69	26.70	26.70	36.52	36.52	56.61	151.9	7.08	311	475	368
1L7	—	9.94	26.80	26.70	36.32	36.27	32.80	151.8	7.09	311	475	276
1L8	—	9.90	27.00	27.10	37.02	37.07	31.83	151.9	6.91	311	475	290
1L9	—	9.63	26.70	26.80	36.04	36.09	57.46	151.8	7.06	311	475	360
1L10	—	9.59	26.70	26.80	36.49	36.54	32.91	152.2	7.26	311	475	291
1L12	—	9.50	27.21	27.39	34.51	33.79	32.24	152.6	6.93	365	531	299
1L13	—	9.51	27.05	27.07	50.24	50.02	31.89	152.4	6.85	365	531	372
1L14	—	9.43	27.32	27.35	33.00	32.96	34.06	76.2 76.5 [1]	6.93	365	531	362
1L10a	—	9.44	27.48	27.54	85.95	86.25	47.36	153.0	6.92	293	446	376
2L1	East angle	9.72	26.99	26.96	36.90	36.78	32.20	151.9	7.04	311	475	400
	West angle	9.87	26.80	26.70	36.50	36.40	32.40	152.3	7.04	311	475	
2L6	East angle	9.77	26.30	26.50	36.45	36.25	31.92	151.8	6.98	311	475	377
	West angle	9.80	26.60	26.80	36.80	36.40	31.90	151.9	6.98	311	475	

Note: Refer to Figure 3-1 for description of the dimensions
[1] Bolt pitch between the middle and bottom bolt hole

Table 5-2 Location of Instantaneous Centre of Rotation and Ratio of Vertical Load to Bolt Force

Test Specimen		L (mm)	r_o (mm)	θ (rad)	θ (degrees)	r_1 (mm)	r_2 (mm)	r_3 (mm)	Vertical force equilibrium P/R_1	Moment equilibrium P/R_1	residual
(1)		(2)	(3)	(4)	(5)	(6)	(7)	(8)	(9)	(10)	(11)
1LA		69.2	83.7	0.737	42.2	113.2	113.2	—	1.4809	1.4809	3.09E-08
1LB		68.6	84.2	0.734	42.1	113.5	113.5	—	1.4844	1.4844	4.82E-09
1L1		68.5	84.4	0.733	42.0	113.5	113.5	—	1.4865	1.4865	3.84E-08
1L2		69.1	83.6	0.738	42.3	113.1	113.1	—	1.4798	1.4798	1.99E-07
1L3		68.0	84.9	0.730	41.8	113.9	113.9	—	1.4901	1.4901	7.16E-08
1L4		68.9	83.9	0.736	42.2	113.3	113.3	—	1.4820	1.4820	1.11E-08
1L5		69.2	83.5	0.738	42.3	113.1	113.1	—	1.4792	1.4792	2.40E-07
1L6		69.0	83.7	0.737	42.2	113.0	113.0	—	1.4810	1.4810	3.21E-08
1L7		69.2	83.5	0.738	42.3	112.9	112.9	—	1.4790	1.4790	7.10E-09
1L8		68.4	84.4	0.733	42.0	113.5	113.5	—	1.4858	1.4858	2.20E-08
1L9		69.5	83.2	0.740	42.4	112.6	112.6	—	1.4763	1.4763	9.72E-08
1L10		69.1	83.7	0.737	42.2	113.1	113.1	—	1.4807	1.4807	1.55E-08
1L12		71.0	81.4	0.751	43.0	111.5	111.5	—	1.4615	1.4615	7.07E-10
1L13		55.2	104.5	0.629	36.0	129.3	129.3	—	1.6176	1.6176	4.01E-11
1L14		70.5	55.8	0.931	53.3	94.5	94.3	55.8	1.7756	1.7756	2.77E-07
1L10a		69.5	83.0	0.741	42.5	112.9	112.9	—	1.4754	1.4754	1.34E-09
2L1	East angle	68.5	84.2	0.734	42.1	113.4	113.4	—	1.4846	1.4846	2.67E-08
	West angle	69.0	83.7	0.737	42.2	113.2	113.2	—	1.4808	1.4808	1.47E-08
2L6	East angle	69.0	83.6	0.738	42.3	112.9	112.9	—	1.4802	1.4802	7.48E-08
	West angle	68.7	84.1	0.735	42.1	113.3	113.3	—	1.4837	1.4837	1.06E-10

Table 5-3 Predicted Capacities of Specimens with Failure of Angle Leg Connected to the Column

Test Specimen	Observed Failure Path	Equation [5-14] Failure Model	T_r (kN)	S_r (kN)	P (kN)	test/ pred.	Equation [5-15] Failure Model	T_r (kN)	S_r (kN)	P (kN)	test/ pred.	Equation [5-19] Failure Model	T_r (kN)	S_r (kN)	P (kN)	test/ pred.	Equation [5-20] Failure Model	T_r (kN)	S_r (kN)	P (kN)	test/ pred.
(1)	(2)	(3)	(4)	(5)	(6)	(7)	(8)	(9)	(10)	(11)	(12)	(13)	(14)	(15)	(16)	(17)	(18)	(19)	(20)	(21)	(22)
1LA	A	E	107.8	92.6	297	0.94	G	107.8	86.3	287	0.97	I	194.0	99.8	435	0.64	K	86.2	99.8	276	1.02
1LB	A	E	128.4	93.2	329	0.88	G	128.4	87.1	320	0.90	I	231.1	100.5	492	0.59	K	102.7	100.5	302	0.95
1L1	B	D	85.9	79.0	245	1.25	F	85.9	83.3	251	1.22	H	154.5	96.1	373	0.82	J	68.7	96.1	245	1.25
1L2	C	E	164.4	97.2	387	0.89	G	164.4	111.3	408	0.85	I	295.9	118.2	613	0.56	K	131.5	118.2	369	0.94
1L3	C	E	171.9	103.0	410	1.05	G	171.9	119.8	435	0.99	I	309.4	125.2	648	0.66	K	137.5	125.2	391	1.10
1L4	C	E	165.3	98.3	391	0.97	G	165.3	113.0	412	0.92	I	297.5	119.5	618	0.61	K	132.2	119.5	373	1.01
1L5	C	E	163.1	96.6	384	0.94	G	163.1	110.5	405	0.89	I	293.6	117.4	608	0.60	K	130.5	117.4	367	0.99
1L6	C	E	163.1	98.2	387	0.95	G	163.1	113.2	409	0.90	I	293.5	119.4	612	0.60	K	130.5	119.4	370	0.99
1L7	B	D	84.3	82.3	246	1.12	F	84.3	87.7	254	1.08	H	151.8	100.0	372	0.74	J	67.4	100.0	248	1.11
1L8	B	D	85.4	79.1	244	1.19	F	85.4	82.8	250	1.16	H	153.7	96.2	371	0.78	J	68.3	96.2	244	1.19
1L9	C	E	164.3	96.0	384	0.94	G	164.3	110.0	405	0.89	I	295.7	116.7	609	0.59	K	131.4	116.7	366	0.98
1L10	B	D	81.8	79.5	239	1.22	F	81.8	85.0	247	1.18	H	147.3	96.7	361	0.81	J	65.5	96.7	240	1.21
1L12	B	D	84.8	91.8	258	1.16	F	84.8	92.3	259	1.16	H	152.6	108.4	381	0.78	J	67.8	108.4	258	1.16
1L13	B	D	122.7	82.1	331	1.12	F	122.7	78.5	325	1.14	H	220.8	97.0	514	0.72	J	98.1	97.0	316	1.18
1L14	B	E	69.0	84.9	273	1.32	G	69.0	82.5	269	1.35	I	124.1	100.3	399	0.91	K	55.2	100.3	276	1.31
1L10a	B	D	218.4	107.5	481	0.78	F	218.4	128.7	512	0.73	H	393.1	130.5	773	0.49	J	174.7	130.5	450	0.83
2L1	B	D	83.6	78.7	485	0.83	F	83.6	82.8	498	0.80	H	150.5	95.7	735	0.54	J	66.9	95.7	486	0.82
2L6	B	D	83.7	78.6	482	0.78	F	67.0	83.5	446	0.85	H	120.6	95.6	642	0.59	J	67.0	95.6	483	0.78
Mean						1.02					1.00					0.67					1.05
COV						0.16					0.17					0.17					0.15

* Refer to Figure 5-4 for a description of various failure paths

112

Table 5-4 Predicted Capacities of Test Specimens with Angle End Tearing Failure

Test Specimen	Observed Capacity	CSA–S16–01						AISC 2005						Equation [5-18]		Proposed plastic collapse load for end distance bearing	
		Angle			Beam			Angle			Beam						
		Net section rupture	Gross area yielding	Bolt bearing	Tension and shear block	Bolt bearing	Test/ Pred.	Net section rupture	Gross area yielding	Bolt bearing	Tension and shear block	Bolt bearing	Test/ Pred.	Angle shear capacity	Test/ Pred.	Angle bearing capacity	Test/ Pred.
		[5-2]	[5-1]	[5-3]	[5-14], [5-15]	[5-3]		[5-2]	[5-1]	[5-5]	[5-16], [5-17]	[5-4]		[5-18]		[5-13]	
	(kN)	(kN)	(kN)	(kN)	(kN)	(kN)		(kN)	(kN)	(kN)	(kN)	(kN)		(kN)		(kN)	
(1)	(2)	(3)	(4)	(5)	(6)	(7)	(8)	(9)	(10)	(11)	(12)	(13)	(14)	(15)	(16)	(17)	(18)
1LAa	299	349	**314**	517	371	562	0.95	349	314	**273**	396	562	1.10	336	0.89	224	1.33
1LBa	342	**329**	330	687	360	750	1.04	**328**	330	358	391	750	1.04	353	0.97	290	1.18
1L1a	312	388	**383**	839	—	655	0.81	388	**383**	459	—	655	0.81	419	0.75	363	0.86
1L2a	321	527	**470**	843	—	682	0.68	527	470	**465**	—	682	0.69	514	0.62	366	0.88
1L2aE	490	568	**500**	847	—	693	0.98	568	**500**	519	—	693	0.98	546	0.90	454	1.08
1L3a	345	529	**471**	841	573	939	0.73	529	471	**464**	617	939	0.74	515	0.67	368	0.94
1L4a	452	521	**468**	836	—	683	0.97	521	468	**459**	—	683	0.98	511	0.88	361	1.25
1L5a	392	533	474	846	**421**	686	0.93	533	474	467	**452**	686	0.87	518	0.76	366	1.07
1L6a	331	532	475	847	**420**	684	0.79	532	475	469	**450**	684	0.74	519	0.64	371	0.89
1L7a	288	384	**378**	835	—	661	0.76	384	**378**	457	—	661	0.76	413	0.70	362	0.80
1L8a	306	390	386	842	**299**	653	1.02	390	386	461	**328**	653	0.93	421	0.73	368	0.83
1L9a	454	523	**473**	846	—	692	0.96	523	**473**	551	—	692	0.96	516	0.88	382	1.19
1L11a	327	389	**386**	842	—	662	0.85	389	**386**	468	—	662	0.85	422	0.77	384	0.85
Mean							0.88						0.88		0.78		1.01
COV							0.13						0.15		0.14		0.18

Note: The numbers in the square brackets are the equation numbers.
The highlighted capacities are the governing failure capacity predicted by each design standard.

113

Table 5-5 Predicted Capacities of Test Specimens with Beam Web Edge Distance Tearing Failure

and Beam Web Tension and Shear Block Failure

Test Specimen	Observed Capacity	CSA–S16–01						AISC 2005						Equation [5-18]		Proposed plastic collapse load for end distance bearing	
		Angle		Beam				Angle			Beam						
		Net section rupture	Gross area yielding	Bolt bearing	Tension and shear block	Bolt bearing	Test/ Pred.	Net section rupture	Gross area yielding	Bolt bearing	Tension and shear block	Bolt bearing	Test/ Pred.	Tension and shear block	Test/ Pred.	Angle bearing capacity	Test/ Pred.
		[5-2]	[5-1]	[5-3]	[5-14], [5-15]	[5-3]		[5-2]	[5-1]	[5-5]	[5-16], [5-17]	[5-4]		[5-18]		[5-13]	
	(kN)	(kN)	(kN)	(kN)	(kN)	(kN)		(kN)	(kN)	(kN)	(kN)	(kN)		(kN)		(kN)	
(1)	(2)	(3)	(4)	(5)	(6)	(7)	(8)	(9)	(10)	(11)	(12)	(13)	(14)	(15)	(16)	(17)	(18)
Specimens failed by beam web edge distance tearing																	
2L1a	476	711	719	1679	—	**706**	0.67	711	719	913	—	**706**	0.67	—	—	708	0.67
2L2	472	1076	982	1860	—	**696**	0.69	1076	982	1015	—	**696**	0.69	—	—	787	0.60
2L3	574	1068	973	1842	—	**973**	0.59	1068	973	1013	—	**973**	0.59	—	—	792	0.72
2L4	551	1072	977	1853	—	**690**	0.80	1072	977	1013	—	**690**	0.80	—	—	786	0.70
2L5a	620	978	891	1678	—	**714**	0.87	978	891	912	—	**714**	0.87	—	—	709	0.87
2L6a	463	**706**	721	1687	—	710	0.66	**706**	721	910	—	710	0.66	—	—	703	0.66
Mean							0.71						0.71				0.70
COV							0.14						0.14				0.13
Specimens failed by beam web tension and shear block																	
2L7	347	785	788	1854	**271**	653	1.28	785	788	1005	**300**	—	1.16	364	0.95	772	0.45
2L8a	415	962	885	1669	**406**	714	1.02	962	885	906	**439**	—	0.95	489	0.85	706	0.59
Mean							1.15						1.06		0.90		0.52
COV							0.16						0.14		0.08		0.19

114

Table 5-6 Predicted Capacities of Test Specimens Failed at the Angle Leg Connected to the Supporting Column

		CSA–S16–01						AISC 2005						Equation [5-18]		Proposed plastic collapse load for end distance bearing	
		Angle			Beam			Angle			Beam						
Test Specimen	Observed Capacity	Net section rupture	Gross area yielding	Bolt bearing	Tension and shear block	Bolt bearing	Test/ Pred.	Net section rupture	Gross area yielding	Bolt bearing	Tension and shear block	Bolt bearing	Test/ Pred.	Angle shear capacity	Test/ Pred.	Angle bearing capacity	Test/ Pred.
		[5-2]*	[5-1]	[5-3]	[5-14], [5-15]	[5-3]		[5-2]	[5-1]	[5-5]	[5-16], [5-17]	[5-4]		[5-18]		[5-13]	
	(kN)	(kN)	(kN)	(kN)	(kN)	(kN)		(kN)	(kN)	(kN)	(kN)	(kN)		(kN)		(kN)	
(1)	(2)	(3)	(4)	(5)	(6)	(7)	(8)	(9)	(10)	(11)	(12)	(13)	(14)	(15)	(16)	(17)	(18)
1LA	280	406	433	604	**404**	618	0.69	406	433	**323**	431	618	0.87	420	0.67	267	1.05
1LB	288	388	453	801	**371**	776	0.78	**388**	453	421	400	776	0.74	440	0.65	345	0.83
1L1	306	**393**	399	937	—	707	0.78	**393**	399	509	—	707	0.78	436	0.70	394	0.78
1L2	346	536	**482**	913	—	685	0.72	536	**482**	502	—	685	0.72	527	0.66	391	0.89
1L3	430	544	**492**	933	—	940	0.87	544	**492**	510	—	940	0.87	539	0.80	396	1.09
1L4	378	532	**484**	916	—	692	0.78	532	**484**	507	—	692	0.78	530	0.71	401	0.94
1L5	362	525	**480**	910	—	688	0.75	525	**480**	503	—	688	0.75	526	0.69	399	0.91
1L6	368	530	**486**	919	—	695	0.76	530	**486**	508	—	695	0.76	532	0.69	404	0.91
1L7	276	**399**	405	943	—	696	0.69	**399**	405	511	—	696	0.69	443	0.62	394	0.70
1L8	290	389	399	939	**276**	678	1.05	389	399	511	**307**	678	0.94	436	0.66	396	0.73
1L9	360	527	**483**	914	—	692	0.74	527	**483**	607	—	692	0.74	529	0.68	424	0.85
1L10	291	**382**	393	910	—	712	0.74	**382**	**393**	505	—	712	0.74	430	0.68	424	0.69
1L12	299	558	**531**	1006	—	656	0.56	558	**531**	652	—	656	0.74	565	0.53	—	—
1L13	372	563	**535**	1007	—	649	0.70	563	**535**	654	—	649	0.92	568	0.65	—	—
1L14	362	559	**531**	1004	—	656	0.68	559	**531**	650	—	656	0.90	565	0.64	—	—
1L10a	376	**374**	389	849	—	683	1.00	**374**	389	469	—	683	1.00	425	0.88	393	0.96
2L1	400	800	793	1860	—	**691**	0.58	800	793	1017	—	**691**	0.58	867	0.46	785	0.51
2L6	377	792	791	1857	—	**685**	0.55	792	791	1020	—	**685**	0.55	866	0.44	792	0.48
Mean							0.75						0.78		0.66		0.82
COV							0.18						0.15		0.16		0.21

Note: The highlighted capacities are the governing failure capacity predicted by each design standard.

115

Table 5-7 Summary of Predicted Capacities by Various Design Models

Test specimen	CSA–S16–01 Bolt bearing capacity		Equation [5-18]		Equation [5-13]	Equation [5-20]	Predicted governing capacity	Predicted governing failure mode	Observed capacity	Observed failure mode
	Angle	Beam web	Angle shear failure	Beam web tension and shear block	Angle end tearing	Angle leg connected to the column failed				
	(kN)	(kN)	(kN)	(kN)	(kN)	(kN)	(kN)		(kN)	
(1)	(2)	(3)	(4)	(5)	(6)	(7)	(8)	(9)	(10)	(11)
IV [1]	546	600 [2]	360	462	230	247	230	angle end tearing	240	end distance tearing
V [1]	713	800 [2]	378	487	311	271	271	ALF	269	end distance tearing
1LAa	517	562	336	443	224	266	224	angle end tearing	299	angle end tearing
1LBa	687	750	353	468	290	303	290	angle end tearing	342	angle end tearing
1L1a	839	655	419	—	363	444	363	angle end tearing	312	angle end tearing
1L2a	843	682	514	—	366	528	366	angle end tearing	321	angle end tearing
1L2aE	847	693	546	—	454	560	454	angle end tearing	490	angle end tearing
1L3a	841	939	515	700	368	527	368	angle end tearing	345	angle end tearing
1L4a	836	683	511	—	361	526	361	angle end tearing	452	angle end tearing
1L5a	846	686	518	515	366	531	366	angle end tearing	392	angle end tearing
1L6a	847	684	519	512	371	532	371	angle end tearing	331	angle end tearing
1L7a	835	661	413	—	362	432	362	angle end tearing	288	angle end tearing
1L8a	842	653	421	396	368	445	368	angle end tearing	306	angle end tearing
1L9a	846	692	516	—	382	547	382	angle end tearing	454	angle end tearing
1L11a	842	662	422	—	384	446	384	angle end tearing	327	angle end tearing

[1] Test specimens from Franchuk *et al.* (2002)
[2] Calculated assuming beam web material properties: F_u = 500 MPa and F_y = 400 MPa

*Note: ALF–angle leg connected to the column failure

116

Table 5-7 Summary of Predicted Capacities by Various Design Models (cont'd)

Test specimen	CSA–S16–01 Bolt bearing capacity		Equation [5-18]		Equation [5-13]	Equation [5-20]	Predicted governing capacity	Predicted governing failure mode	Observed capacity	Observed failure mode
	Angle	Beam web	Angle shear failure	Beam web tension and shear block	Angle end tearing	Angle leg connected to the column failed				
	(kN)	(kN)	(kN)	(kN)	(kN)	(kN)	(kN)		(kN)	
(1)	(2)	(3)	(4)	(5)	(6)	(7)	(8)	(9)	(10)	(11)
2L1a	1679	706	785	—	708	680	680	ALF	476	beam web edge distance tearing
2L2	1860	696	1075	—	787	727	696	bolt bearing on beam web	472	beam web edge distance tearing
2L3	1842	973	1065	—	792	707	707	ALF	574	beam web edge distance tearing
2L4	1853	690	1070	—	786	720	690	bolt bearing on beam web	551	beam web edge distance tearing
2L5a	1678	714	973	—	709	875	709	angle end tearing	620	beam web edge distance tearing
2L6a	1687	706	787	—	703	683	683	ALF	463	beam web edge distance tearing
2L7	1858	653	862	364	772	490	364	beam web tension and shear block	347	beam web tension and shear block
2L8a	1669	714	967	489	706	865	489	beam web tension and shear block	415	beam web tension and shear block

*Note: ALF—angle leg connected to the supporting column failure

117

Table 5-7 Summary of Predicted Capacities by Various Design Models (cont'd)

Test specimen	CSA–S16–01 Bolt bearing capacity Angle	Beam web	Equation [5-18] Angle shear failure	Beam web tension and shear block	Equation [5-13] Angle end tearing	Equation [5-20] Angle leg connected to the column failed	Predicted governing capacity	Predicted governing failure mode	Observed capacity	Observed failure mode
	(kN)	(kN)	(kN)	(kN)	(kN)	(kN)	(kN)		(kN)	
(1)	(2)	(3)	(4)	(5)	(6)	(7)	(8)	(9)	(10)	(11)
1LA	604	618	420	468	267	276	267	angle end tearing	280	ALF
1LB	801	776	440	457	345	302	302	ALF	288	ALF
1L1	937	707	436	—	394	245	245	ALF	306	ALF
1L2	913	685	527	—	391	369	369	ALF	346	ALF
1L3	933	940	539	—	396	391	391	ALF	430	ALF
1L4	916	692	530	—	401	373	373	ALF	378	ALF
1L5	910	688	526	—	399	367	367	ALF	362	ALF
1L6	919	695	532	—	404	370	370	ALF	368	ALF
1L7	943	696	443	—	394	248	248	ALF	276	ALF
1L8	939	678	436	368	396	244	244	ALF	290	ALF
1L9	914	692	529	—	424	366	366	ALF	360	ALF
1L10	910	712	430	—	424	240	240	ALF	291	ALF
1L12	1006	656	565	—	—	258	258	ALF	299	ALF
1L13	1007	649	568	—	—	316	316	ALF	372	ALF
1L14	1004	656	565	—	—	276	276	ALF	362	ALF
1L10a	842	683	425	—	393	450	393	angle end tearing	376	ALF
2L1	1860	691	867	—	785	486	486	ALF	400	ALF
2L6	1857	685	866	—	792	483	483	ALF	377	ALF

*Note: ALF—angle leg connected to the supporting column failure

118

a) End Distance Failure

b) Collapse Load Mechanism
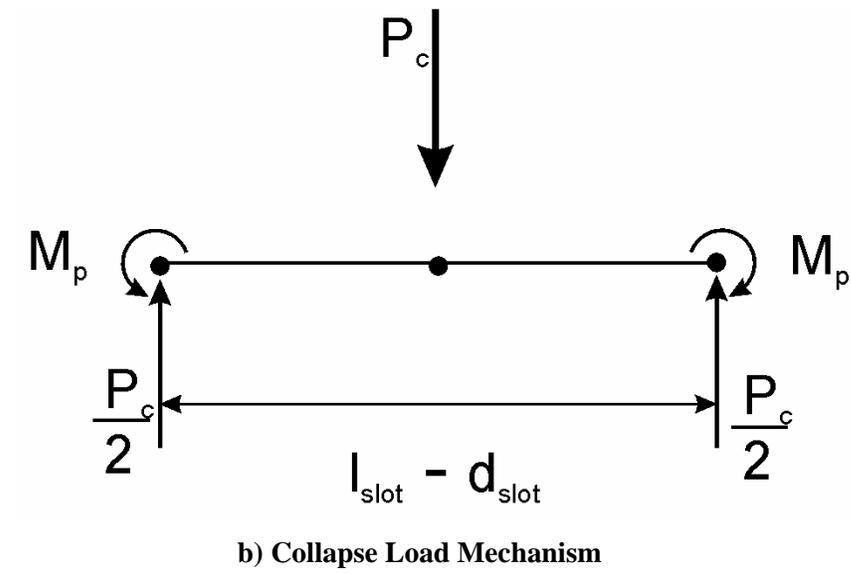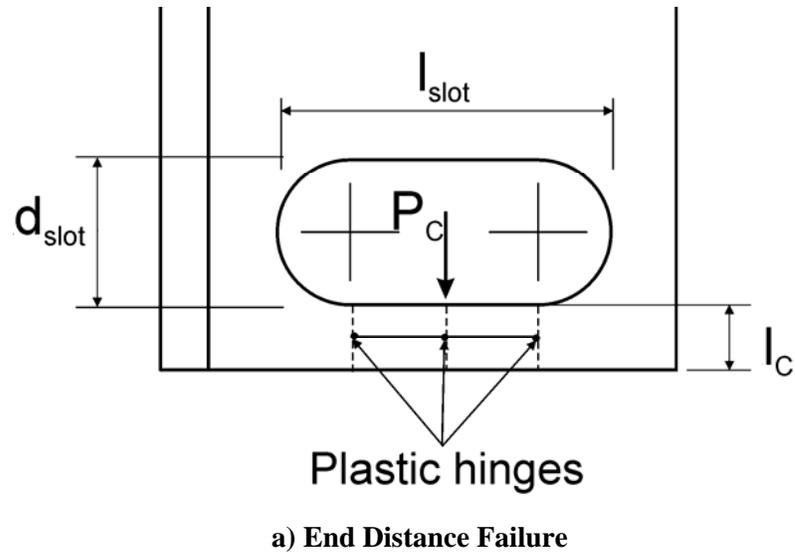
Figure 5-1 Collapse Load Capacity of End Distance in a Slotted Hole Connection
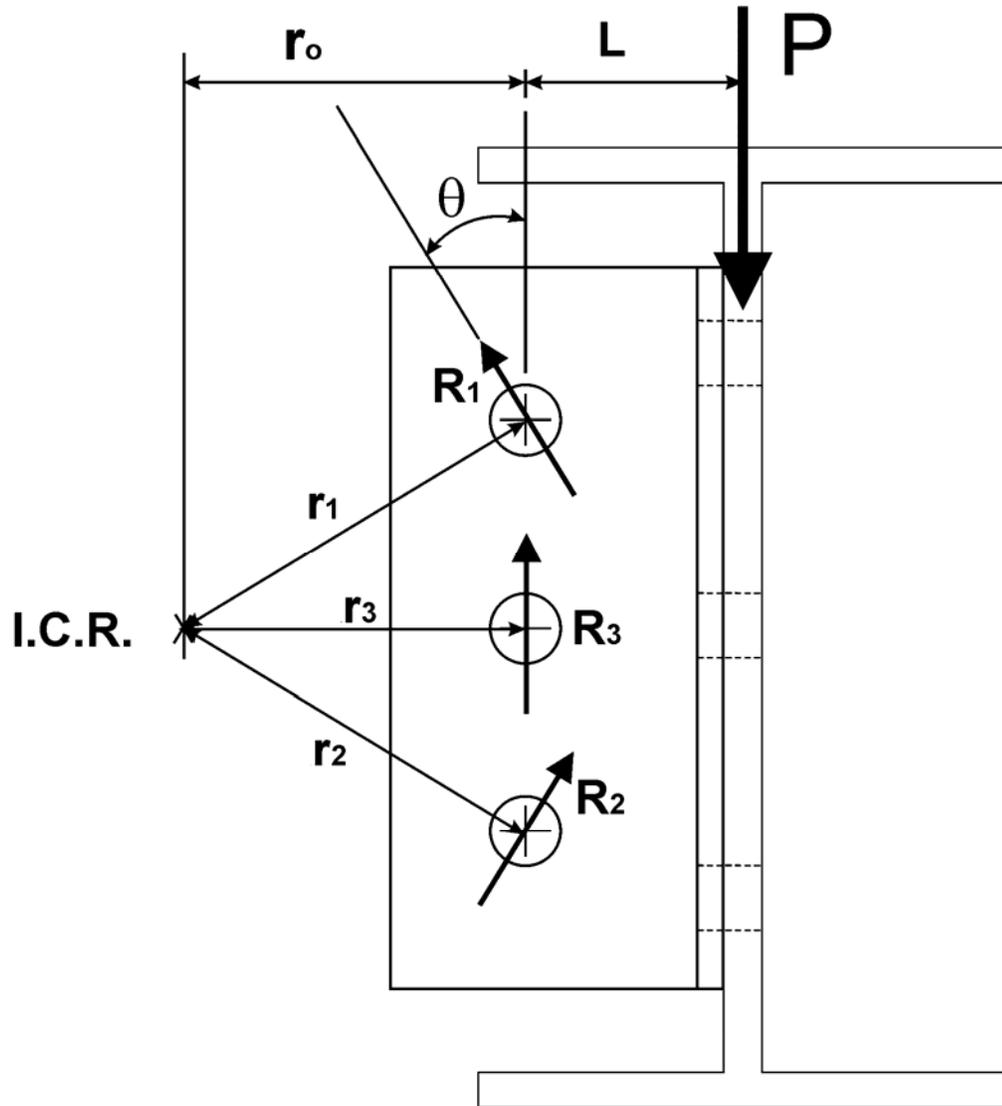
Figure 5-2 Typical Eccentrically Loaded Single Angle Shear Connection
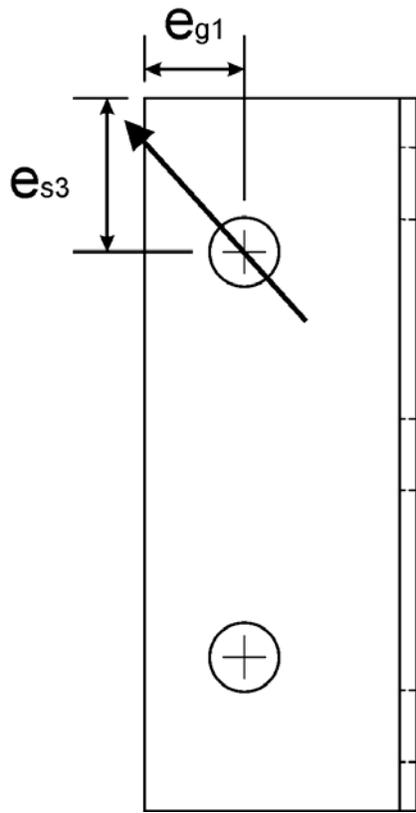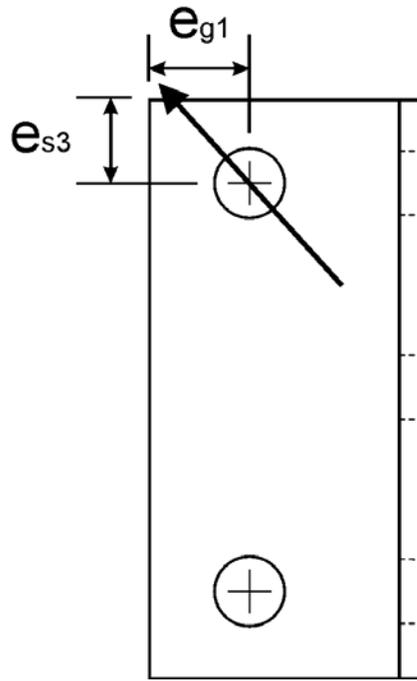
a) Bolt Force Crosses the Edge   b) Bolt Force Crosses the Top End

Figure 5-3 Direction of Bolt Force
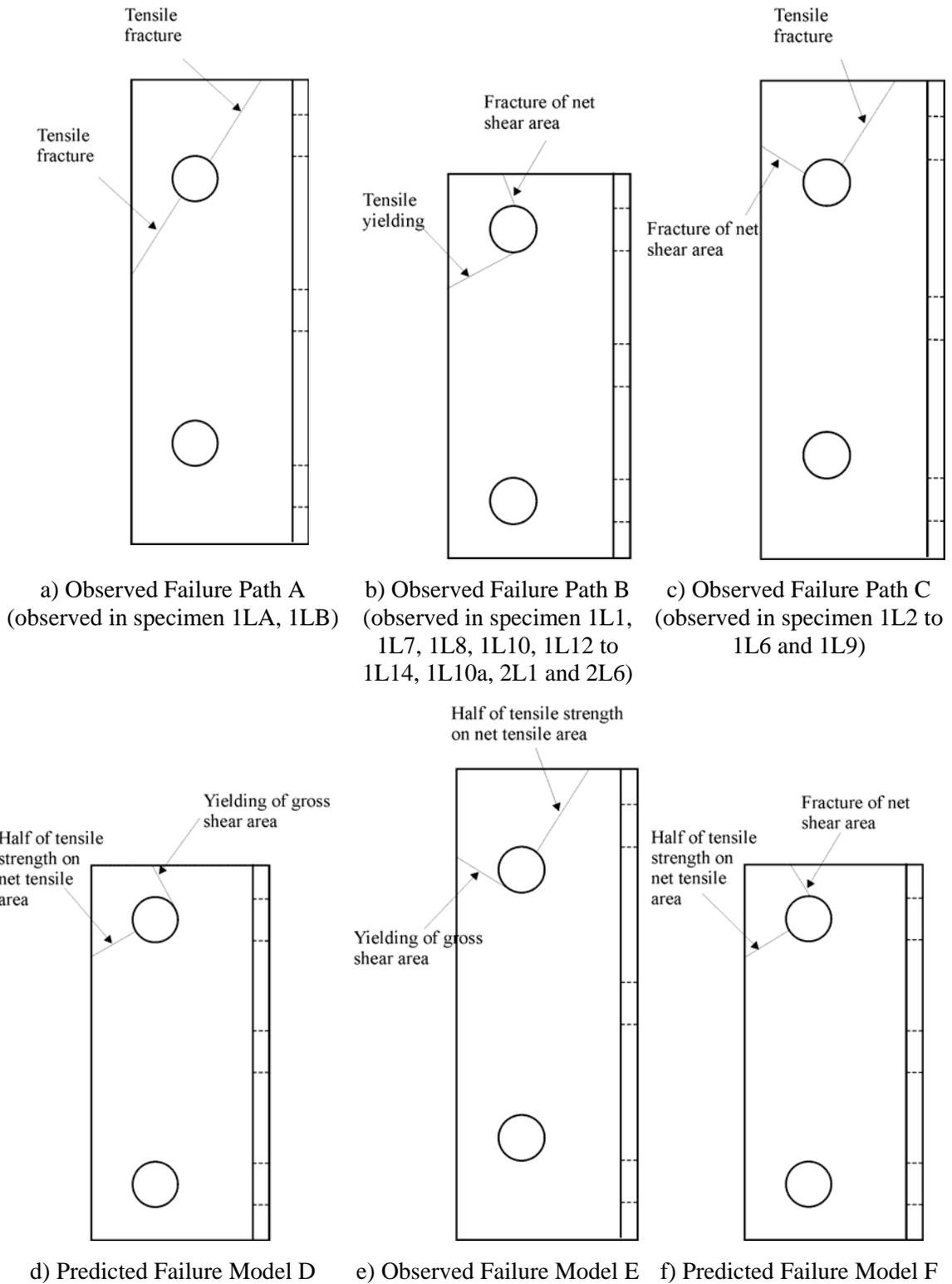
a) Observed Failure Path A (observed in specimen 1LA, 1LB)

b) Observed Failure Path B (observed in specimen 1L1, 1L7, 1L8, 1L10, 1L12 to 1L14, 1L10a, 2L1 and 2L6)

c) Observed Failure Path C (observed in specimen 1L2 to 1L6 and 1L9)

d) Predicted Failure Model D

e) Observed Failure Model E

f) Predicted Failure Model F

Figure 5-4 Observed Failure Paths and Predicted Failure Model

122

g) Predicted Failure Model G   h) Predicted Failure Model H   i) Predicted Failure Model I

j) predicted Failure Model J   k) Predicted Failure Model K
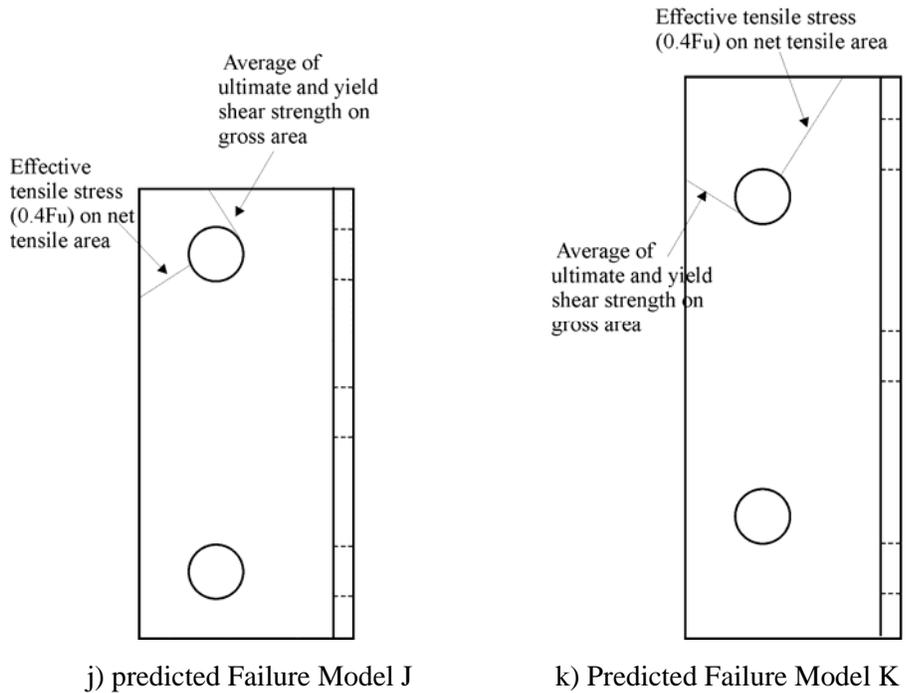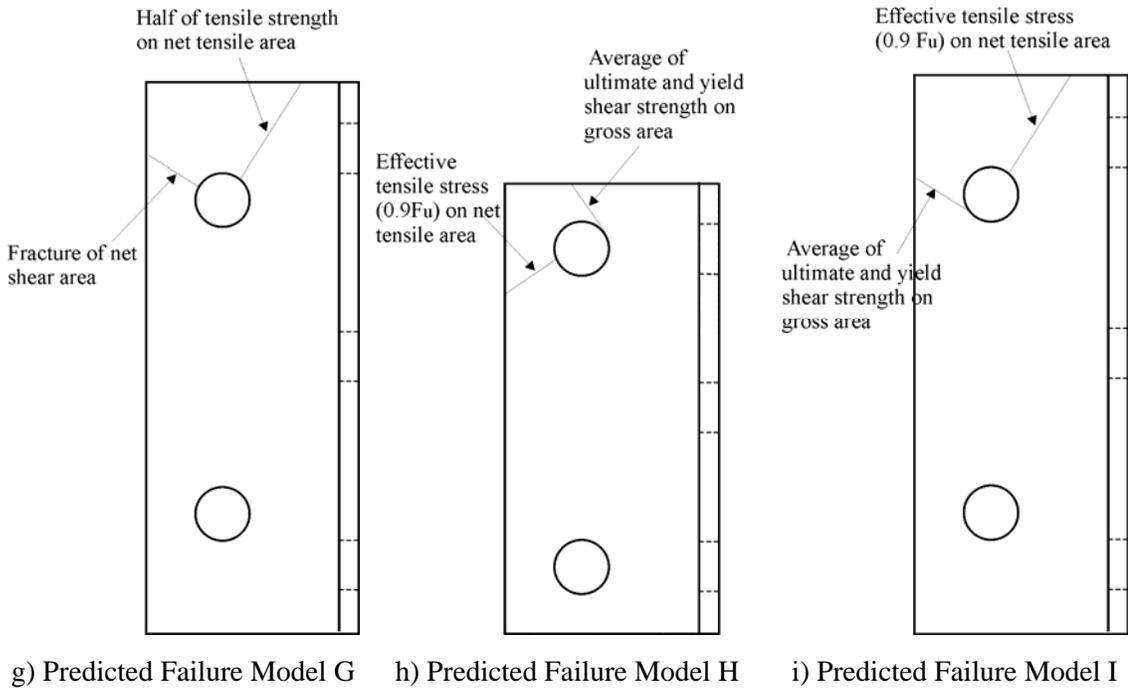
Figure 5-4 Observed Failure Paths and Predicted Failure Models (cont'd)
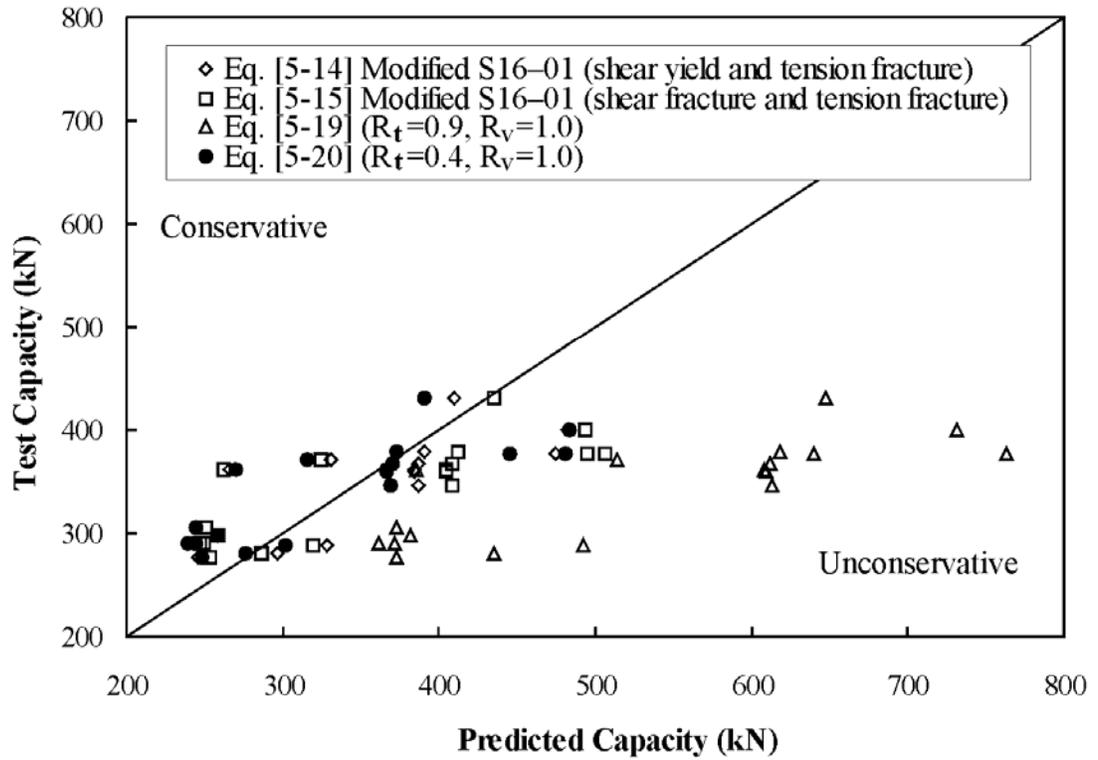
**Figure 5-5 Comparison of Proposed Prediction Models for Specimens Failed at the Leg
Connected to the Column**

6 Summary and Conclusions

6.1 Summary

It has been shown that research in the past few decades on single and double angle connections has emphasized the moment-rotation behaviour of connections, rather than the shear capacity or the ultimate limit state of the connections. Moreover, no tests had been conducted on slotted hole connections with the slots on the outer plies. The current North American steel design standards, namely CSA–S16–01 and AISC 2005, require that plate washers with standard size holes have to be installed on the outer plies of joints in a connection with long slots to completely cover the slots with the loading direction perpendicular to the length of slot. The purpose of the plate washer is to prevent bolt pull-out in a bearing type connection. However, bolt pull-out has not been identified as an ultimate limit state in the past. The effects of a plate washer on the strength and behaviour of connections with slotted holes are not clearly identified yet. Therefore, a research program was initiated to assess the effect of plate washers as well as other parameters on the strength and behaviour of the connections.

An experimental research program consisting of 40 tests on full-scale beam-to-column connections was carried out to investigate the strength and behaviour of connections with slotted holes. A wide range of parameters were investigated: bottom end distance, plate washer, slot length, bolt pretension, torsion brace, bolt pitch, coped flange, beam end rotation, web thickness and bolt diameter. In assessing the effect of the above parameters, the load vs. deformation response and load carrying capacity were used as bases for comparison. Two of the test specimens from the current research program were compared with two single angle specimens tested by Franchuk *et al.* (2002) to investigate the effect of plate washers on single angle connections further. In addition, a failure mode that consisted of failure of the angle leg connected to the column was observed. The failure mode was similar to the tension and shear block failure in coped beams, except that the tension and shear block was inclined to the line of action of the applied force. In order to investigate this failure mode further, parameters related to the angle leg connected to the column were varied. These parameters included: top end

distance and edge distance, thickness of angle, number of bolts and the effect of single or double angles.

A comparison between the test results and capacities predicted by the current North American steel design standards, namely, CSA–S16–01 and AISC 2005, as well as Equation [5-18] was presented. In addition, new prediction models were developed for failure by angle bottom end tearing and failure of the angle leg connected to the supporting column.

6.2 Conclusions

The following conclusions are drawn from this research program:

1. Plate washers are beneficial to slotted holes connections with 6.4 mm thick single angles. The thin single angle specimens without plate washers (IV and V from Franchuk *et al.* (2002)) failed by tearing of bottom end of the angle and top edge of the beam web, followed by tilting of the middle bolt. In contrast, the specimens with plate washers failed by bottom end distance tearing, followed by shear failure of angle. The capacities of specimens with plate washers showed an increase in capacity of 24% to 27% over the ones without plate washers.

2. Specimens with 9.5 mm thick angles with plate washers also showed increased capacity compared to the ones without plate washers. The single angle specimen (1L2a) without a plate washer showed a 29% lower angle end tearing capacity compared to the specimen with a plate washer (1L4a). The double angle specimen with plate washers (2L4) showed a 14% higher capacity over the one without plate washers (2L2). Both of the specimens without plate washers did not reach the expected capacity predicted by the current North American steel design standards. Specimen 1L2a had a test-to-predicted ratio of 0.68 and 0.69 predicted by CSA–S16–01 and AISC 2005, respectively, and specimen 2L2 had a ratio of 0.69 predicted by both CSA–S16–01 and AISC 2005. Only the single angle specimen with plate washer (1L4a) reached the expected capacity (test-to-predicted ratio of 0.97 and 0.98 predicted by CSA–S16–01 and AISC 2005, respectively). The double angle connection with plate washer (2L4) did not reach

the expected capacity (test-to-predicted ratio of 0.80 predicted by both standards). It is likely due to the failure of the edge distance, and the bearing strength of the beam web was not fully developed.

3. It was found that the size of the loaded bottom end distance in single angle connections has a significant effect on angle end tearing capacity. An increase in as-built bottom end distance by from 34.0 mm to 46.3 mm resulted in an increase in the angle end tearing capacity of 53%.

4. Single angles with short slots (1L9a) showed 41% higher end tearing capacity than its long slot counterpart (1L2a).

5. It was found that increasing the bolt pitch did not lead to a significant increase in capacity for the single angle connections (3% to 8% increase) and double angle connections with uncoped beam (1% increase). That is because the former failed by angle end tearing and the latter by beam web edge distance tearing. Double angle connections with a coped beam failed by tension and shear block of the beam web. The increase of bolt pitch (from 76 mm to 102 mm) and the associated increased shear area led to a 20% increase in capacity for double angle specimens with coped beams (2L7 and 2L8a) that failed in a tension and shear block mode.

6. Single web framing angles with minimum bottom end distances that failed by end tearing showed a resistance as low as 68% of the capacity predicted using CSA–S16–01 and AISC 2005.

7. The beam web edge distance used in the research program was 30 mm, which is close to the minimum requirement of 28 mm. The test specimens with an uncoped beam and double angles failed by beam web edge distance tearing. The possible failure mode of bolt bearing on the beam web was investigated. It was observed that the edge distance tearing failure resulted in a reduction in capacity of as much as 41%. None of the test specimens with double angles and an uncoped beam reached the bolt bearing capacity.

8. Connections with pretensioned bolts showed higher stiffness (about 50%) and higher capacity (18% increase in angle end tearing capacity for single angle

specimens and 13% increase in beam web failure capacity for double angle specimens) than the ones with snug tight bolts, possibly due to some load transfer by friction between the faying surfaces at the connection.

9. Torsionally braced specimens showed only a 5% increase in web framing angle capacity. However, torsion bracing reduced twisting of the beam by as much as 7° at peak load (at about 25 mm bottom flange deflection).

10. For specimens that failed in the angle leg connected to the column, it was found that top end distance, edge distance and number of bolts connecting the angle to the column affect the connection capacity. Increasing the top end distance from 32 mm to 58 mm resulted in an increase in capacity of 29% on average. An increase in edge distance from 32 mm to 50 mm resulted in an increase of 24% in the connection capacity. For the same size of angle, an increase in the number of bolts from two to three connecting to the column also results in an increase of 21% in the capacity. The double angle connection with this failure mode also showed a 34% higher capacity than its single angle counterpart.

11. The current North American steel design standards, namely, CSA–S16–01 and AISC 2005, have provisions for the following failure modes: fracture at the net section of web-framing angles, tension and shear block failure of beam web and web crippling failure under a concentrated load. In the current test program, the test-to-predicted ratio of the test specimens with the above failure modes was found to range from 0.87 to 1.28 calculated using CSA–S16–01 and range from 0.87 to 1.16 calculated using AISC 2005. However, CSA–S16–01 does not have provisions for angle end tearing failure, and neither North American standards has provisions for the failure of the angle leg connected to the column that failed by corner tearing of the connected material, as well as tearing of the beam web edge distance.

12. Equation [5-13] is proposed for the prediction of capacity of web framing angles failing by end tearing and bearing. The equation combines the failure of the end distance by plastic collapse or shear failure with the bearing strength of the remaining interior bolts. For 13 specimens that failed by angle bottom end

distance tearing, Equation [5-13] resulted in a mean test-to-predicted ratio of 1.01 and a COV of 0.18, compared to a mean of 0.88 and a COV of 0.13 predicted by CSA–S16–01, and a mean of 0.88 and a COV of 0.15 predicted by AISC 2005.

13. A calculation procedure was proposed to predict the capacity of eccentrically loaded angles failing by loaded end tearing. The formulation is based on a tension and shear block failure mode limiting the strength of the critical bolt in the eccentrically loaded connection. The resulting Equation [5-20] results in a mean test-to-predicted ratio of 1.05 and a COV of predicted values of 0.15 for 18 specimens that failed in this manner. Other possible failure modes predicted by CSA–S16–01 and AISC 2005, such as rupture of net shear area of angle, yielding of gross shear area of angle, bolt bearing on beam and angle, and tension and shear block failure of coped beams, were investigated. Neither design standard has provisions for corner tearing of angle leg connected to the column. The mean test-to-predicted ratio obtained from CSA–S16–01 is 0.75 and COV of 0.18, and the mean test-to-predicted ratio obtained from AISC 2005 is 0.78, with a COV of 0.15.

6.3 Design Recommendations

From the results of this research program, several recommendations are made for the design of connections with slotted holes:

1. Angle thickness – It was found that the single angle connections with thinner angles (6.4 mm) and without plate washer (specimens IV and V from Franchuk *et al.* (2002)) could fail by tearing of the loaded end distance followed by bolt-tilting. The test-to-predicted ratios for these two specimens were substantially lower than expected (0.69 and 0.76). The bolt-tilting phenomenon was not observed on the single angle connections with thicker angles (9.5 mm). It is suspected that the angle used in specimens IV and V was too flexible. Moreover, the minimum recommended thickness suggested in AISC Manual of Steel Construction (AISC, 1999) is 9.5 mm. Therefore, it is recommended that the minimum angle thickness used in web-framing angles be at least 9.5 mm.

2. Plate washers for connections with slotted holes – It was found that connections with plate washers had higher capacities than the one without plate washers. This is likely caused by the increased rigidity and confinement within the connections with plate washers. Although no bolt pull-out was observed in this research program, the plate washers are required in both single and double angle slotted hole connections in order to reach the predicted capacity. It should be noted that an increase in end and edge distances might be sufficient to waive the requirement for plate washers in double angle connections. This was not investigated in this research program.

3. Edge distance requirements – In this research program, the edge distance used on beam web was 30 mm, which satisfies the edge distance requirement of 28 mm for 7/8 in. diameter A325 bolts as described in CSA–S16–01. The failure mode of beam web edge distance tearing was likely caused by the small edge distance used in the beam web. The test-to-predicted ratio for specimens that failed by rupture of the edge distance ranged from 0.59 to 0.87, as predicted by the bolt bearing capacity equation in CSA–S16–01. The bolt bearing strength on beam web was not reached for all the specimens with edge distance tearing. It is suspected that the edge distance has to be larger in order to develop the bearing strength on the beam web. According to CSA–S16–01, the bearing strength, σ_b, is taken as three times material the tensile strength at the ultimate limit state. To achieve equilibrium of forces and assuming the edge distance on either side of the bolt shares equal loads at the ultimate limit state, the clear edge distance has to be at least 1.5 times the bolt diameter in order to develop the bearing stress of 3 times the material tensile strength. Therefore, it is recommended that a minimum clear edge distance of 1.5 times the bolt diameter, or a minimum edge distance (from center of bolt to the edge of material) of 2.0 times the bolt diameter, if the connection is designed for bolt bearing on the beam web. Validation of this increased edge distance is recommended.

4. End distance requirements – All the angles in the test program were fabricated with minimum end distance as required by CSA–S16–01 for ASTM high strength

bolts, except for specimen 1L2aE, which was fabricated with 47 mm bottom end distance. As shown in Kulak *et al.* (1987), the relationship between the bearing stress, end distance and bolt diameter can be expressed as:

$$\frac{l_e}{d} \geq 0.5 + 0.715 \frac{\sigma_b}{F_u} \qquad [6\text{-}1]$$

In terms of clear end distance, l_c:

$$\frac{l_c}{d} \geq 0.715 \frac{\sigma_b}{F_u} \qquad [6\text{-}2]$$

If the bearing strength of 3.0 F_u has to be achieved at the end distance, the clear end distance has to be about 2.0 times the bolt diameter. For instance, the clear end distance has to be 45 mm for a 7/8 in. diameter bolt. Therefore, a minimum clear end distance of 2.0 times the bolt diameter is recommended.

6.4 Recommendations for Future Research

From the result of this research program, the understanding of the behaviour of connections with slotted holes had been improved significantly. However, further research is required in the following areas:

1. It was found that the loaded end distance had significant effect on the connection capacity. However, only one test specimen (1L2aE) had a loaded end distance greater than the minimum permitted, whereas the remaining specimens had minimum loaded end distances. It seems that the minimum end distance currently used in design standards may be too small to develop the full capacity of a connection. Further testing is recommended to determine the minimum end distance required to develop the full connection potential.

2. Several of the test specimens with a double angle shear connection and uncoped beam failed by edge distance tearing. However, only one edge distance (30 mm) was investigated in this test program. Therefore, the effect beam edge distance on the connection capacity should be investigated. The bolt bearing capacity was not

reached in any of these specimens. It is therefore expected that a larger edge distance would result in a significant increase in connection shear capacity.

3. A reliability analysis is recommended to assess the level of safety of the connections as designed by current North American steel design standards, as well as the newly proposed prediction models. In this research program, only the test-to-predicted ratios and the COV of test-to-predicted values by various prediction models are presented. A wide range of failure modes were observed in the test program. As a result, there are only a few specimens under each group of failure mode. There is a need to expand the pool of experimental data for specimens with the same failure mode. The information on angle end tearing and beam web edge distance failure is the most deficient in this respect. More experimental work is recommended in this area. A reliability analysis is also recommended to assess the level of safety provided by the newly developed prediction models in this research program.

4. For double angle connections with coped or uncoped beams, the location of beam web edge distance tearing varied. The specimens with a large bolt pitch failed by beam web edge distance tearing at the middle bolt hole, whereas the specimens with standard pitch failed at the bottom bolt hole. This phenomenon should be investigated further. The effects of parameters that affect the location of edge distance tearing need to be identified.

5. The use of plate washers resulted in a significant increase in shear capacity of connections with slotted holes in the outer plies. The possible causes were a change in failure mode and increased rigidity at the connection. However, the failure mechanism of angle end tearing with plate washer on the outer plies of the joint and how the plate washer increased the rigidity of the connection is not clearly identified yet. More experimental testing and numerical analyses are recommended to investigate the effect of plate washers on connections with slotted holes further.

References

AISC (1999). "*Manual of Steel Construction - Load and Resistance Factor Design (LRFD), Second Edition, Vol. 2, Connections,*" American Institute of Steel Construction (AISC), Chicago, Illinois.

AISC (2005). "*Specification for Structural Steel Buildings,*" American Institute of Steel Construction, Chicago, IL.

ASTM (1997). "*A370-97 Standard Test Methods and Definitions for Mechanical Testing of Steel Products,*" American Society for Testing and Materials, Philadelphia, PA, USA.

Allan, R.N. and Fisher, J.W. (1968). "*Bolted Joints with Oversized or Slotted Holes,*" Proceedings of the ASCE, No. ST9, pp. 2061-2080.

Astaneh, A., Call, S.M., and McMullin, K.M. (1989). "*Design of Single Plate Shear Connections,*" Engineering Journal, AISC, First Quarter, pp. 21-32.

Bergson, P.M. and Galambos, T.V. (1998). "*Experimental Tests on Bolted Single-Angle Connections with Horizontal Short-Slotted Holes,*" Structural Engineering Report No. ST-98-3, Department of Civil Engineering, University of Minnesota, Minneapolis, MN.

Birkemoe, P.C. and Gilmor, M.I. (1978). "*Behavior of Bearing Critical Double-Angle Beam Connections,*" Engineering Journal, AISC, Vol. 15, No. 4, Fourth Quarter, pp. 109-115.

CISC (2004). "*Handbook of Steel Construction,*" Eighth Edition, CISC, Toronto, Ontario.

Crawford, S.F. and Kulak, G.L. (1971). "*Eccentrically Loaded Bolted Connections,*" Proceedings of the ASCE, Journal of Structural Division, ST3, March 1971, pp. 765-783.

Crocker, J.P. and Chambers, J.J. (2004). "*Single Plate Shear Connection Response to Rotation Demands Imposed by Frames Undergoing Cyclic Lateral Displacements,*" Journal of Structural Engineering, ASCE, Vol. 130, No. 6, pp. 934-941.

CSA (1998). "*CAN/CSA–G40.21–98 Structural Quality Steel,*" Canadian Standards Association, Toronto, ON, Canada.

CSA (2001). "*CSA–S16–01 Limit State Design of Steel Structures,*" Canadian Standards Assocation, Toronto, ON.

Franchuk, C.R., Driver, R.G. and Grondin, G.Y. (2002) "*Block Shear Behavior of Coped Steel Beams*," Structural Engineering Report no. 244, Department of Civil and Environmental Engineering, University of Alberta, Edmonton, AB, Canada.

Hormby, D.E., Richard, R.M. and Kriegh, J.D. (1984). "*Single Plate Framing Connections with Grade-50 Steel and Composite Construction*," Engineering Journal, AISC, Third Quarter, pp. 125-138.

Kulak, G. L., Fisher, J. W., and Struik, J. H. A. (1987). "*Guide to Design Criteria for Bolted and Riveted Joints*," Second Edition, Wiley-Interscience, New York, New York.

Lipson, S.L. (1968), "*Single-Angle and Single-Plate Beam Framing Connections*," Proceedings, Canadian Structural Engineering Conference, Toronto, Ontario, Canada, Feb., 1968, pp. 141-162.

Lipson, S.L. (1977) "*Single-Angle Welded-Bolted Connections*," Journal of Structural Engineering, ASCE, Vol. 103, No. ST3, pp. 559-570.

Munse, W.H., Bell, W.G., and Chesson, E. Jr.(1961). "*Behavior of Beam-to-Column Connections*," Transactions, ASCE, Vol. 126, Part II, Paper No. 3241, pp. 729-749.

Rathbun, J.C. (1936), "*Elastic Properties of Riveted Connections*," Transactions, ASCE, Vol. 101, Paper No. 1933, pp. 524-563.

RCRBSJ (1976), "*Specifications for Structural Joints Using ASTM A325 or A490 Bolts*," Research Council on Riveted and Bolts Structural Joints, Feb., 1976.

Richard, R. M., Gillett, P.E., Kriegh, J. D. and Lewis, B.A. (1980). "*The Analysis and Design of Single Plate Framing Connections*." AISC Engineering Journal, American Institute of Steel Construction, Second Quarter, pp. 38-52.

Ricles, J.M., and Yura, J.A. (1983). "*Strength of Double-Row Bolted-Web Connections*," Journal of Structural Engineering, ASCE, Vol. 109, No. 1, pp. 126-142.

Shneur, V. (2003). "*57 tips for Reducing Connection Costs*," Modern Steel Construction, July, 2003, pp. 20-22.

Wald, F., Mazura, V., Moal, M. and Sokol, Z. (2002). "*Experiments of Bolted Cover Plate Connections with Slotted Holes*," CTU Reports, Vol. 6, 2/2002, pp. 79-96.

Yura, J.A., Birkemoe, P.C., and Ricles, J.M. (1982). "*Beam Web Shear Connections: An Experimental Study*," Journal of the Structural Division, ASCE, Vol. 108, No. ST2, pp. 311-325.

Appendix A
Photos of Failed Specimens
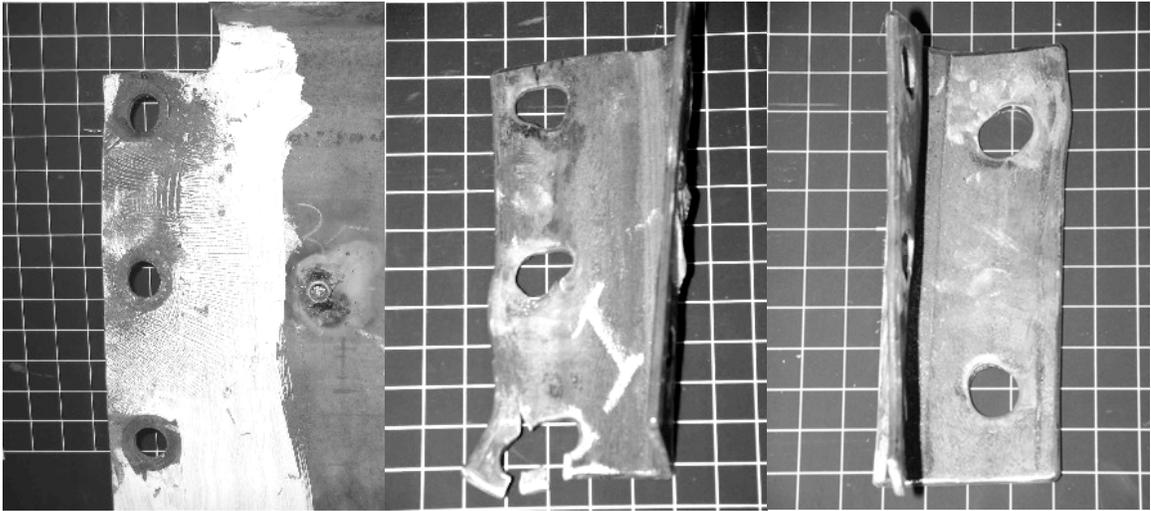
| Beam | Angle leg on connection side | Angle leg connected to the column |

Figure A-1 Test Specimen 1LA
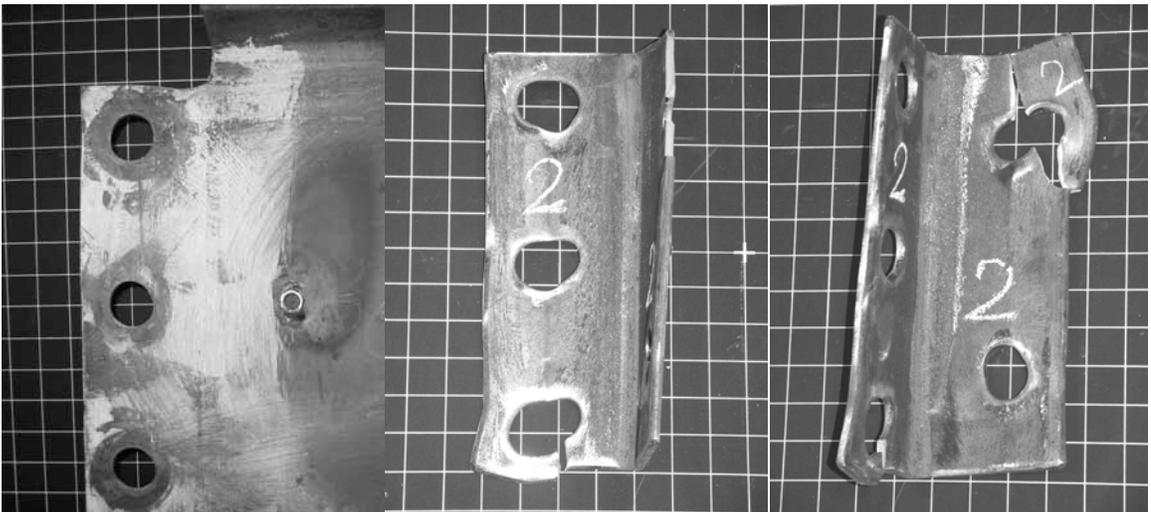
| Beam | Angle leg on the connection side | Angle leg connected to the column |

Figure A-2 Test Specimen 1LB
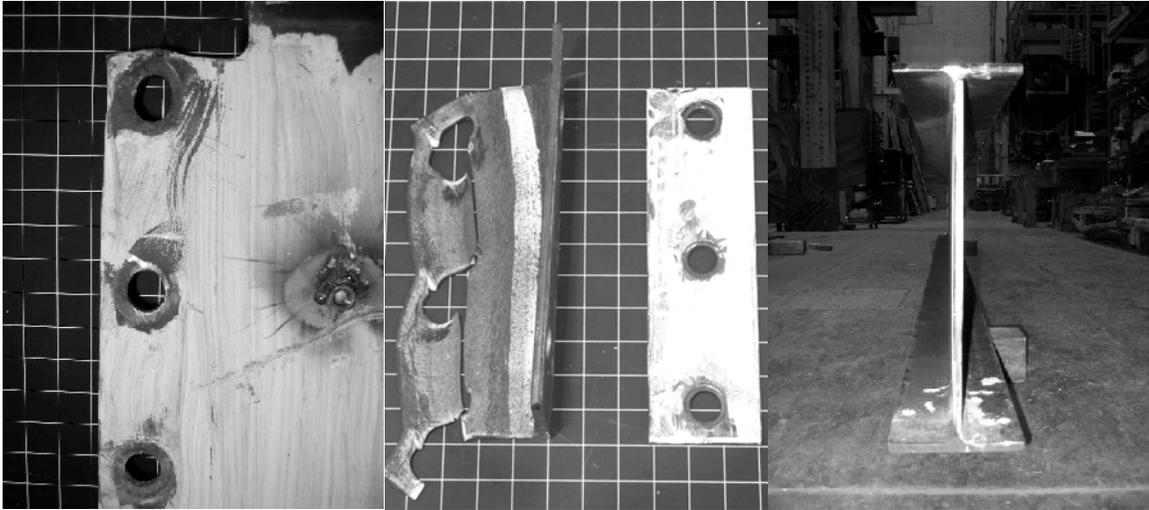
| Beam | Angle and the plate washer | Side view of beam web |

Figure A-3 Test specimen 1LAa
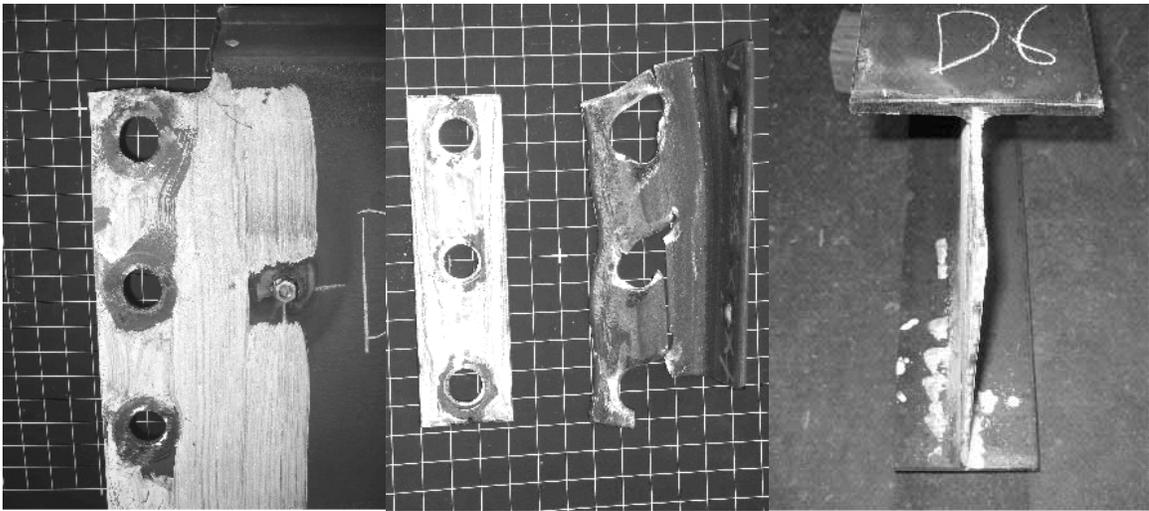
| Beam | Angle and the plate washer | Side view of beam web |

Figure A-4 Test Specimen 1LBa
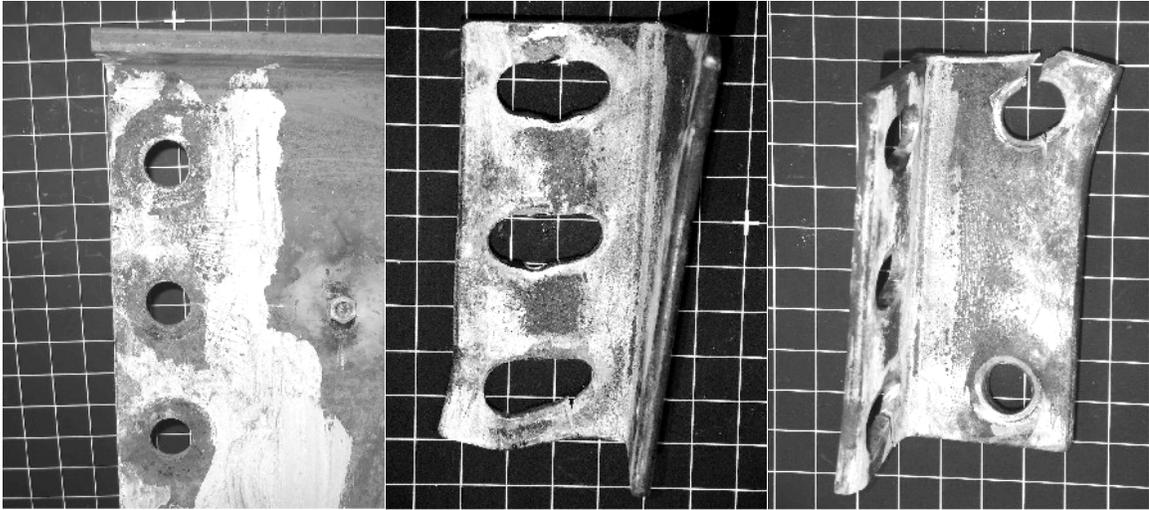
| Beam | Angle | Angle leg connected to the column |

Figure A-5 Test specimen 1L1
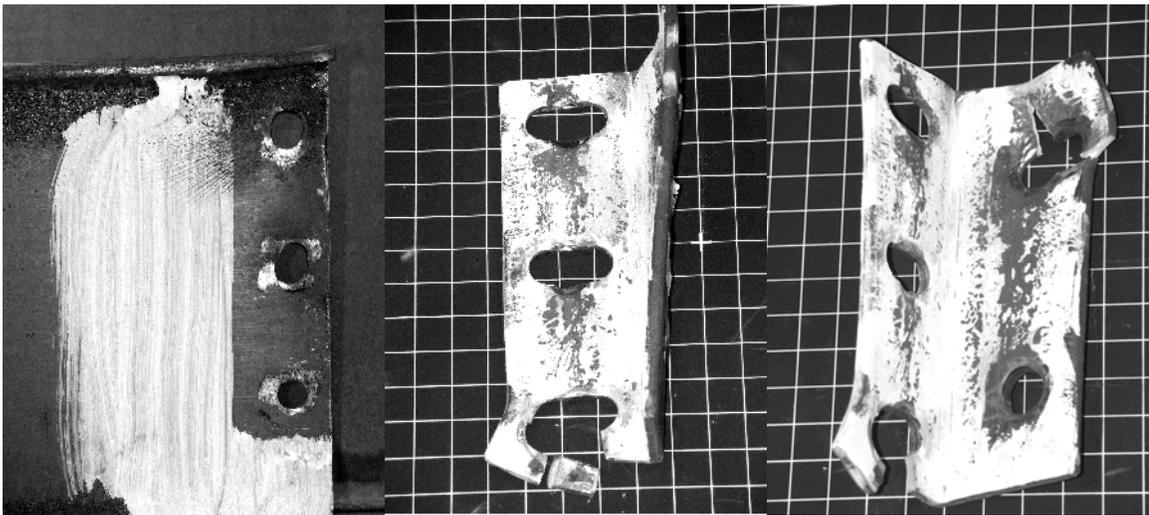
| Beam | Angle leg on connection side | Angle leg connected to the column |

Figure A-6 Test specimen 1L2
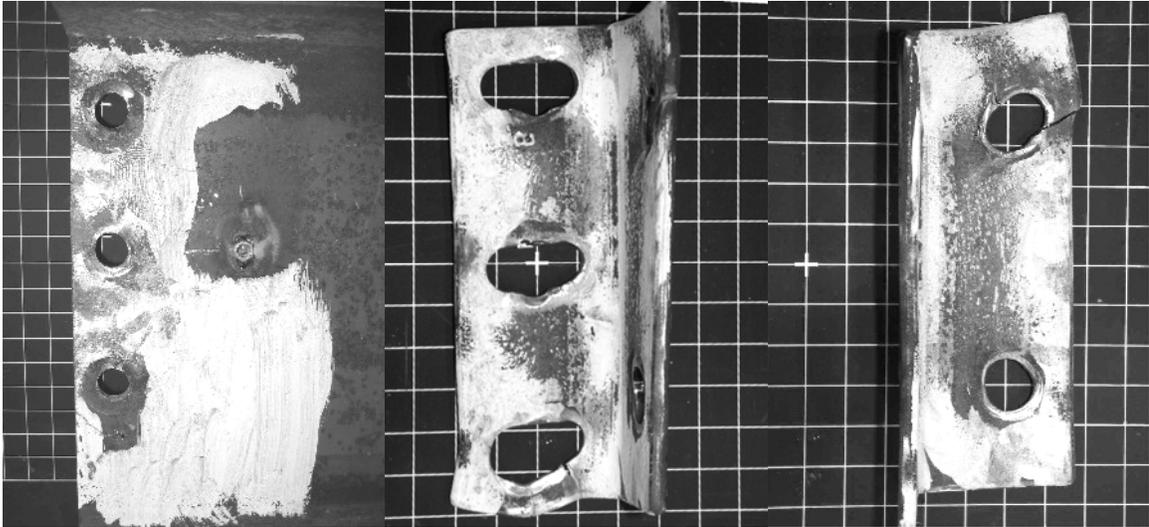
| Beam | Angle | Angle leg connected to the column |

Figure A-7 Test specimen 1L3

| Beam | Angle | Angle leg connected to the column |

Figure A-8 Test specimen 1L4
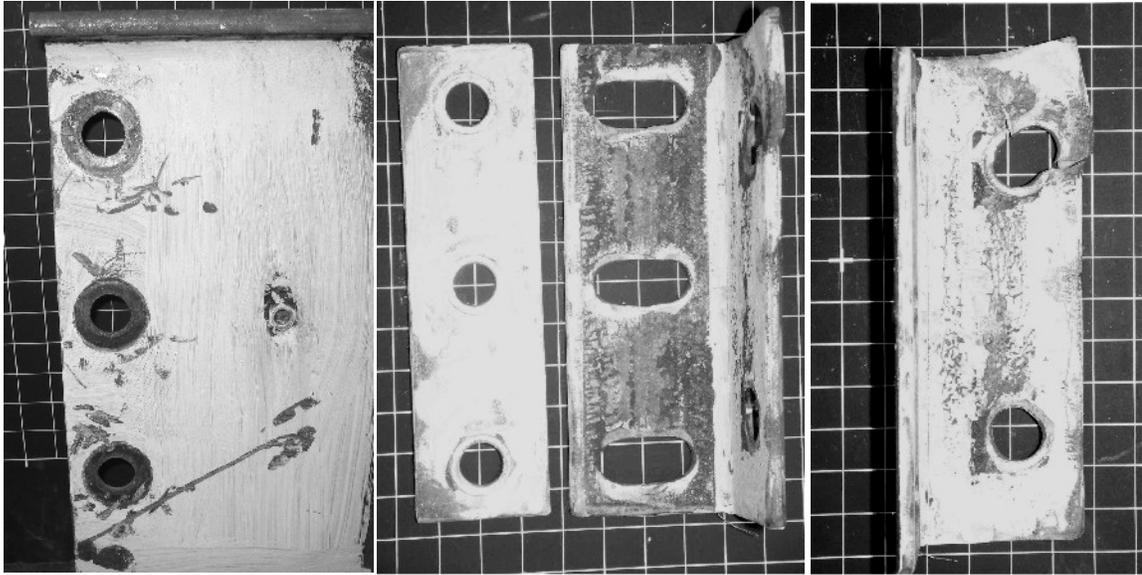
| Beam | Angle and the plate washer | Angle leg connected to the column |

Figure A-9 Test specimen 1L5
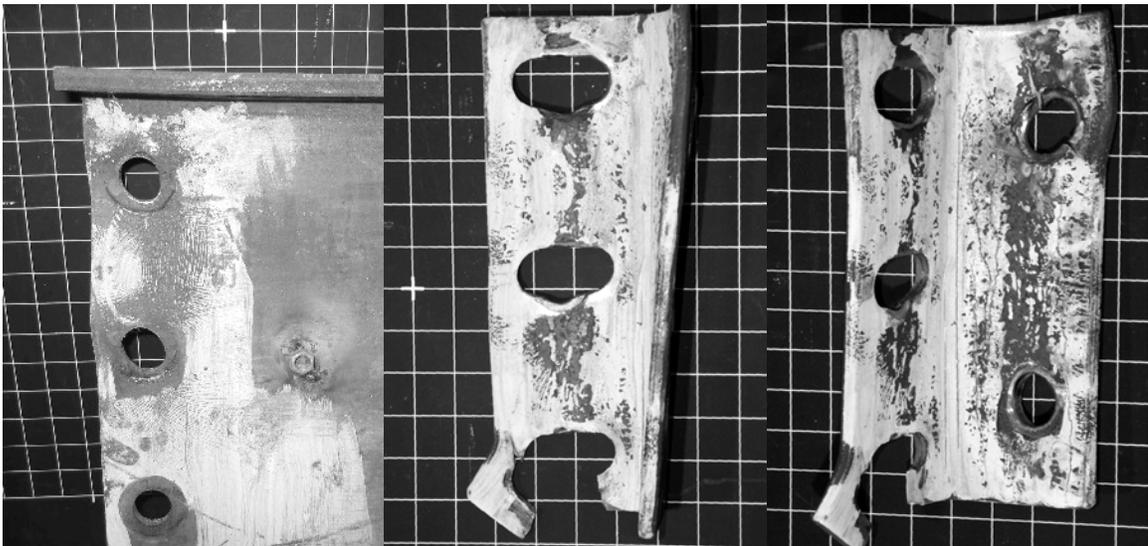
| Beam | Angle | Angle leg connected to the column |

Figure A-10 Test specimen 1L6
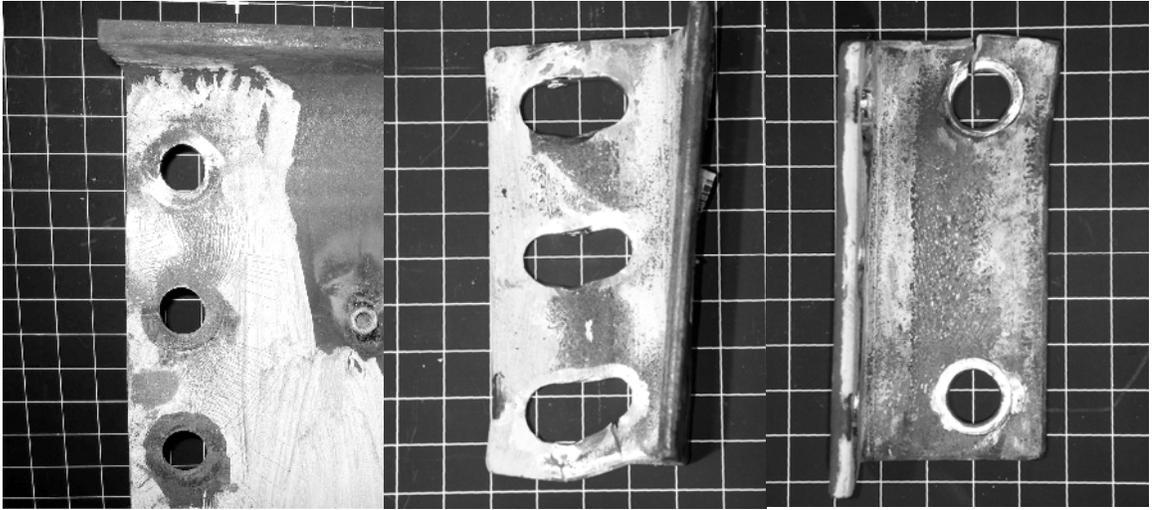
| Beam | Angle on connection side | Angle leg connected to the column |

Figure A-11 Test specimen 1L7
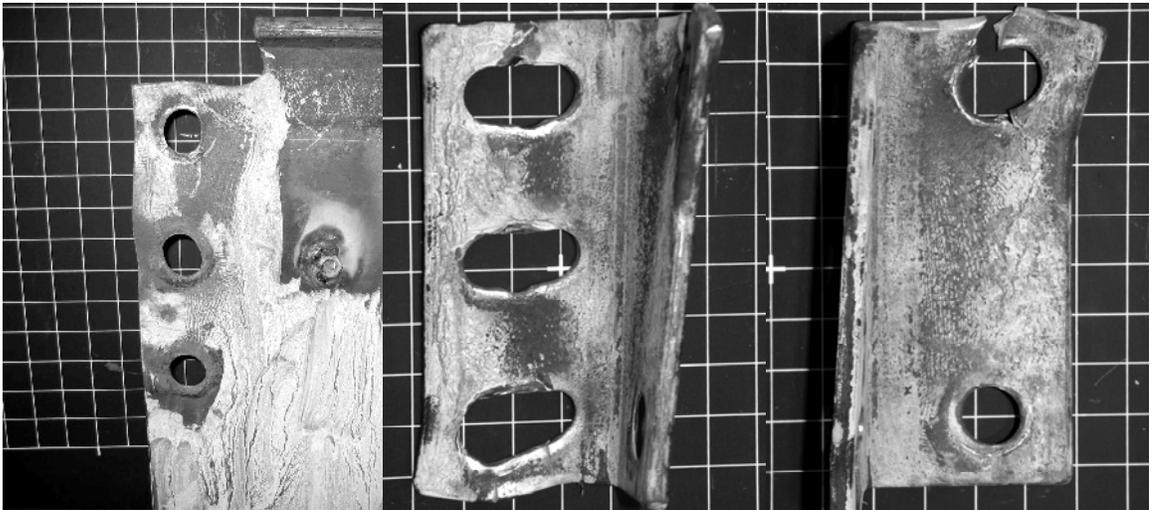
| Beam | Angle on connection side | Angle leg connected to the column |

Figure A-12 Test specimen 1L8
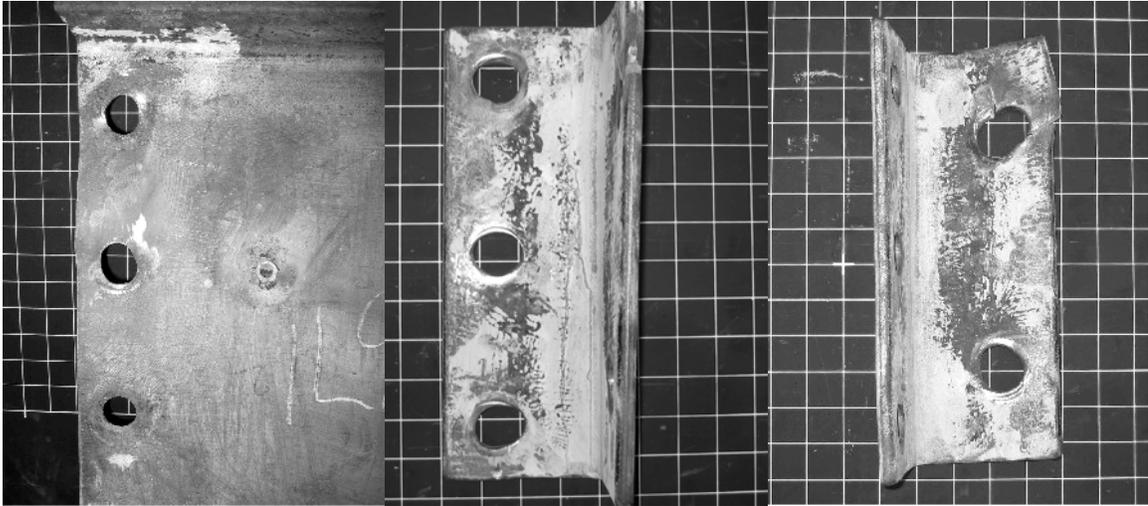
| Beam | Angle on connection side | Angle leg connected to the column |

Figure A-13 Test specimen 1L9
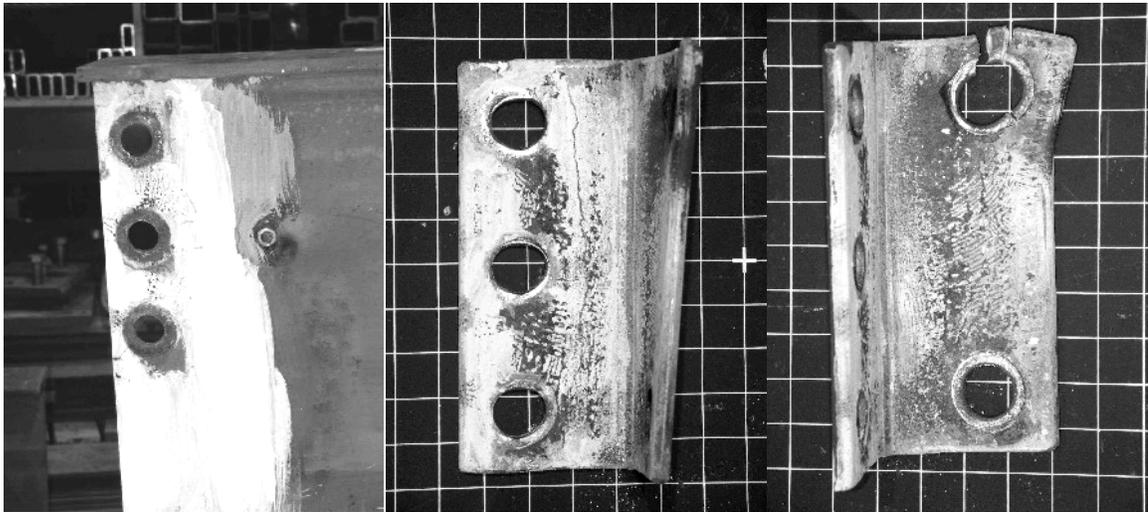
| Beam | Angle on connection side | Angle leg connected to the column |

Figure A-14 Test specimen 1L10
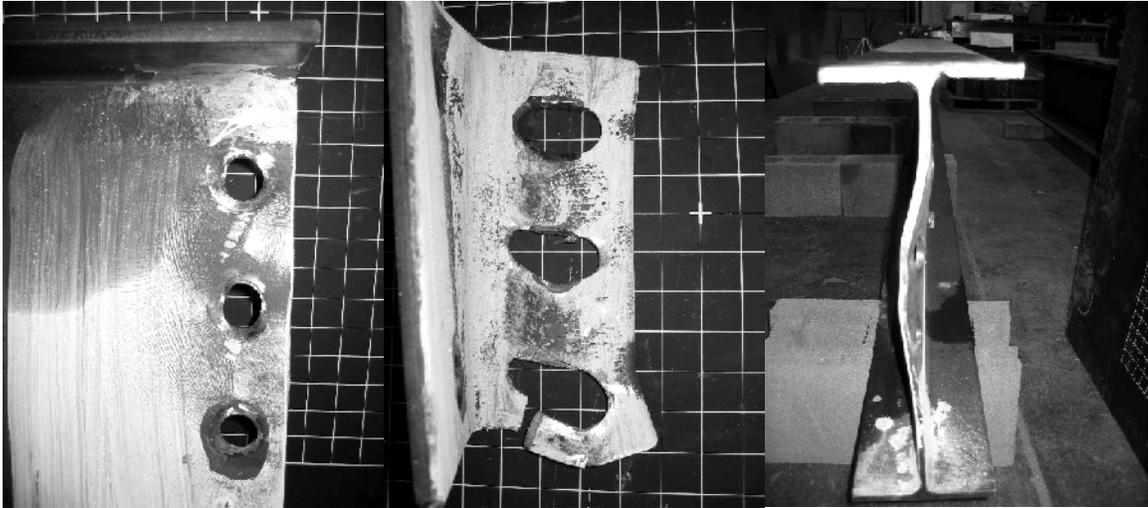
| Beam | Angle on connection side | Distorted beam web at connection |

Figure A-15 Test specimen 1L1a
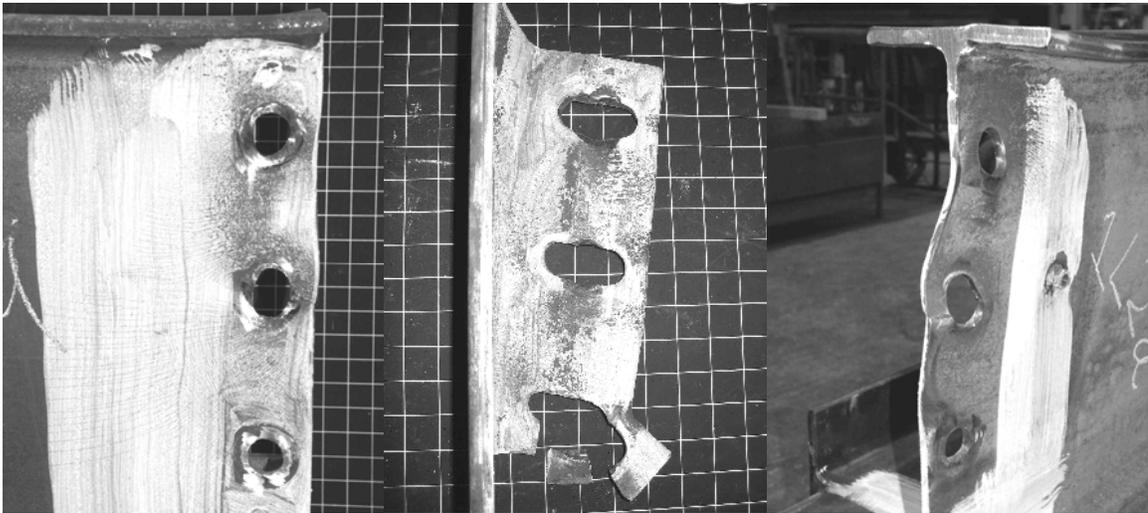
| Beam | Angle on connection side | Distorted beam web at connection |

Figure A-16 Test specimen 1L2a
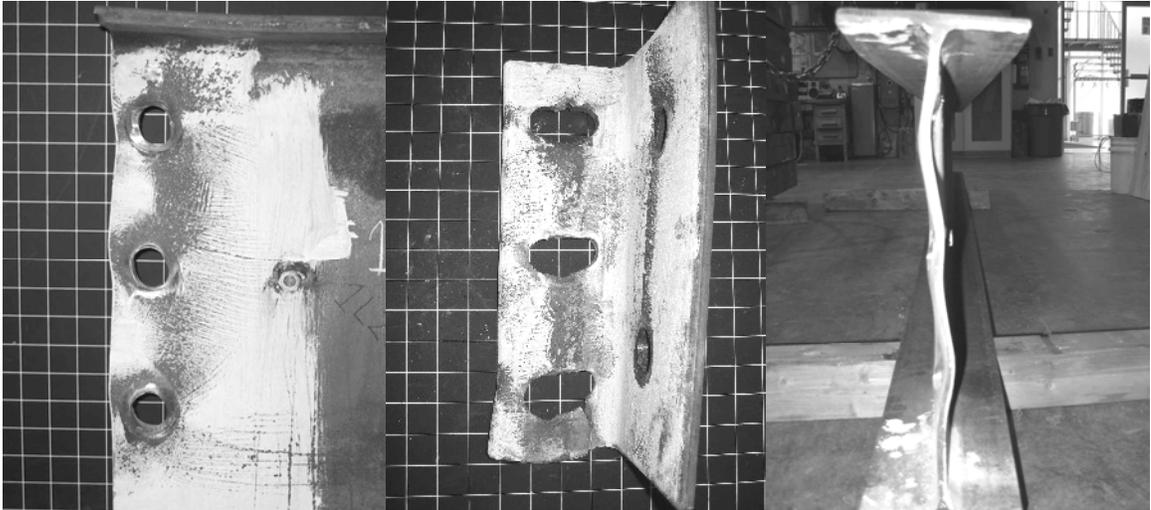
| Beam | Angle | Distorted beam web at connection |

Figure A-17 Test specimen 1L2aE

| Beam | Angle | Distorted beam web at connection |

Figure A-18 Test specimen 1L3a
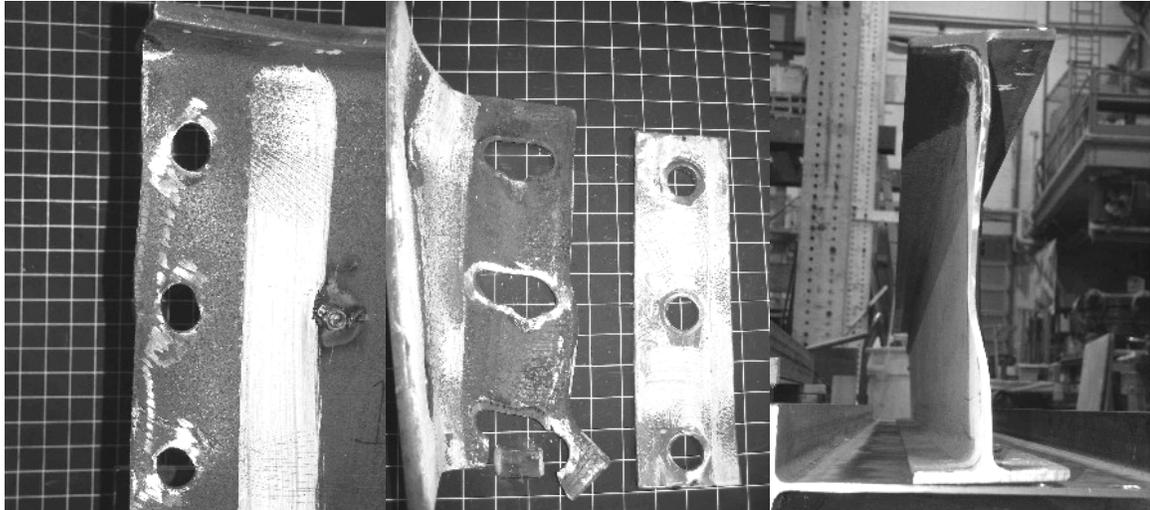
| Beam | Angle and plate washer | Distorted beam web at connection |

Figure A-19 Test specimen 1L4a
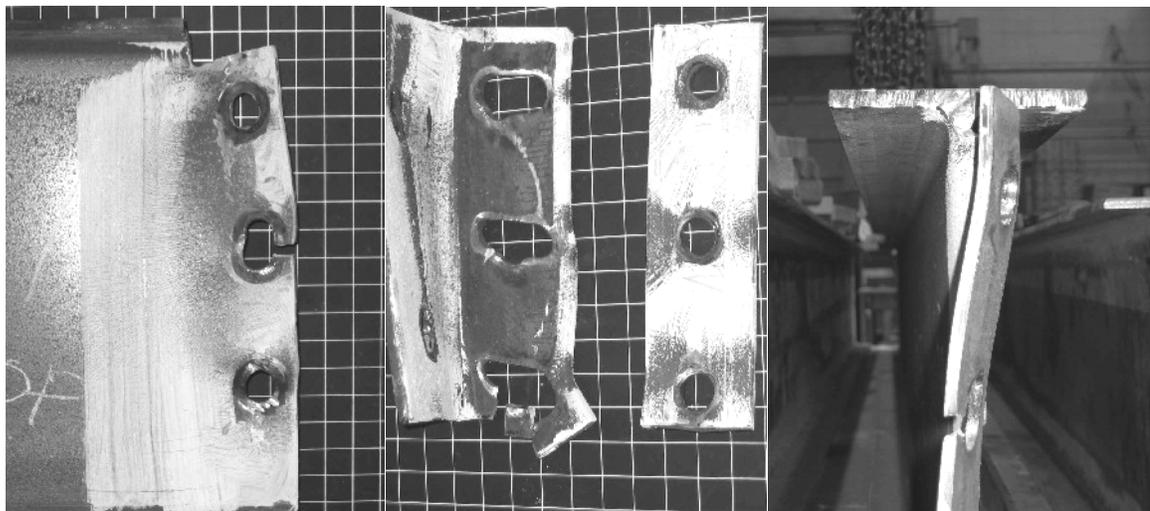
| Beam | Angle and plate washer | Distorted beam web at connection |

Figure A-20 Test specimen 1L5a
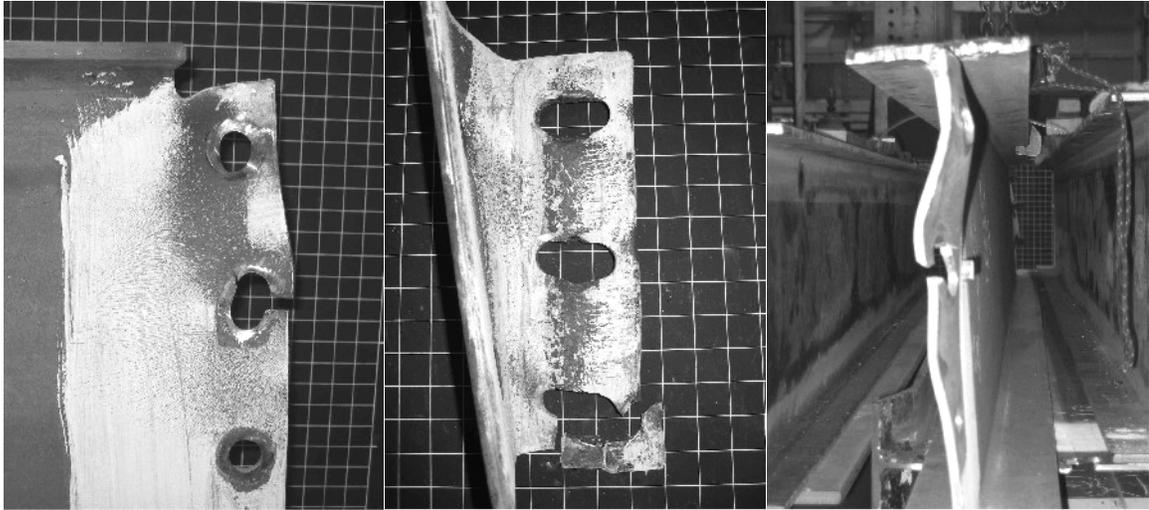
Beam	Angle	Distorted beam web at connection

Figure A-21 Test specimen 1L6a
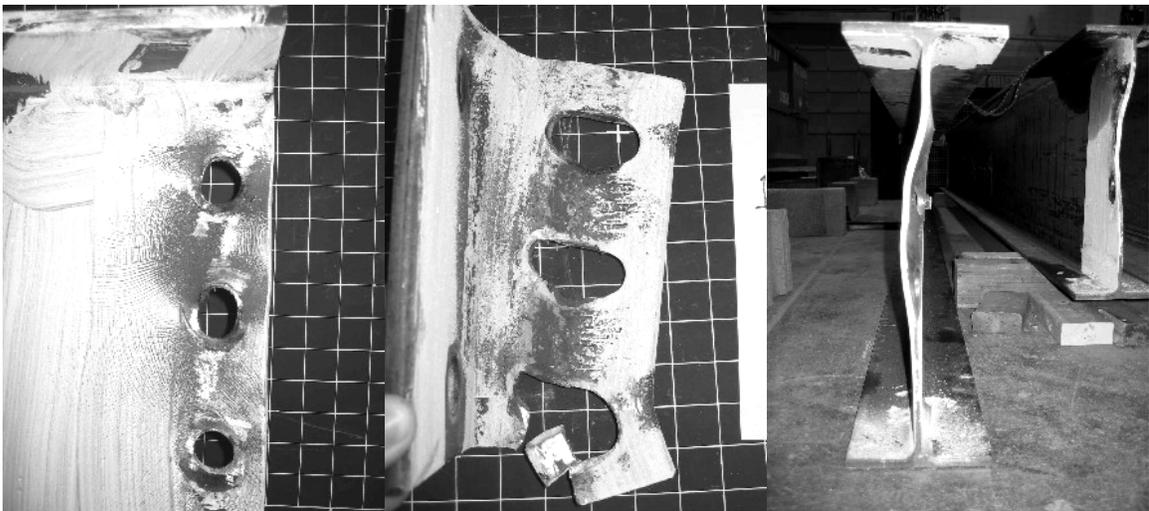
Beam	Angle	Distorted beam web at connection

Figure A-22 Test specimen 1L7a

146
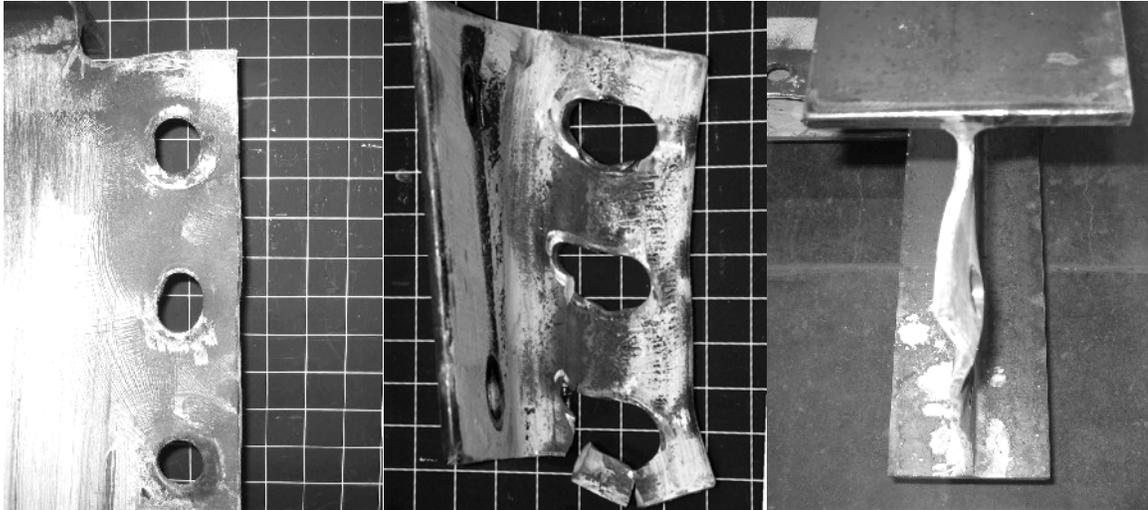
| Beam | Angle | Distorted beam web at connection |

Figure A-23 Test specimen 1L8a
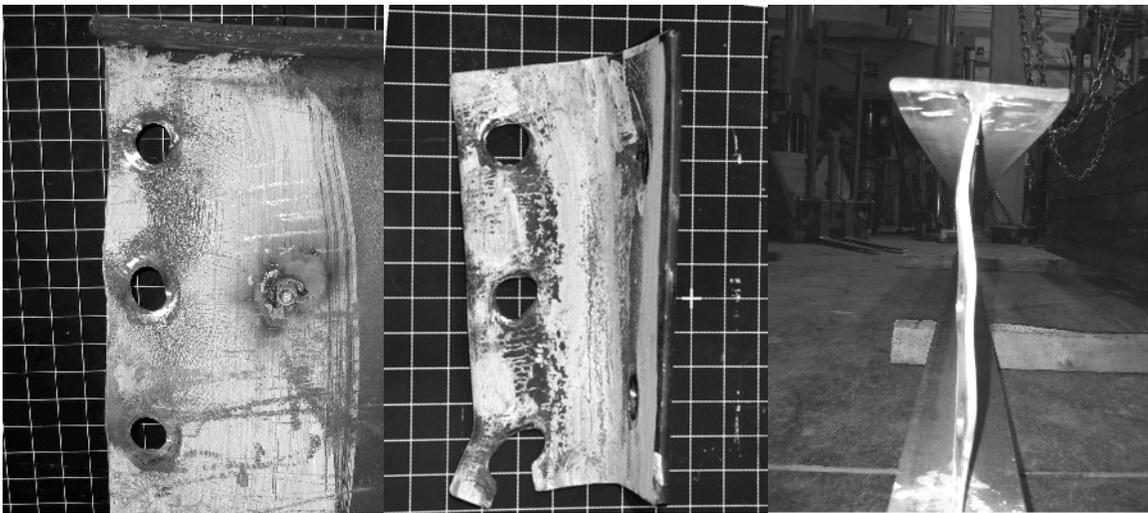
| Beam | Angle | Distorted beam web at connection |

Figure A-24 Test specimen 1L9a
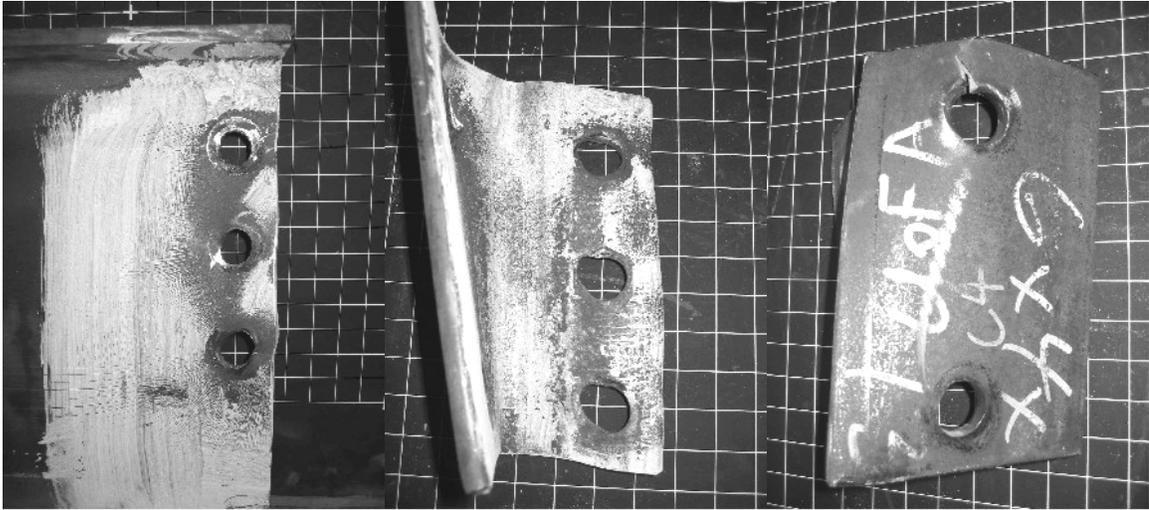
| Beam | Angle leg on the connection side | Angle leg connected to the column |

Figure A-25 Test specimen 1L10a
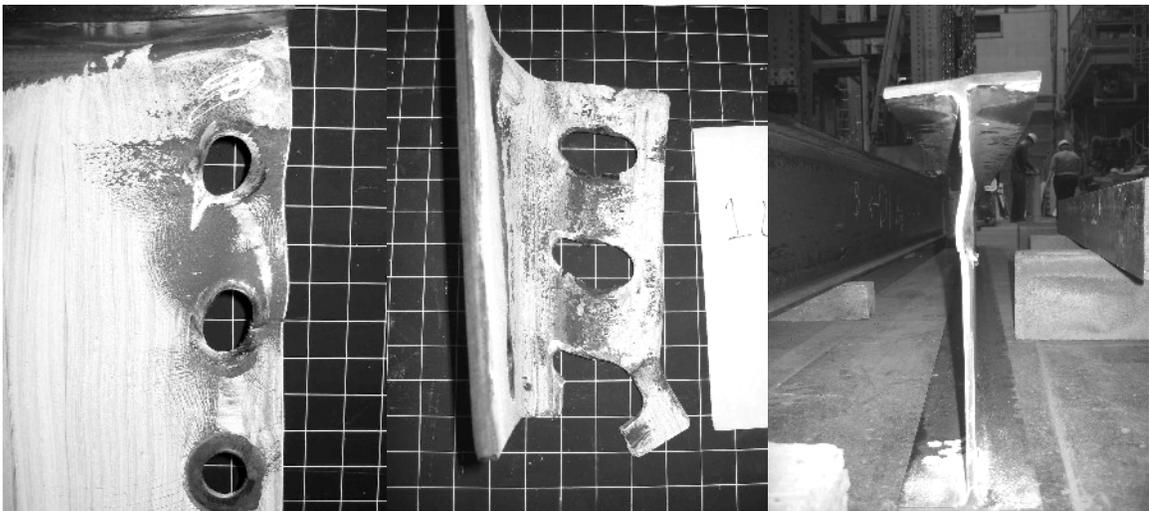
| Beam | Angle leg on the connection side | Beam web |

Figure A-26 Test specimen 1L11a
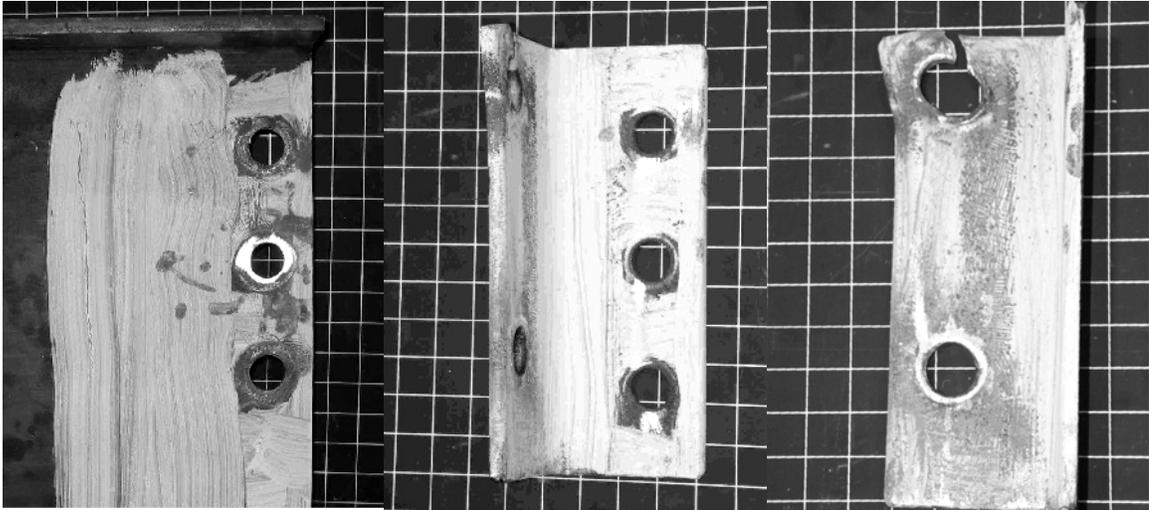
| Beam | Angle leg on the connection side | Angle leg connected to the column |

Figure A-27 Test specimen 1L12
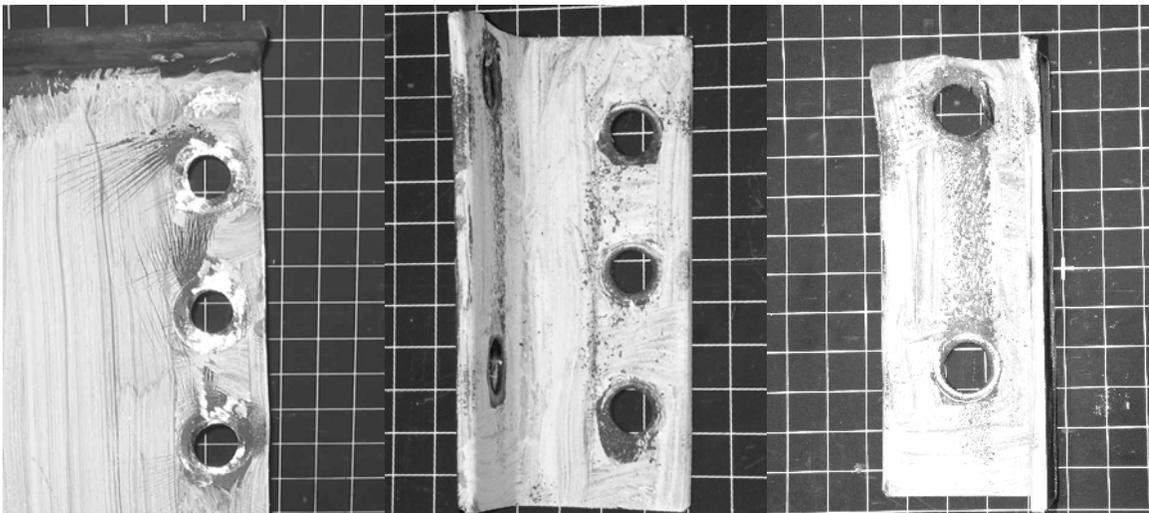
| Beam | Angle leg on the connection side | Angle leg connected to the column |

Figure A-28 Test specimen 1L13
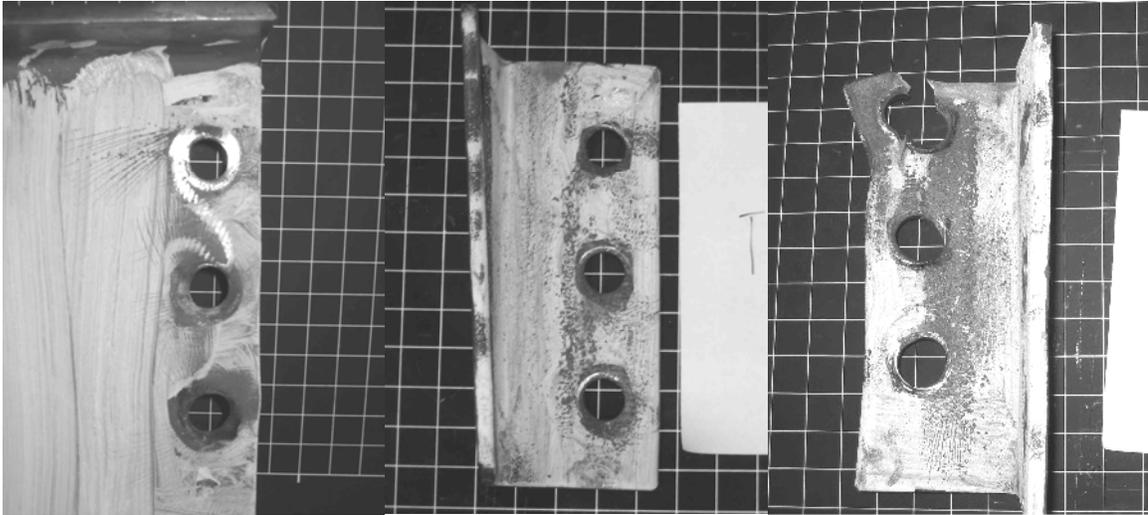
| Beam | Angle leg on the connection side | Angle leg connected to the column |

Figure A-29 Test specimen 1L14
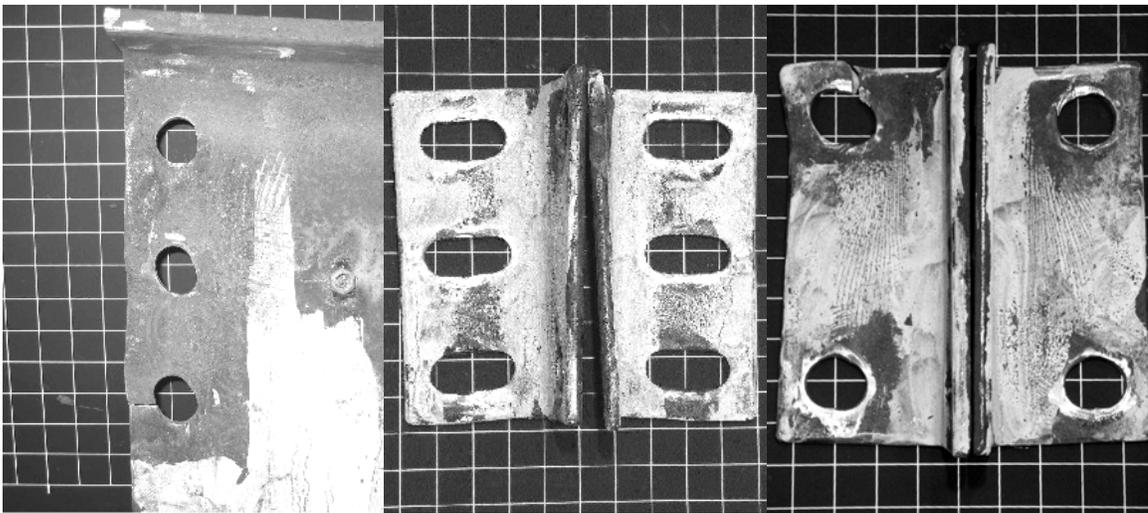
| Beam | Angle leg on the connection side | Angle leg connected to the column |

Figure A-30 Test specimen 2L1

Beam   Angle leg on the connection side

Figure A-31 Test specimen 2L2
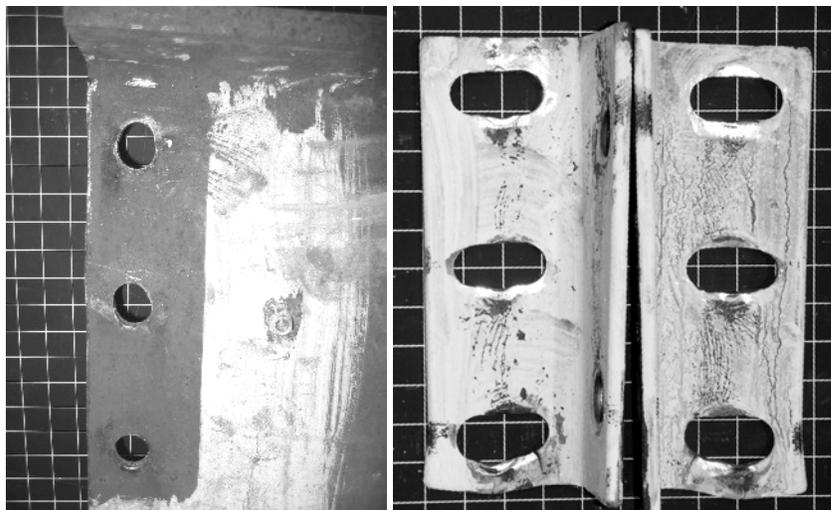
Beam   Angle leg on the connection side

Figure A-32 Test specimen 2L3
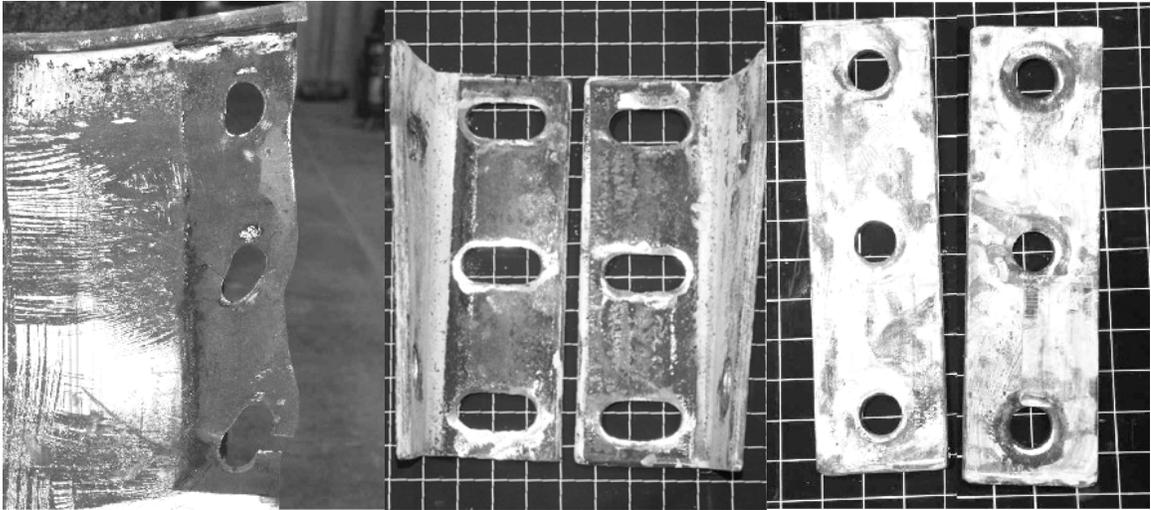
| Beam | Angle leg on the connection side | Plate washers after testing |

Figure A-33 Test specimen 2L4
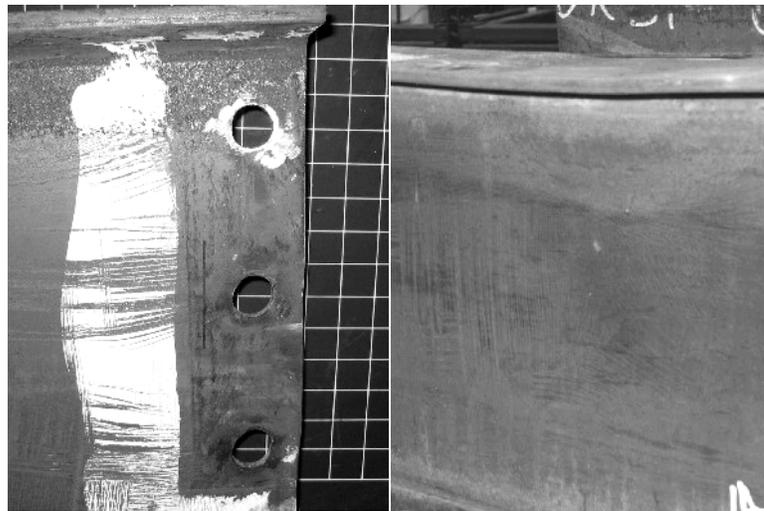
| Beam | Crushed beam web under the load point |

Figure A-34 Test specimen 2L5
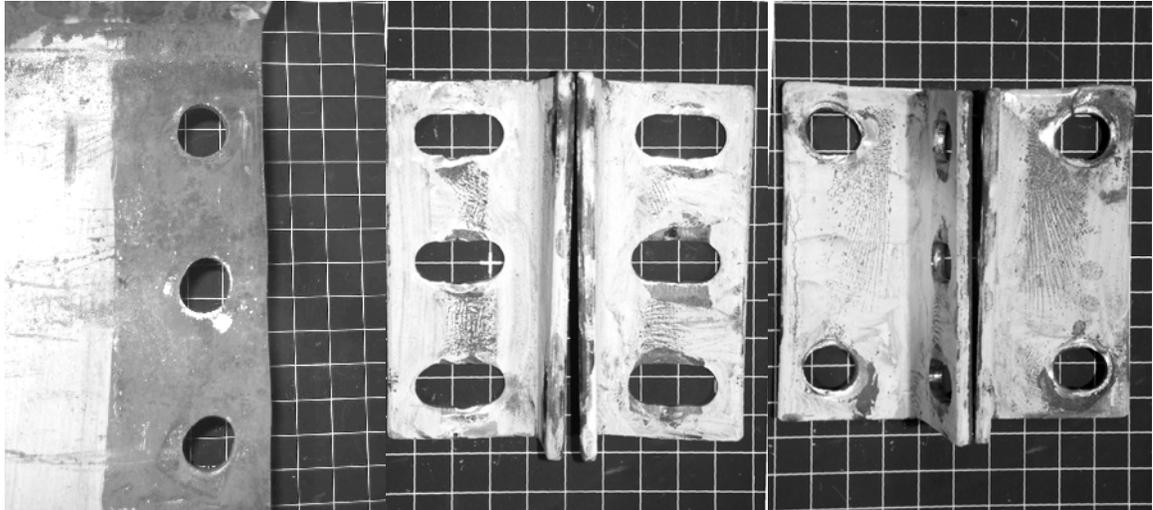
Beam   Angle legs on the connection side   Angle legs connected to the column

Figure A-35 Test specimen 2L6

Beam   Angle legs on the connection side

Figure A-36 Test specimen 2L7
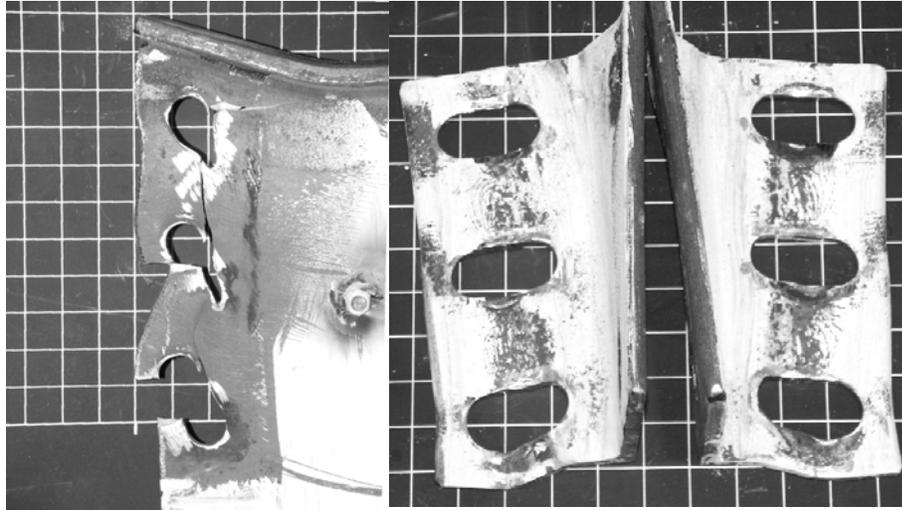
Beam   Angle legs on the connection side

Figure A-37 Test specimen 2L1a
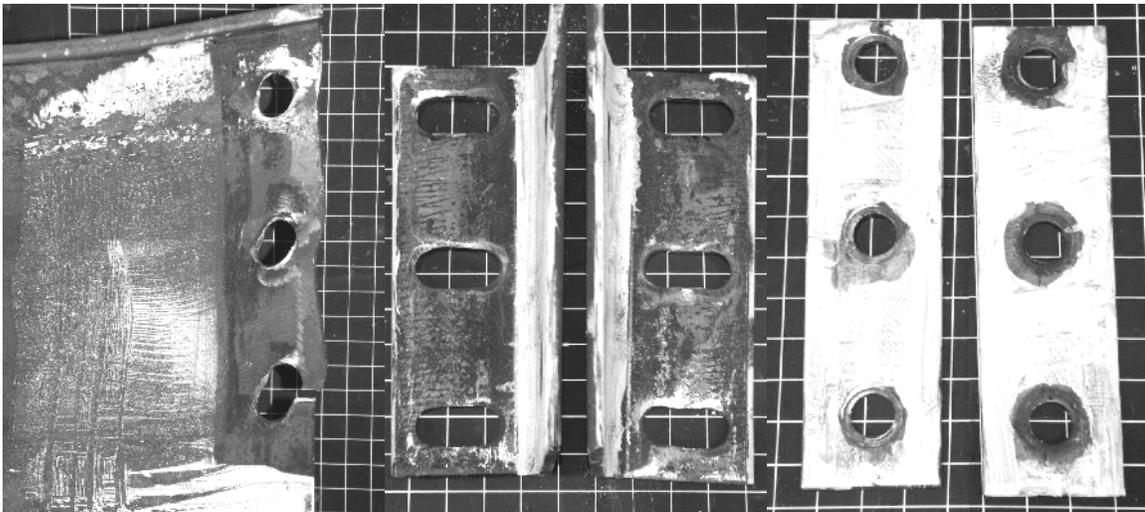
Beam   Angle legs on the connection side   Plate washers after testing

Figure A-38 Test specimen 2L5a
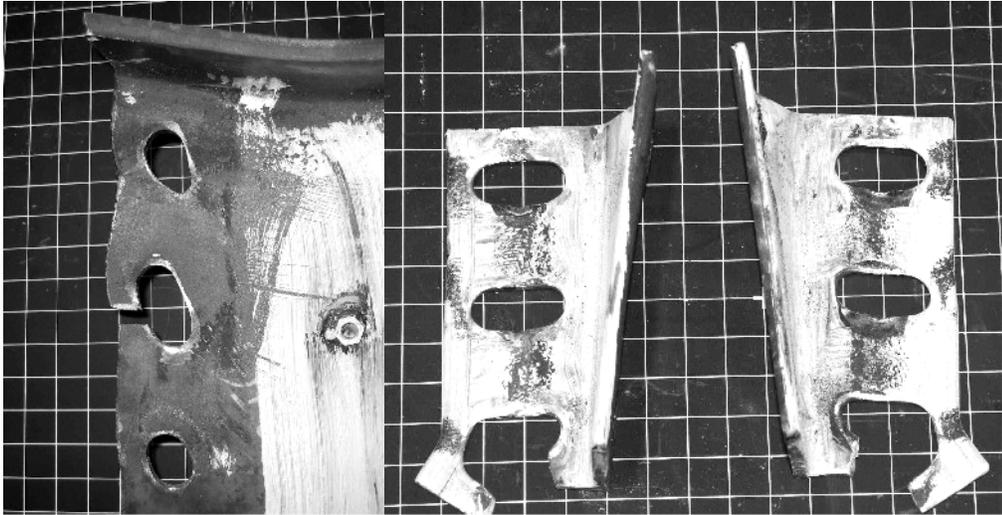
Beam   Angle legs on the connection side

Figure A-39 Test specimen 2L6a
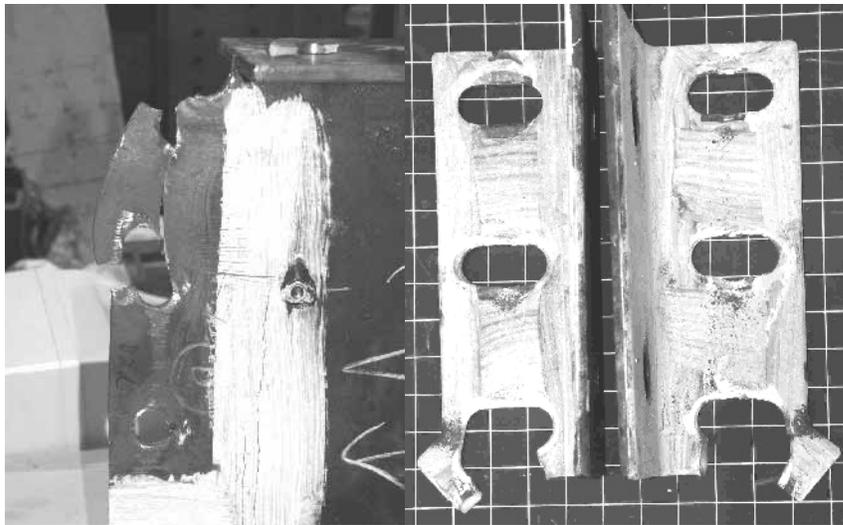
Beam   Angle legs on the connection side

Figure A-40 Test specimen 2L8a

Appendix B
Load vs. Deformation Response and
Twist of Connection vs. Deformation of Test Specimens
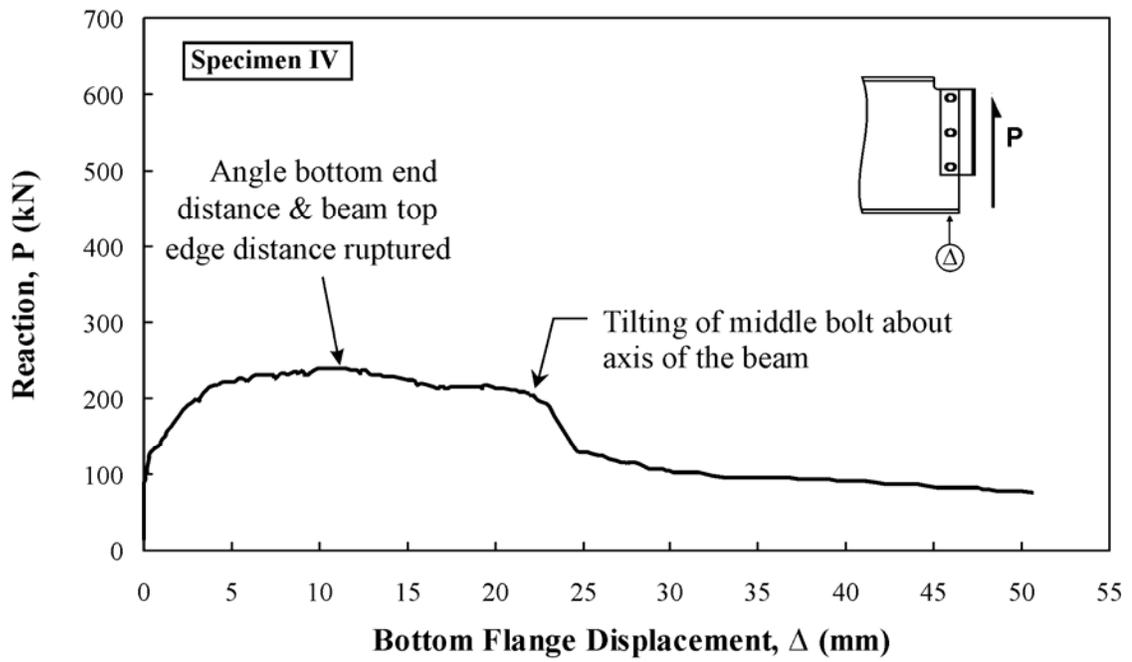
Figure B-1 Connection Reaction vs. Bottom Flange Displacement, Test Specimen IV (Franchuk *et al.*, 2002)
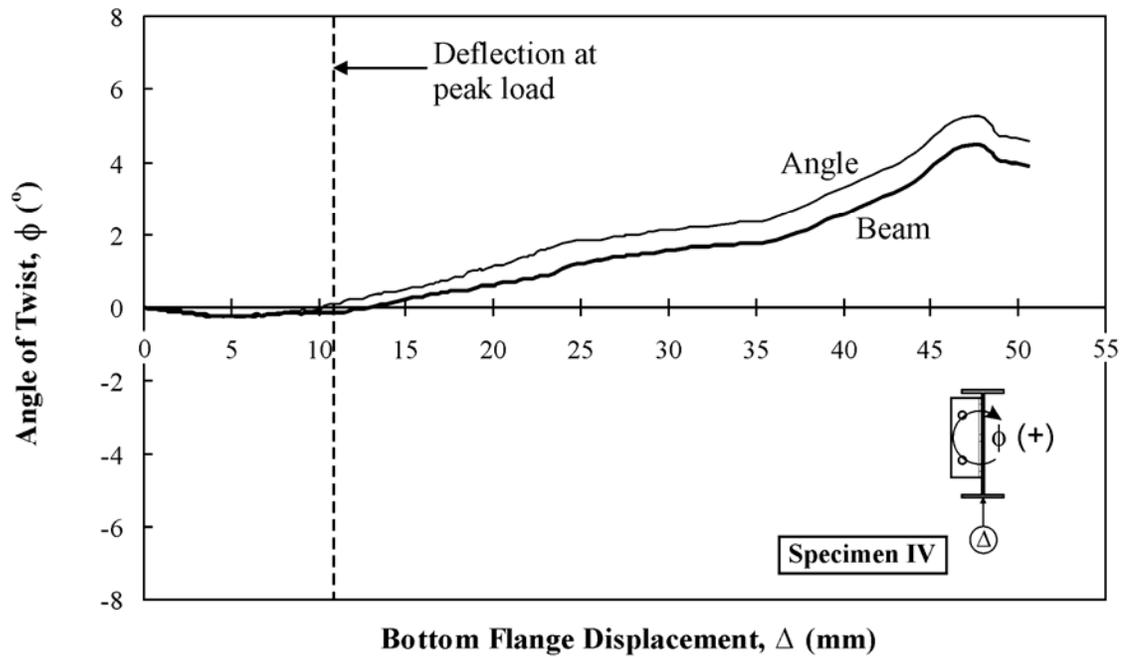
Figure B-2 Twist vs. Bottom Flange Displacement, Test Specimen IV (Franchuk *et al.*, 2002)
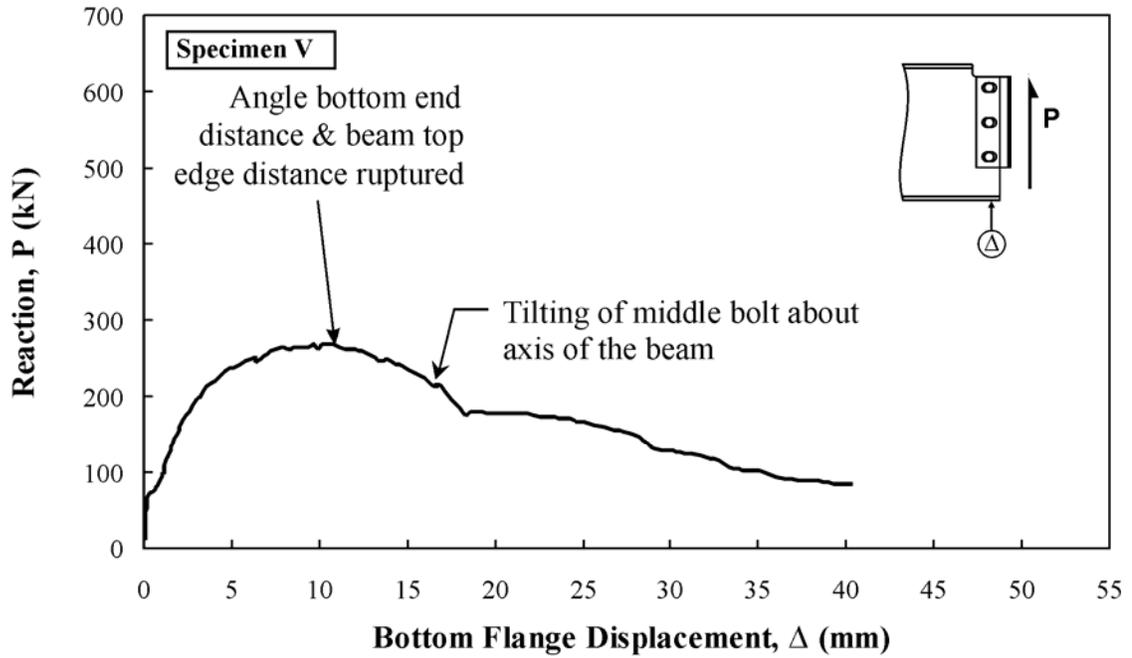
Figure B-3 Connection Reaction vs. Bottom Flange Displacement, Test Specimen V (Franchuk *et al.*, 2002)
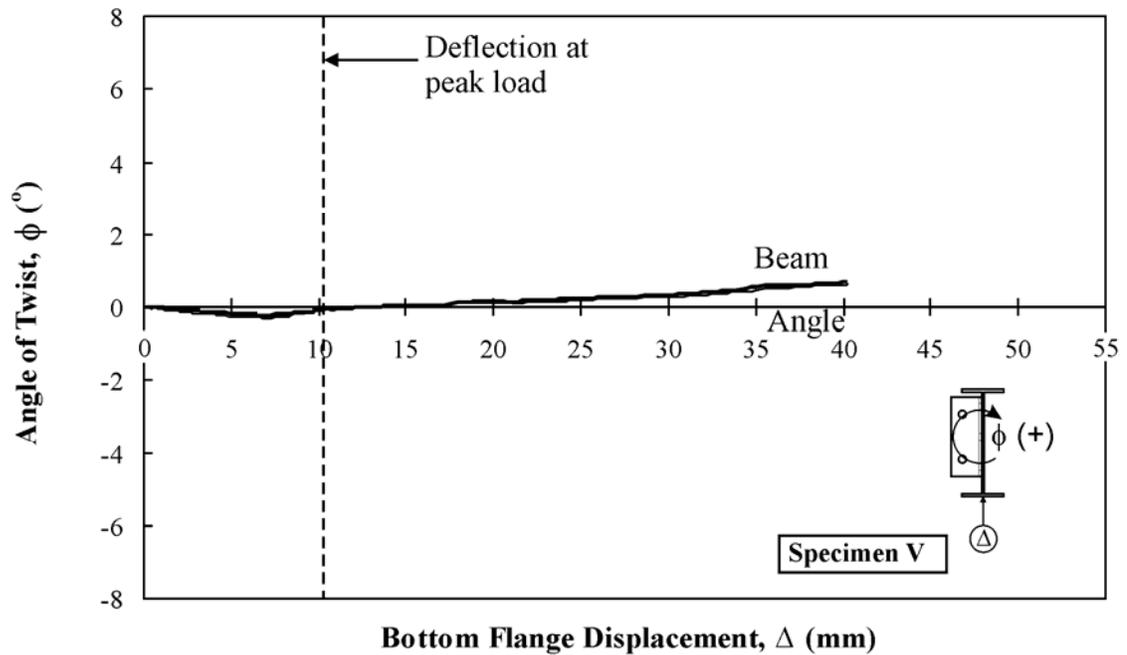
Figure B-4 Twist vs. Bottom Flange Displacement, Test Specimen V (Franchuk *et al.*, 2002)

158
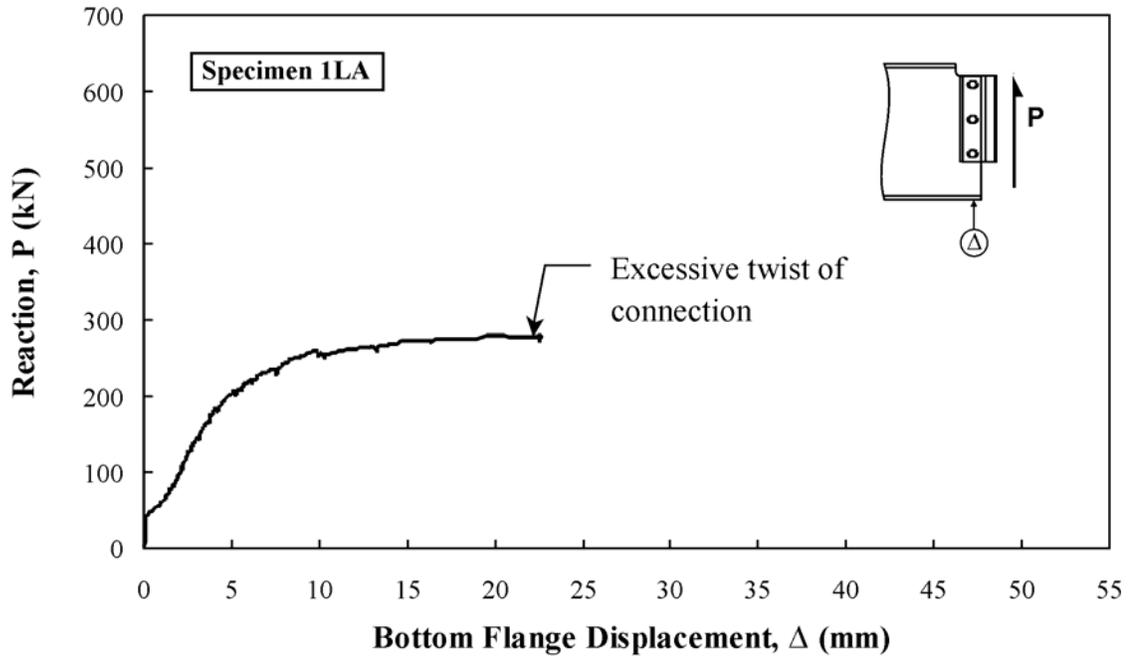
**Figure B-5 Connection Reaction vs. Bottom Flange Displacement, Test Specimen 1LA**
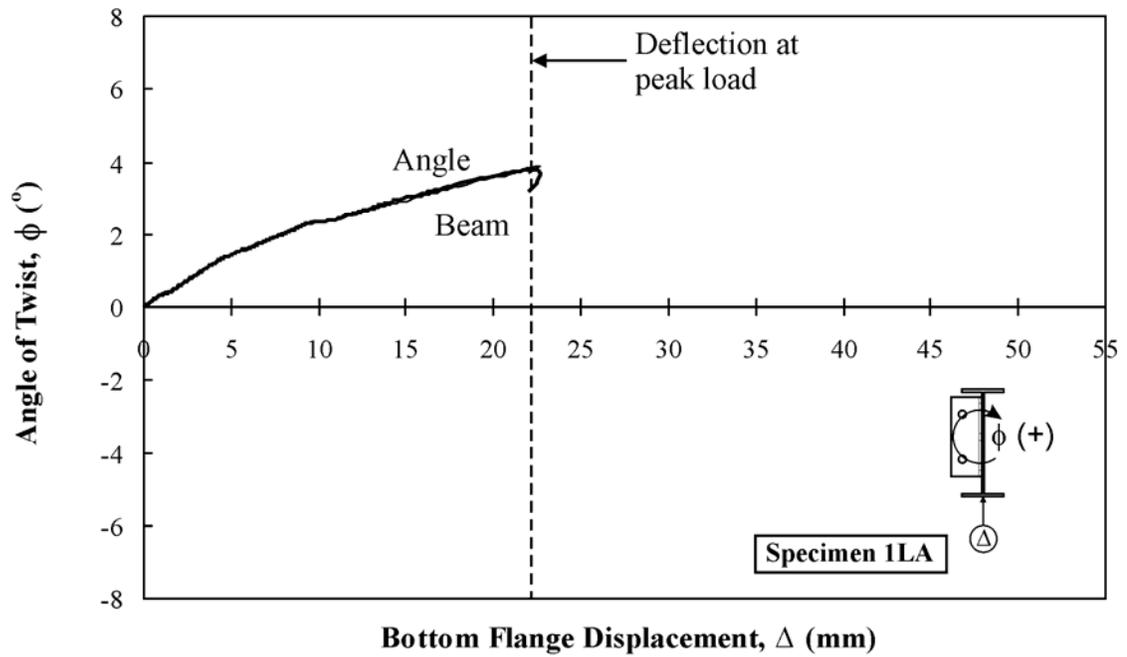

Figure B-6 Twist vs. Bottom Flange Displacement, Test Specimen 1LA
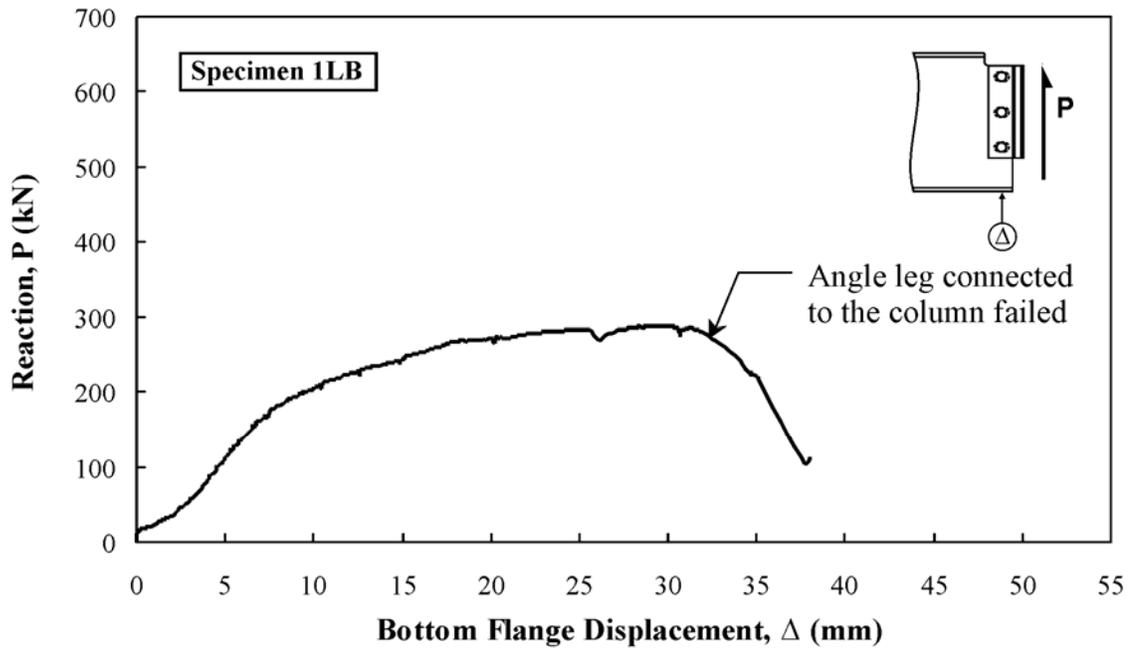
Figure B-7 Connection Reaction vs. Bottom Flange Displacement, Test Specimen 1LB
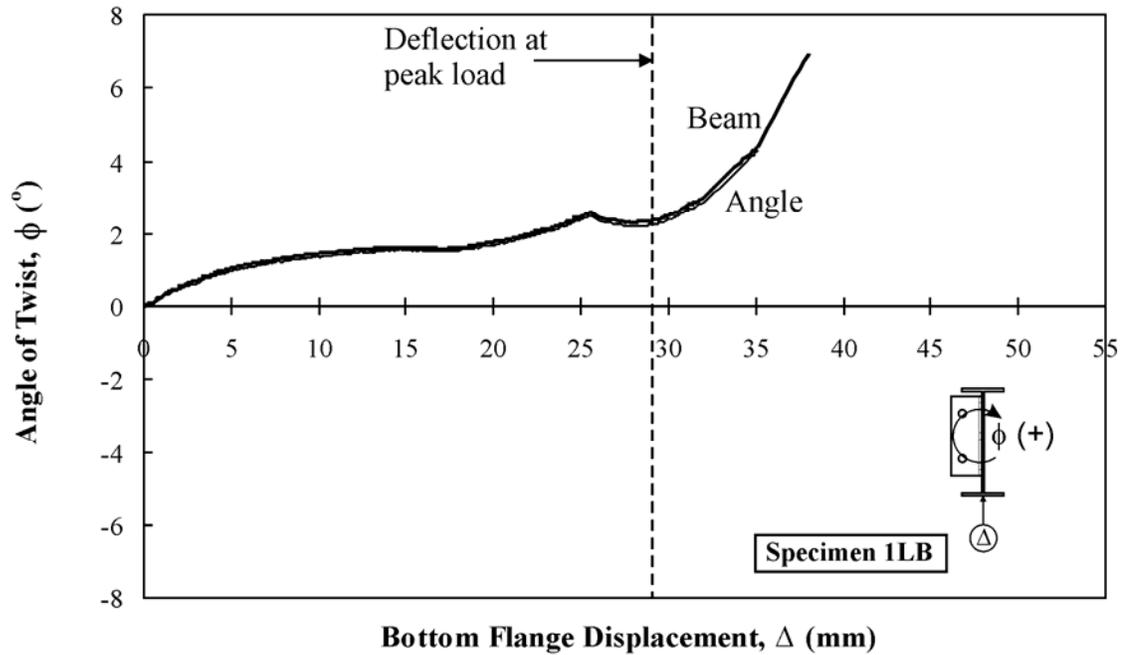
Figure B-8 Twist vs. Bottom Flange Displacement, Test Specimen 1LB
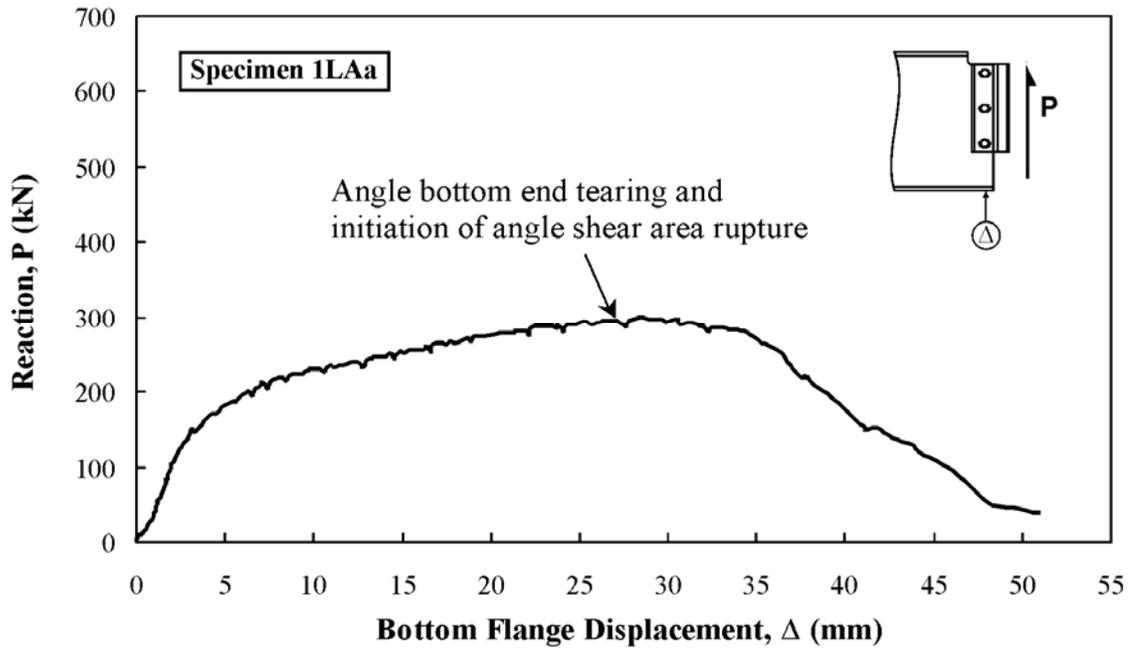
**Figure B-9 Connection Reaction vs. Bottom Flange Displacement,
Test Specimen 1LAa**
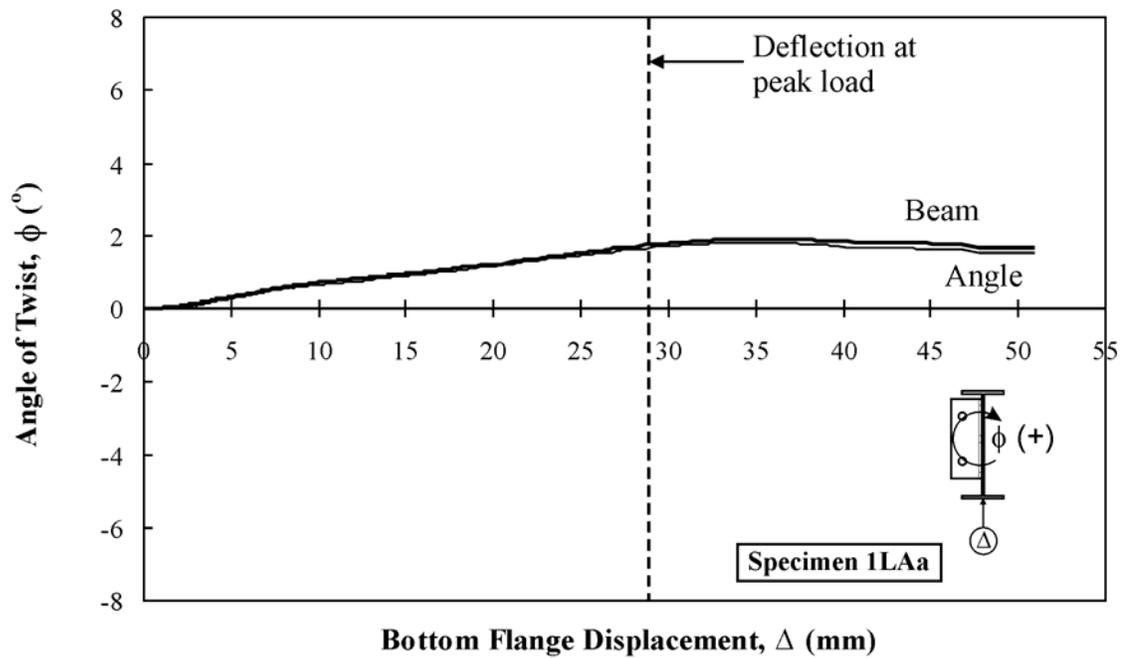
Figure B-10 Twist vs. Bottom Flange Displacement, Test Specimen 1LAa

161
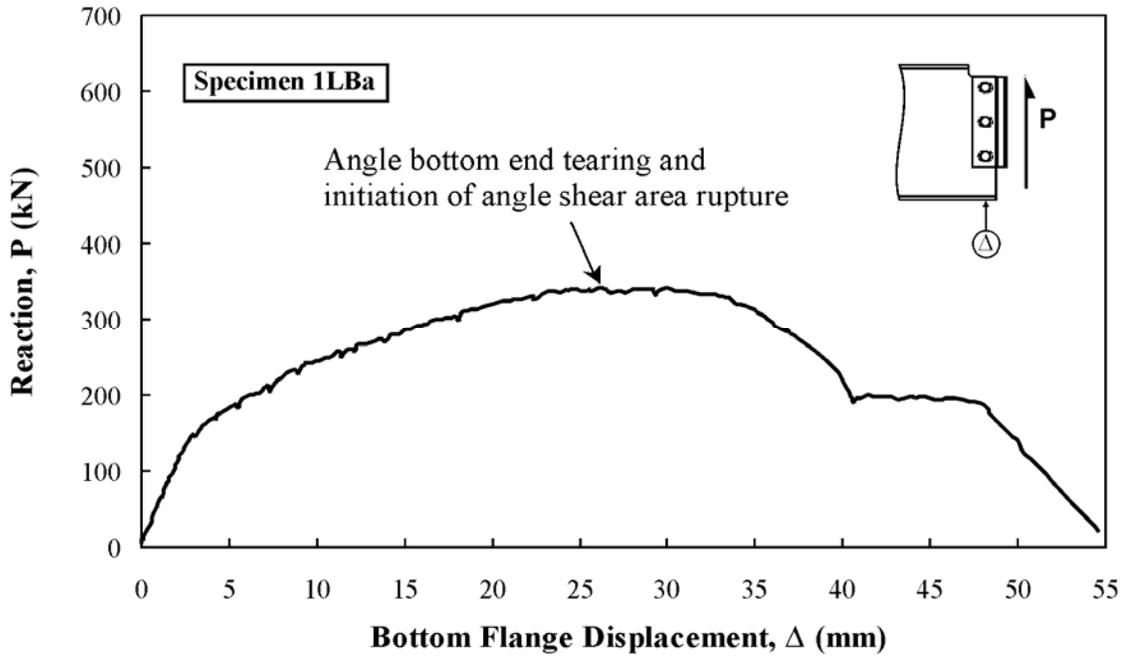
Figure B-11 Connection Reaction vs. Bottom Flange Displacement, Test Specimen 1LBa
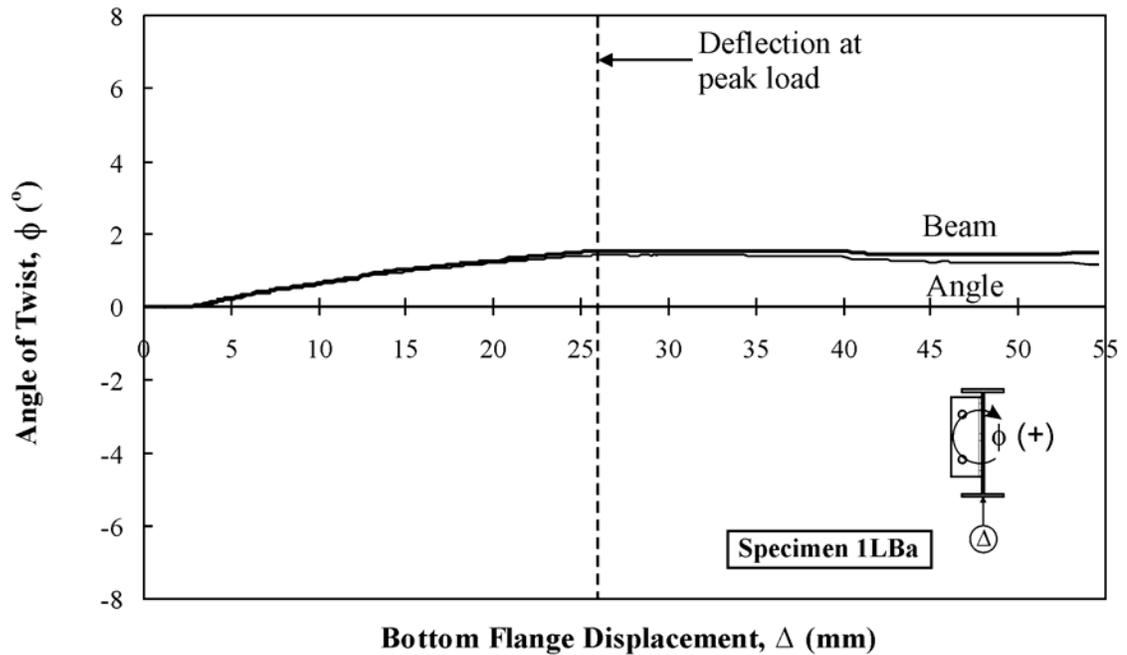
**Figure B-12 Twist vs. Bottom Flange Displacement, Test Specimen 1LBa**

162
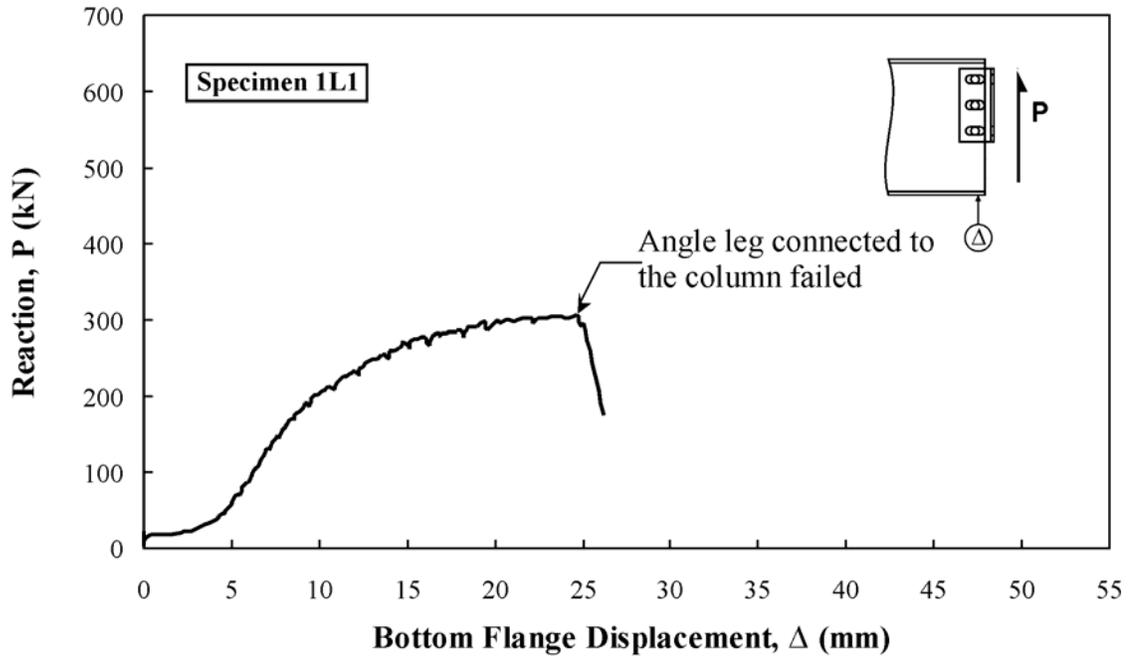
Figure B-13 Connection Reaction vs. Bottom Flange Displacement, Test Specimen 1L1
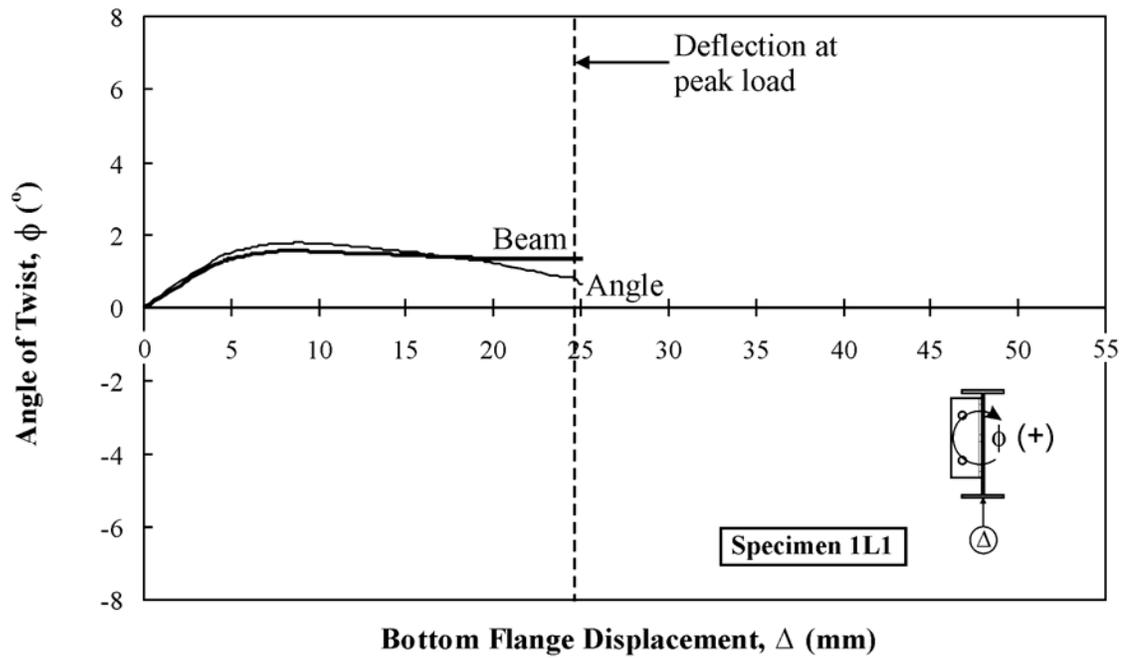
Figure B-14 Twist vs. Bottom Flange Displacement, Test Specimen 1L1

163
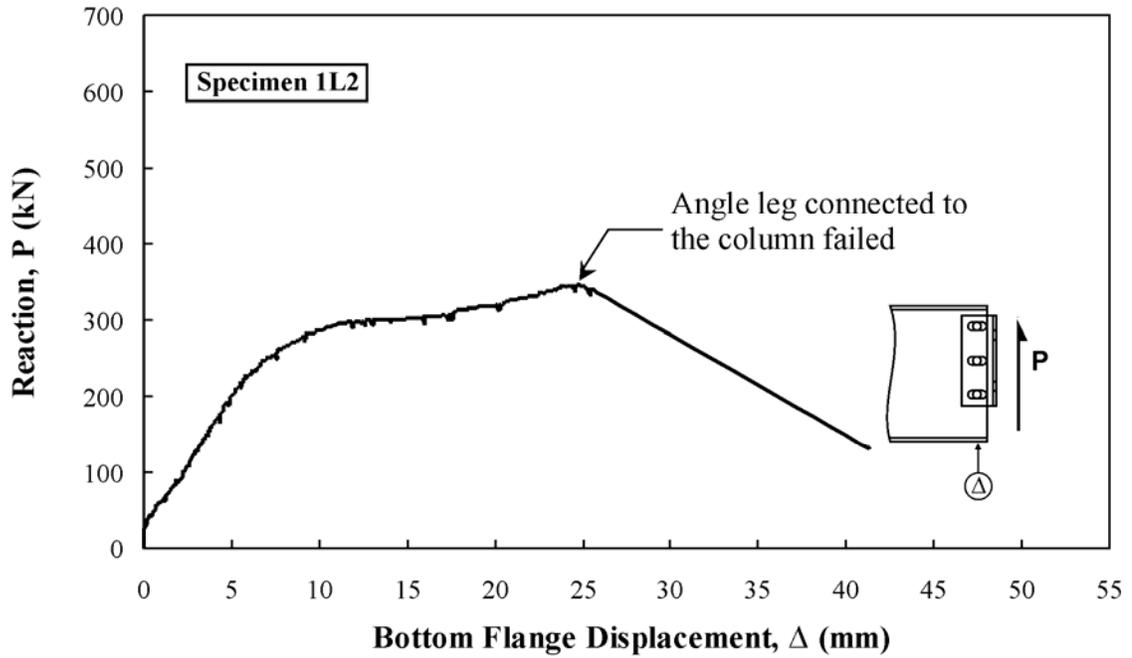
Figure B-15 Connection Reaction vs. Bottom Flange Displacement, Test Specimen 1L2
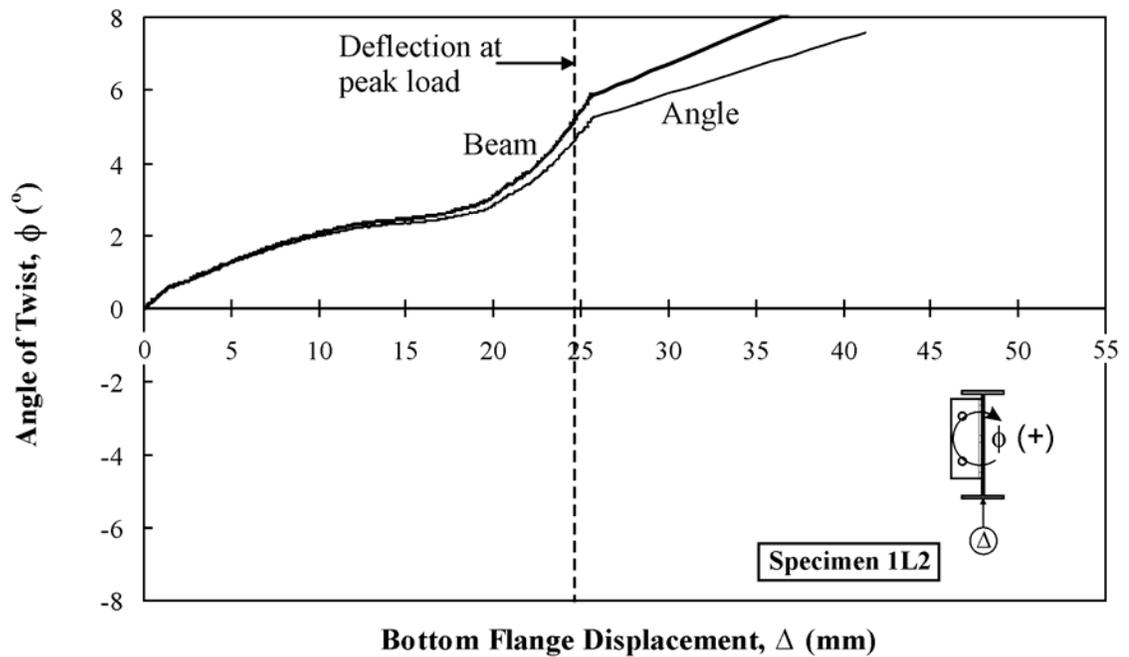
Figure B-16 Twist vs. Bottom Flange Displacement, Test Specimen 1L2
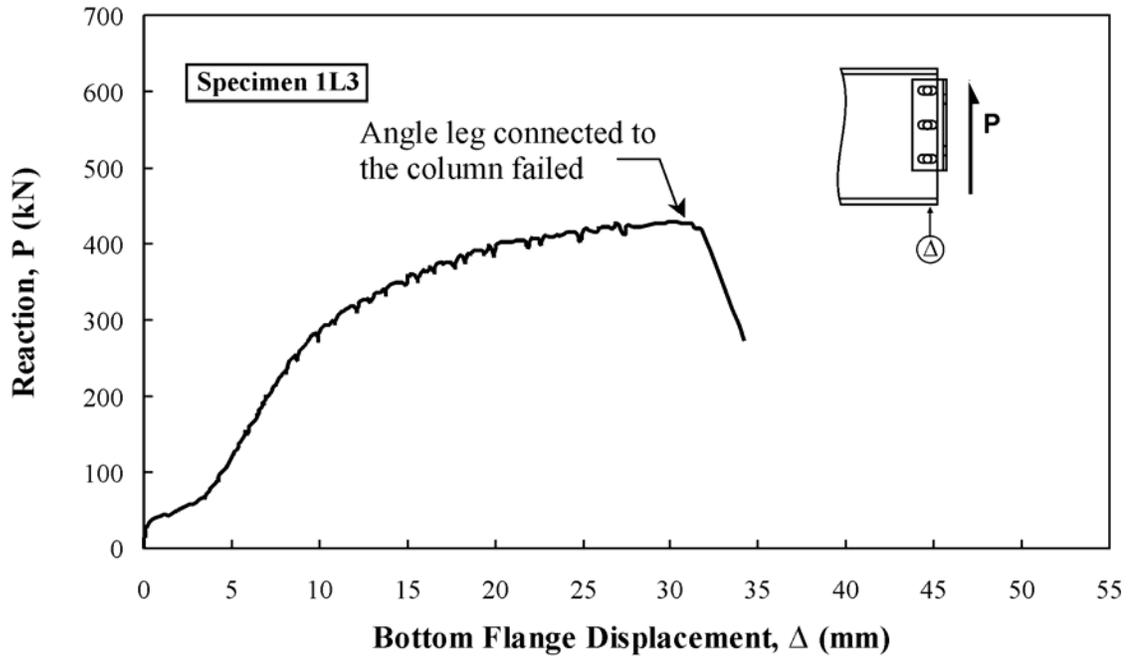
**Figure B-17 Connection Reaction vs. Bottom Flange Displacement, Test Specimen 1L3**
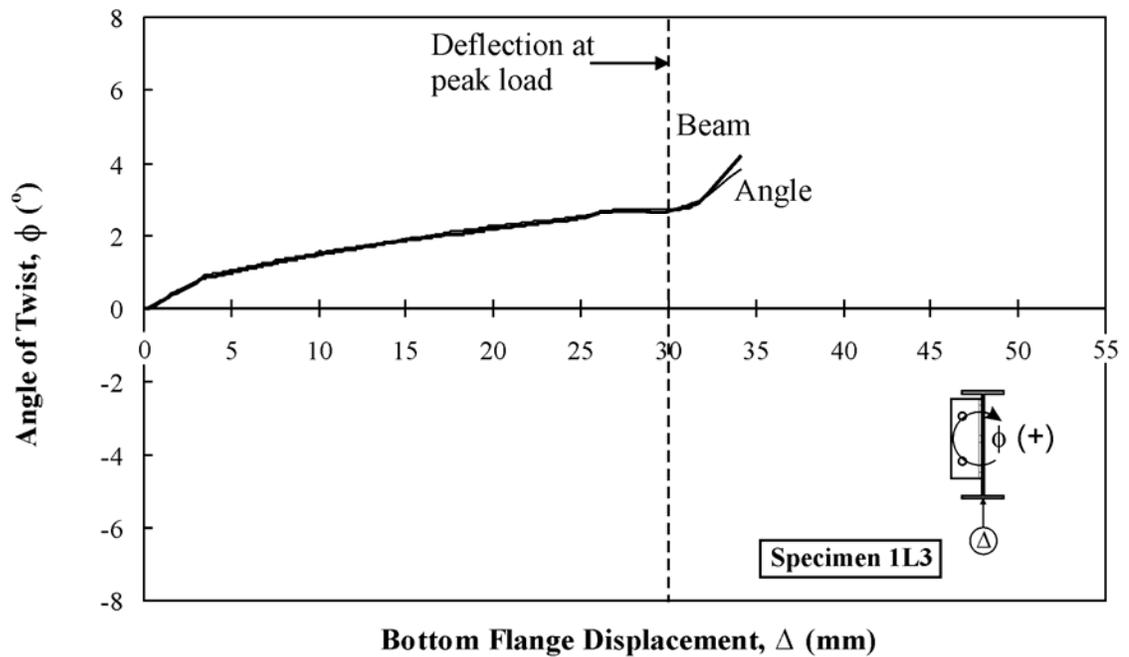
Figure B-18 Twist vs. Bottom Flange Displacement, Test Specimen 1L3

165
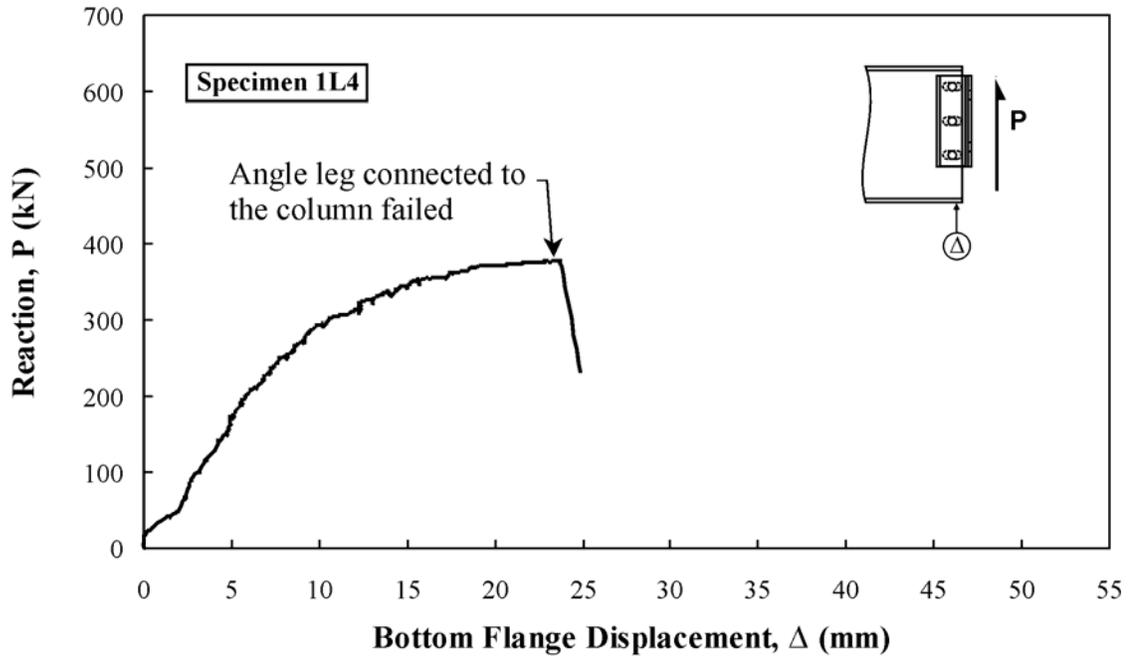
**Figure B-19 Connection Reaction vs. Bottom Flange Displacement, Test Specimen 1L4**
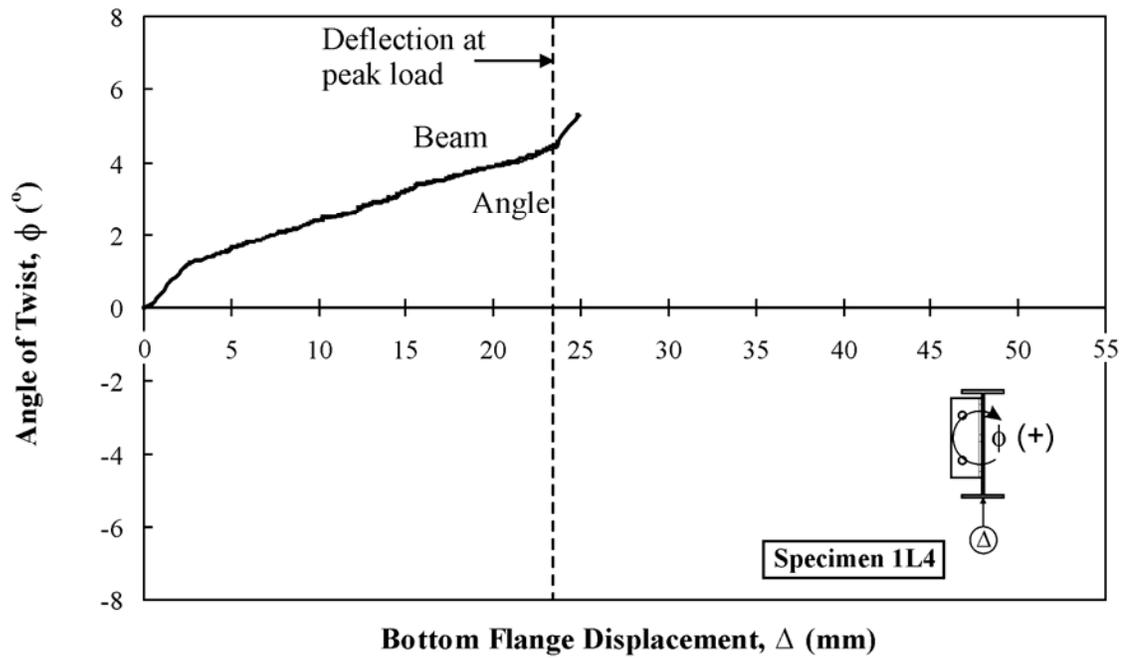
Figure B-20 Twist vs. Bottom Flange Displacement, Test Specimen 1L4
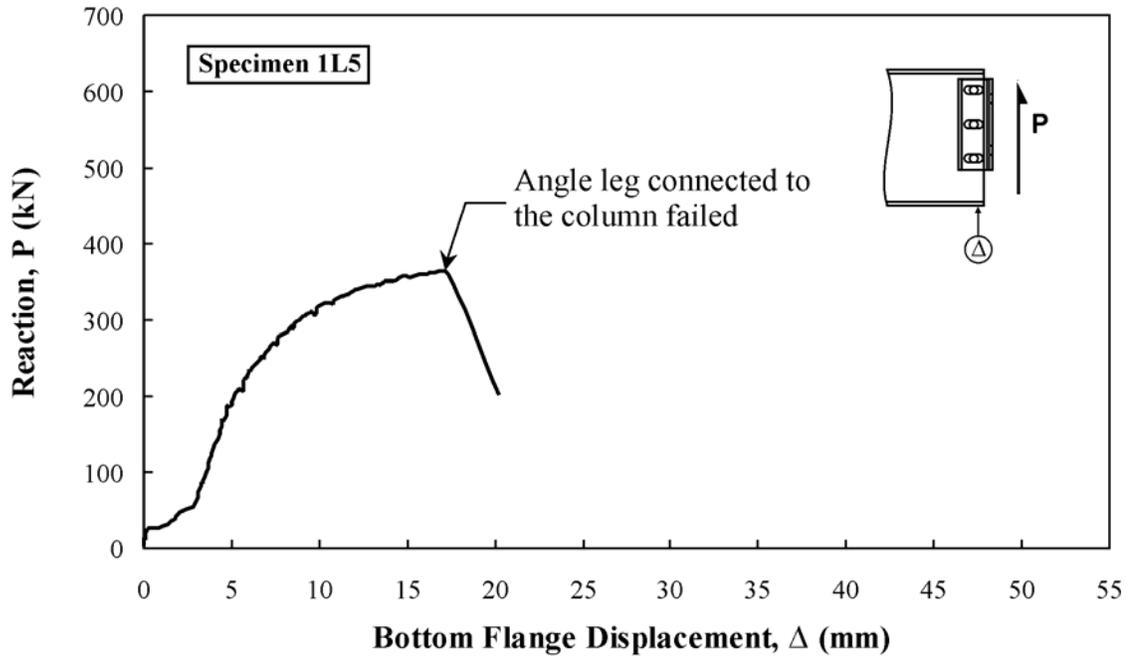
Figure B-21 Connection Reaction vs. Bottom Flange Displacement, Test Specimen 1L5
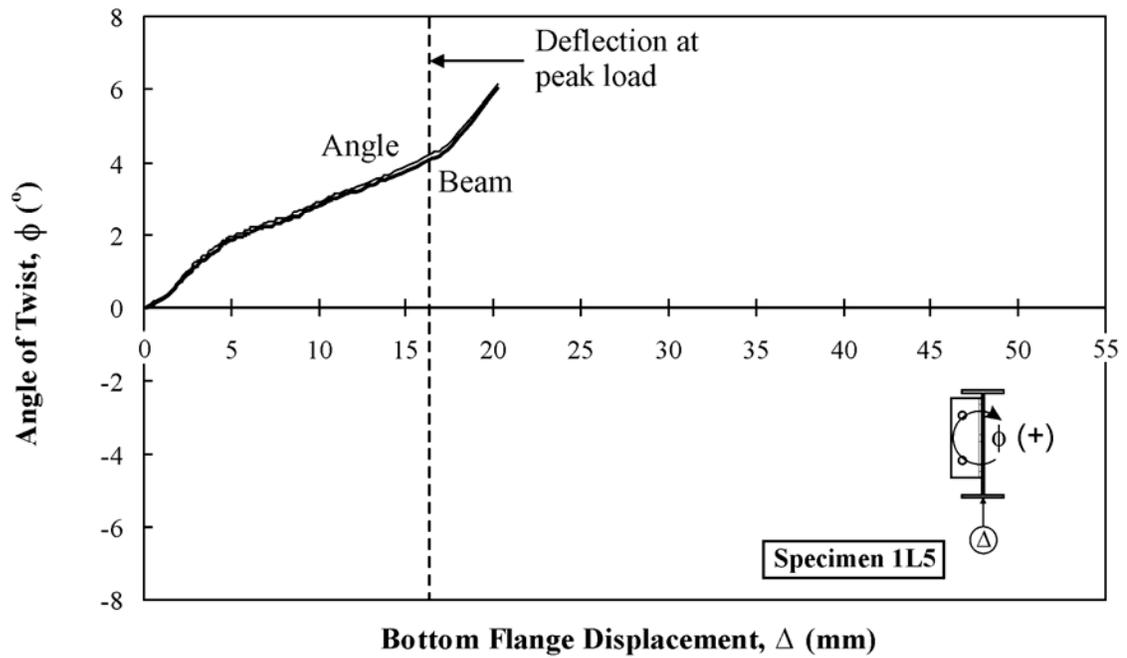
Figure B-22 Twist vs. Bottom Flange Displacement, Test Specimen 1L5
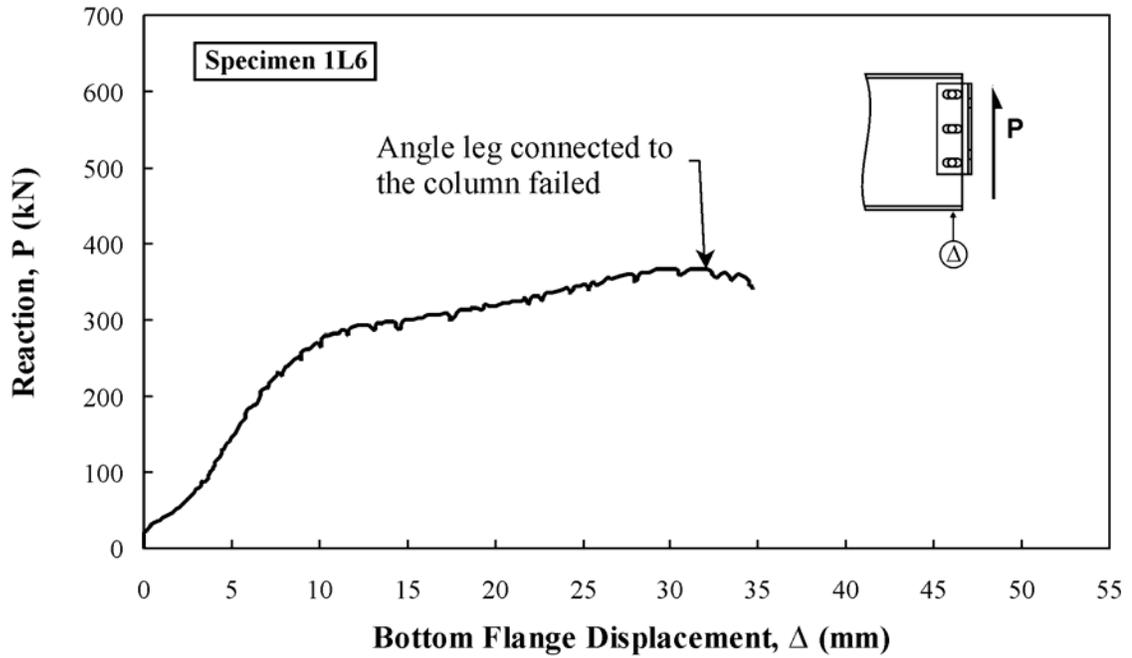
Figure B-23 Connection Reaction vs. Bottom Flange Displacement, Test Specimen 1L6
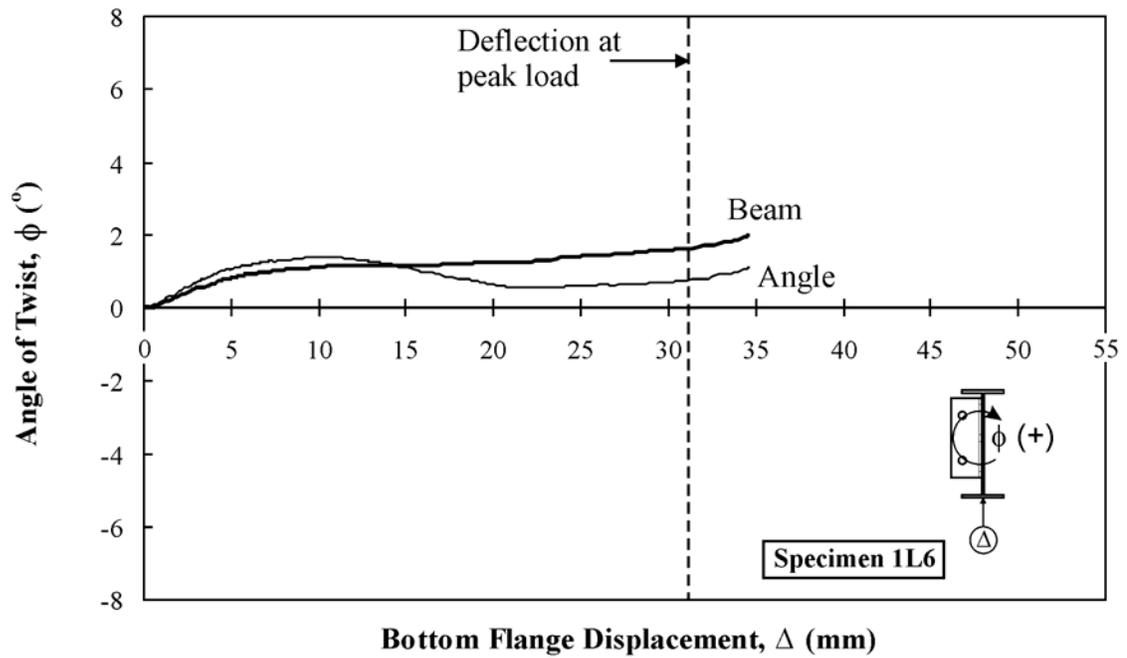
Figure B-24 Twist vs. Bottom Flange Displacement, Test Specimen 1L6
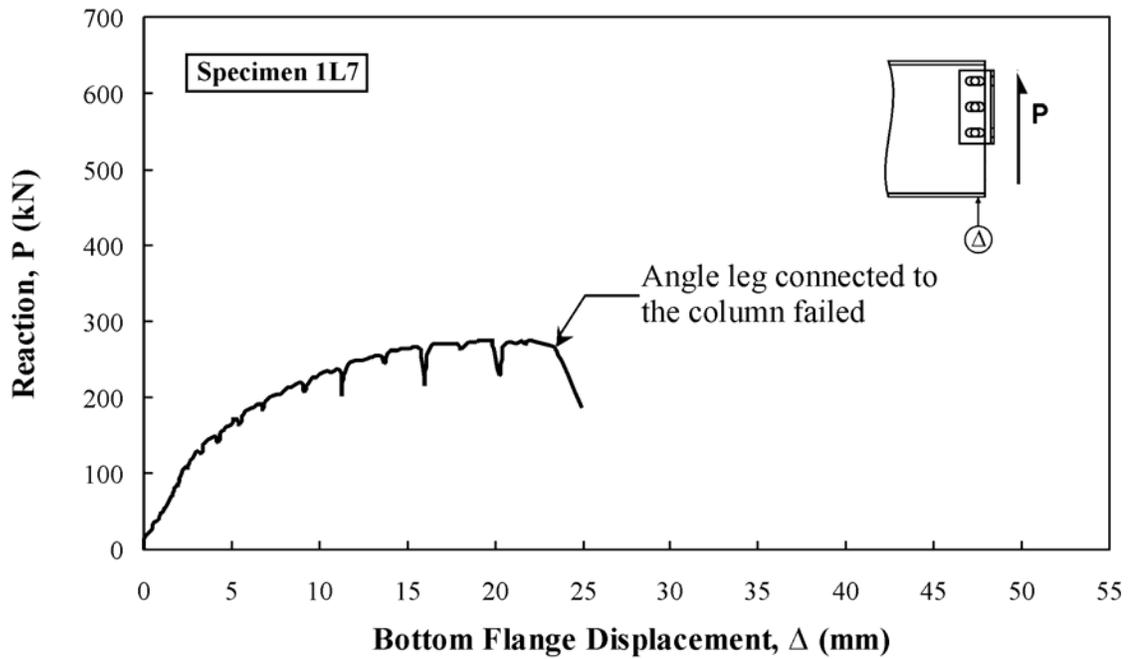
Figure B-25 Connection Reaction vs. Bottom Flange Displacement, Test Specimen 1L7
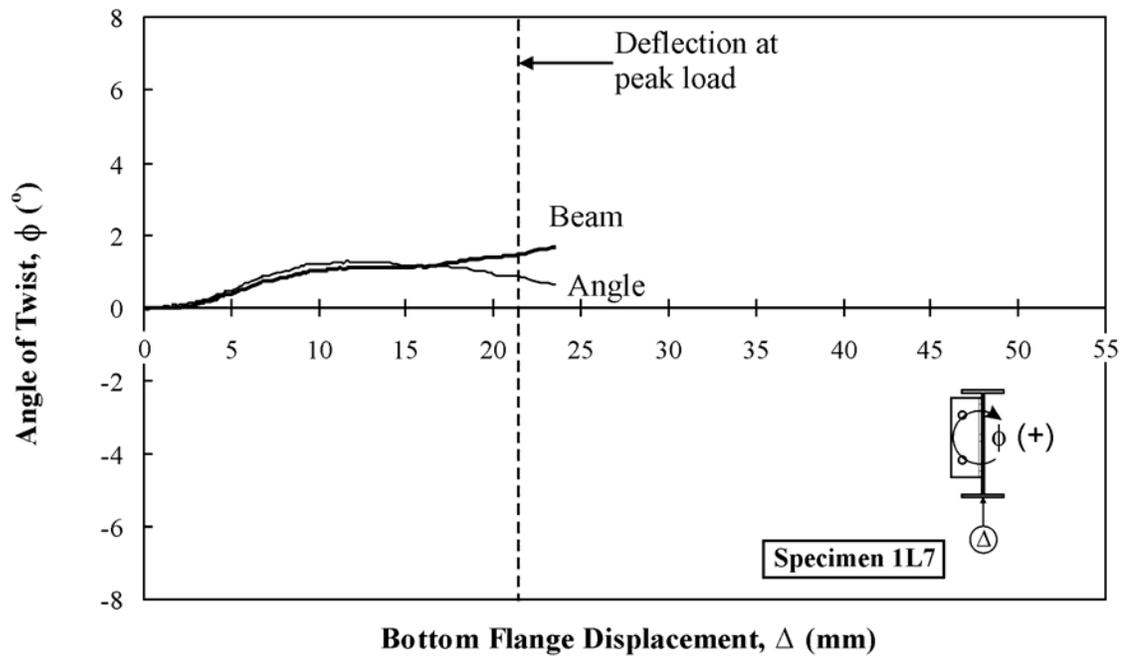
Figure B-26 Twist vs. Bottom Flange Displacement, Test Specimen 1L7
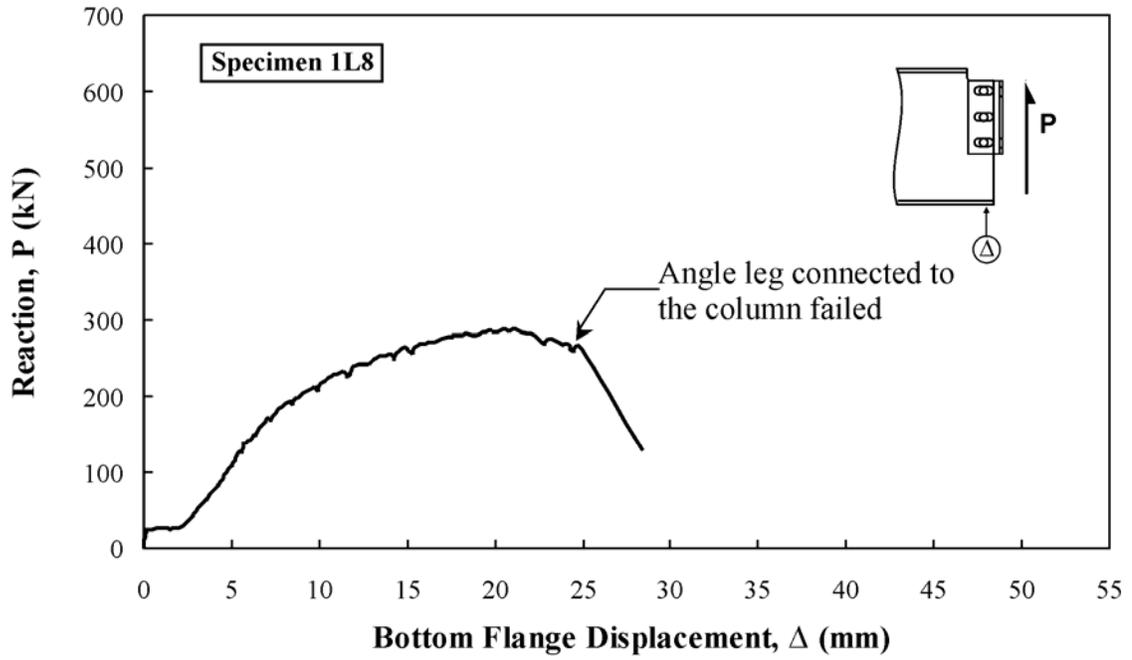
Figure B-27 Connection Reaction vs. Bottom Flange Displacement, Test Specimen 1L8
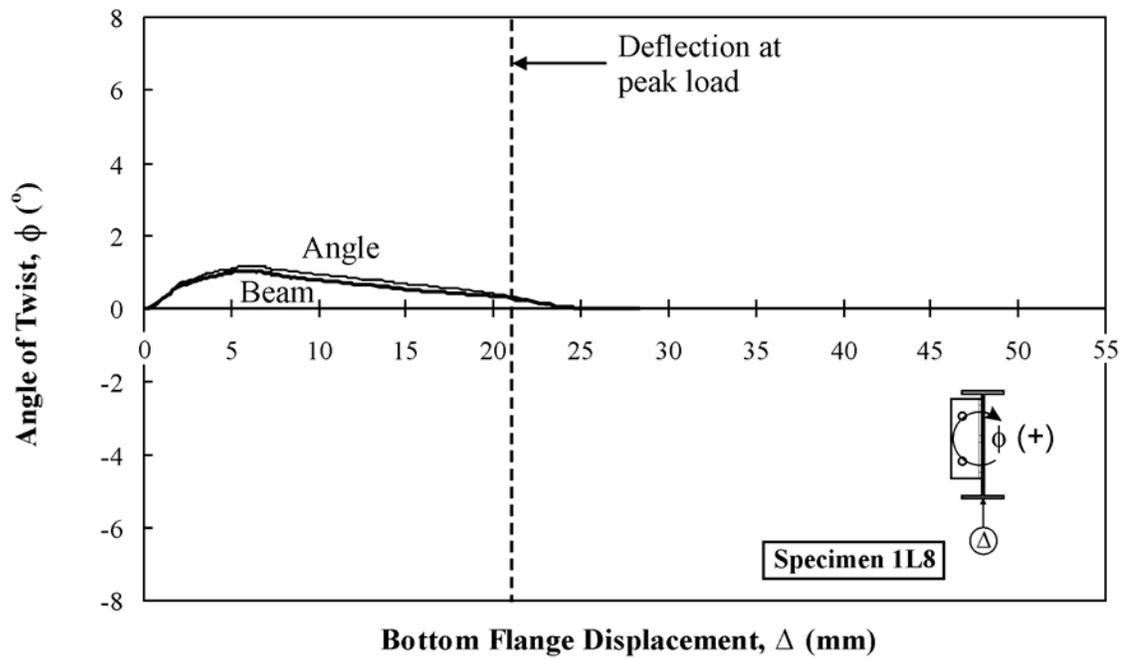
**Figure B-28 Twist vs. Bottom Flange Displacement, Test Specimen 1L8**
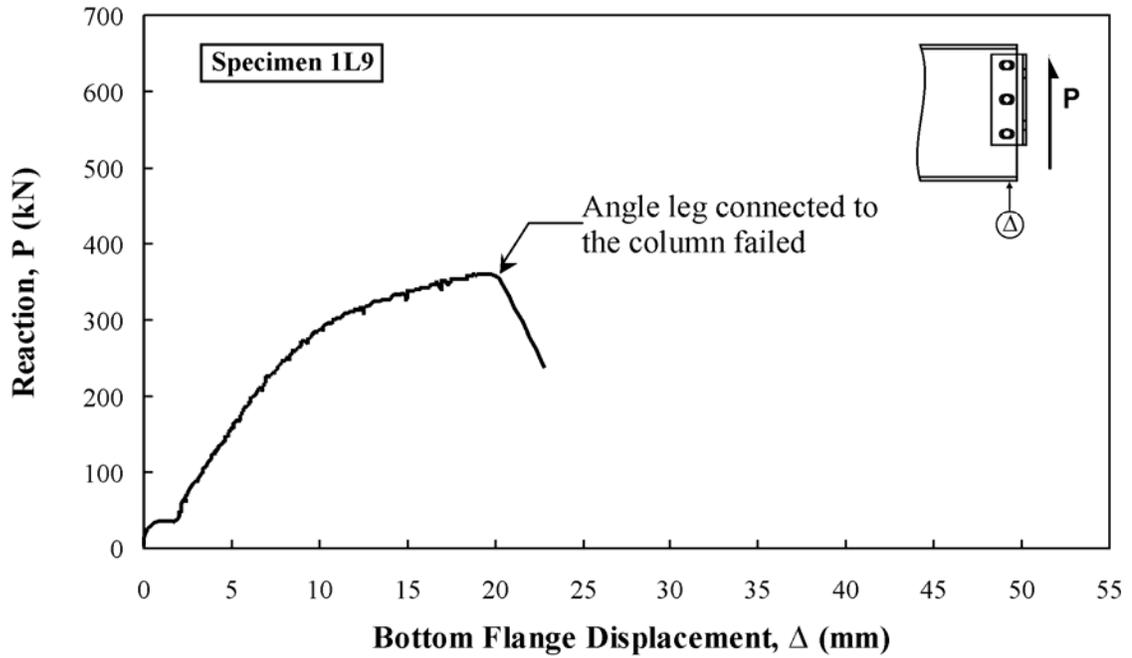
Figure B-29 Connection Reaction vs. Bottom Flange Displacement, Test Specimen 1L9
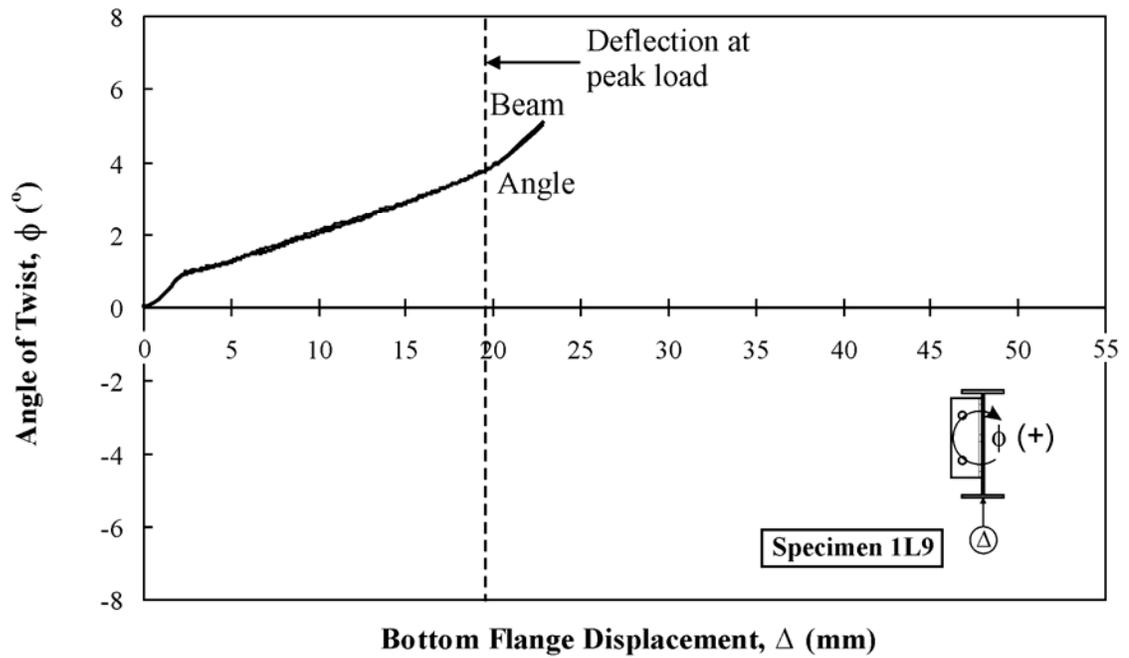

Figure B-30 Twist vs. Bottom Flange Displacement, Test Specimen 1L9
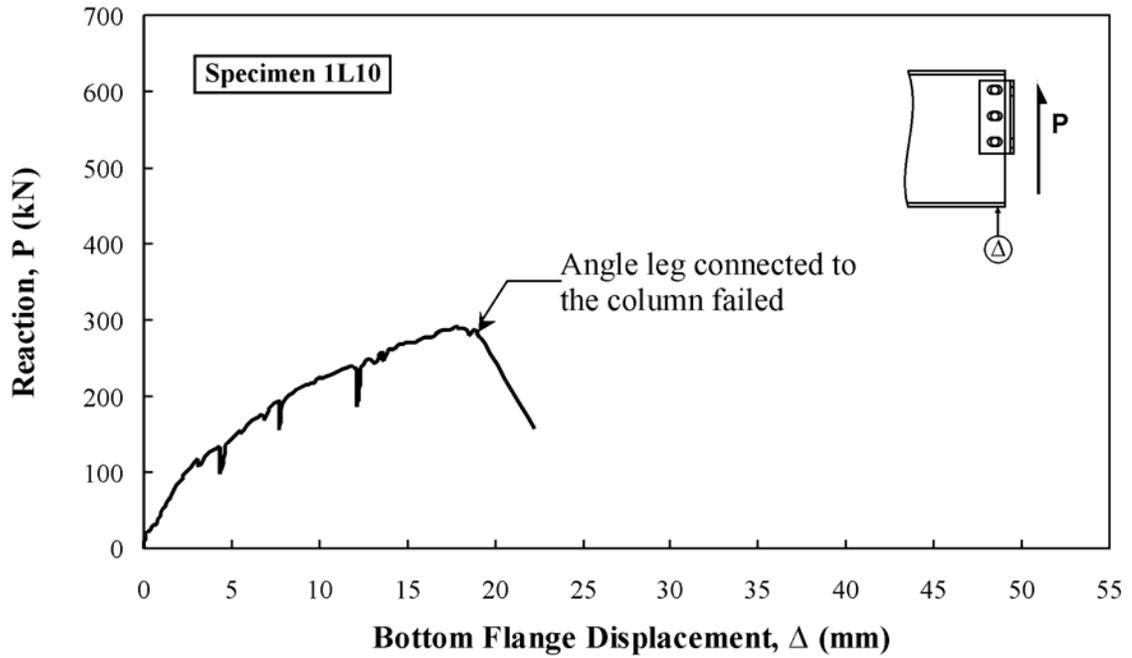
Figure B-31 Connection Reaction vs. Bottom Flange Displacement, Test Specimen 1L10
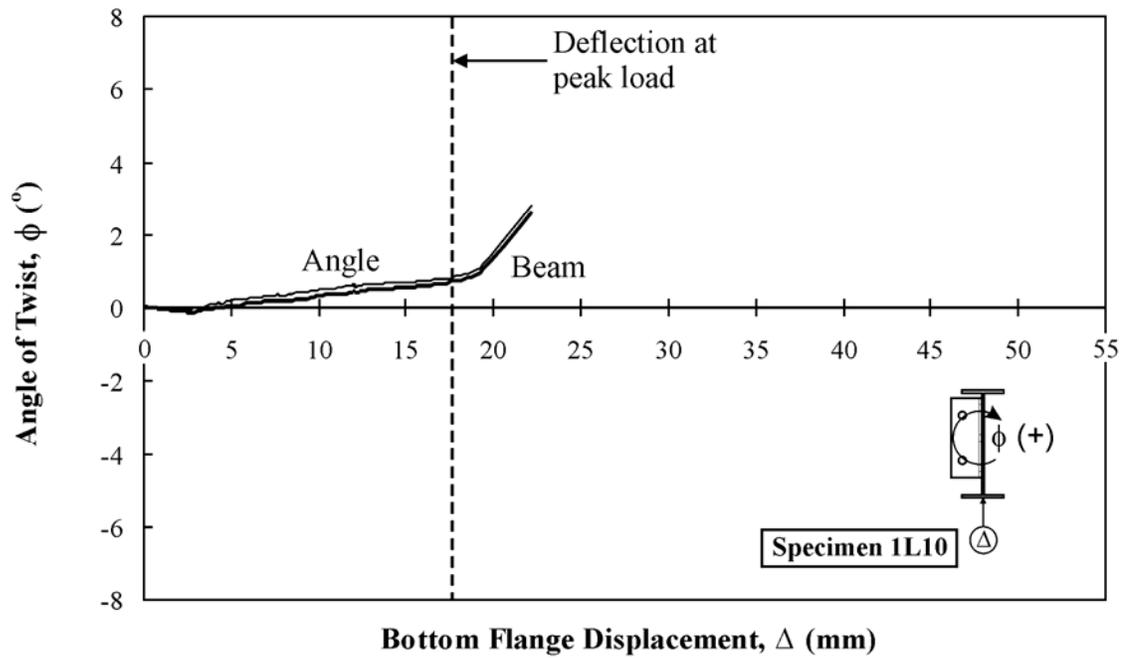
Figure B-32 Twist vs. Bottom Flange Displacement, Test Specimen 1L10

172
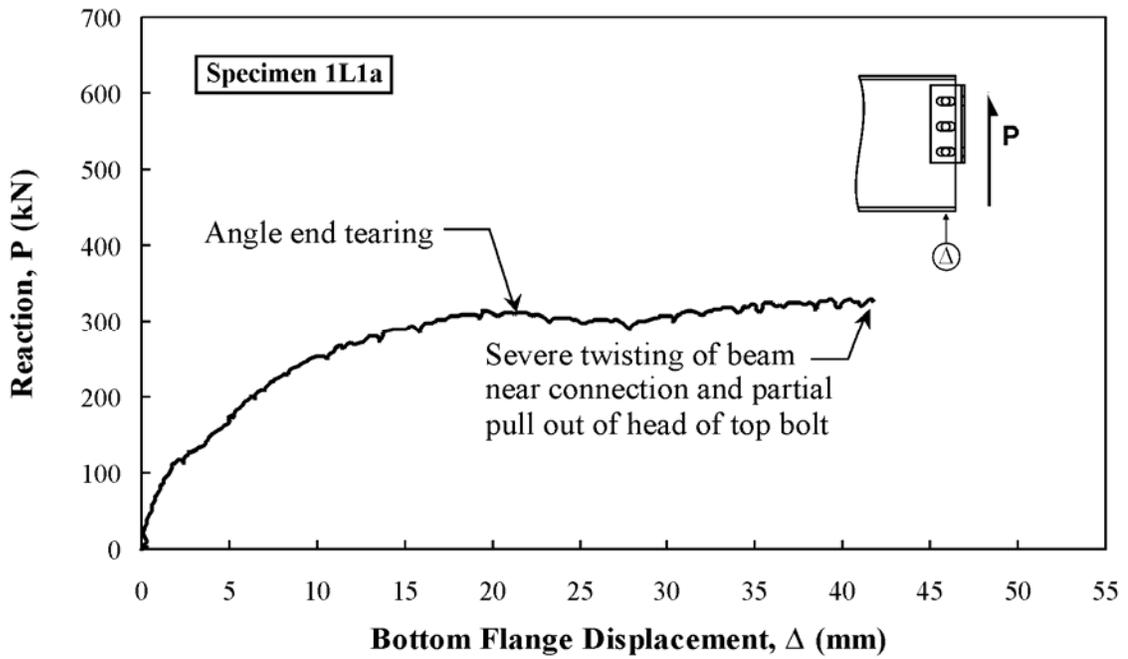
Figure B-33 Connection Reaction vs. Bottom Flange Displacement, Test Specimen 1L1a
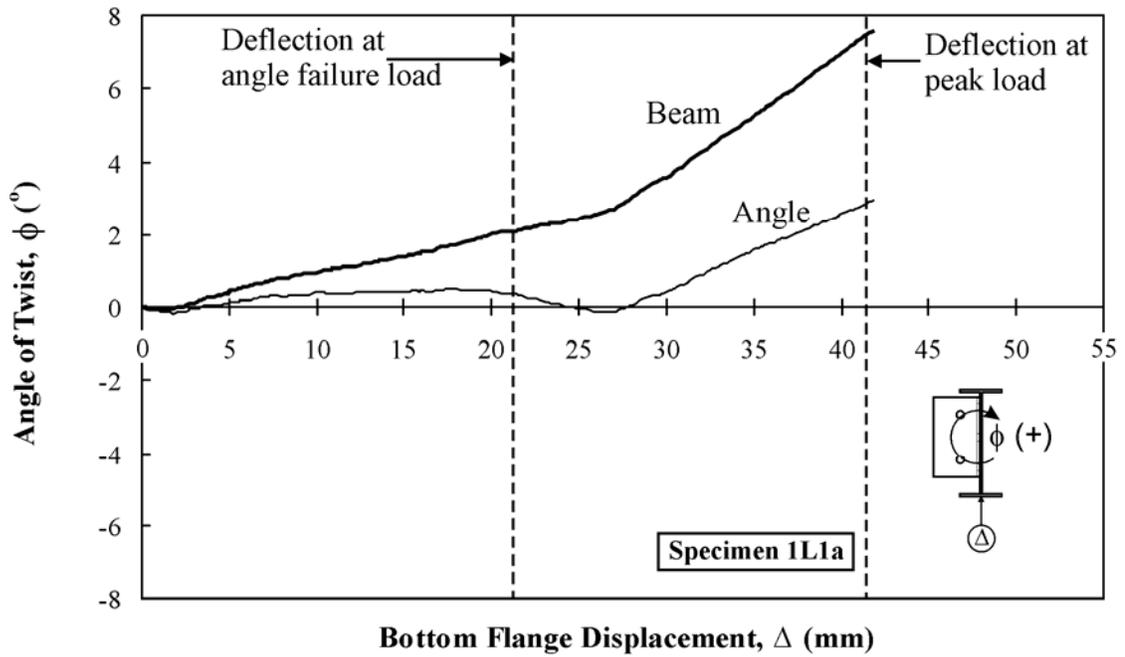
**Figure B-34 Twist vs. Bottom Flange Displacement, Test Specimen 1L1a**

173
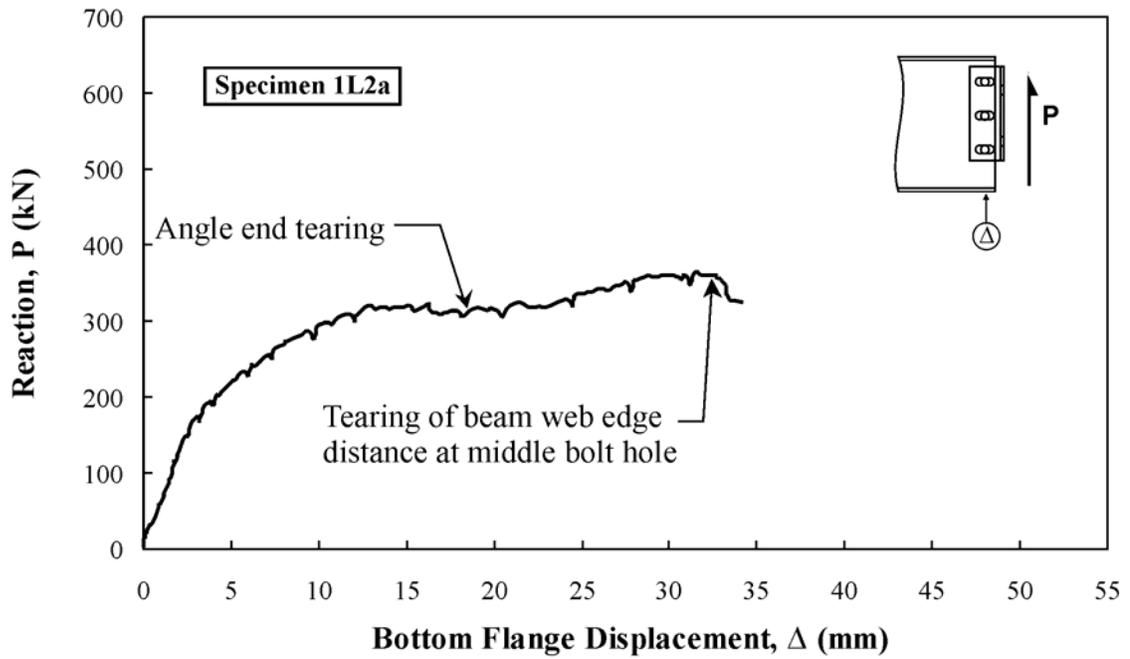
Figure B-35 Connection Reaction vs. Bottom Flange Displacement, Test Specimen 1L2a
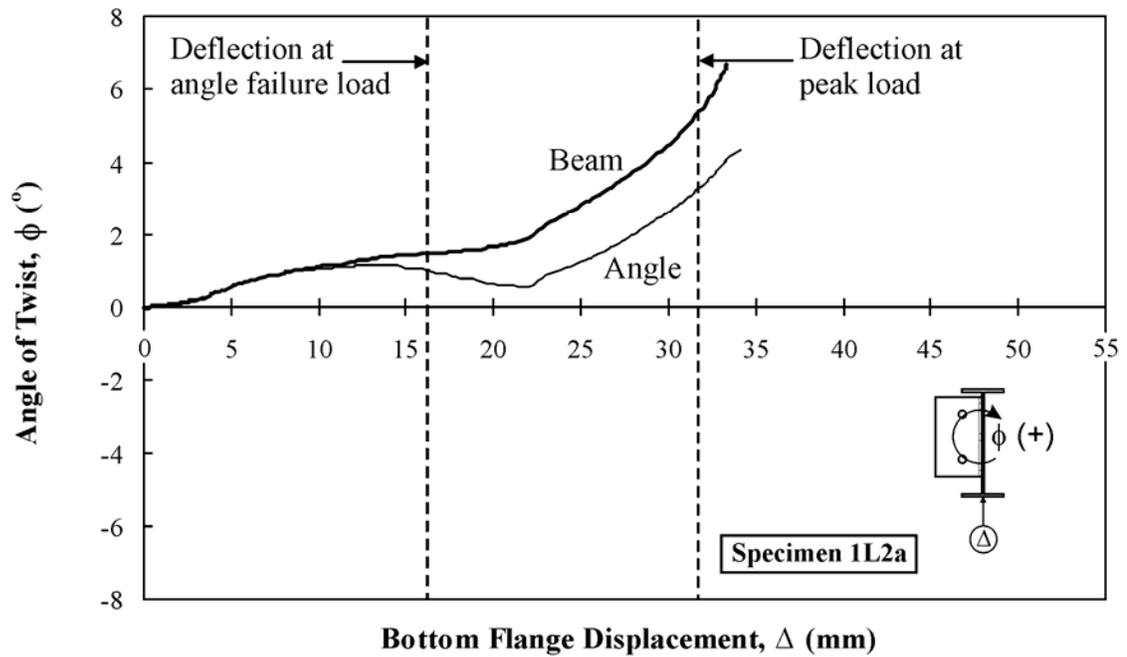

Figure B-36 Twist vs. Bottom Flange Displacement, Test Specimen 1L2a

174
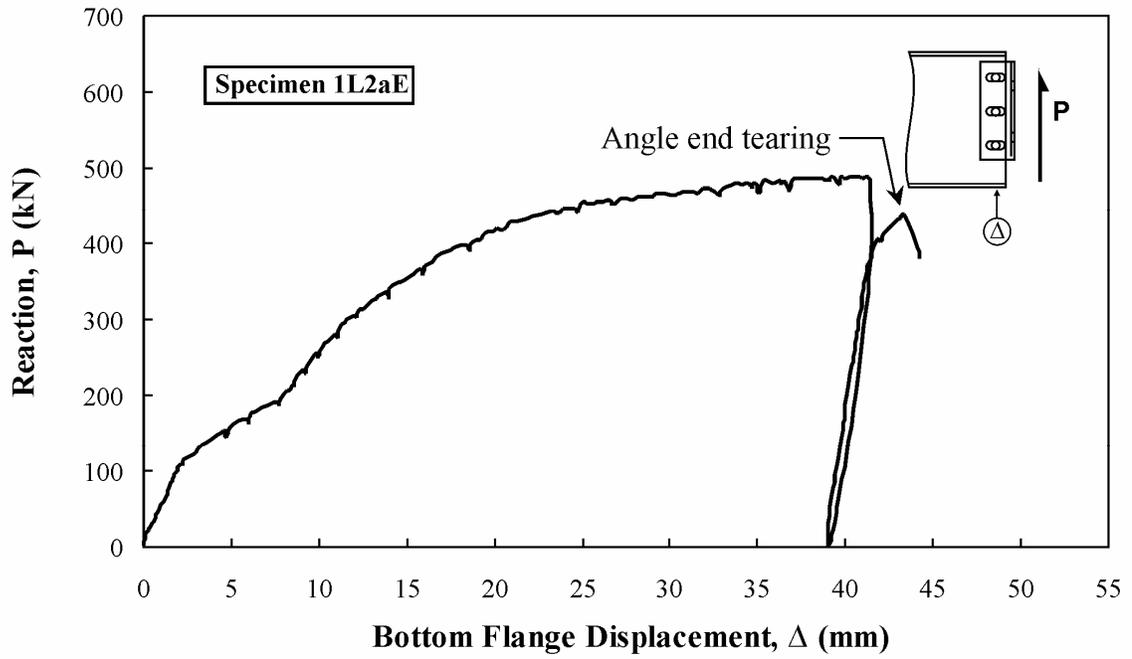
Figure B-37 Connection Reaction vs. Bottom Flange Displacement, Test Specimen 1L2aE
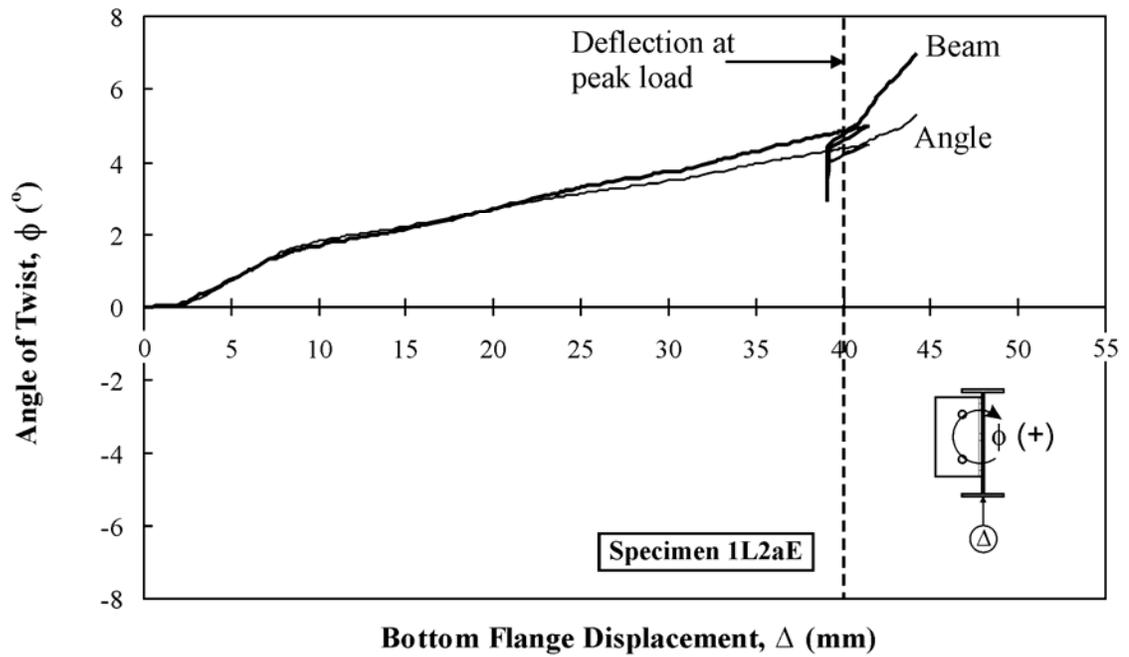
Figure B-38 Twist vs. Bottom Flange Displacement, Test Specimen 1L2aE

175
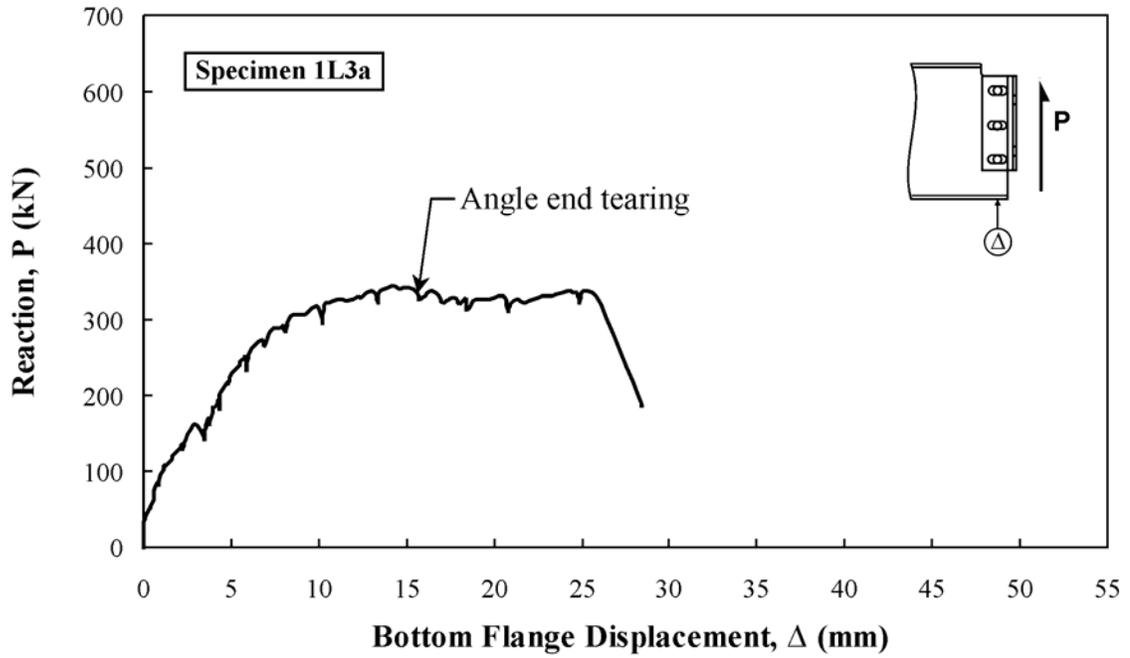
Figure B-39 Connection Reaction vs. Bottom Flange Displacement, Test Specimen 1L3a
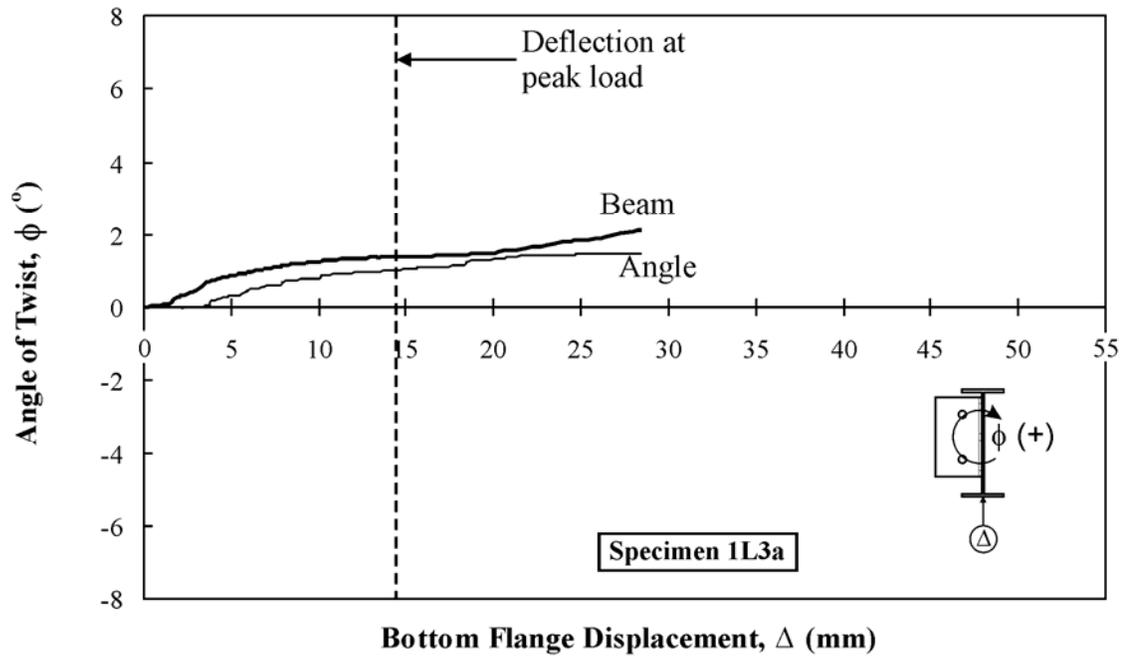

Figure B-40 Twist vs. Bottom Flange Displacement, Test Specimen 1L3a

176
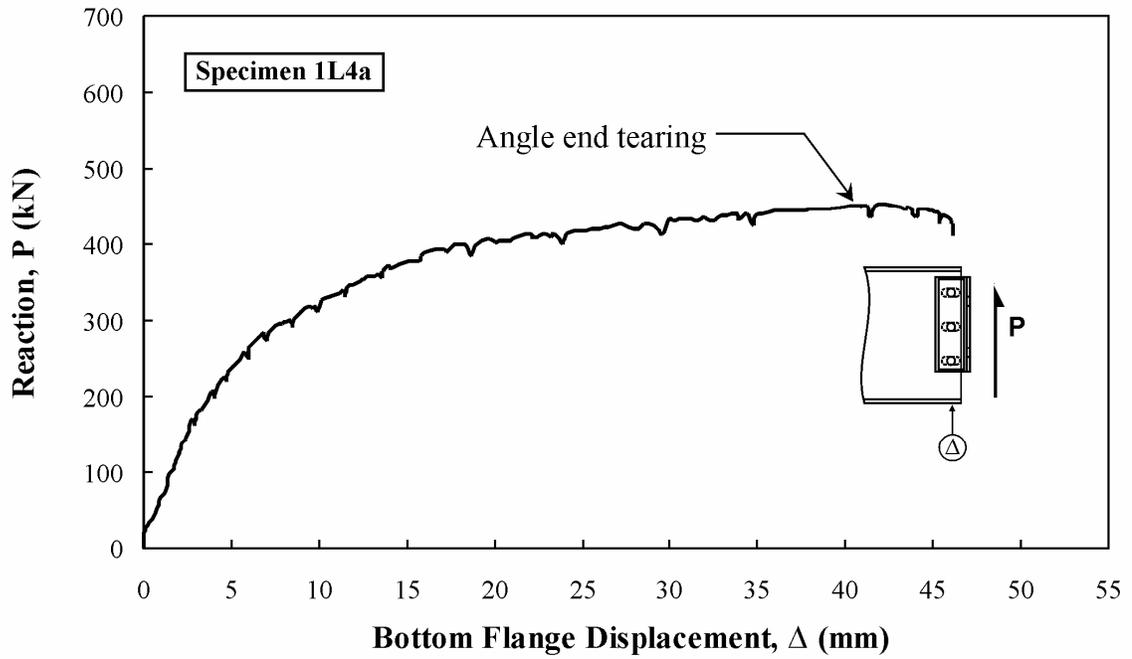
Figure B-41 Connection Reaction vs. Bottom Flange Displacement, Test Specimen 1L4a
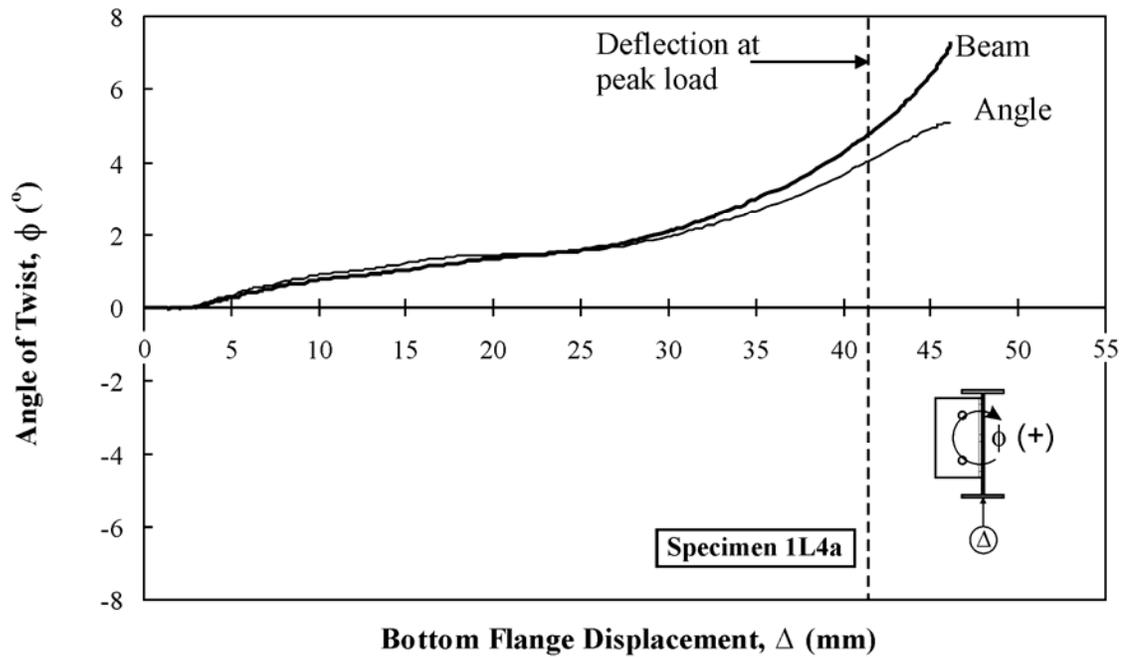
Figure B-42 Twist vs. Bottom Flange Displacement, Test Specimen 1L4a

177
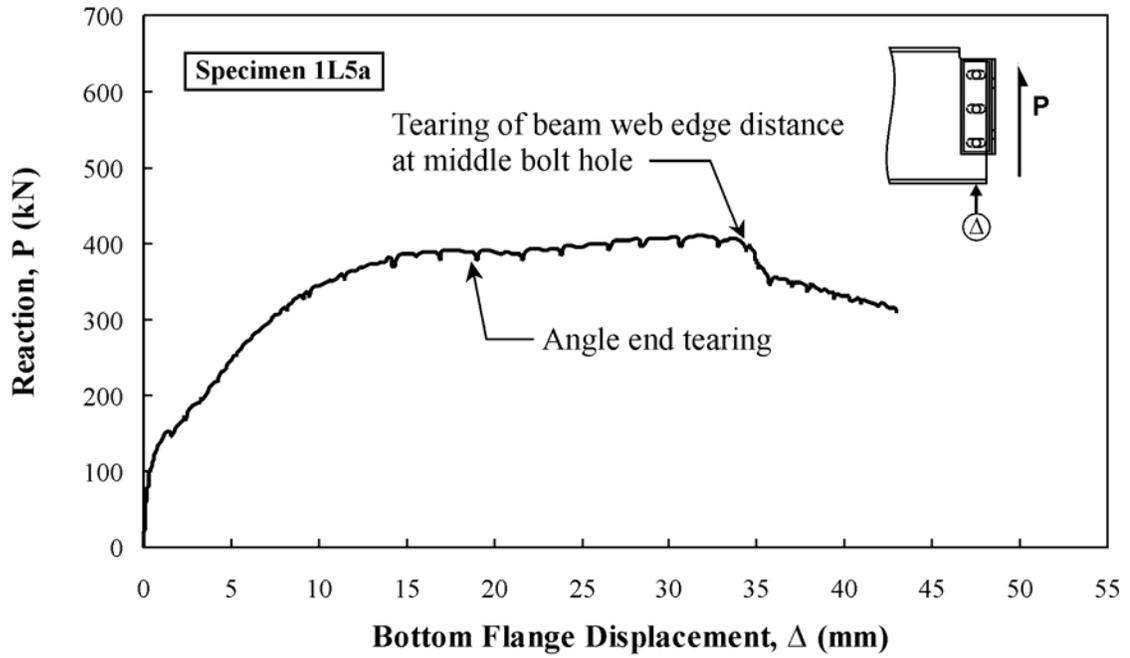
Figure B-43 Connection Reaction vs. Bottom Flange Displacement, Test Specimen 1L5a
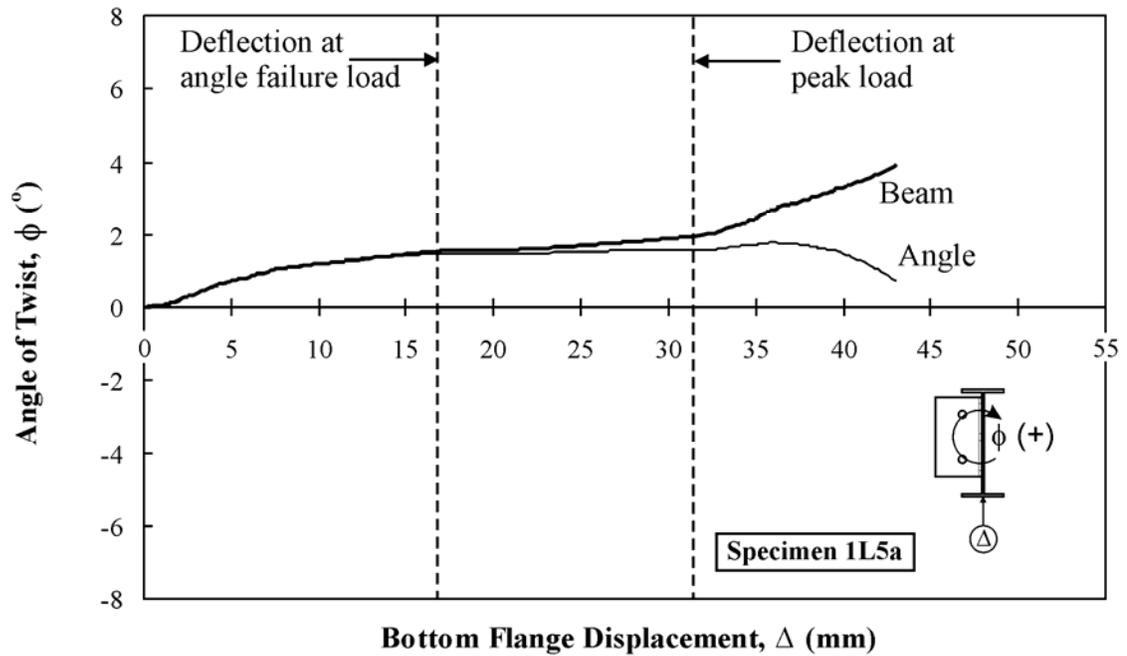
Figure B-44 Twist vs. Bottom Flange Displacement, Test Specimen 1L5a
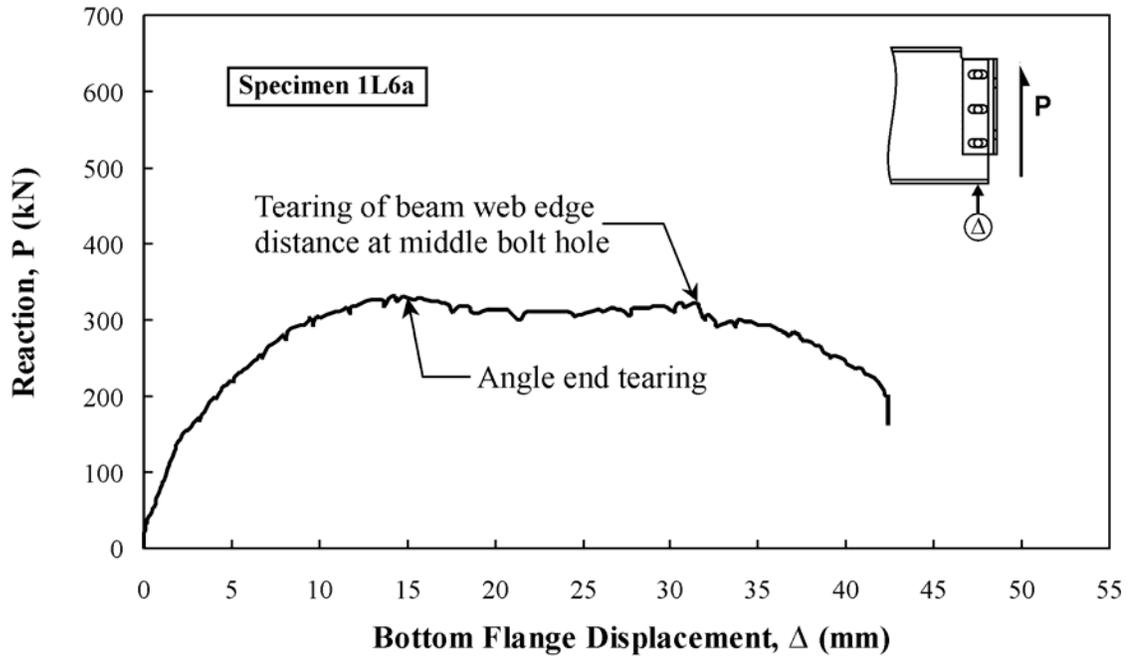
**Figure B-45 Connection Reaction vs. Bottom Flange Displacement, Test Specimen 1L6a**
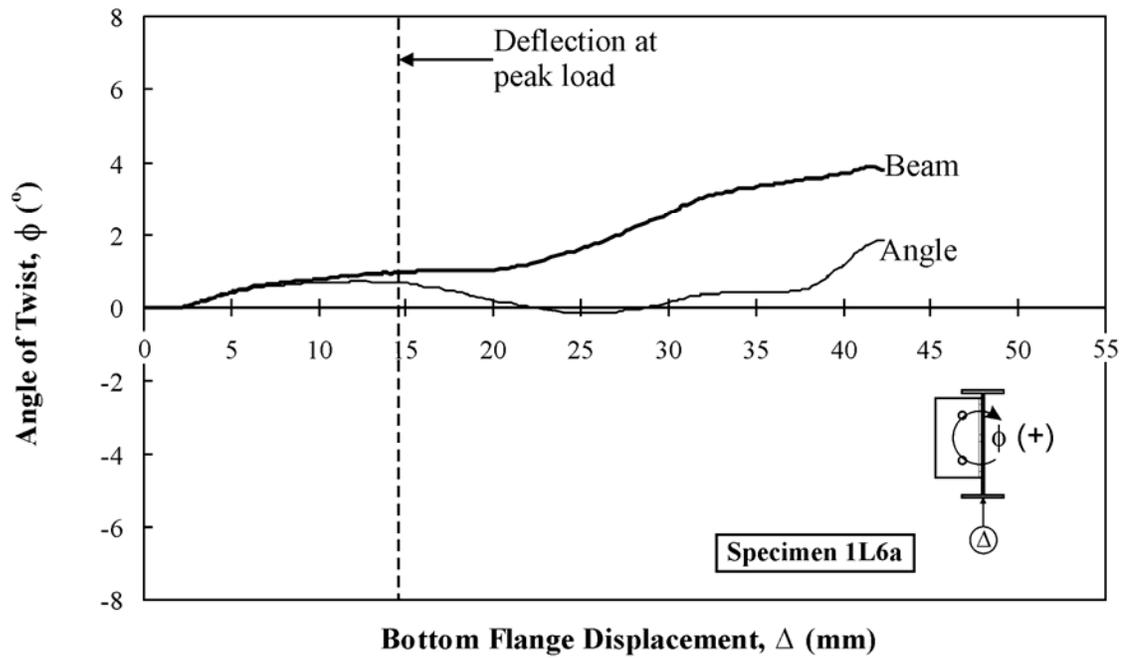
Figure B-46 Twist vs. Bottom Flange Displacement, Test Specimen 1L6a

179
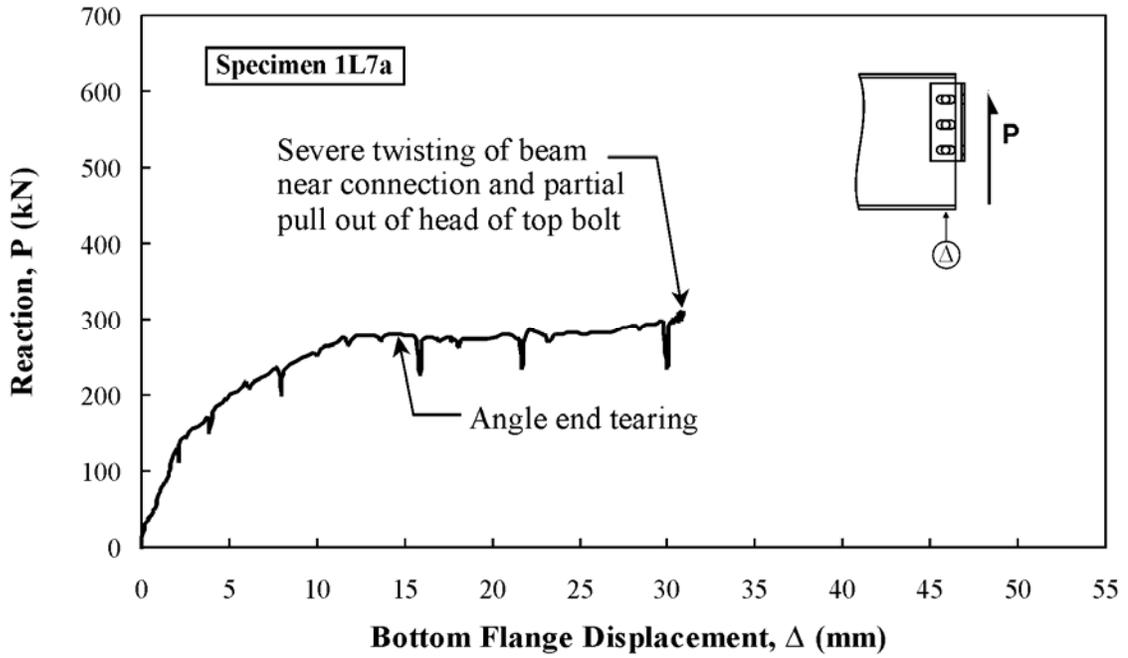
Figure B-47 Connection Reaction vs. Bottom Flange Displacement, Test Specimen 1L7a
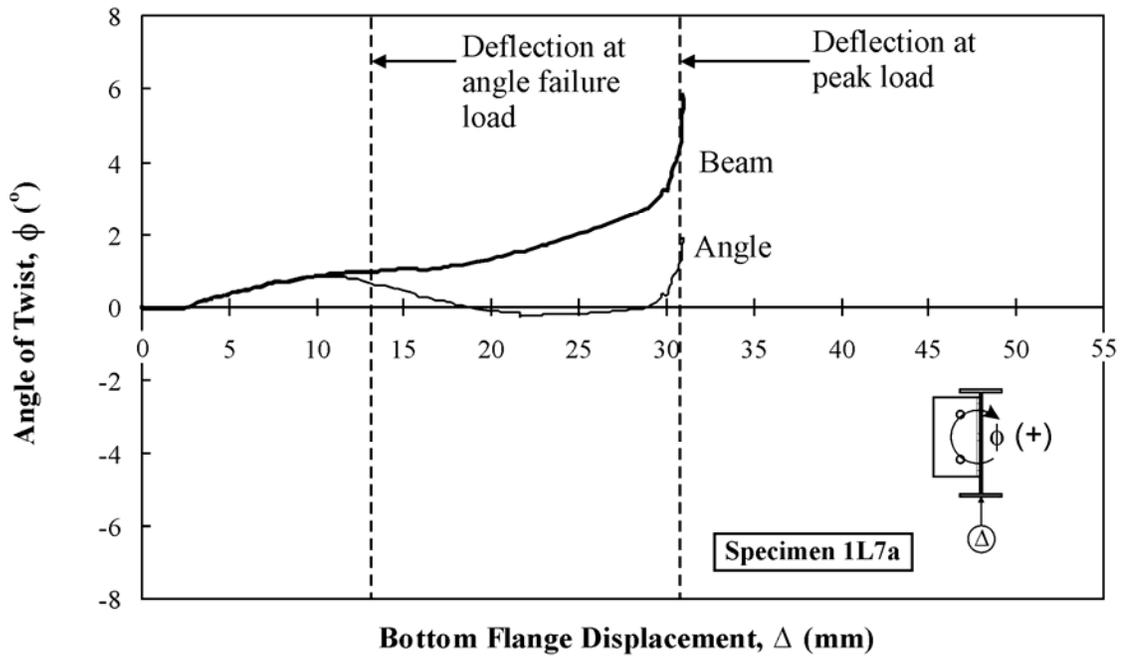
Figure B-48 Twist vs. Bottom Flange Displacement, Test Specimen 1L7a

180
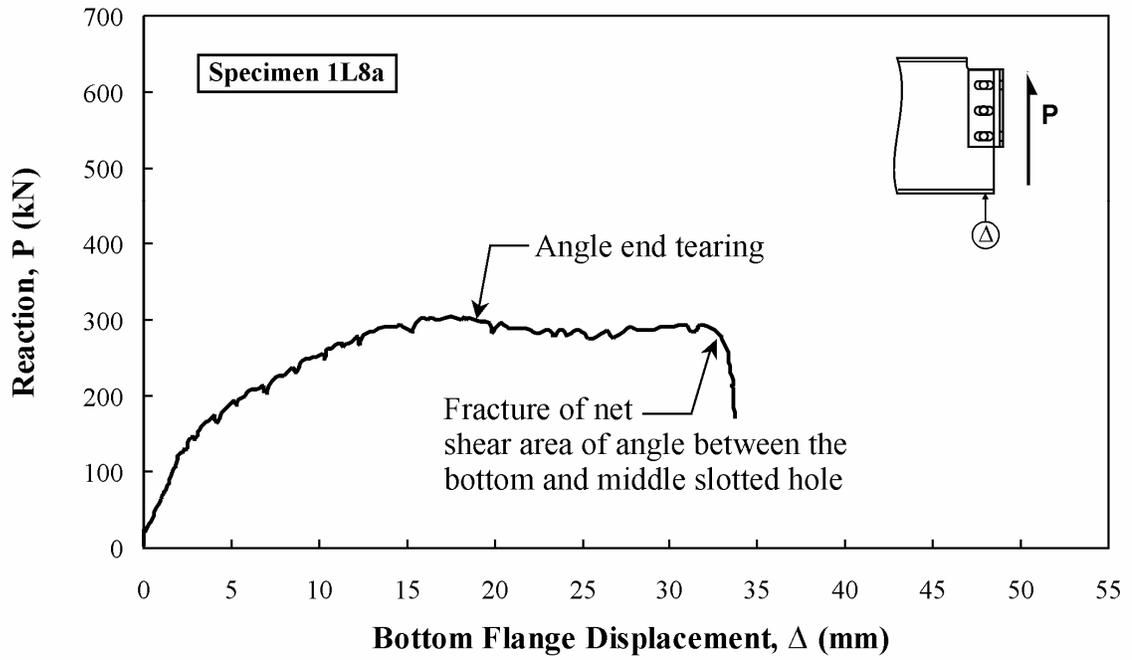
Figure B-49 Connection Reaction vs. Bottom Flange Displacement, Test Specimen 1L8a
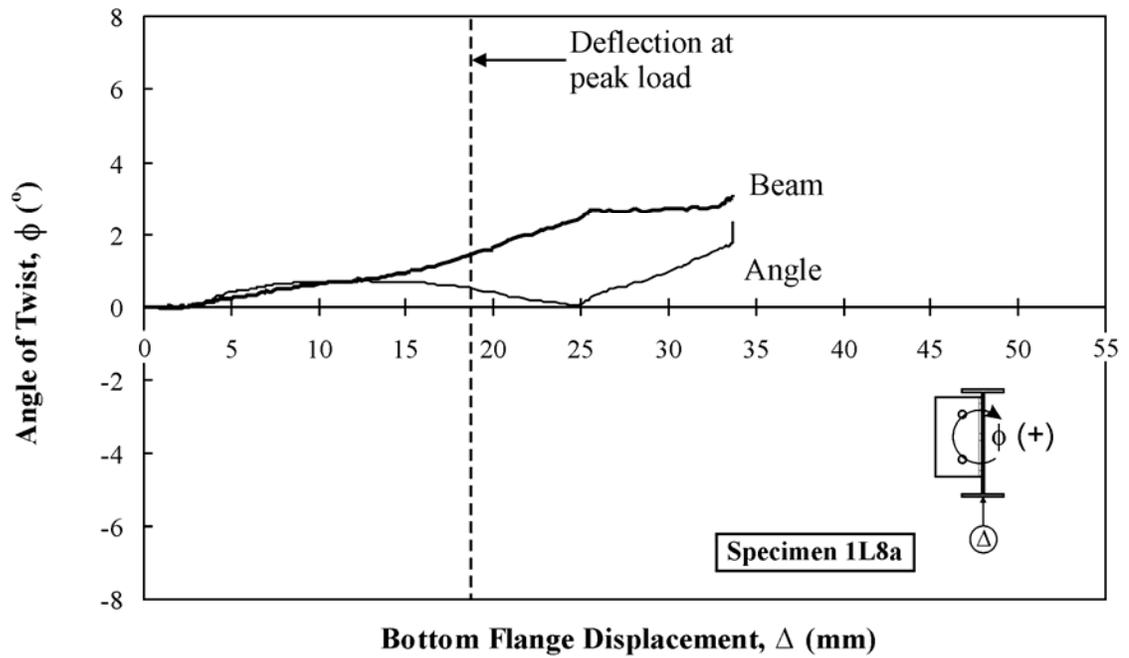
**Figure B-50 Twist vs. Bottom Flange Displacement, Test Specimen 1L8a**
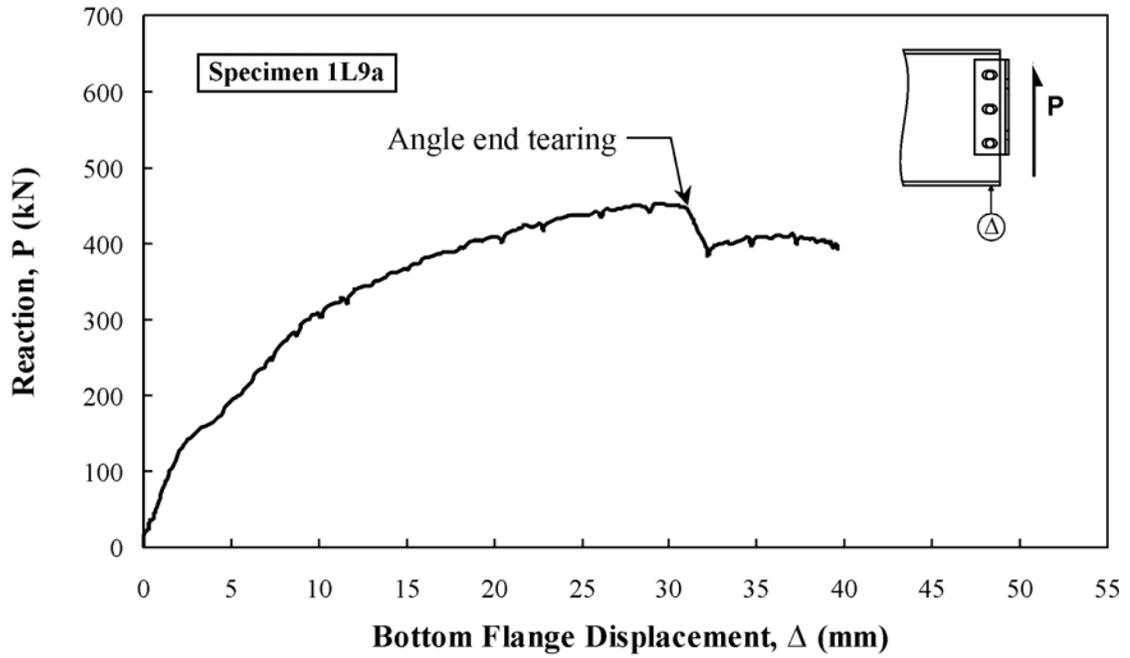
**Figure B-51 Connection Reaction vs. Bottom Flange Displacement, Test Specimen 1L9a**
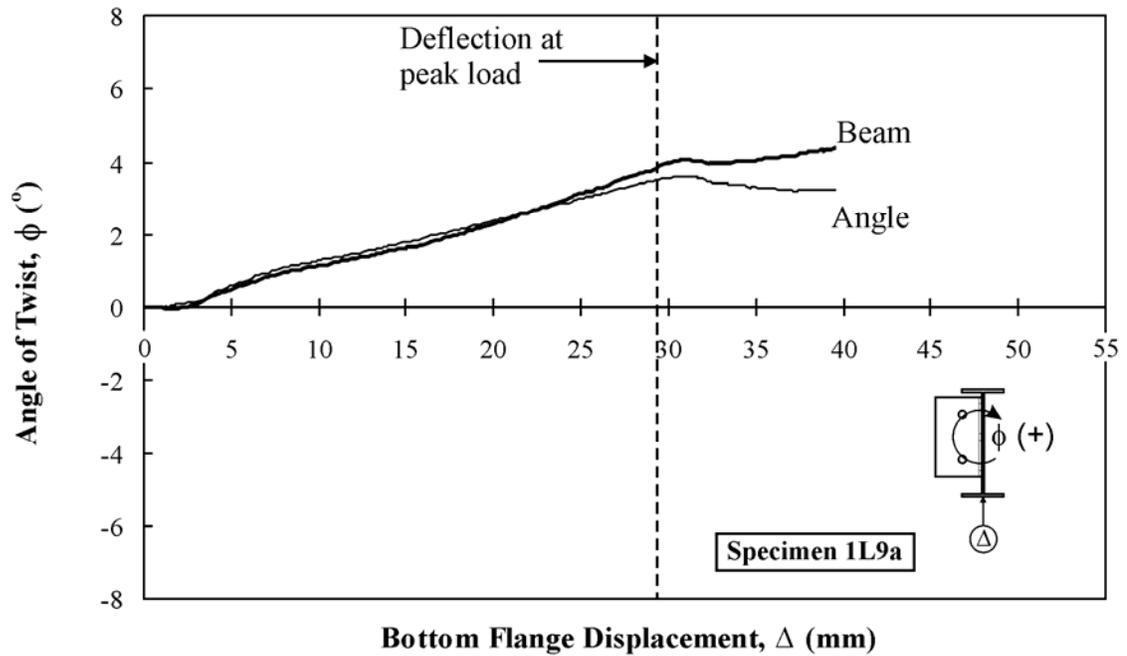
**Figure B-52 Twist vs. Bottom Flange Displacement, Test Specimen 1L9a**
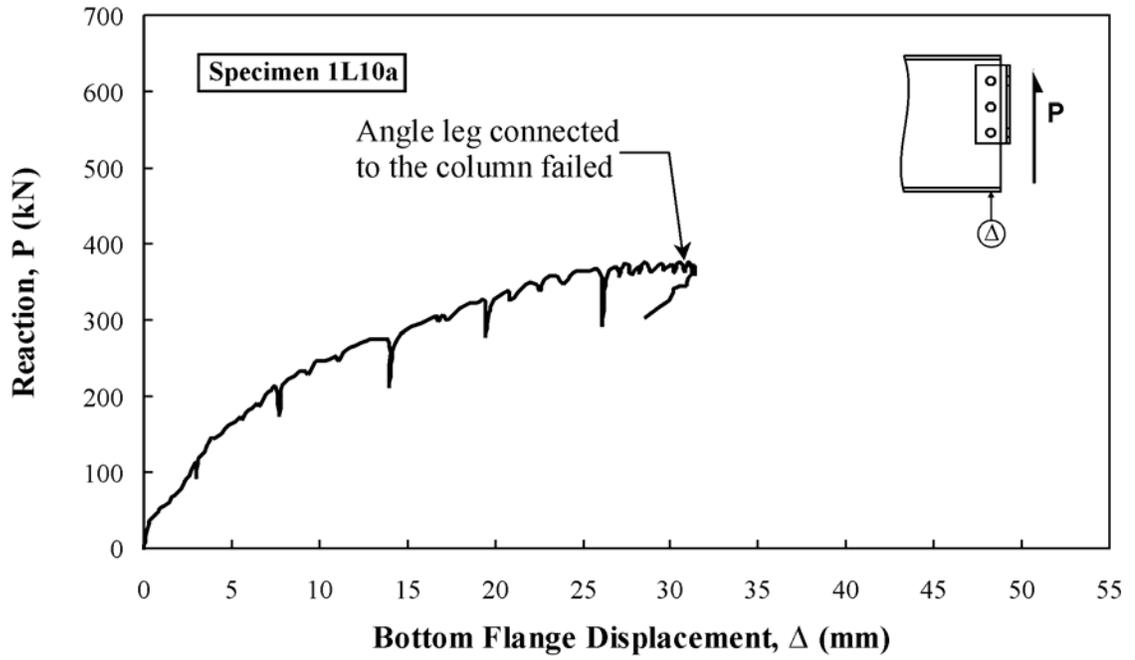
Figure B-53 Connection Reaction vs. Bottom Flange Displacement, Test Specimen 1L10a
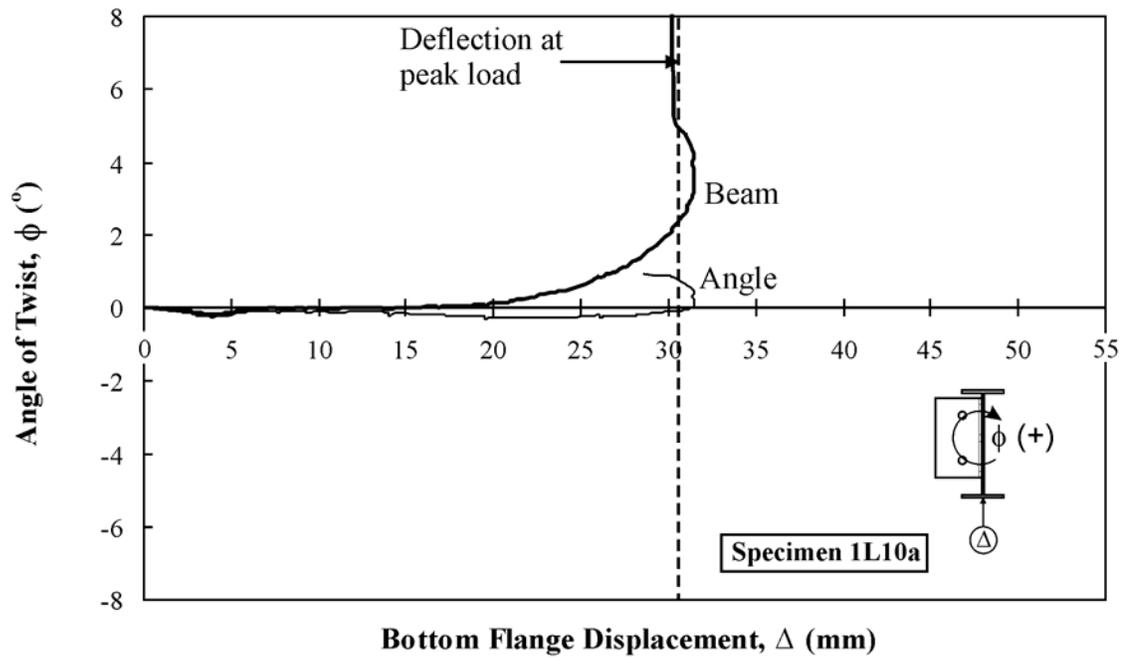
Figure B-54 Twist vs. Bottom Flange Displacement, Test Specimen 1L10a
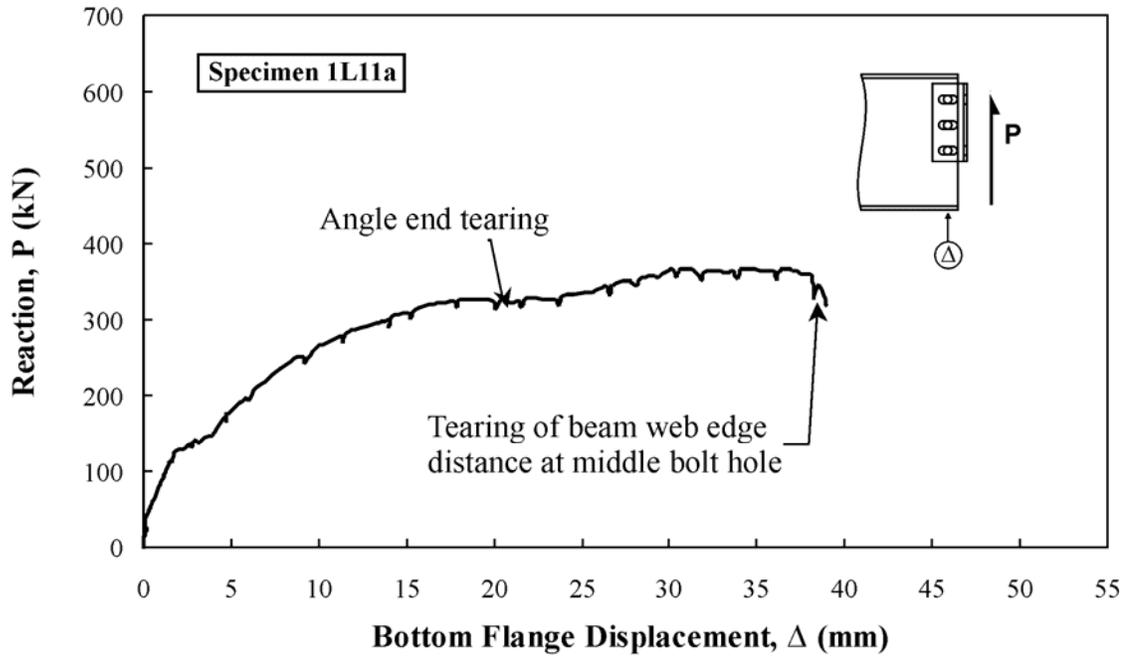
Figure B-55 Connection Reaction vs. Bottom Flange Displacement, Test Specimen 1L11a
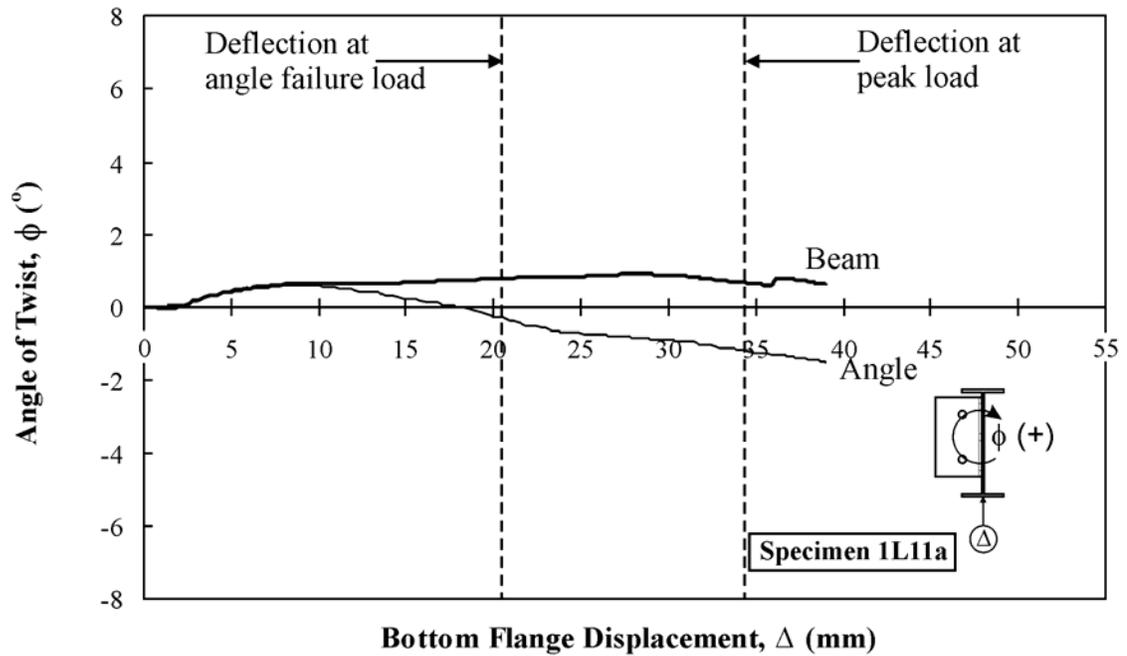
Figure B-56 Twist vs. Bottom Flange Displacement, Test Specimen 1L11a

184
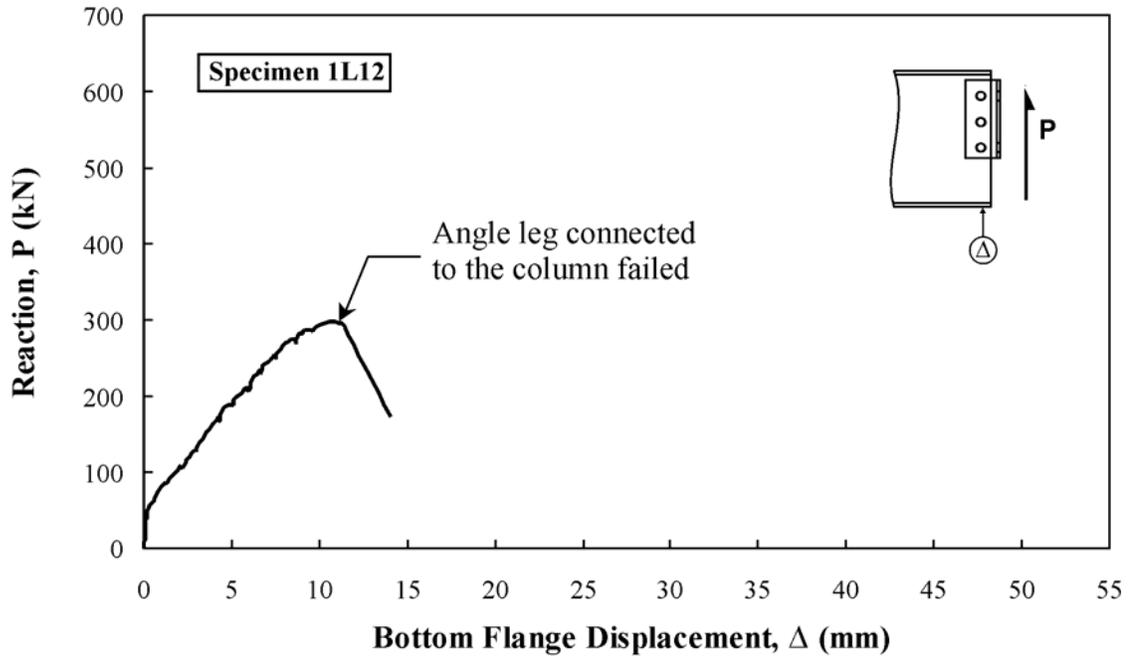
Figure B-57 Connection Reaction vs. Bottom Flange Displacement, Test Specimen 1L12
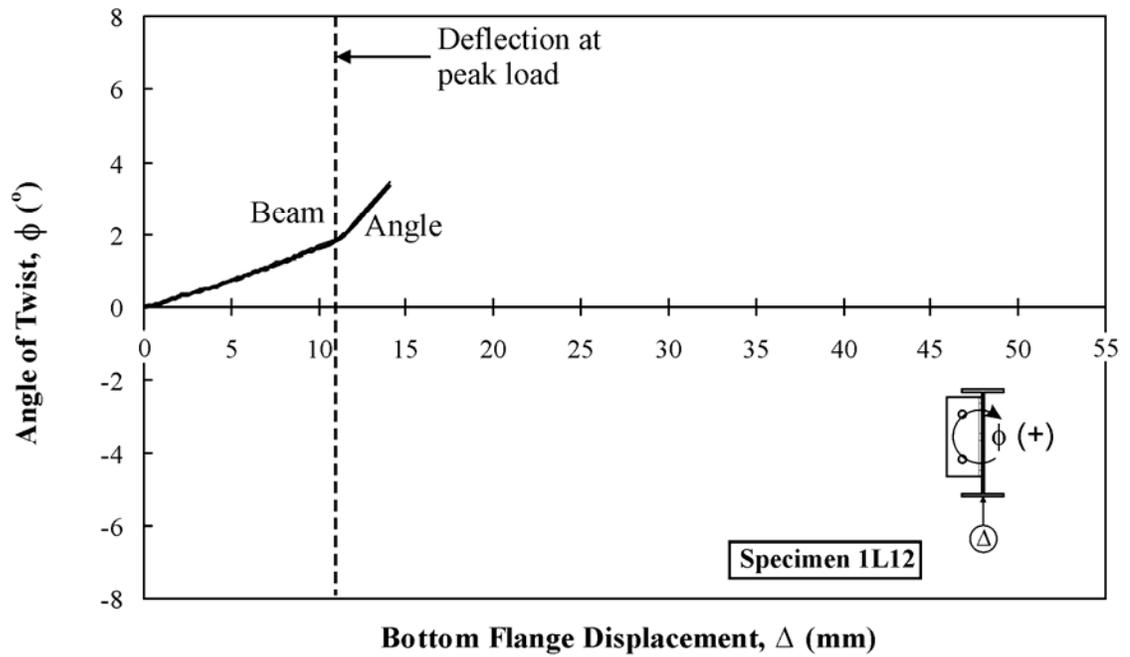

**Figure B-58 Twist vs. Bottom Flange Displacement, Test Specimen 1L12**
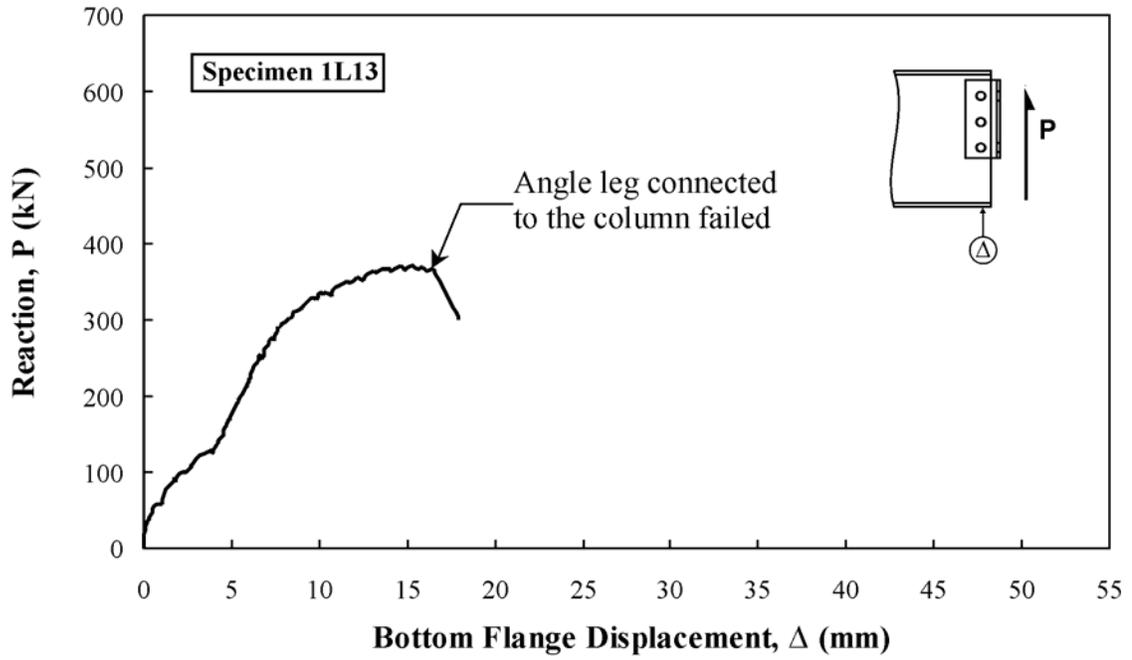
Figure B-59 Connection Reaction vs. Bottom Flange Displacement, Test Specimen 1L13
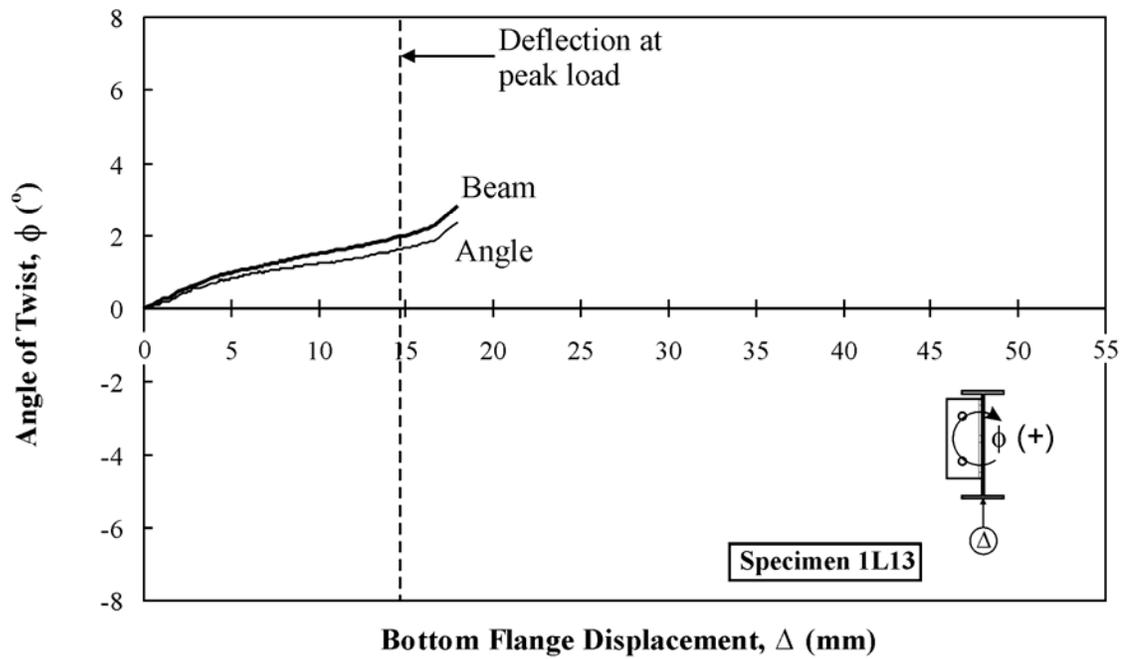
Figure B-60 Twist vs. Bottom Flange Displacement, Test Specimen 1L13

186
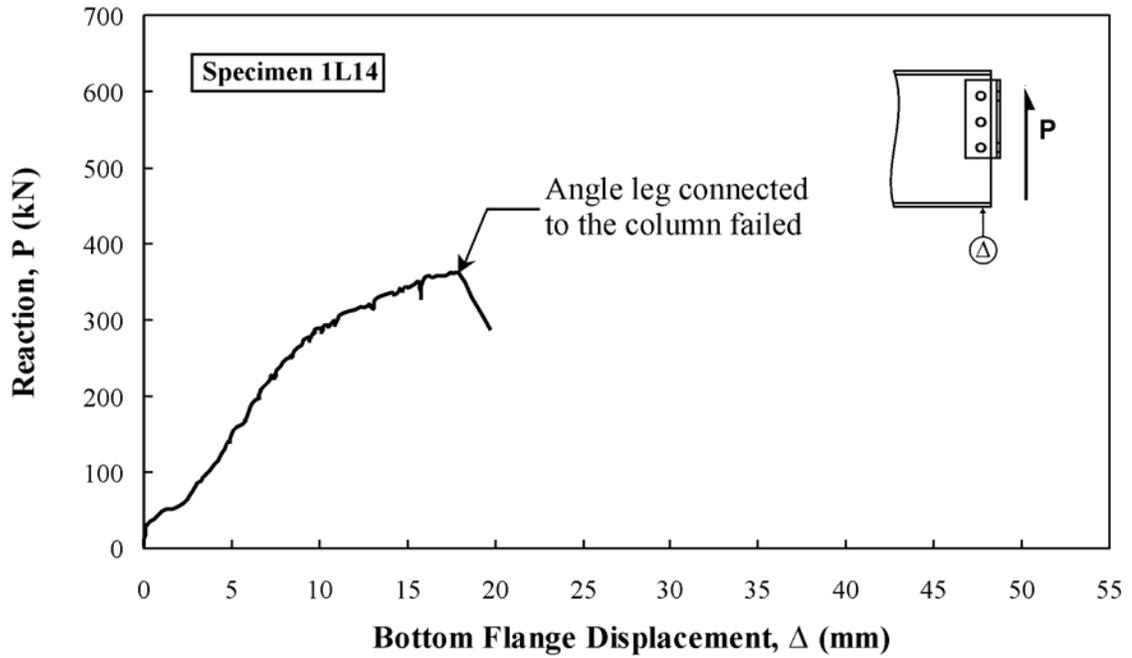
Figure B-61 Connection Reaction vs. Bottom Flange Displacement, Test Specimen 1L14
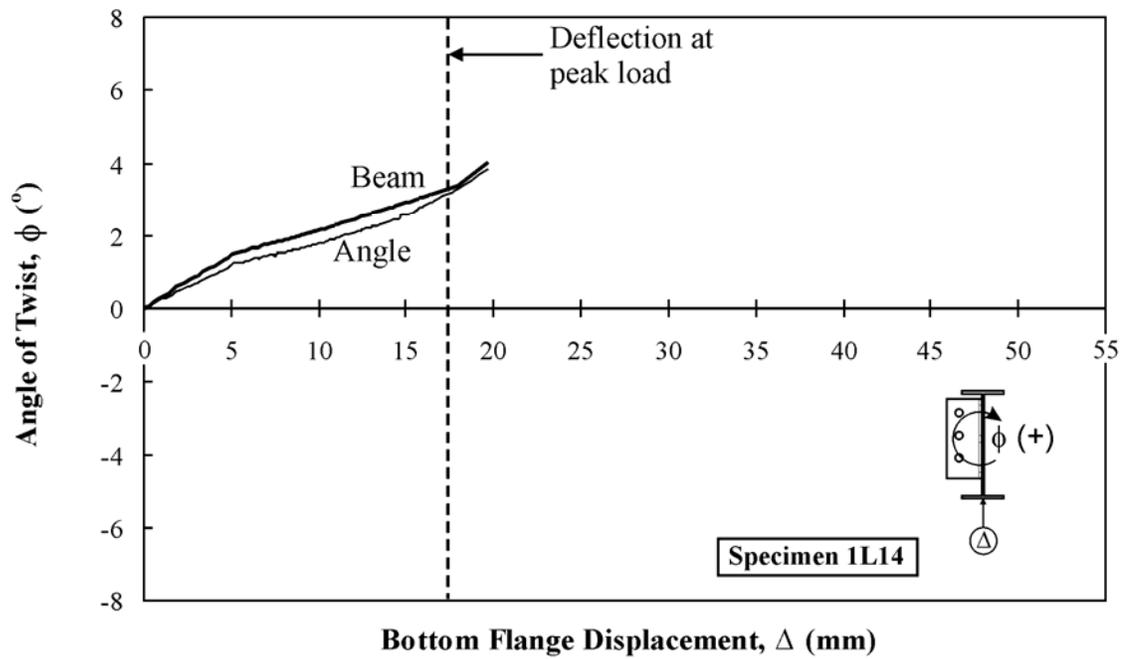
Figure B-62 Twist vs. Bottom Flange Displacement, Test Specimen 1L14

187
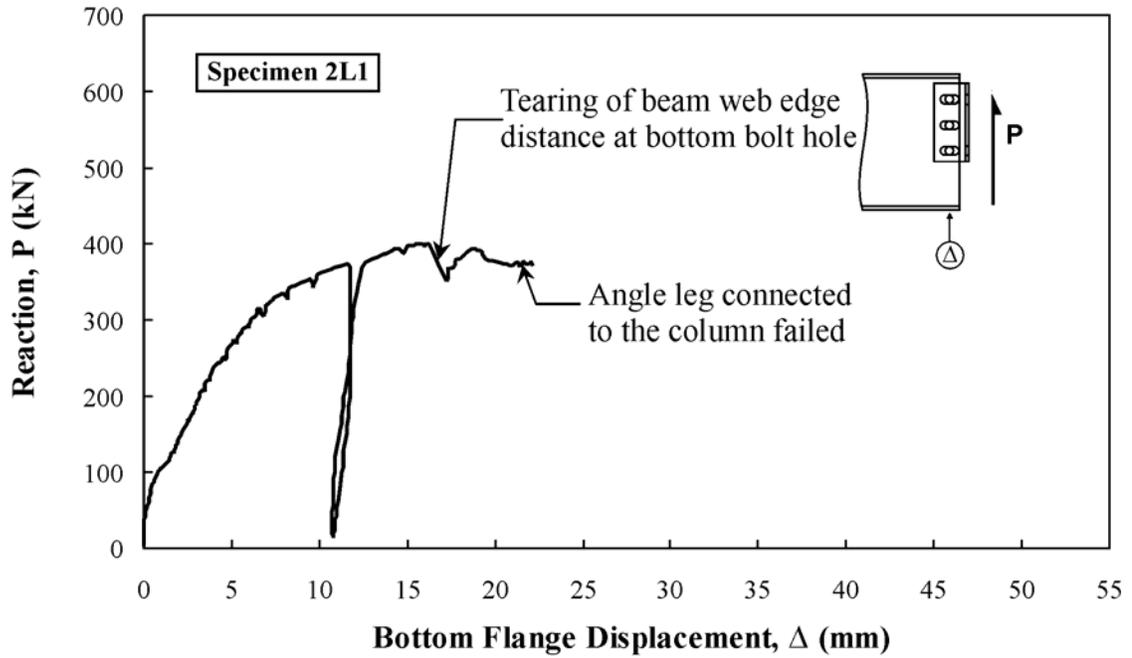
Figure B-63 Connection Reaction vs. Bottom Flange Displacement, Test Specimen 2L1
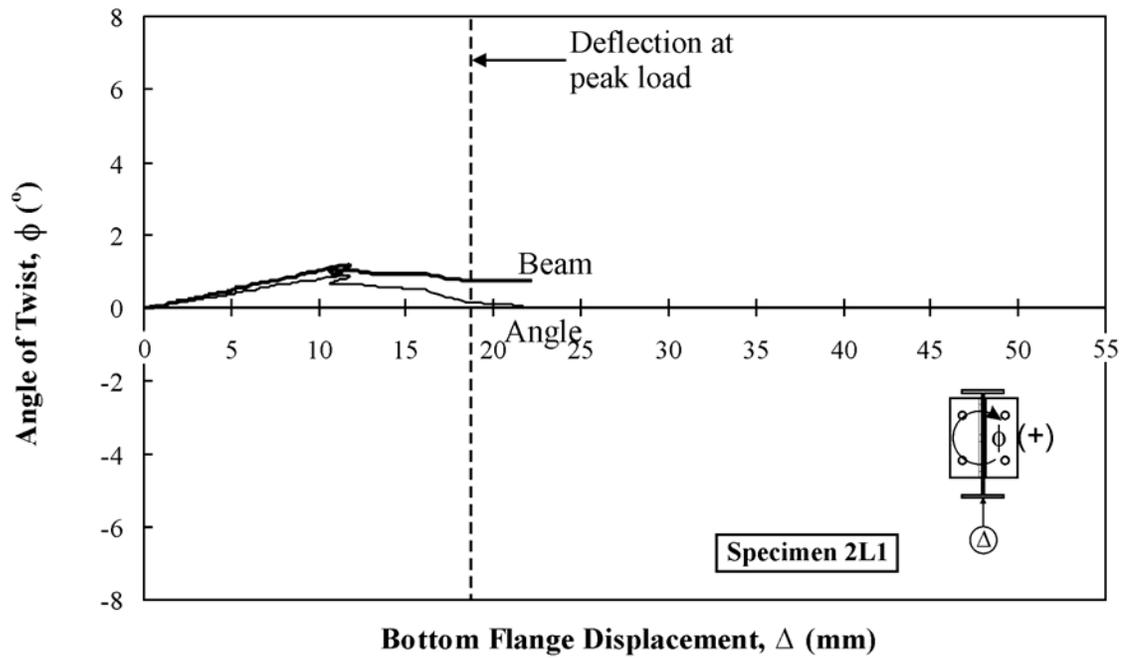

Figure B-64 Twist vs. Bottom Flange Displacement, Test Specimen 2L1

188
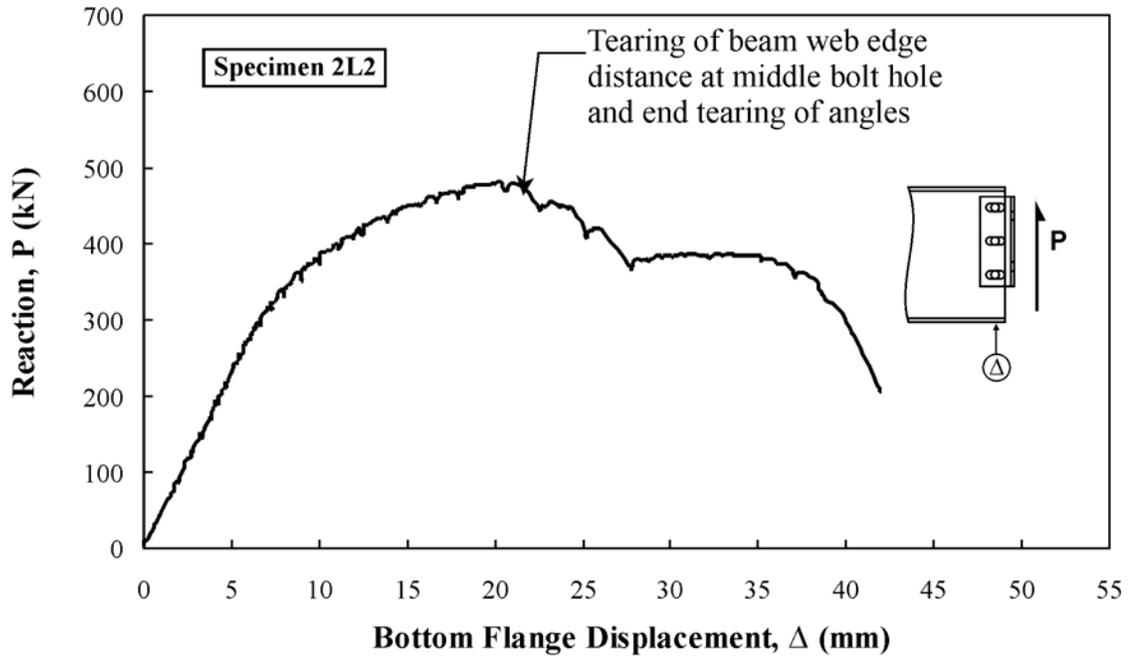
Figure B-65 Connection Reaction vs. Bottom Flange Displacement, Test Specimen 2L2
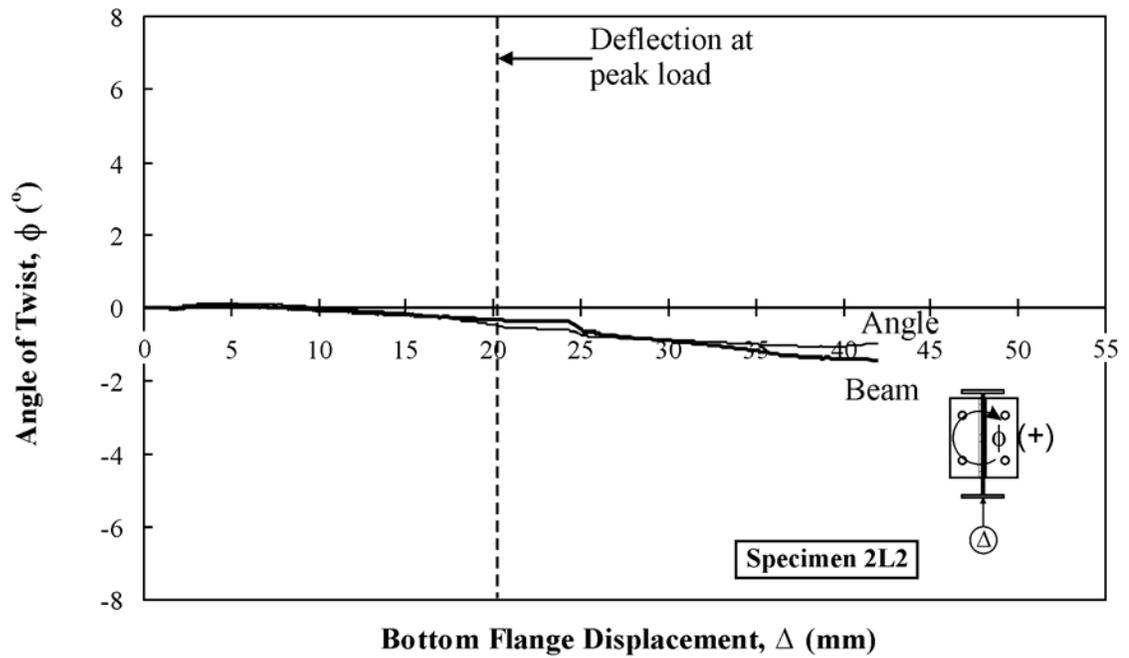
**Figure B-66 Twist vs. Bottom Flange Displacement, Test Specimen 2L2**
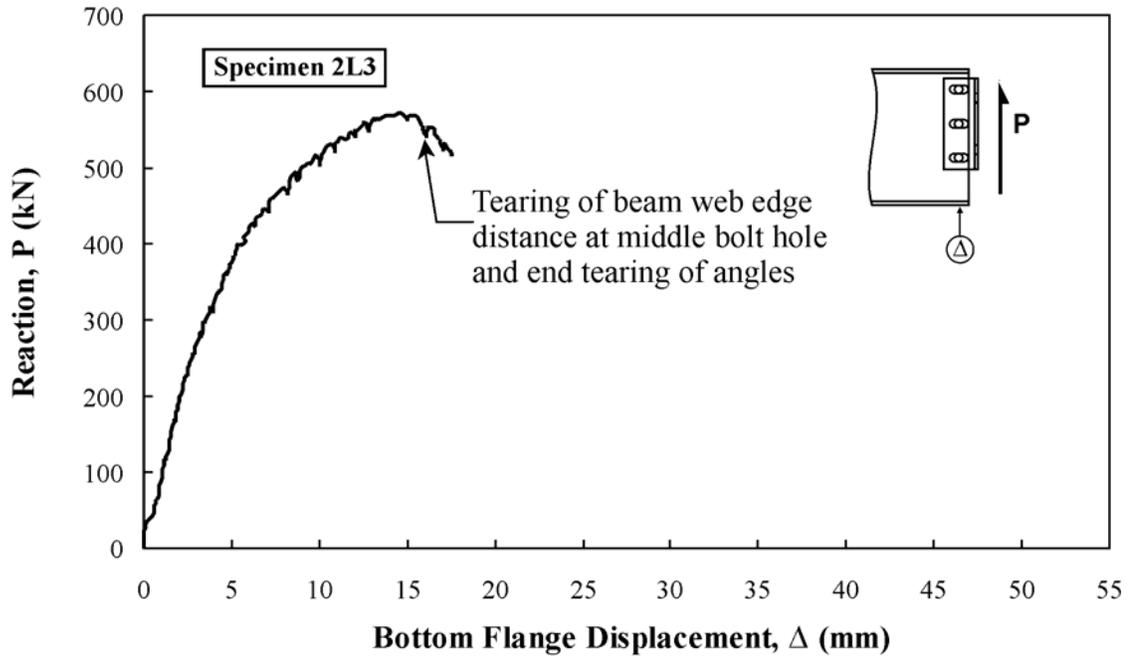
**Figure B-67 Connection Reaction vs. Bottom Flange Displacement, Test Specimen 2L3**
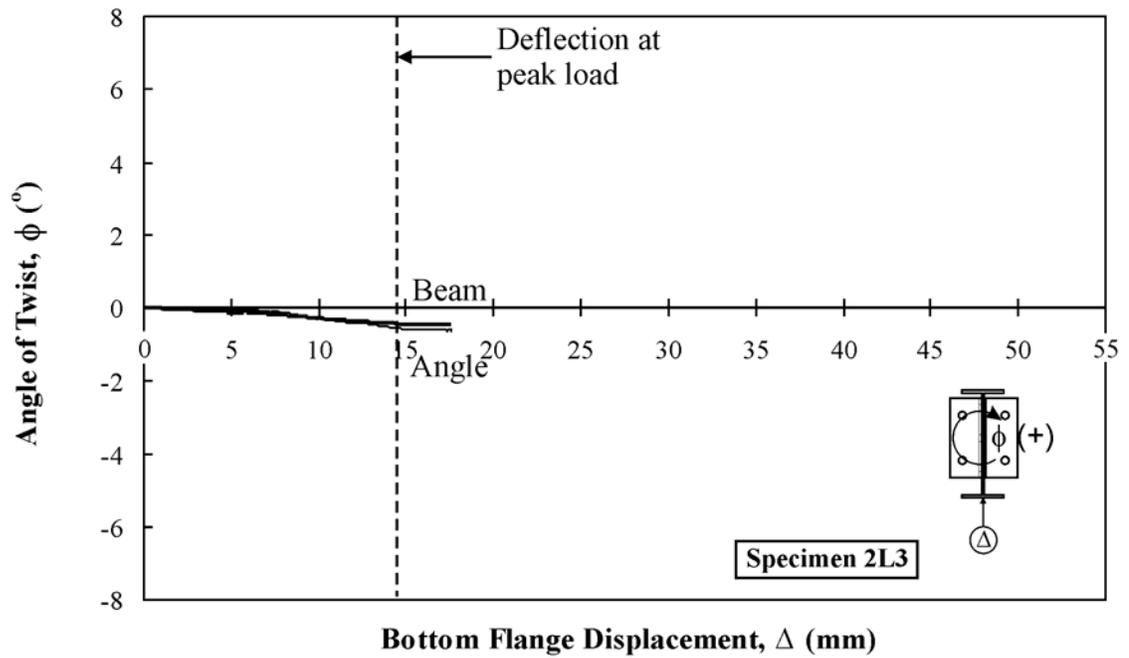
Figure B-68 Twist vs. Bottom Flange Displacement, Test Specimen 2L3
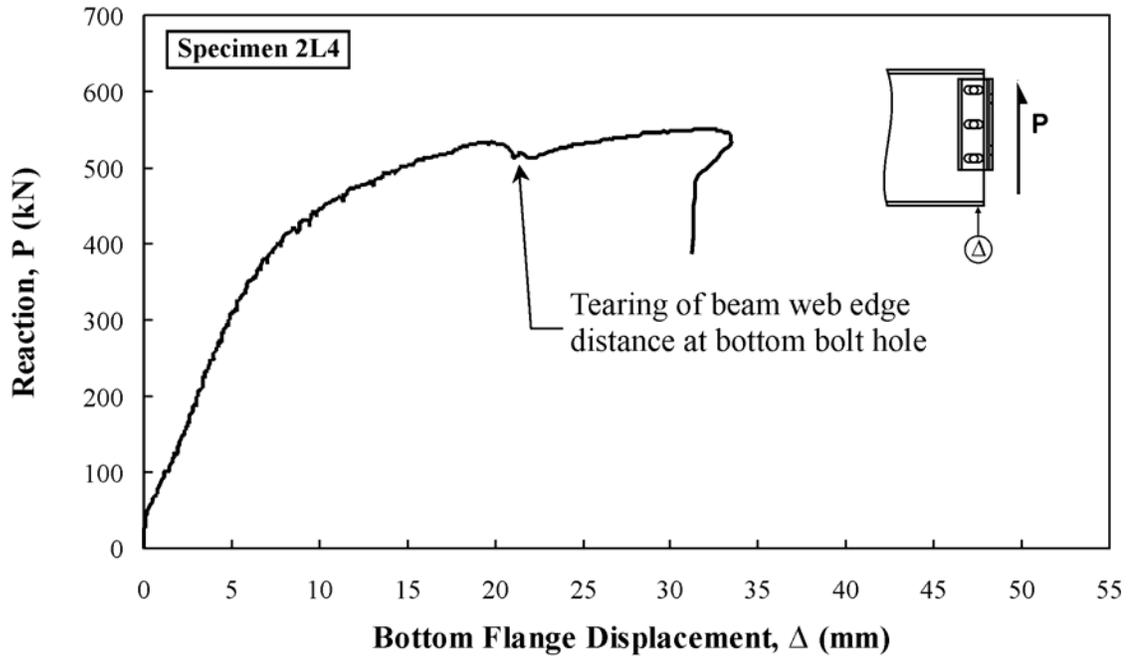
Figure B-69 Connection Reaction vs. Bottom Flange Displacement, Test Specimen 2L4
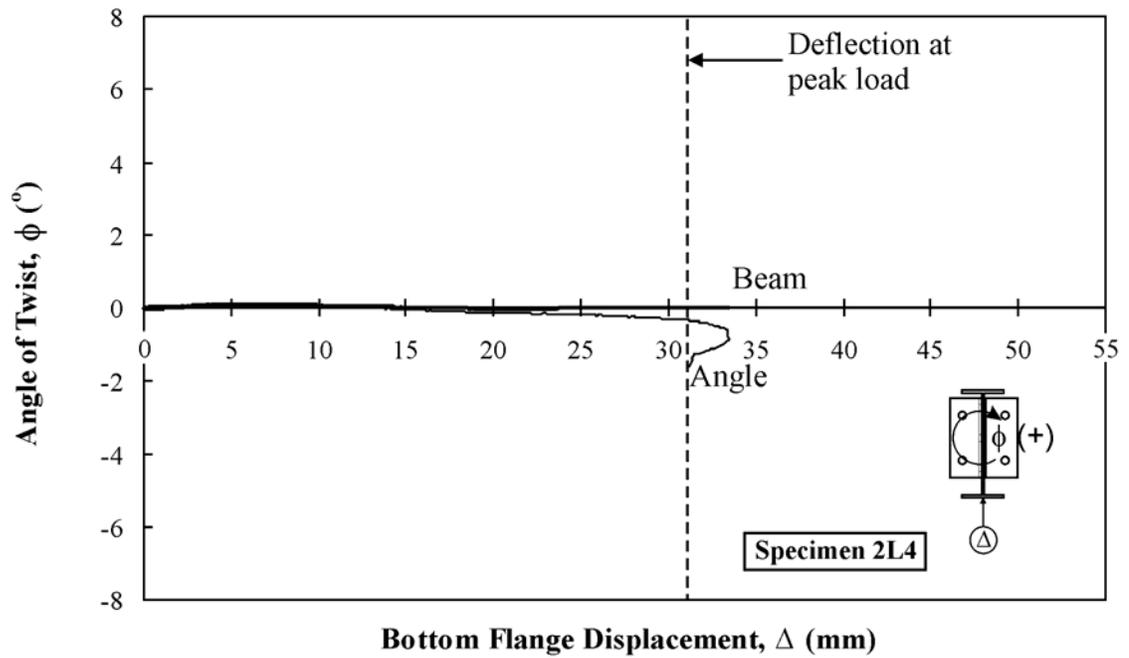
Figure B-70 Twist vs. Bottom Flange Displacement, Test Specimen 2L4

191
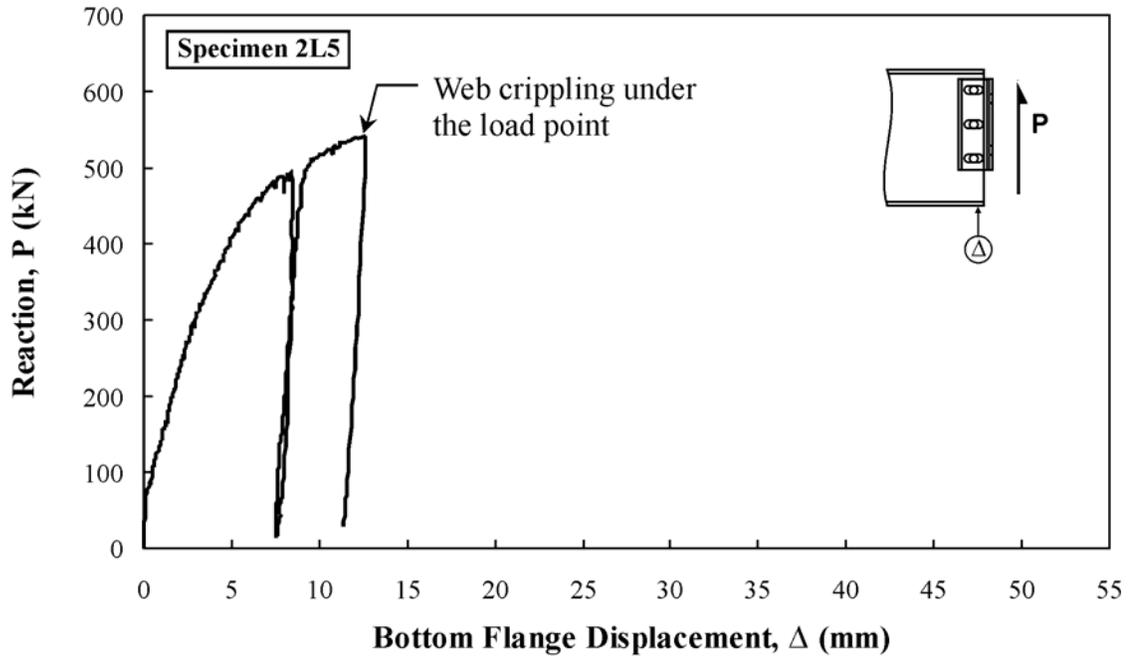
Figure B-71 Connection Reaction vs. Bottom Flange Displacement, Test Specimen 2L5
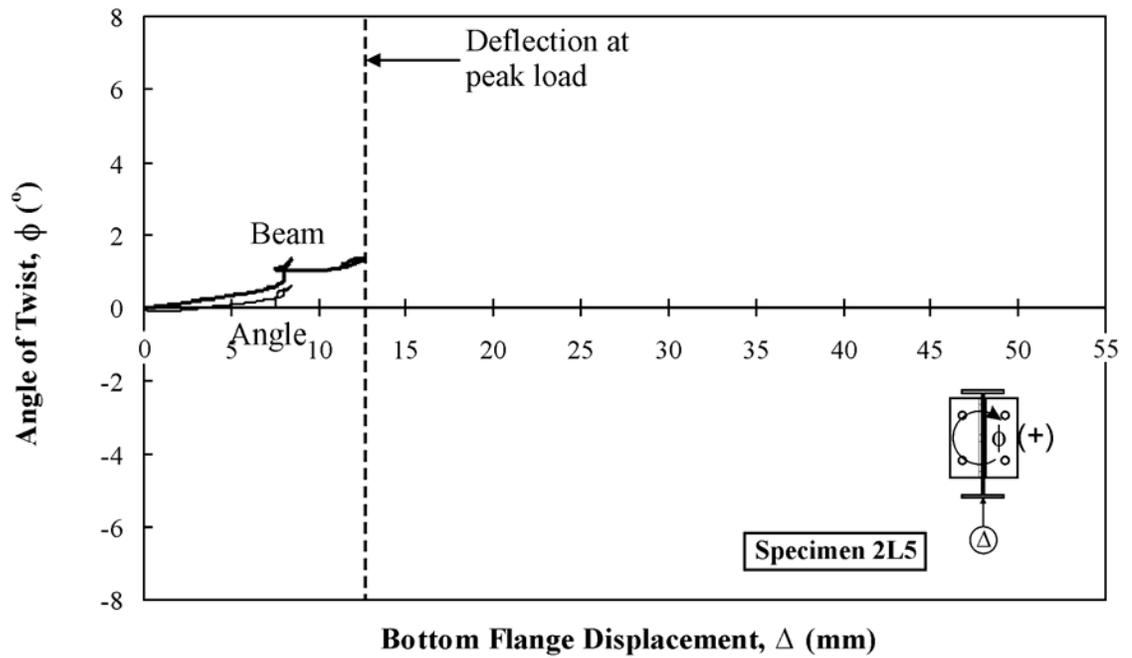
Figure B-72 Twist vs. Bottom Flange Displacement, Test Specimen 2L5
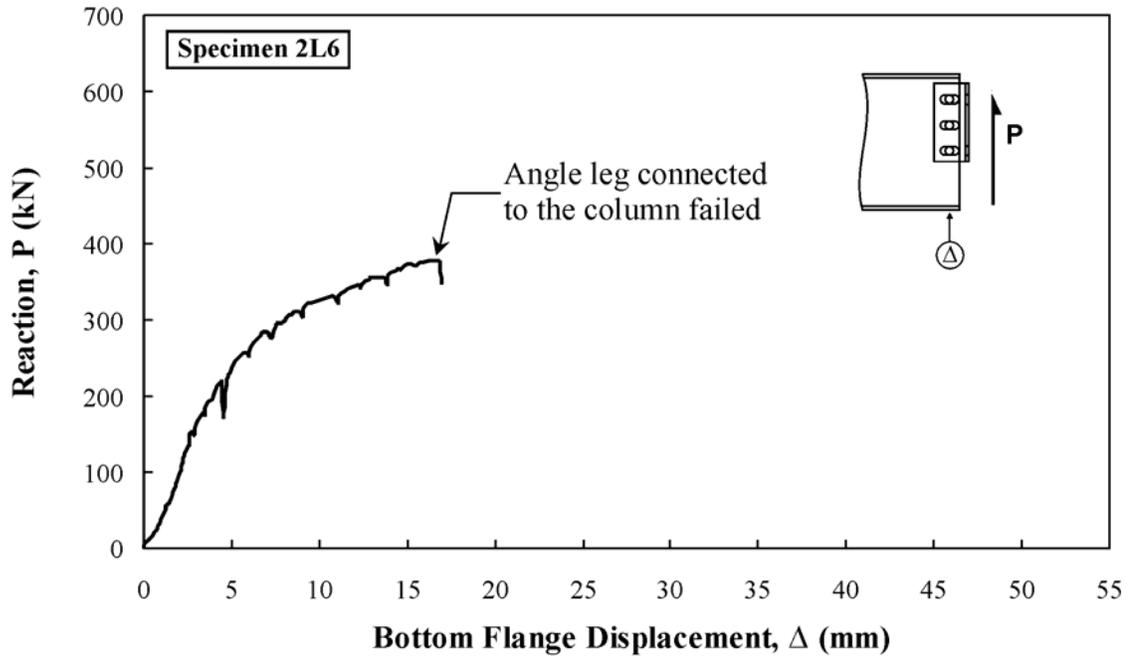
**Figure B-73 Connection Reaction vs. Bottom Flange Displacement, Test Specimen 2L6**
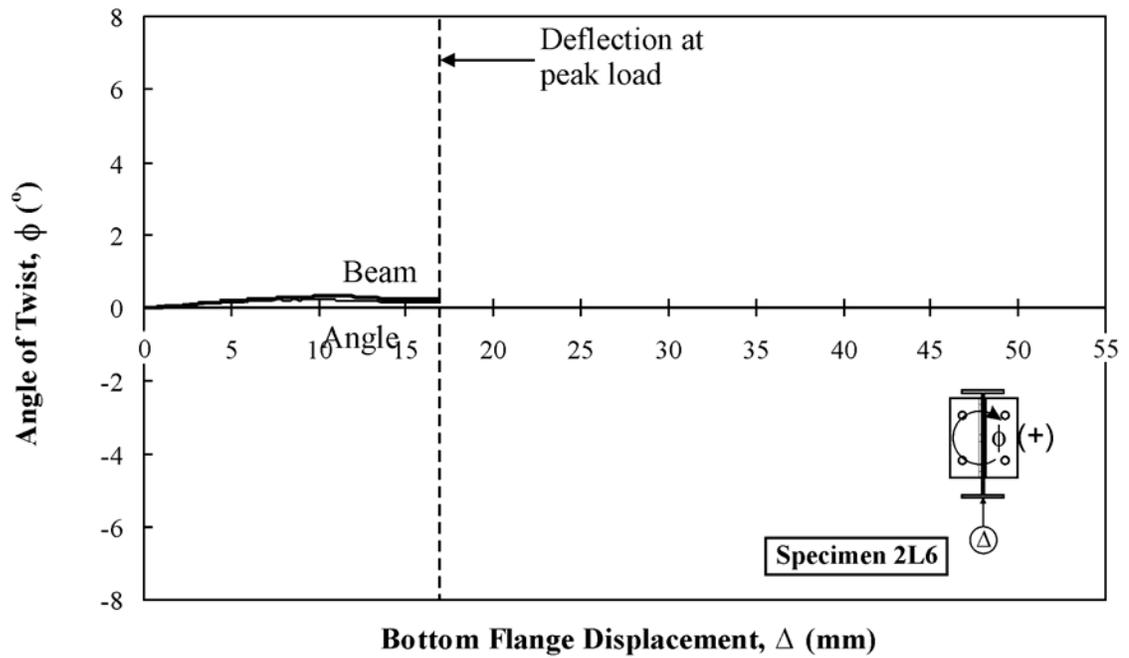
Figure B-74 Twist vs. Bottom Flange Displacement, Test Specimen 2L6
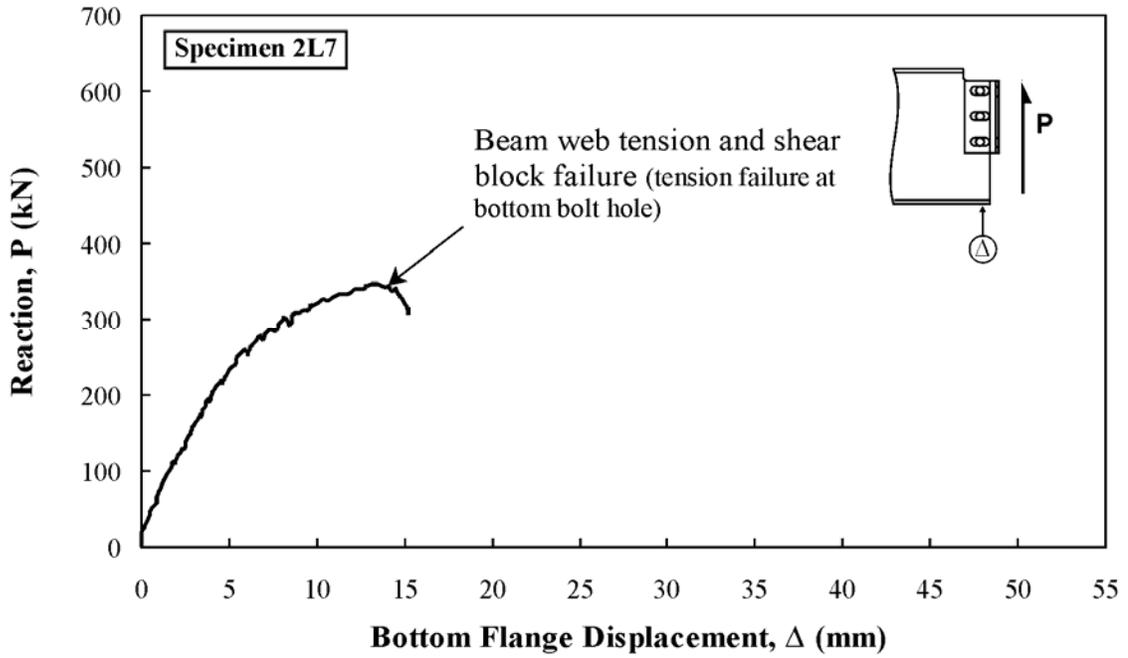
Figure B-75 Connection Reaction vs. Bottom Flange Displacement, Test Specimen 2L7
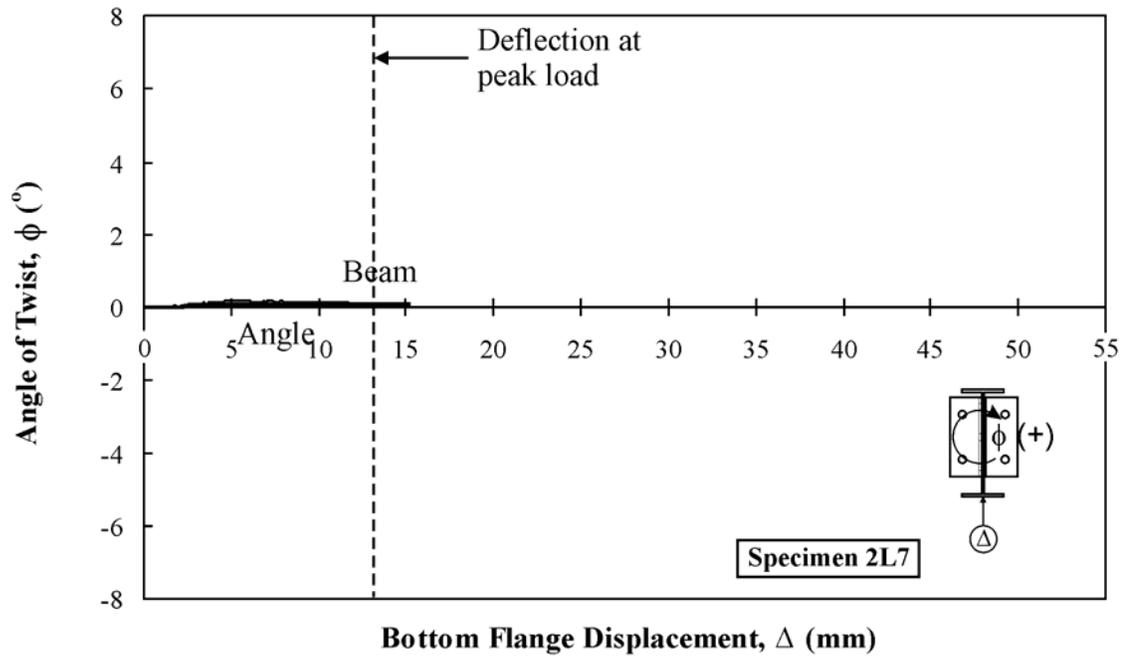
Figure B-76 Twist vs. Bottom Flange Displacement, Test Specimen 2L7

194
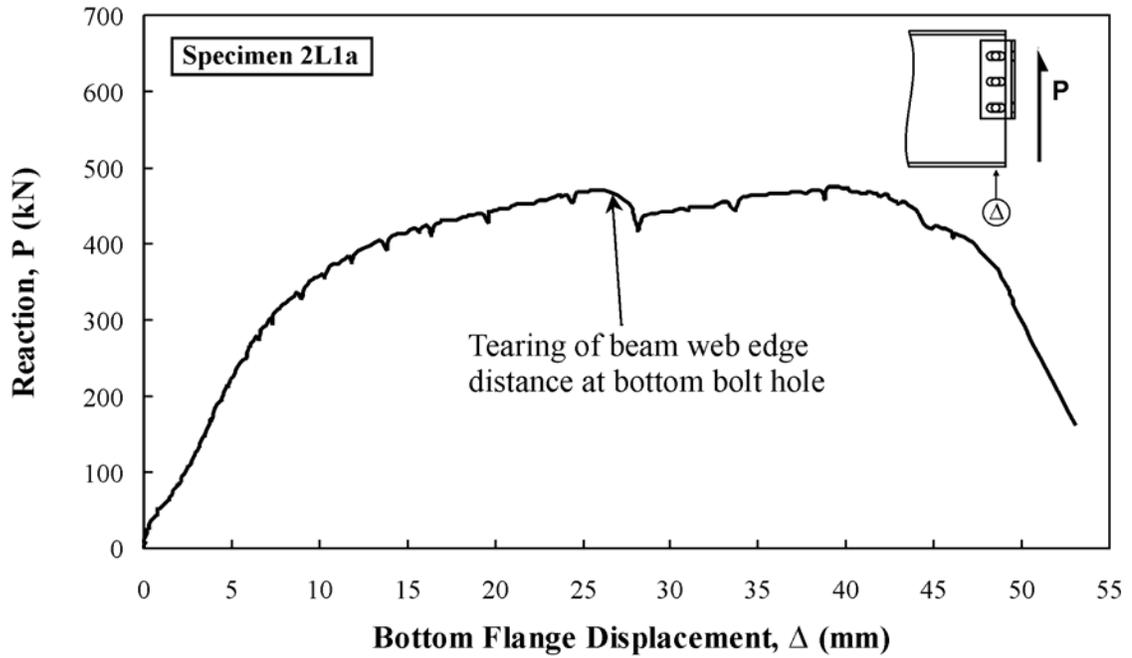
Figure B-77 Connection Reaction vs. Bottom Flange Displacement, Test Specimen 2L1a
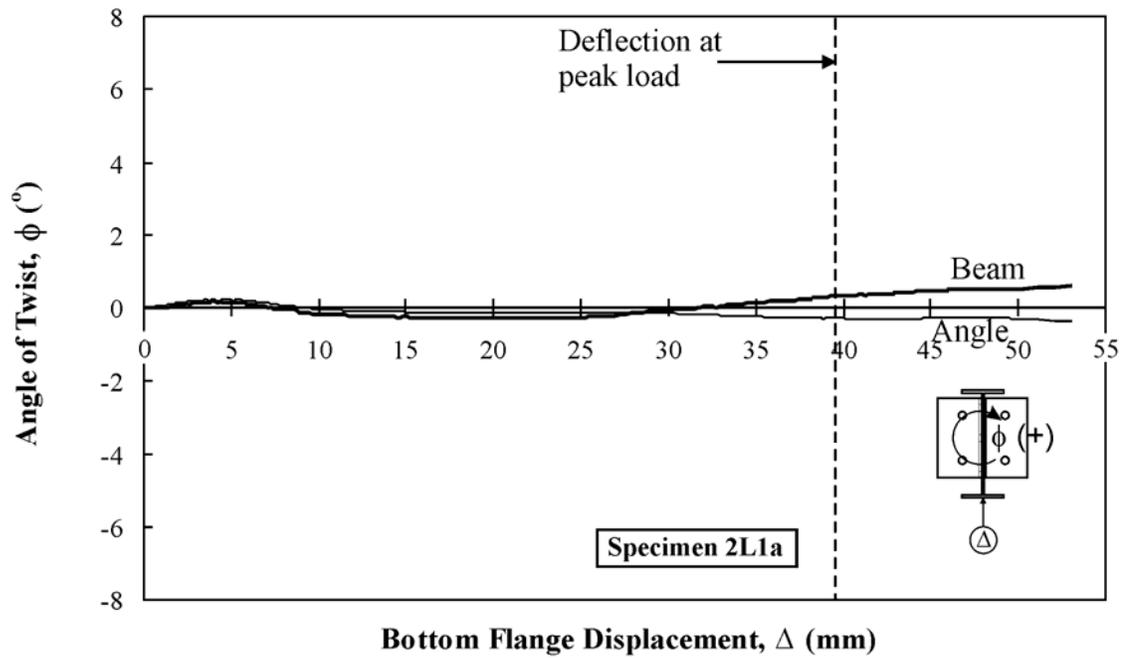
**Figure B-78 Twist vs. Bottom Flange Displacement, Test Specimen 2L1a**

195
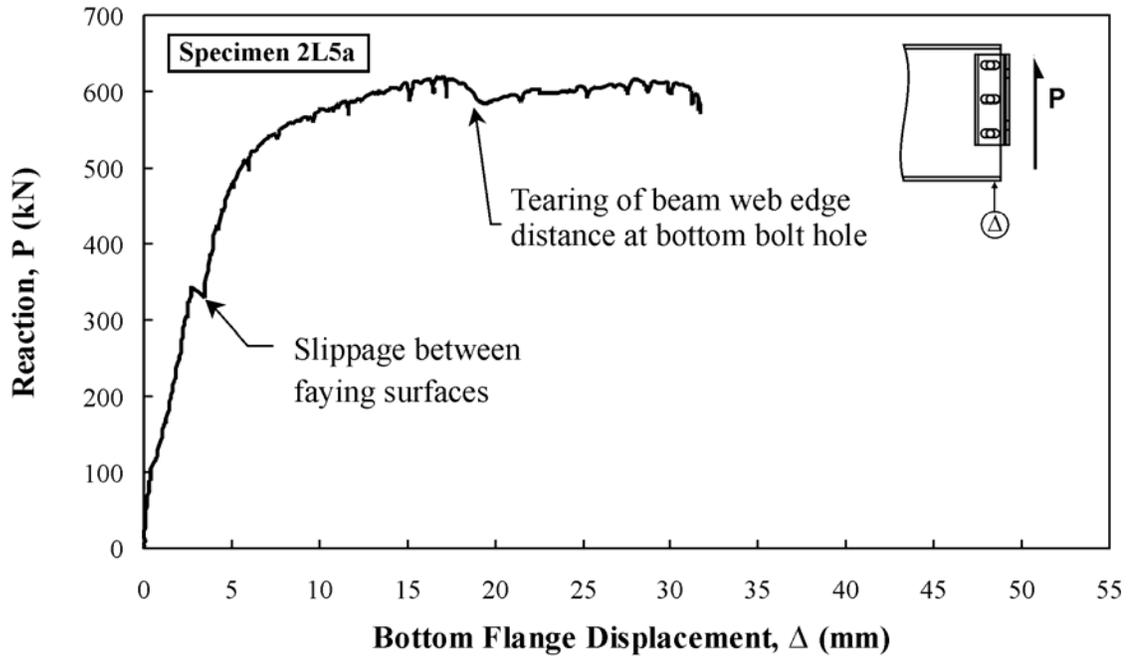
Figure B-79 Connection Reaction vs. Bottom Flange Displacement, Test Specimen 2L5a
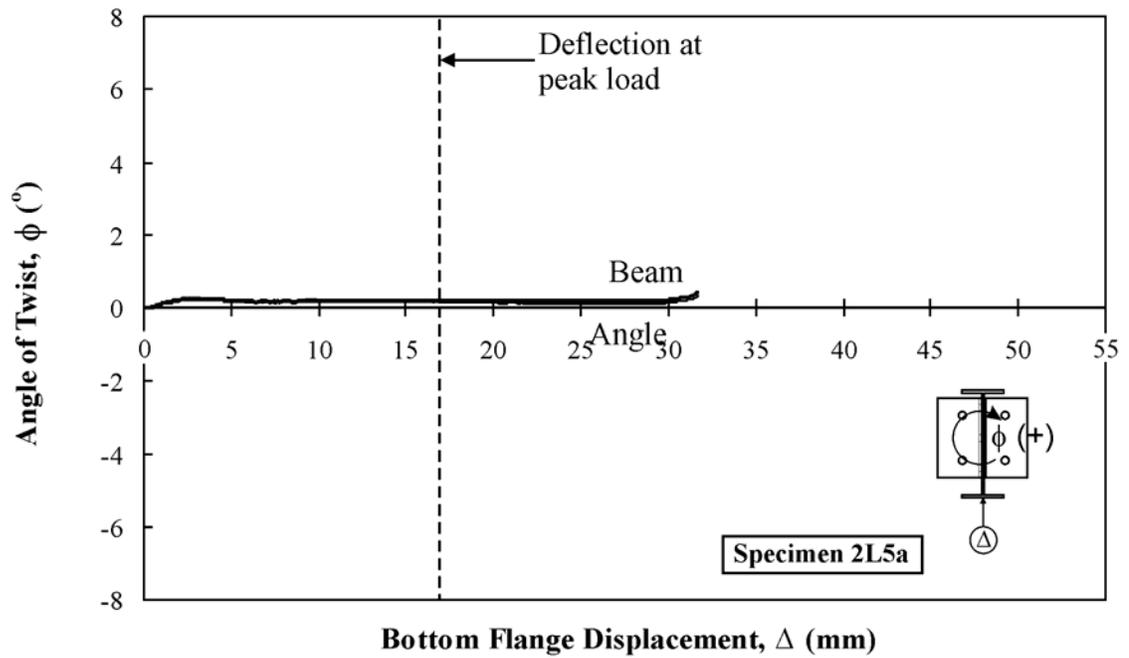
Figure B-80 Twist vs. Bottom Flange Displacement, Test Specimen 2L5a

196
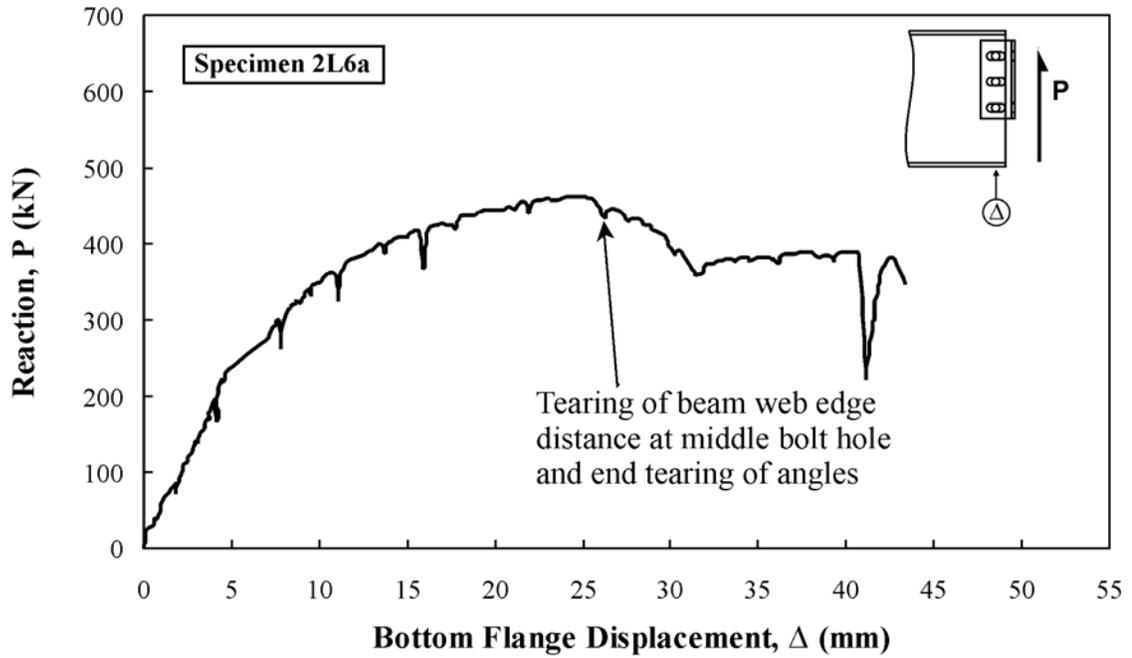
**Figure B-81 Connection Reaction vs. Bottom Flange Displacement, Test Specimen 2L6a**
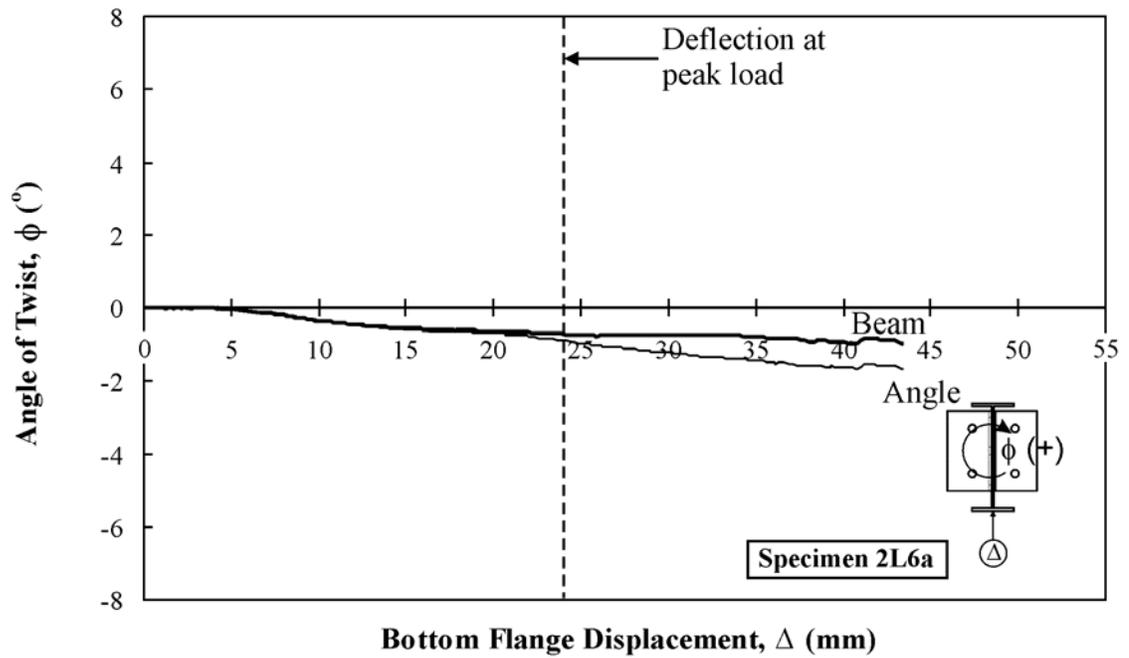
**Figure B-82 Twist vs. Bottom Flange Displacement, Test Specimen 2L6a**

197
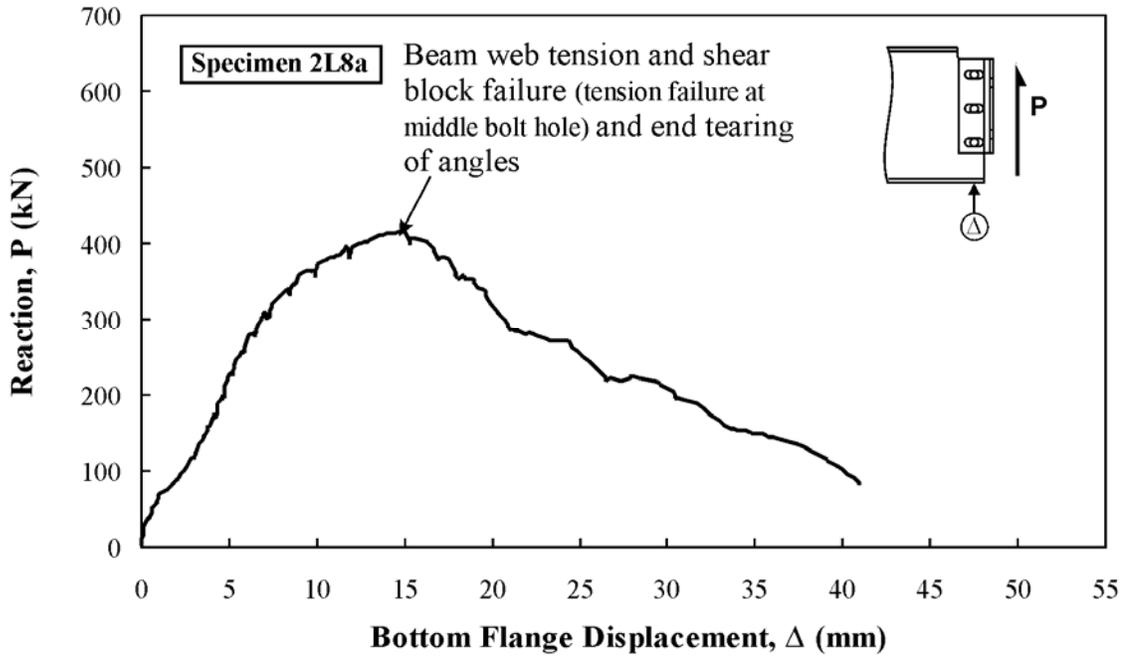
**Figure B-83 Connection Reaction vs. Bottom Flange Displacement, Test Specimen 2L8a**
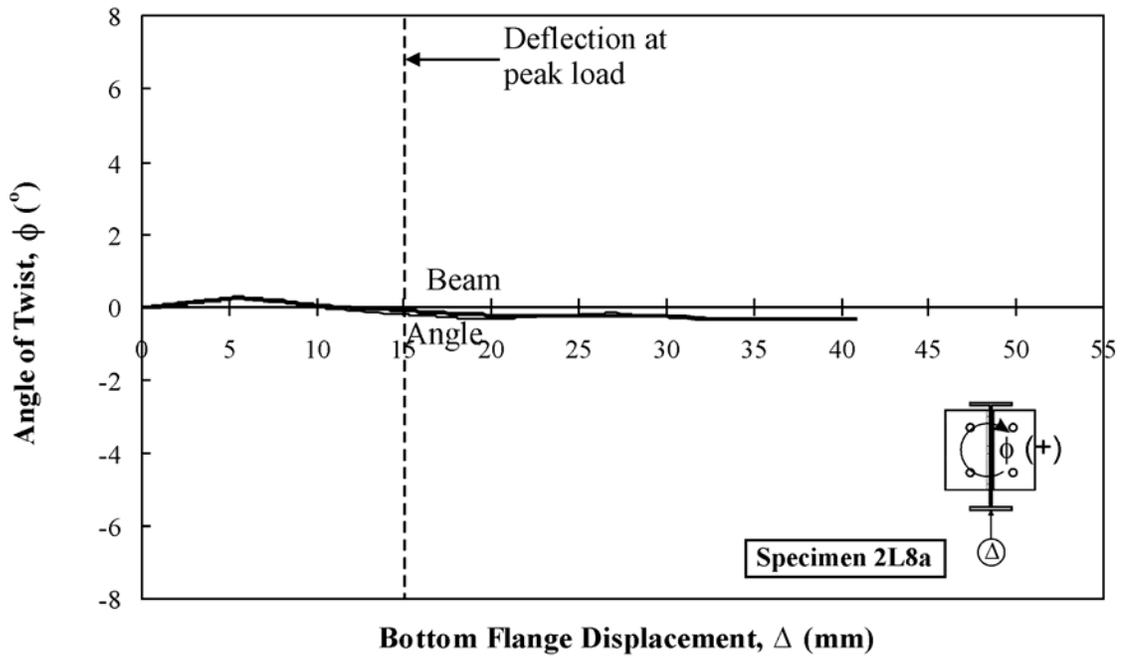
Figure B-84 Twist vs. Bottom Flange Displacement, Test Specimen 2L8a